THE UNIVERSITY *of* EDINBURGH

Integrated Assessment of Quality of Supply in Future Electricity Networks

Ignacio Hernando Gil

Doctor of Philosophy

THE UNIVERSITY OF EDINBURGH

2014

Abstract

Although power system reliability analysis is a mature research area, there is a renewed interest in updating available network models and formulating improved reliability assessment procedures. The main driver of this interest is the current transition to a new flexible and actively controlled power supply system with a high penetration of distributed generation (DG) and energy storage (ES) technologies, wider implementation of demand-side management (DSM) and application of automated control, monitoring, protection and communication infrastructures. One of the aims of this new electricity supply network ('the smart grid') is an improved reliability and power quality performance, realised through the delivery of an uninterrupted and high-quality supply of electrical energy. However, there is currently no integrated methodology to measure the effects of these changes on the overall system reliability performance.

This PhD research aims to update the standard power system simulation engine with improved numerical software models offering new capabilities for the correct assessment of quality of supply in future electricity networks. The standard reliability analysis is extended to integrate some relevant power quality aspects, enabling the classification of short and long supply interruptions by the correct modelling of network protection and reconfiguration schemes. In addition, the work investigates the formulation and analysis of updated reliability indicators for a more accurate validation and benchmarking of both system and end-user performance.

A detailed database with typical configurations and parameters of UK/European power systems is established, providing a set of generic models that can correctly represent actual distribution networks supplying a mix of residential, commercial and industrial demand for different load sectors. A general methodology for reducing system complexity by calculating both electrical and reliability equivalent models of LV and MV distribution networks is also presented. These equivalent models, based on the aggregation of individual component models, help to reduce calculation times while preserving the accuracy assessment of network's reliability performance at bulk supply points. In addition, the aggregated counterparts (same and mixed-type) of different 'smart' component models (DG, ES and DSM) are also included in the analysis, showing how their co-ordinated implementation and control could improve quality of supply.

Conventional reliability assessment procedures are also extended in this thesis to include accurate reliability equivalent models, network contingency statistics, actual load profiles and empirical fault probability distributions, which are employed to assess the frequency and duration of interruptions in the supply system for different scenarios. Both analytical and probabilistic simulation techniques (Monte Carlo method) are developed to include up-to-date security of supply legislation, introducing a new methodology for calculating the standard set of indices reported annually to energy regulators.

Acknowledgements

Firstly, I would like to thank my supervisor, Dr Saša Djokić, for his constant guidance and support during the PhD study, and specially for his patience and honesty on difficult occasions when nothing seemed to make sense, which kept me motivated to make the most out of my PhD. I would like to acknowledge the support from the EPSRC project (under the grant award EP/G052530/1) for funding this PhD research.

Thanks are also extended to my other 'half' in the project, Dr Irinel-Sorin Ilie, who was always of great help for introducing me to the 'fabulous world' of network reliability, and for sharing all his knowledge to lay the foundations of this research. Also, thanks to the thesis examiners, Prof. Markus Mueller, Prof. Matti Lehtonen and Dr Andrew Keane, for their time and effort in reviewing the thesis.

I am also indebted to Ziming Song, Richard Ball and Graham Stein, for setting up my very useful and productive placement with National Grid, and for agreeing on being my professional mentors during my time in Warwick. That work experience would not have been possible without the help and support of Jose Luis Barba from Madrid, and the Leigh family (Mike and Julia) from Leamington Spa. Also, thanks to Math Bollen from Lulea University of Technology, and Alastair Ferguson from Scottish Power, for providing a large part of the data used in this thesis.

Many thanks to my colleagues and friends at the Institute for Energy Systems, particularly all those who have passed through Rm 4.120, who have been a real pleasure both to work and socialise with. Special mention goes to Dr Adam Collin, Dr Jorge Acosta and Dr Barry Hayes for their efforts in collaboration, and also for providing such a good working environment. I would also like to thank my friends, Roger Fenske and Lee Noquet, for making my new life in Edinburgh as easy as possible, and for providing me with a 'family' away from home.

A very special acknowledgment goes to my family, for their endless love, and for giving me all of the encouragement, advice and support I could need. I am grateful to Mum, Dad, Raquel, Pedro, Rodrigo, and also to Antonio, Mari and Maruja, for their continued belief in me.

Finally, and most importantly, thank you to my best friend and beloved girlfriend Natalia, for always being there for me. Arriving at this point would not have been possible without the stability and love she provided me, and thus, I will be forever grateful to her.

Declaration

I declare that this thesis was composed by myself, that the work contained herein is my own except where explicitly stated otherwise in the text, and that this work has not been submitted for any other degree or professional qualification except as specified.

Ignacio Hernando Gil

Contents

Abstract ii

Acknowledgements iii

Declaration iv

List of Figures x

List of Tables xiv

Acronyms and abbreviations xvi

Nomenclature xx

1 Introduction 1
- 1.1 The Need for an Improved Quality of Supply Assessment . . . 1
- 1.2 Context for Quality of Supply Research . . . 2
- 1.3 Research Objectives and Scope . . . 3
- 1.4 Thesis Contributions to Knowledge . . . 5
- 1.5 Thesis Structure . . . 6

2 Network Reliability and Power Quality in Perspective 8
- 2.1 Introduction . . . 8
  - 2.1.1 Costs of Reliability . . . 9
  - 2.1.2 New Challenges for the Power System Quality of Supply . . . 10
- 2.2 Security and Quality of the Electricity Product . . . 11
  - 2.2.1 Definitions and Quantities of Security . . . 11
  - 2.2.2 Definition of Reliability/Availability/Security . . . 13
  - 2.2.3 Focus of Reliability Research . . . 16
  - 2.2.4 Definition of Power Quality . . . 17
- 2.3 Metrics for Quality of Supply . . . 19
  - 2.3.1 Reliability Indices . . . 20
  - 2.3.2 New Available Reliability Concepts . . . 29
  - 2.3.3 Power Quality Indices . . . 31
- 2.4 Security and Regulator-imposed Requirements for Supply Restoration Times . . . 31
  - 2.4.1 UK Security of Supply Requirements . . . 32

2.4.2 UK Regulator Requirements for Supply Restoration Times 33
2.4.3 Time to Restore the Supply After Temporary Faults 34
2.5 Power System Component Failure Rates and Repair Times 35
2.5.1 Power Component Bathtub Curves and Models of Operation 36
2.6 Analysis of Distribution Equipment Reliability Data 37
2.6.1 Reliability Case Study: 64 Swedish DNOs 39
2.6.2 Analysis of SPEN Reliability Performance 41
2.6.3 Fault Probability Analysis of the UK Transmission System - NG 43
2.7 Chapter Summary 47

3 Modelling of Generic Distribution Networks 48
3.1 Introduction 48
3.1.1 Typical UK Distribution Networks 49
3.2 Distribution Network Component Database 50
3.2.1 Component Database Sample: Distributed Generation 51
3.2.2 Component Database Sample: Transformers 52
3.3 Development of Sub-Transmission Network Equivalents 53
3.4 Identification of Load Structure for Network Representation 57
3.4.1 Load Modelling 57
3.4.2 Aggregate Residential Load Model 59
3.4.3 Residential Load Subsectors 62
3.4.4 Typical 'After Diversity Demand' Values per Residential Load Subsector 63
3.5 Modelling of Generic LV/MV Distribution Networks 66
3.6 Detailed Representation of LV Residential Networks 66
3.6.1 Highly-Urban Generic LV Distribution Network 69
3.6.2 Urban Generic LV Distribution Network 70
3.6.3 Suburban Generic LV Distribution Network 71
3.6.4 Rural Generic LV Distribution Network 72
3.7 MV Distribution Network Modelling 73
3.7.1 MV Underground Network Model Design 75
3.7.2 MV Overhead Network Model Design 79
3.8 Chapter Summary 80

4 Distribution System Equivalents: Aggregation Methodology and Network Analysis 83
4.1 Analysis and Calculation of LV System Supply Impedances 83
4.1.1 Supply Impedances: Typical Residential Premises 84
4.1.2 UK Case Study: MV/LV Fault Levels and Supply Impedances 85
4.2 Network and Load Aggregation Methodology 89
4.2.1 LV/MV Distribution Network Equivalents 90

4.2.2 Validation of Equivalent Network Methodology . . . 92
4.2.3 Network Influence on Aggregate Load Model Parameters . . . 93
4.2.4 MV Aggregate Load Model . . . 95
4.3 Modelling and Aggregation of the MV and LV Networks . . . 96
4.3.1 Definition of Supplying Network Subsectors . . . 97
4.3.2 Modelling the Interconnecting 33 kV Networks . . . 98
4.3.3 Aggregation of 33 kV Networks . . . 99
4.3.4 Aggregated Polynomial and Exponential Load Models Incorporating Network Effects . . . 101
4.4 Inclusion of Micro-Generation Models in Network Aggregation Methodology . 102
4.4.1 Modelling of Micro-Generation . . . 103
4.4.2 Aggregate Network and Load Characteristics with Micro-Generation . 106
4.5 Impact of DSM and Distributed Generation/Storage on Network Performance . 108
4.5.1 Case Study: Smart Grid Applications in an Urban Residential Network 109
4.5.2 Case Study: Smart Grid Applications in a Suburban Residential Network 112
4.6 Reliability Equivalents of LV and MV Distribution Networks . . . 115
4.6.1 Input Data for Reliability Equivalent Models and Analysis . . . 116
4.6.2 Reliability Equivalent Parameters with Alternative Supply . . . 117
4.7 Conclusions . . . 119

5 Risk and Reliability Modelling of Power Supply Systems 120
5.1 Reliability Criteria and Techniques . . . 120
5.1.1 General Overview . . . 120
5.1.2 Approaching Reliability Analysis . . . 121
5.2 Application of Monte Carlo Simulation Procedure . . . 123
5.2.1 Classification of Long and Short Interruptions . . . 124
5.2.2 Inclusion of Actual Load Profiles in MCS . . . 126
5.2.3 Assessment of Input Probability Distributions . . . 128
5.2.4 Impact of Time-Varying Failure Rates on Distribution Reliability . . . 130
5.2.5 Integrated Code for Monte Carlo Simulation . . . 134
5.3 Precision Estimation of Monte Carlo Method . . . 134
5.3.1 Uncertainty Assessment of MCS . . . 135
5.3.2 Multiple/Simultaneous Fault Analysis . . . 138
5.3.3 Convergence Analysis of MCS . . . 140
5.4 Empirical Model for Customer Interruption Process . . . 143
5.4.1 Theoretical Interruption Model . . . 144
5.4.2 Application and Effectiveness of the Outage Model . . . 146
5.5 Conclusions . . . 149

6 Integrated Reliability Analysis of Active Distribution Networks 151

6.1 Reliability Performance of a Real Power Supply System 151
6.1.1 Assessment of Energy Not Supplied (ENS) 153
6.1.2 Estimation of Conventional Reliability Indices 154
6.2 Risk Assessment of Interruption Times Affecting Customers 156
6.2.1 Deterministic Algorithm for Customer Interruption Risk Assessment . . 157
6.2.2 Duration of Interruptions Assessment 159
6.2.3 Reliability Indices Reported to Regulator 160
6.3 Quantification of Network Functionalities through Monte Carlo Simulation . . 162
6.3.1 Reliability Equivalents of Aggregate LV Networks 164
6.3.2 Network Scenarios for Reliability Assessment 165
6.3.3 Reliability Results: MCS vs. Analytical Contingency Analysis 167
6.3.4 Monte Carlo Simulation Results: Network Stochastic Behaviour 170
6.4 "Smart Grid" Reliability Performance Assessment 180
6.4.1 Application of Energy Storage and Demand-side Management Resources 180
6.4.2 Reliability Performance Analysis with ES and DSM 182
6.5 Conclusions 185

7 Summary and Conclusions 187
7.1 Synopsis 187
7.2 Implications of Results 188
7.2.1 Modelling of Generic Networks and Load Identification 188
7.2.2 Electrical and Reliability Network Equivalents 189
7.2.3 Impact of the Smart Grid Functionalities on QoS Performance 190
7.2.4 Integrated Reliability Analysis of Active Distribution Networks 190
7.3 Research Limitations 191
7.4 Recommendations for Further Work 193

References 196

Appendices

A Reliability Case Studies: DNOs/TSOs Performance Analysis 211
A.1 Analysis of Swedish Reliability Performance 211
A.1.1 Aggregate Customer Impact in Year 2010 211
A.1.2 Classification of SAIFI and CAIDI Indices by Type of Customer Interruptions (Year 2010) 213
A.1.3 Classification of Customer Interruptions by Voltage Level (Year 2010) . 213
A.1.4 Comparison of 64 Swedish DNOs' Data (Years 2008 vs. 2010) 216
A.2 SPEN - Distribution Reliability Performance 2009/10 216
A.2.1 Analysis of Pre-arranged Network Interruptions 216

A.3 NG - Fault Probability Analysis (6-10 years data) . . . 218
A.3.1 NG - Transient/Sustained Transformer Trips . . . 218
A.3.2 NG - Planned Circuit Outages . . . 219
A.3.3 NG - Overall Component Fault Statistics . . . 219

B Power Component Database Sample 221
B.1 Sample Database: Circuits . . . 221
B.1.1 Overhead Lines . . . 221
B.1.2 Cables . . . 222
B.2 Sample Database: Reactive Compensation & FACTS Devices . . . 222
B.3 Sample Database: Protections . . . 223
B.4 MV Distribution Transformers: Specifications Summary . . . 224

C Report on Typical UK Transformer Ratings 225

D Full-Specification Modelling of Secondary Distribution Transformers 239
D.1 Development of Full Transformer Models . . . 239
D.1.1 Transformer's Series Impedance Calculation . . . 241
D.1.2 Transformer's Parallel Impedance Calculation . . . 242
D.2 Transformer Full-Specification Models per Load Subsector . . . 244

E MV Load Subsector Classification in the SPTL System 246

F Matlab Model for Monte Carlo Simulation 248

G DNO's Interruption Probability Analysis 257
G.1 Probability Distributions of Long Interruptions . . . 257
G.2 Probability Distributions of Short Interruptions . . . 259

List of Figures

2.1 Costs according to reliability of the system 10
2.2 UK average 2008/09 proportion of customer interruptions by voltage 10
2.3 Diagram of average reliability times 15
2.4 Annual demand and LDC of a 33/11 kV substation in the UK 21
2.5 Bathtub curves for the risk of faults over a network component's lifetime 37
2.6 Operational models of power components 38
2.7 Classification of 64 Swedish DNOs into different load sectors. 40
2.8 SPEN - Number of unplanned LIs by voltage level and equipment (09/10). 41
2.9 SPEN - Average duration of unplanned LIs (09/10). 42
2.10 SPEN - Unplanned CI and CML by voltage level and equipment (09/10). 42
2.11 SPEN - Probability of duration of unplanned LIs (09/10). 43
2.12 NG - Cumulative distributions of the duration of sustained circuit trips (6 years). . . 44
2.13 NG - CDFs of the duration of sustained trips of overhead lines (6 years). 45
2.14 NG - CDFs of urgent events in different transformers (6 years). 46
2.15 NG - PDFs of urgent events in different transformers (6 years). 46
2.16 NG - Outage rate distributions for power components' lifetime. 47

3.1 The UK context for electricity distribution 49
3.2 Methodology for building the MV network component database. 50
3.3 Comparison of typical UK transformer ratings. 52
3.4 IEEE 14-bus network: original and UK revised variant. 54
3.5 IEEE 14-bus network vs. reference UK sub-transmission network. 56
3.6 Active power demand created by 1 kW of each of the three load types, as a function of the supply voltage. 58
3.7 Typical aggregate daily load demand curves for the UK residential load sector for three characteristic loading conditions. 60
3.8 Decomposition of the UK residential load sector into load types for average loading conditions 61
3.9 Typical UK domestic profile classes 63
3.10 Highly-urban generic LV distribution network model. 70
3.11 Urban generic LV distribution network model. 71
3.12 Suburban generic LV distribution network model. 72
3.13 Rural generic LV distribution network model. 73
3.14 Highly-urban generic MV distribution network model 77
3.15 Urban generic MV distribution network model 78

3.16 Suburban generic MV distribution network model 81
3.17 Rural generic MV distribution network model 82

4.1 Typical arrangement for overhead LV distribution systems 84
4.2 Typical arrangements for underground LV distribution systems 85
4.3 Existing urban network arrangement considered for system fault level analysis (SHEPD) 86
4.4 Network model for determining MV/LV system fault levels and supply impedances in urban areas. 87
4.5 Single-line circuit diagram for MV/LV fault levels calculated. 88
4.6 Overview of the aggregation methodology 89
4.7 MV and LV equivalent network configurations. 90
4.8 Comparison of example MV polynomial/ZIP load model coefficients obtained using detailed and equivalent network models. 93
4.9 Network influence on MV aggregate load characteristics (reactive power). 95
4.10 Comparison of MV and LV aggregate load models for UK urban load subsector example, expressed in exponential form. 96
4.11 Map illustrating the 33 kV distribution system in the Edinburgh city region. 97
4.12 Govan GSP 33 kV network. 99
4.13 GSP load aggregation methodology. 100
4.14 Polynomial ZIP model coefficients calculated at BAGA 33 kV node. 101
4.15 Exponential coefficients calculated at BAGA 33 kV node. 102
4.16 Estimated minimum, maximum and average power outputs of aggregated wind and solar-PV microgeneration systems for Spring. 104
4.17 Impact of aggregate LV wind-based MG model for maximum residential demand. . 105
4.18 Urban network with connected microgeneration. 106
4.19 Equivalent network configuration with connected microgeneration. 106
4.20 Comparison of active and reactive power flows at 11 kV aggregate load supply point for detailed and equivalent network models for maximum loading conditions. 107
4.21 Exponential load model interpretation of MV aggregate load for maximum loading conditions with installed microgeneration. 108
4.22 Typical UK network configuration supplying urban residential load. 109
4.23 Comparison of aggregate active and fundamental reactive power demands with devised urban DSM schemes. 111
4.24 Comparison of LV voltage profiles and transformer tap settings with devised urban DSM schemes. 112
4.25 Typical UK network configuration supplying suburban residential load. 113
4.26 Combined power outputs of solar-PV and wind-based microgeneration systems. . . 113

4.27 Comparison between aggregate active and reactive power demands for the implemented suburban DSM scenarios. . . . 114
4.28 Comparison between LV voltage profiles and transformer tap settings for the implemented suburban DSM scenarios. . . . 115
4.29 Aggregate LV and MV network models, with equivalent network impedances and reliability equivalent model parameters. . . . 116

5.1 General algorithm of the applied MCS procedure. . . . 125
5.2 Demand identification of a mixed load profile at 33 kV GSP. . . . 127
5.3 Input probability distributions for modelling the fault repair time of a 33 kV bus. . 129
5.4 Example application of Bathtub (Beta) distribution for the expected lifetime of a power component. . . . 131
5.5 Suburban test distribution network (residential + commercial load). . . . 132
5.6 Comparison of average duration of interruptions per network load point. . . . 133
5.7 Uncertainty distribution of reliability indices over simulation time. . . . 136
5.8 Comparison of average duration of load interruptions for uncertainty analysis. . . . 137
5.9 Standard deviation and probabilities associated with a normal distribution. . . . 139
5.10 Kernel density function of permanent double faults after a 34,000-year simulation. 140
5.11 Convergence of SAIFI mean value for three different 1,000-year simulations. . . . 141
5.12 Convergence of mean value of frequency of interruptions (SAIFI and MAIFI indices) over a 34,000-year simulation. . . . 141
5.13 Convergence tolerance of SAIFI index over a 1,000-year simulation. . . . 142
5.14 Convergence tolerance of SAIFI index over a 34,000-year simulation. . . . 142
5.15 Zoom into the convergence tolerance of SAIFI index over a 34,000-year simulation. 143
5.16 Daily probability distributions of short and long interruptions. . . . 144
5.17 Theoretical model approximation of the average empririal distributions. . . . 145
5.18 Simplified MV system supplying aggregate load point. . . . 146
5.19 Moment of interruption modelling for real distributions and theoretical CDFs. . . . 147

6.1 Distribution system with typical highly-urban and suburban configurations. . . . 152
6.2 Estimations of ENS index for several probability distributions. . . . 153
6.3 Probabilistic estimations of reliability indicators for different PDFs. . . . 155
6.4 Estimated durations of interruptions for different customer classes in a typical UK distribution system. . . . 160
6.5 Probabilistic comparison of reliability indices with SQS and repair time thresholds. 161
6.6 Typical MV/LV urban distribution network with underground meshed configuration (divided in group demand classes). . . . 163
6.7 Average duration of interruptions for 48 load points and all network scenarios. . . . 170
6.8 Frequency of long interruptions analysis: SAIFI index for all network scenarios. . . 172
6.9 Frequency of short interruptions analysis: MAIFI index for all network scenarios. . 174

6.10 Duration of long interruptions analysis: SAIDI index for all network scenarios. . . 175
6.11 Impact of network functionalities on duration of customer interruptions. 177
6.12 Energy not supplied analysis: ENS index for all network scenarios. 179
6.13 Decomposition of typical UK daily load curves for maximum demand (winter). . . 181
6.14 Frequency of interruptions probability (SAIFI and MAIFI Indices). 183
6.15 Effect of energy storage on the duration of LIs (Base case vs. E. Storage). 184
6.16 Impact of 'smart grid' scenarios on energy not supplied (ENS). 184

A.1 Frequency and average outage duration by type of customer interruptions. 213
A.2 Average duration of customer interruptions (CAIDI) per voltage. 215
A.3 SAIFI and SAIDI indices - Unplanned long customer interruptions inside own network 216
A.4 SPEN - Number of planned LIs by voltage level and equipment (09/10). 217
A.5 SPEN - Average duration of planned LIs (09/10). 217
A.6 SPEN - Planned CI and CML by voltage level and equipment (09/10). 217
A.7 SPEN - Probability of duration of planned LIs (09/10). 218
A.8 NG - Number and duration of outages for different transformer types. 218
A.9 NG - Cumulative distribution of the duration of planned outages. 219

B.1 Specifications summary of MV power distribution transformers 224

D.1 Simplified transformer equivalent circuit. 240
D.2 Transformer equivalent circuit: Z_{TOT} components referred to their own winding. . . 241
D.3 Transformer equivalent circuit: Z_{TOT} components referred to the secondary winding. 241
D.4 Electrical characteristics of MV distribution transformers (Ormazabal) 243

G.1 SPEN - Daily probability of all long interruptions in year 2009. 258
G.2 SPEN - Daily probability of planned long interruptions in year 2009. 258
G.3 SPEN - Daily probability of LIs due to incidents on other systems in year 2009. . . 258
G.4 SPEN - Daily probability of all short interruptions in years 2009/10. 259
G.5 SPEN - Daily probability of week-day short interruptions in years 2009/10. 259
G.6 SPEN - Daily probability of weekend-day short interruptions in years 2009/10. . . 260
G.7 SPEN - Daily probability of spring-time short interruptions in years 2009/10. . . . 260
G.8 SPEN - Daily probability of summer-time short interruptions in years 2009/10. . . 260
G.9 SPEN - Daily probability of autumn-time short interruptions in years 2009/10. . . . 261
G.10 SPEN - Daily probability of winter-time short interruptions in years 2009/10. . . . 261

List of Tables

2.1 Two approaches/concepts used in PQ definitions. 19
2.2 Characteristics of reliability metrics for network performance assessment. 28
2.3 Annual values of UK DNOs' reliability indices 32
2.4 UK security of supply requirements for interrupted customers 33
2.5 UK regulator-imposed requirements for supply restoration times 34
2.6 Fault clearance times of typical UK protection systems 34
2.7 Failure rates and mean repair times for main network components 36
2.8 Swedish regulator statistics for unplanned interruptions, sorted by load sector . . . 39

3.1 Medium/small generation embedded within UK distribution networks 51
3.2 Selection of the 'most typically used' power distribution transformer in the UK. . . 53
3.3 Typical 33/11 kV distribution transformers in the UK 53
3.4 OHL specifications for UK sub-transmission network equivalent. 55
3.5 Transformer specifications for UK sub-transmission network equivalent. 55
3.6 Seasonal percentage contributions to the annual energy demand in SPEN networks. 64
3.7 Annual average domestic electricity consumption per meter in 2009 65
3.8 After diversity demand (ADD) values per load subsector, class of customer and yearly season. 65
3.9 Typical UK LV line cross-sections per residential load subsector 67
3.10 Typical configurations and parameters of LV lines in the UK 67
3.11 Parameters of typical 11/0.4 kV secondary distribution transformers 68
3.12 Maximum distribution radius of secondary distribution transformers 68
3.13 Typical configurations and parameters of MV lines 74
3.14 Parameters of typical 33/11 kV primary distribution transformers 74

4.1 Comparison of MV/LV system fault levels and supply impedances. 88
4.2 UK residential consumers' complex supply impedance (IEC/TR 60725:2005) . . . 88
4.3 MV and LV equivalent network impedances per load subsector. 92
4.4 Values for example of network influence on the aggregate MV load model. 94
4.5 Example of MV system classification at GOVA bus. 98
4.6 Comparison of total daily energy supplied for two urban network scenarios. 111
4.7 Comparison of daily system energy losses for two urban network scenarios. 111
4.8 Reliability equivalent parameters per network and load subsector. 118

5.1 Comparison of input analytical parameters for modelling the fault repair time of a 33 kV bus (MTTR = 140 hours). 129

5.2 Comparison of average reliability indices for constant and time-varying failure rate. 133
5.3 Uncertainty evaluation of Monte Carlo simulation method. 136
5.4 Comparison of average reliability indicators for uncertainty analysis. 137
5.5 Comparison of absolute values for multiple/simultaneous fault analysis. 139
5.6 Comparison of relative values for multiple/simultaneous fault analysis. 139
5.7 Polynomial coefficients of theoretical interruption curves - SI and LI approx. . . . 146
5.8 ENS results with real distributions and theoretical model for different load types. . 148

6.1 Comparison of mean values and standard deviations of estimated reliability indicators with different probability distributions. 156
6.2 Penalty risk for durations of interruptions above Regulator-imposed time thresholds. 159
6.3 Mean reliability indices (urban network) following Monte Carlo simulation. 167
6.4 Mean reliability indices (urban network) following analytical contingency analysis. 169
6.5 Average reduction of energy not supplied (ENS) for different 'smart grid' scenarios. 185

A.1 Unplanned long customer interruptions. 211
A.2 Planned long customer interruptions. 212
A.3 Total (planned + unplanned) long customer interruptions. 212
A.4 Short customer interruptions. 212
A.5 Type of customer interruptions by voltage level. 214
A.6 Reliability indicators per voltage level. 215
A.7 NG - Overall component fault statistics (6-10 years) 220

B.1 MV Overhead lines data (11, 33 & 132 kV). 221
B.2 MV Distribution cable data (11, 33 & 132 kV). 222
B.3 Sample of typical reactive compensation equipment 223
B.4 UK network fault clearance times. 223
B.5 Back-up protection fault clearance times. 223

D.1 Full specification of phase constants for secondary transformers in highly-urban areas 245
D.2 Full specification of phase constants for secondary transformers in urban areas . . . 245
D.3 Full specification of phase constants for secondary transformers in suburban areas . 245
D.4 Full specification of phase constants for secondary transformers in rural areas . . . 245

E.1 Results from load subsector classification at the 89 GSPs in the SPTL network . . . 247

Acronyms and abbreviations

1-ph	Single-Phase
3-ph	Three-Phase
ac	Alternating Current
ADD	After Diversity Demand
AeT	Annual Effective Time
Al	Aluminium
ASAI	Average Service Availability Index
ASIDI	Average System Interruption Duration Index
ASIFI	Average System Interruption Frequency Index
BSP	Bulk Supply Point
CAIDI	Customer Average Interruption Duration Index
CAIFI	Customer Average Interruption Frequency Index
CDF	Cumulative Distribution Function
CE	Consumer Electronics
CEER	Council of European Energy Regulators
$CEMSMI_n$	Customers Experiencing Multiple Sustained Interruption and Momentary Interruption Events
CENS	Customer Energy Not Supplied
CFL	Compact Fluorescent Lamp
CHP	Combined Heat and Power
CI	Customer Interruptions
CML	Customer Minutes Lost
CPNS	Customer Power Not Supplied
CSA	Cross Sectional Area
CSP	Customer Supply Point
CTAIDI	Customer Total Average Interruption Duration Index
Cu	Copper
dc	Direct Current
DG	Distributed Generation
DHW	Domestic Hot Water
DNO	Distribution Network Operator
DPLVC	Daily Peak Load Variation Curve
DSM	Demand-side Management

EEA	European Energy Authority
EENS	Expected Energy Not Supplied
EeNS	Energy equipment Not Supplied
EHV	Extra High Voltage
EIU	Energy Index of Unreliability
EIR	Energy Index of Reliability
EL	Expected Lifetime (of a power component)
ENA	Energy Networks Association
ENS	Energy Not Supplied
EPR	Ethylene Propylene Rubber
EPRI	Electric Power Research Institute
ES	Energy Storage
EU	European Union
EUE	Expected Unserved Energy
EV	Electric Vehicle
FACTS	Flexible ac Transmission System
GB	Great Britain
GD	Group Demand
GIL	General Incandescent Lamp
GS	Guaranteed Standards
GSP	Grid Supply Point
GW	Gigawatt
HU	Highly-Urban
HV	High Voltage
ICT	Information and Communication Technology
IEEE	Institute of Electrical and Electronic Engineers
IES	Institute for Energy Systems
IIS	Interruption Incentive Scheme
ISO	International Organisation for Standardisation
LDC	Load Duration Curve
LI	Long Interruption
LOEE	Loss of Energy Expectation
LOLE	Loss of Load Expectation
LTDS	Long Term Development Statement
LV	Low Voltage
MAIFI	Momentary Average Interruption Frequency Index
$MAIFI_E$	Momentary Average Interruption Event Frequency Index
MCS	Monte Carlo Simulation

MDT	Mean Down Time
MG	Micro-Generation
MTBF	Mean Time Between Failures
MTTF	Mean Time To Fail
MTTR	Mean Time To Repair
MUT	Mean Up Time
MV	Medium Voltage
MVA	Megavolt Amperes
MW	Megawatt
NERC	North American Electric Reliability Council
NG	National Grid
OFGEM	Office of Gas and Electricity Markets
OHL	Overhead Line
OLTC	On Load Tap-Changing
PC	Power Component
PCC	Point of Common Coupling
PDF	Probability Density Function
PeNS	Power equipment Not Supplied
PES	Power and Energy Society
PQ	Power Quality
PSSE	Power System Simulator for Engineering
p.u.	per unit
PV	Photovoltaic
PVC	Polyvinyl Chloride
QoS	Quality of Supply
RER	Renewable Energy Resources
RI	Re-Interruptions
rms	Root-mean-square
Ru	Rural
SAIDI	System Average Interruption Duration Index
SAIFI	System Average Interruption Frequency Index
SI	Short Interruption
SG	Smart Grid
SHEPD	Scottish Hydro Electric Power Distribution
SMRCR	SAIFI/MAIFI Relative Cost Ratio
SPEN	Scottish Power Energy Networks
SQS	Security and Quality of Supply
SSE	Scottish and Southern Energy

SU	Sub-Urban
SVC	Static VAr Compensator
TCB	Tele-controlled Circuit Breaker
TSO	Transmission System Operator
TTF	Time to Fail
TTR	Time to Repair
TTRS	Time to Restore Supply
U	Urban
UK	United Kingdom
UKRI	United Kingdom and Republic of Ireland
US	United States
WT	Wind turbine
XLPE	Cross-linked Polyethylene
ZIP	Polynomial Load Model

Nomenclature

α	Time-varying scaling factor
α_B	Parameter of Beta distribution model
β_B	Parameter of Beta distribution model
ε	Coefficient of variation
λ	(Power component's) Fault rate
λ_c	Constant failure rate
λ_{eq}	Equivalent failure rate
τ	Tolerance of MCS
$A(t)$	Availability (over time)
B	Susceptance
$CNT_{(k>n)}$	Total number of customers experiencing more than n interruptions
d	(Power component's) Repair time
d_{eq}	Equivalent mean repair time
E_{ik}	Expected energy interrupted when power component i fails
I_0	Transformer's primary no-load current
$I_{3ph-rms-break}$	Short circuit 3-ph symmetrical current
I_C	Transformer's primary core loss current
I_m	Transformer's primary magnetising current
I_{NOM}	Nominal current
I_p	Constant current coefficient for active power
I_q	Constant current coefficient for reactive power
Iz_{ph}	Maximum phase current
m_i	Number of failures experienced by power component i
n_p	Coefficient of active power exponential load model
n_q	Coefficient of reactive power exponential load model
N_T	Total number of customers served
n_T	Transformer's phase voltage ratio
P	Active power
P_{IRON}	Transformer's core loss
p_k	Probability of power outage
P_o	Nominal/rated active power
P_{PVagg}	Power output of the aggregate photovoltaic MG model
P_p	Constant power coefficient for active power
P_q	Constant power coefficient for reactive power

P_{WTagg} Power output of the aggregate wind-based MG model
PF_1 Displacement power factor
Q Reactive power
Q_o Nominal/rated reactive power
R Resistance
r Average outage duration
R_0 Zero-sequence resistance
R_1 Transformer's primary resistance
R'_1 Transformer's primary resistance, referred to the secondary winding
R_2 Transformer's secondary resistance
R_{FE} Transformer's core resistance
r_i Interruption restoration time
R_{LV} Resistance of 11/0.4kV transformer on LV winding
$R_{Neutral}$ Resistance of neutral conductor
R_{ph} Phase resistance
R_{TOT} Transformer's total resistance
S Apparent power
S_{BASE} Base apparent power
S_{irr} Solar irradiance
S_i Apparent power interrupted
S_{NOM} Nominal apparent power
S_{SC} Short circuit apparent power
S_T Total installed apparent power
T_k Time interval of undelivered energy
U Unavailability
V RMS supply voltage
v Input wind speed (wind turbine model)
V_n Nominal voltage
V_o Nominal/rated rms supply voltage
W Watts (active power)
W_{cu} Transformer's load loss
w_i Number of interruptions experienced by customer i
X Reactance
X_0 Zero-sequence reactance
X_1 Transformer's primary reactance
X'_1 Transformer's primary reactance, referred to the secondary winding
X_2 Transformer's secondary reactance
X_{LV} Reactance of 11/0.4kV transformer on LV winding
X_M Transformer's magnetising reactance

X_{ph}	Phase reactance
X_{TOT}	Transformer's total reactance
Z	Impedance
Z_{BASE}	Base impedance
$Z_{eq,LV}$	Equivalent LV network impedance
$Z_{eq,MV}$	Equivalent MV/LV network impedance
Z_L	Line (OHL/cable) impedance
Z_p	Constant impedance coefficient for active power
Z_q	Constant impedance coefficient for reactive power
Z_{SYS}	System supply impedance
Z_T	Transformer impedance

Chapter 1

Introduction

The electricity grid infrastructure is currently experiencing a transformation in terms of system visibility and controllability, which will result in higher levels of system-user interactions, but will also increase overall system complexity by modifying current operating conditions. Moreover, the United Kingdom (UK) Government has committed to reduce overall carbon emissions by 80% by 2050 (relative to 1990 levels) [1], and to meet renewable generation targets of respectively 15% and 100% of the UK and Scottish demand for electricity by 2020 [2].

In order to achieve these targets, there will be a significant increase of small-to-medium size renewable-based distributed generation (DG) connected nearer to the points of consumption (i.e. at the distribution system level), a large-scale upgrade and replacement of transmission and distribution networks (including flexible energy storage (ES) facilities), and the introduction of new highly efficient smart technologies through automated control, monitoring and communication infrastructures [3, 4, 5]. The latter functionalities will serve as a base for the implementation of different demand-side management (DSM) schemes in actively managed distribution networks, which will help distribution network operators (DNOs) to alleviate network congestions, improve system performance and therefore provide lower costs for electricity customers (residential, commercial and industrial).

1.1 The Need for an Improved Quality of Supply Assessment

In future networks, existing analysis tools and methodologies will become inadequate for studying the increased dynamics of two-way power flows and higher levels of harmonic emissions, waveform distortions, direct current (dc) offsets and unbalances [6]. The calculation of short circuit currents and fault levels will become increasingly complex, while the contributions of distributed and end-user resources to voltage/frequency regulation and capacity evaluation must be included in the analysis [7, 8, 9]. Therefore, new methodologies and tools are necessary for the correct evaluation of system performance, where the load and system dynamic behavior should be analysed accurately enough to reflect the response of future plants and loads, when even a brief disturbance in power supply (e.g. voltage sag or short interruption) can lead to a plant or process shutdown or failure.

As a consequence of the aforementioned changes, one of the aims of this future network, so called 'Smart Grid' (SG), will be to increase reliability and power quality for the delivery of an uninterrupted and high-quality supply of electrical energy. However, there is currently no integrated methodology to predict or measure the effects of these changes on the overall system performance. The assessment of quality of supply (QoS) is usually undertaken as a combination of different power system studies in which the analysis of system and end-user performance is performed separately. Therefore, this approach requires additional analytical efforts as the outputs of these studies have to be post-processed and combined before the overall quality of supply can be assessed.

Quality of supply assessment is commonly performed using different power system analysis tools, including computer simulation software for power flow analysis, short circuit fault calculation, voltage/frequency regulation and protection coordination studies. However, these 'power system simulators' must be adequately updated with the models of recently introduced power components (i.e. DG or ES systems) and those expected to be employed in the future (i.e. DSM-enabled loads) to provide additional functionalities for the operation and control of smart electricity networks. Besides, they are not specifically designed or capable of performing an overall assessment of the quality of supply in large distribution networks.

1.2 Context for Quality of Supply Research

This PhD research is part of the EPSRC funded Grant EP/G052530/1 Project "Integrated Assessment of Quality of Supply in Future Electricity Networks", which was designed to propose a new methodology for the successful integration of reliability, power quality, security and other relevant aspects of quality of supply analysis in an all-inclusive procedure, including assessment of both system and end-user performance [10]. One of the aims of the project was to define a set of new indicators, capable of quantifying any improvement or deterioration of the quality of supply performance due to, for example, a change in system configuration, the installation of new components or upgrading of the old ones, and the application of new automation/control functionalities. This would allow for a direct correlation of the achieved benefits with the known or estimated costs of each applied action. In that way, a more accurate cost-benefit analysis and economic assessment tools can be applied in order to allocate the correct value to different planned or unplanned changes in the system and end-user assets, functions and services.

The existing quality of supply assessment procedures result in separate sets of indicators, where each set provides measures (i.e. numeric values) only applicable to either system or end-user performance [11, 12, 13, 14, 15]. In addition, reliability and power quality studies are currently performed independently, resulting in two different sets of data and indices, although they often describe phenomena or events with the same origin and impact on the

analysed power supply system [16, 17, 18]. Therefore, existing reliability and power quality indices were critically reviewed and used as a basis for introduction of new performance indicators. As each 'smart grid' component model became available from previously completed tasks in the EPSRC Project, it was implemented for the assessment of the effects each new technology would pose to the improvement/deterioration of the quality of supply performance. Consequently, similarities between different parts of the quality of supply analysis have been identified during the initial work of the project [10], and then investigated further to propose a robust and comprehensive methodology for their integration.

In order to obtain more realistic values for the calculated system indices, additional factors were introduced and divided in three general categories. The first category consists of system-related factors, e.g. type and length of circuits, supply voltage level and strength of the network. The second category takes into account user-related factors, e.g. load density, load peak power and load sector, while the third category reflects external data factors, e.g. annual variations in weather conditions and exceptional events, or differences in applied measurement/monitoring systems.

To answer all these challenges, this PhD research has concentrated on the development of improved numerical modeling and simulation tools and their use for the analysis of realistic distribution networks using high-performance computing resources. According to the rest of work streams in the EPSRC Project, this would create a fully applicable methodology for the correct analysis of future flexible and actively controlled electricity networks.

The first main objective of the proposed research (within the EPSRC Project context) was to integrate key elements of the dynamic analysis of distributed generation, MV/LV system and load contributions to the overall quality of supply performance in a numerical simulation model that can accurately resolve responses at different levels of accuracy (steady-state and transient analysis). The second main objective was planned to use this numerical simulation model to introduce and formulate a set of new reliability indicators for a more accurate validation and benchmarking of the overall system performance.

1.3 Research Objectives and Scope

The presented PhD work aims to extend the standard three-phase calculation engine in order to allow the implementation of multiple numerical software models offering new capabilities and distinctive properties for the correct assessment of quality of supply in future electricity networks. The proposed research has, therefore, been divided into four main streams of work in order to address all the issues previously defined.

The first work stream is designed to identify and develop missing power component models, update the existing ones, and apply them after identifying typical UK and European network

models. Therefore, a detailed database with typical configurations and parameters of electricity transmission/distribution systems is built. The aim of this work is to provide a set of generic models that can easily represent actual sub-transmission and distribution networks supplying a mix of residential, commercial and industrial demand, while allowing the efficient modelling and simulation of current and future power system functionalities. For different load sectors, from metropolitan to rural areas, detailed demand decomposition and generic network models are identified. Accordingly, detailed and updated specifications for all power components and relevant system loading conditions are collected based on data from UK/European DNOs and manufacturers of power equipment. This information is considered essential for steady state network analysis, such as active/reactive power flows, system losses, voltage profiles, etc., as well as for any network planning stage, where issues such as security and reliability of supply are of primary importance. *Publications arising from this research: [19, 20, 21, 22, 23, 24, 25, 26]*

However, due to their volume and complexity, LV and MV networks are often represented by lumped aggregate models in order to reduce computation times in power system analysis. These aggregate load models, which often provide only information on active and reactive power demands downstream the grid supply point (GSP), represent highly dispersed loads and, as the load aggregation proceeds from lower to higher voltage levels, more and more network components are being neglected. In addition, as most of the smart grid technologies and functionalities (DG, ES and DSM) will be implemented at lower voltage levels, this may have a strong impact on their possible benefits on quality of supply [27], as system faults within the lumped parts of the network are inaccurately assessed. Therefore, in order to avoid the underestimation of network's reliability performance at bulk supply points (BSP), a general methodology is developed for reducing system complexity by calculating the electrical and reliability equivalent models of LV and MV distribution networks. These equivalent models, based on the aggregation of individual component models, help to reduce calculation times while preserving the accuracy of the assessment of power system reliability performance. *Publications arising from this research: [19, 24, 26]*

The following work stream analyses the impact on relevant steady state, transient operating conditions, and quality of supply of active distribution networks, due to the inclusion of 'smart grid' component models, such as renewable-based micro-generation (MG) systems, ES and wide-scale implementation of DSM. Accordingly, this work is partly based on research collaboration with colleagues within the Institute for Energy Systems (IES), providing access to an updated library of load models, DG models and models of advanced ES. Some examples of the 'smart grid' component models used for network analysis include inverter-interfaced and directly-connected DG/MG technologies with and without ES. Also, for intermittent types of DG, data on availability of their primary energy sources is included in the analysis. Additional examples of the analysed models are the new types of end-user loads (with new typical load

demand curves), including plug-in electric vehicle (EV) chargers, modern non-linear power electronic equipment and demand-manageable loads. In addition, their aggregated counterparts (same and mixed-type aggregate DG and load models) are combined with the previously calculated network equivalent models (for different load sectors), in order to allow a simplified but still accurate analysis of the overall system-load-DG interactions and responses of several DG units (of different sizes and types) connected in the same part of network, or at the same supply feeder. *Publications arising from this research: [20, 21, 28, 29, 30, 31, 32]*

Finally, regarding the approach for reliability analysis of active distribution networks, analytical and simulation techniques (Monte Carlo Simulation (MCS) method) are employed to assess the frequency and duration of interruptions in the supply system for different 'smart grid' scenarios, considering a coordinated deployment of DG, ES and DSM. Recordings and contingency statistics related to the analysed network models are used as inputs for the simulation method, in which output reliability indices (e.g. SAIFI, SAIDI, MAIFI, CAIDI, ENS, etc. [33]) are expressed as probability distributions, rather than simple average values and standard deviations. Therefore, this study introduces a new methodology for quantifying in a most realistic manner the standard set of indices reported annually to energy regulators. Particular attention is given to continuity of supply of low voltage residential customers and potential scenarios to improve service quality by reducing the frequency and duration of customer interruptions. *Publications arising from this research: [22, 23, 25, 34]*

Conventional reliability assessment procedures are extended to include accurate reliability equivalent models, actual load profiles, and empirical (i.e. recorded non-uniform) fault probability distributions, allowing to make a clear distinction between short and long supply interruptions. Besides these modifications, the conventional Monte Carlo Simulation approach is modified in order to include UK security of supply legislation, which specifies required supply restoration times for interrupted customers. Different scenarios are considered in order to validate the proposed methodology and demonstrate its accuracy and applicability. *Publications arising from this research: [35, 36]*

1.4 Thesis Contributions to Knowledge

The results from this research have been jointly presented in 4 journal papers [28, 29, 35, 36] as a co-author of the main scientific work, and 12 international conference papers [19, 20, 21, 22, 23, 24, 25, 26, 30, 31, 32, 34], from which the author was the main/lead contributor to the published work in [20, 23, 25, 26, 34]. Part of this work, as a research collaboration within the IES, was awarded the Basil Papadias prize for best student paper at the IEEE PowerTech Conference 2011. In addition, the work was awarded with the best student presentation (runner up prize) at the 3^{rd} Durham "Risk and Reliability Modelling of Energy Systems Day" 2012, organised by the IEEE-PES UKRI Chapter.

Regarding the reliability stream of this research, the author also contributed (through workshop participation) to the production of the Electric Power Research Institute (EPRI) White Paper, published in August 2012, on *Bulk System Reliability Assessment and the Smart Grid* [37]. Moreover, a collaboration work with the UK Transmission Network Operator, National Grid (NG), over the summer 2012 resulted in one of the NG internal reports (July 2012): *The Probability of Faults and Trips on the UK Grid System* [38].

The main contributions (both as lead and co-author), and their associated publications, can be summarised as:

- Modelling of generic sub-transmission and distribution networks:
  - development of improved load and network aggregation methodology [19, 26].
- Investigation into the network influence of load models and 'smart grid' functionalities:
  - with locally connected micro-generation [20, 30, 31],
  - responsive demand scenarios [20, 21, 30, 32],
  - application of energy storage applications [20, 23, 25],
  - quality of supply in MV/LV distribution networks (power flows, system losses, voltage profiles, harmonic emissions, etc.) [20, 21, 31].
- Reliability performance assessment in smart grids:
  - improved Monte Carlo simulation method for application in future networks [22, 23, 25].
- Reliability equivalents of LV and MV distribution networks [24, 26]:
  - with energy storage and demand-side resources [25, 34].
- Risk assessment of interruption times affecting domestic and non-domestic electricity customers [35].
- Theoretical interruption model for reliability assessment of power supply systems [36].

In further collaborations with colleagues in the IES, the developed network and reliability models have also been applied for micro-wind generation analysis [28, 39], transmission level studies [29, 40] and load modelling analysis [41].

1.5 Thesis Structure

This thesis is divided into seven chapters, with additional material provided in the Appendices.

Chapter 2 provides the background and literature review for the thesis. First, the expected challenges for assessing quality of supply in power distribution systems are discussed, by providing an overview of the most widely used reliability metrics and concepts. A review of security and regulator-imposed requirements for supply restoration times is also presented, in combination with a comprehensive database with failure rates and mean repair times of network components. Moreover, several reliability case studies are provided with the analysis of actual component failure statistics and reliability performance of different European DNOs.

Chapter 3 contains information on the modelling of typical/generic sub-transmission and power distribution systems, and their equivalent representations at different network locations and voltage levels. First, the work focuses on the development of a comprehensive component database for network modelling, providing a wide range of specifications and parameters of actual power equipment. In addition, this chapter reviews the main principles of load modelling for power system analysis, identifies typical load structures at different residential subsectors, and proposes an aggregate residential load model for an accurate network design and operation.

In **Chapter 4**, the modelling, aggregation and analysis of distribution network equivalents is discussed. A novel approach is proposed for the calculation of public supply network impedances at different voltage levels. A methodology for aggregating LV and MV distribution networks, which enables the correct assessment of quality of supply at bulk supply points including microgeneration models and distributed generation/storage functionalities, is presented and validated. Accurate electrical and reliability equivalent models are formulated for different distribution networks and load subsectors.

Chapter 5 describes the main reliability criteria and techniques used in this thesis for the calculation of system and end-users' reliability indices. The conventional Monte Carlo Simulation method is modified with the inclusion of actual load profiles, the use of different input probability distributions, as well as the impact analysis of time-varying failure rates of network components. The uncertainty and convergence of the resulting reliability indices is also discussed, in combination with a study of multiple-fault occurrence. Finally, a new theoretical outage model is introduced for assessing more accurately the moment in time when interruptions of electricity customers are likely to occur.

The applicability of the proposed Monte Carlo simulation algorithm, including different network functionalities and equivalent models, is assessed in **Chapter 6** for an integrated reliability analysis of active distribution networks (i.e. "smart grids"). A reliability deterministic approach is undertaken in order to acknowledge the protection of electricity customers from extremely long outages. The integrated time-sequential methodology is used to assess the potential improvements that different demand-side management and energy storage schemes could have on the frequency and duration of customer interruptions.

Finally, **Chapter 7** reviews the main results of the thesis, and discusses the implications of the results as they apply to network quality of supply assessment. Lastly, suggestions for future research work and final conclusions are provided.

Chapter 2

Network Reliability and Power Quality in Perspective

This chapter discusses the background, literature review and new challenges related to the two general concepts that define QoS in power systems: *reliability* and *power quality*, by defining all the relevant terminology as used in this thesis. This is followed by an overview of the most widely used metrics for assessing QoS in power distribution networks, with consideration to new available reliability concepts. A review of security and regulator-imposed requirements for supply restoration times is also presented, focusing on the applicability of this concept to the reliability analysis of both sustained and temporary system outages. In addition, a comprehensive database with failure rates and mean repair times of network components is provided, building the base for modelling their different operation modes for reliability assessment. The final section of this chapter presents the analysis of the actual component failure statistics and reliability performance of different European DNOs and transmission system operators (TSOs), considering several reliability case studies.

2.1 Introduction

Deregulation and competition in the electricity market put a significant pressure on generators, network operators and power suppliers to improve quality and reliability of the services they provide. Failure to deliver electrical energy on promises of better quality and higher reliability can result in severe financial penalties and, more importantly, may affect their ability to gain new and keep existing customers [42]. Accordingly, Energy Regulators impose annual reliability and continuity of supply targets for the frequency and duration of customer interruptions.

The reliability performance of supply systems is quantified through a series of indices, which varies from one country to another. In most European countries and the United States (US), DNOs report the reliability performance of their networks using the energy not supplied (ENS) index [43] and indices defined in accordance with [33]: system average interruption frequency index, SAIFI; system average interruption duration index, SAIDI; and momentary average interruption frequency index, MAIFI. The main difference is in the defined duration of long interruption (LI)-in Europe is at least three minutes [44], whereas one minute duration limit is

used in the US [33]. In the UK, DNOs report to the Regulator (Office of Gas and Electricity Markets, OFGEM) two reliability indices for which targets are established [45]: customer interruptions (CI) and customer minutes lost (CML), which basically correspond to SAIFI and SAIDI indices. Further details are given in Section 2.3, providing information on the calculation and definition of quality of supply indicators. In addition, the UK DNOs report to OFGEM the number of short interruptions (SI), although there are currently no specified targets for them.

Recent statistics suggest that current planning strategies are not always successfully implemented when reliability network performance is assessed, even though DNOs may be confident with the methods they use. For example, more than 14% of DNOs have recently been penalised in the UK for not achieving the specified CI limits, whereas 50% of them have not been able to meet the CML targets [27]. In addition, further development of highly sensitive electrical and electronic loads will have a big influence on load and power supply responses to different steady state and transient disturbances [46]. Therefore, power quality disturbances, until now not considered to be as severe as reliability-related events, must be included in the analysis of the overall system performance. For example, the effects of voltage sags or short interruptions on modern continuous and automated processes are often as detrimental as the effects of outages and long interruptions.

Nevertheless, power quality (PQ) has only been partially considered as part of QoS studies until now [47]. Current regulation considers voltage, frequency variations and maximum restoration times, while other issues such as voltage sags, voltage swells, or short interruptions, are neglected. Recently, the importance of new and additional PQ performance indicators has been considered in the UK with the new introduction of mandatory monitoring and reporting on the number of SI, which is also being widely adopted within the European Union (EU). This clearly signals the beginning of a more comprehensive regulation of the overall quality of supply performance and confirms the need for the proposed research.

2.1.1 Costs of Reliability

Another relevant issue for the analysis of quality of supply is the fact that the level of system reliability is interrelated with the economic aspects [48]. A certain amount of investments are needed to obtain an optimal reliability level. Accordingly, in order to undertake an appropriate estimation of system's reliability and economics, it is always necessary to compare the cost required to reach a certain level of reliability with the potential benefit to be obtained from it. The basic concept can be easily illustrated by using the costs curves in Figure 2.1, which shows the increasing trend that investment costs must follow if an increased reliability is desired for the energy supply to consumers. On the other hand, the consumer cost associated with the power interruptions decreases as the quality of supply of the network increases. The total cost is therefore the sum of these two individual costs, showing a minimal point for which the "optimal" level of reliability is reached.

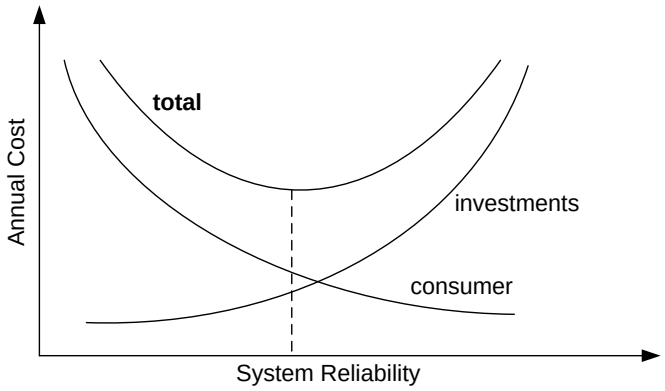

Figure 2.1: Costs according to reliability of the system [15].

2.1.2 New Challenges for the Power System Quality of Supply

Reliability performance is now a very important factor in the processes of designing, planning and operating electricity networks. The primary objective of DNOs is to increase the market value of the services by providing the right amount of reliability, and at the same time, provide lower expenses for customers. However, present distribution systems are designed such that performance of the MV and LV networks have a dominant impact on the quality of service seen by the end customers. In the UK, it is reported that about 90% of CI and 97% of CML have their cause at voltages from 0.4 kV (i.e. LV) up to 20 kV (i.e. MV) [27]. Figure 2.2 provides a disaggregation of the number and duration of interruptions by the voltage level at which they occurred (according to the typical nomenclature used by DNOs to disaggregate the MV concept), which are classified as follows:

- 132kV
- Extra High Voltage (EHV) - voltages greater than 20 kV but less than 132 kV;
- High Voltage (HV) - voltages from 1 kV up to 20 kV;
- Low Voltage (LV) - voltages less than 1 kV; and
- LV Services - the service line connecting the electricity main to the distribution company's protection device situated upon the customer's premises.

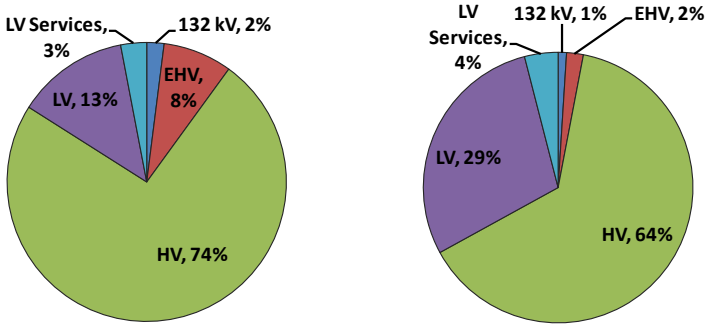

(a) Proportion of CI by Voltage (b) Proportion of CML by Voltage

Figure 2.2: UK average 2008/09 proportion of customer interruptions by voltage [27].

In order to alleviate this problem, the structures and operation of today's traditional distribution systems will feature an evolution through the fast development of new technologies and further deregulation of the electricity market. This will need an alteration and adaptation to the approaches for studying reliability. In existing literature, related analysis mostly concentrates on the operation, control and planning aspects of the new "smart grids", while their impact on, and potential for improving system reliability performance is less researched.

The changes in power distribution networks due to the new challenges of the electricity market can be summarised as follows [49]:

- the use of existing installations whilst avoiding excessive investments. Special attention is paid to minimising the operation and maintenance costs;
- the inclusion of uncertainties in the computer methods, thus, the probabilistic methods find more applications;
- the different appreciation of the reliability value amongst end customers. Some consumers would be willing to pay additional tariffs for a higher quality of supply.

2.2 Security and Quality of the Electricity Product

Security and Quality of Supply (SQS, as in e.g. [50]) denotes a general concept commonly used for the quantitative and qualitative analysis of the planning, operation and maintenance of power supply systems. SQS is a common denominator incorporating three main aspects into analysis: reliability (or continuity of supply), power quality, and (quality of) technical services, which are all of importance to both end-users (electricity customers) and power supply companies (DNOs), as well as to the other subjects involved with generation, transmission, distribution and utilisation of electrical energy. In the context of this thesis, however, reliability and power quality are seen as two aspects of the highest techno-economic interest, capable of providing comprehensive and factual information on the overall system/load performance. Customer services, which generally refer to the service quality provided to the electricity customers (i.e. connection, customer care, technical service, metering and billing), as the third element of the general SQS analysis, are not considered in this work.

2.2.1 Definitions and Quantities of Security

There are a number of important definitions and terminology related to quality of supply which should be given a preliminary attention. As the terms may vary in different texts [49], the terminology used in this thesis is defined as follows:

- *Customer/End-user*:

A customer or end-user is defined as a group of loads connected to the power supply system at a dedicated individual supply/measurement point. Accordingly, one electricity meter will determine one and only one individual customer. Individual customers can be further grouped or

aggregated, for example to represent aggregate system load at higher voltage levels. Moreover, aggregate clusters of residential customers connected at LV level, or commercial/industrial customers connected at both LV and MV levels, can be established, based on their aggregate load profiles.

- *Supply Interruptions and Outages*:

Outage can be defined as the total loss of supply (in all phases of a poly-phase supply system), which is a consequence of a physical disconnection of an end-user from the power supply system (e.g. after a circuit breaker/recloser opens). Outages may result from either planned (e.g. maintenance or servicing) or forced (e.g. lightning strike or component malfunction) actions and events [51], and are main subject of reliability analysis.

(Long) Interruption can be defined as either total or almost total loss of supply (i.e. zero or close to zero voltage in all phases of a poly-phase supply system), which is not caused by a physical disconnection of an end-user from the power supply system, but is a consequence of a de-energisation or a loss of supply voltage in the interconnecting system components. (Short) Interruptions are main subject of PQ analysis.

Disconnection can be defined as the process which physically separates two parts of a power system (e.g. a customer from a supply system, or a generating unit from a transmission system, etc.) for a generally undefined period of time. Accordingly, two normally connected parts of the system are disconnected when there is no electrical connection between them and no intentional flow of power or exchange of energy between them.

Incident/Fault is the consequence of a failure in the electricity network which can result in an interruption or outage of a customer or group of loads.

Failure is the suspension of the aptitude of a power component (PC) to achieve a necessary function. After a failure, the PC is found in a state of breakdown. A failure is a transition from one state to another, in opposition to a breakdown, which is a different state.

Breakdown is defined as the state of a PC unfit to achieve a required function. Lack of fitness due to preventive maintenance or other programmed actions or to a lack of external means is not included.

- *Outage Probability*:

Failure Rate is the probability that a PC loses its capacity to achieve a function during the interval $[t, t+dt]$, knowing that it functioned between $[0, t]$.

Repairing Rate is defined as the probability that a PC is repaired or replaced during the interval $[t, t+dt]$, knowing that it was broken down between $[0, t]$.

Operational Failure Rate is the probability that a PC refuses to change state when required to operate.

- *Voltage Sag and Swell*:

Voltage Sag or Dip is defined as a sudden reduction of the supply voltage magnitude between 0.1 and 0.9 p.u. of the nominal voltage, for a time period of 0.5 cycles to 1 min, according to [52], and from 10 ms to 1 min according to [44], during which the load remains connected with the power supply system.

Voltage Swell refers to a sudden increase of the supply voltage magnitude between 1.1 and 1.8 p.u. with a duration of 0.5-30 cycles for instantaneous variations, 1.1-1.4 p.u. and a duration of 30 cycles-3 s for momentary variations, and 1.1-1.2 p.u. and a duration greater than 3 s to 1 min for temporary variations [52].

- *Maintenance*:

Corrective Maintenance is carried out after detection of a breakdown and intended to put a PC in a state allowing it to achieve a necessary function.

Preventive Maintenance is carried out at predetermined intervals or according to prescribed criteria intended to reduce the probability of failure or degradation in the operation of a PC.

The computation of failure rate only considers the forced outages. Accordingly, the planned outages are not considered failures of power components and can be counted as preventive maintenance rate. Moreover, events such as extreme weather conditions, flooding or natural disasters are not counted by DNOs as customer interruptions, so are included in the category of exceptional events.

2.2.2 Definition of Reliability/Availability/Security

Continuity of power supply, when expressed and assessed as the ability of the power system components to perform their functions as intended (i.e. to operate normally), is known as *reliability*. As the occurrence of system faults and malfunctions of system components is inherently stochastic and unpredictable, reliability analysis involves concepts of probability and statistical theory, where both continuous and discrete variables should be used as inputs for the analysis.

Concepts like *availability* and *security* have usually been included in the reliability analysis as they are closely related. Therefore, a clear distinction between the actual meaning of reliability, availability and security analysis is initially needed. All three concepts are used for the analysis of a power system as a whole, but only reliability and availability can focus on individual network components (e.g. a generator or transformer). The results of reliability and availability analysis, even when defined for a particular network component, can be extended to the whole system, in order to observe whether the performance of the whole system is influenced by particular component(s) exhibiting poor reliability and/or availability. Although reliability and availability have different connotations, there is a mutual dependence between them, which involves another concept known as *maintainability*. A high reliability associated with a high

level of maintainability is usually translated into a high availability of component(s), or whole power system, when a global analysis is carried out.

Reliability, in its most general meaning, can be defined as the ability of a device or equipment to operate without interruptions for a time period specified by the manufacturer (usually equipment lifetime) under normal operating conditions. As mentioned, the reliability concept can be easily extended to the whole system, or part of it, which then directly introduces reliability analysis from the end-users/customers point of view. Accordingly, the North American Electric Reliability Council (NERC) defines power system reliability as "the degree to which the performance of the elements of the electrical system result in power being delivered to consumers within accepted standards and in the amount desired" [53]. Moreover, NERC considers that terms like *adequacy* and *security* are of major significance for reliability analysis.

Adequacy is defined as "the ability of the system to supply aggregate electric power and energy requirements of the consumers at all the times" [54]. Adequacy refers to static system conditions, e.g. for long-term planning and investment purposes. Accordingly, the concept of availability of generation and transmission resources/capacities can be analysed with respect to how they are meeting the demand during peak conditions, or what capacity reserves are available for various contingencies.

Availability ($A(t)$) can be defined as the total number of hours in which a system component, or the whole system is available, i.e. operates normally. Different formulas are often provided in the literature for availability. An example definition is [55]:

$$A(t) = \frac{\text{up time}}{\text{up time} + \text{down time}} \tag{2.1}$$

where: $uptime$ is the time for which the considered system component is in operation, and $downtime$ is the time when it is not operating (due to a fault, or servicing).

The studies of security enable to quantify the optimal compromise between the various quantities. To characterise reliability, in addition to the terms and probabilities defined previously, it is also possible to use average temporal quantities (see Figure 2.3).

In Figure 2.3:

- MTTF (*mean time to fail*): average time of good operation before the first failure;
- MTTR (*mean time to repair*): average time required for the faulted component to achieve the initial operational state;
- MTBF (*mean time between failures*): average time between two consecutive failures of a repairable system;
- MUT (*mean up time*): average time of good operation after repair;
- MDT (*mean down time*): average time of failure (time of detection of the breakdown, duration of the intervention, time of repair and time taken putting it back into operation.

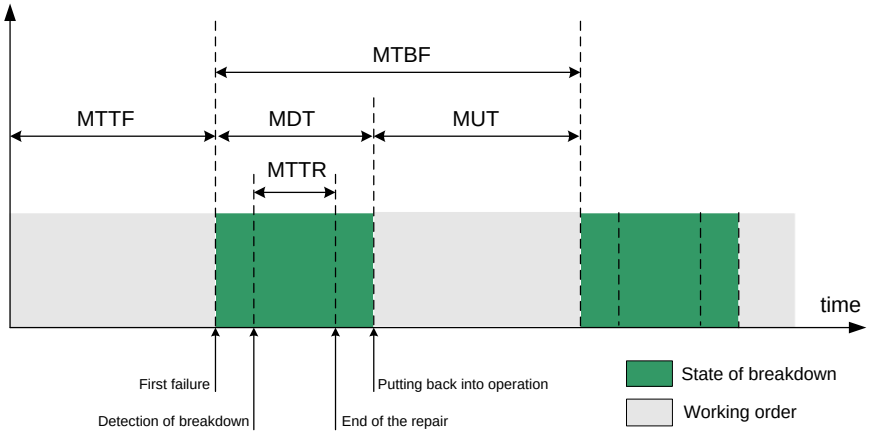

Figure 2.3: Diagram of average reliability times [49].

Another *availability* definition that uses the normal operation time of a power component, i.e. time between two failures, and the time for which the component is not able to operate normally, i.e. time during which the component is repaired ("two-times concept"), is given by [56]:

$$A(t) = \frac{\text{MTBF}}{\text{MTBF} + \text{MTTR}} \tag{2.2}$$

MDT incorporates MTTR and the time period before the fault condition becomes apparent and maintenance procedures begin. Nonetheless, MDT is applied in the computation of Formula 2.2 only in case of forced outages, while MTTR is considered for planned outages or maintenance. The availability calculation does not make distinction between forced and planned outages, so it can be defined to count both types of outages in its analysis.

Security is another concept defined and associated with reliability analysis, representing the ability of a power supply system to respond to disturbances/transient events without becoming unstable and/or resulting in faults that require disconnection of customers or not satisfying customers' supply requirements [15]. The term *security* is therefore associated with the system dynamics, occurring when the system moves from one state to another, typically within relatively short time periods. According to [54], security is "the ability of the system to withstand sudden disturbances".

2.2.3 Focus of Reliability Research

Reliability analysis should answer what parts of the system should be disconnected, and for what time periods, in order to isolate and clear a system fault, or repair faulted system component(s) causing supply interruption to customers. It is generally assumed that faults may occur anywhere in the system, and that a probability of any system component to get faulted can be expressed and quantified through the corresponding fault (or failure) component rates. When a system fault, or a system component failure results in the disconnection of some end-users' loads (i.e. outage of some customers), reliability analysis should answer what is the (expected) number of disconnected customers, the (expected) duration for which they are disconnected, and the (expected) amount of load or energy which is not supplied.

However, during the reliability analysis, self-extinguishing faults and faults cleared by automatic reclosing, as well as the other transient events (i.e. PQ-related events that do not result in sustained faults), are usually neglected. In other words, if supply to the end-users is disconnected (or disturbed) for a period of time shorter than a few minutes [1], the common practice is not to include it in the reliability analysis. This clearly confirms the need for the presented research, offering a general methodology capable of integrating both PQ and reliability aspects of power system analysis.

Moreover, in current reliability analysis, the specific characteristics of different customers are usually ignored (it is assumed that all affected end-users and load/equipment will stop to operate after an outage). Therefore, reliability analysis is mainly system-related, i.e. it mostly quantifies and describes "system performance", while "end-user performance" (particularly of individual end-users) has been less investigated. However, the new "smart" distribution networks will pose a big change to this situation, as end-users will start to have a more active position through the use of new functionalities, such as DG, ES or DSM applications. Accordingly, reliability indices, which have normally been considered to be system indices (and can be defined for the whole system, part of the system, or specific BSP) should be adapted to correctly measure the impacts of different "smart" scenarios on distribution networks.

The following definition of ***Reliability*** will be used in this thesis:

> *Reliability* can be considered as one of the critical elements of the analysis of a power system, as it emphasises the performance of the system as a consequence of the ability of individual system components to operate without interruptions and to assure a continuous supply of electrical energy to all end-users in normal operational conditions during the lifetime given for those power components or equipment.

---

1. Different durations are specified in different standards, e.g. 3 min in [44] and [45], and 1 min in [52].

2.2.4 Definition of Power Quality

Similarly to reliability, *Power Quality* (PQ) also denotes a general concept which includes different subjects and elements into analysis. In existing literature, PQ is defined in different ways, but, regardless of the definition, PQ also considers two sides of the power system: power suppliers and electricity customers. Accordingly, two primary areas of interest to the PQ analysis are the supply system (or network) performance on one side, and the end-user (or equipment/load) performance on the other [57].

It can be generally concluded that PQ considers the aspects of the power supply system which are not covered by the reliability concept. Therefore, PQ analysis includes transient events and phenomena that do not result in an outage and (full/physical) disconnection of the end-users' equipment from the supply system, but in the de-energising and loss of supply voltage for a limited time period (i.e. resulting in a short supply interruption). Based on that, PQ can be closely related to the quality of electricity as the "delivered product", i.e., to the level of acceptance of the electrical characteristics of a power supply system. Various standards (e.g. [44]) set tolerances and limits for electrical characteristics, but these limits are not always consistent with the levels of acceptance. Exactly that discrepancy is the main reason why there is no simple approach for dealing with PQ issues. Different end-users utilise different types of equipment in different ways and, accordingly, have different levels of acceptance and expectations of power quality. [2]

Dominant Concepts in PQ Definitions

There are two dominant concepts in existing PQ definitions, both derived from the definitions of *quality* as a more general category. The first concept is "user-related", and defines PQ with regard to the end-user satisfaction with the service provided. The International Organisation for Standardisation (ISO) defines *quality* as: "the ability of a product or service to satisfy user's needs". Similarly, the standard [58] defines *quality of service* as: "a collective effect of service performance which determines the degree of satisfaction of a user of the service". Also, the standard [59] defines quality as: "the totality of features and characteristics of a product or service that bear on its ability to satisfy stated or implied needs." The two keywords used ("user's satisfaction") are the main source of ambiguity in the related PQ definitions, simply because different end-users may have different "PQ expectations". These differences are mainly driven by the characteristics and ways of utilisation of the end-user's equipment, i.e. differences in the equipment susceptibility/sensitivity to various PQ disturbances. With these definitions, power quality is defined in a "relative" sense, assuming that PQ is "good or satisfactory" if there are no complaints from the particular end-user, i.e. when the end-user is satisfied with the

2. The operation of a power supply system in a way that it meets the requirements of the most sensitive end-users' loads is not an optimal solution because the overall costs of the distributed electrical energy for the majority of end-users will be far too high.

power supply conditions no matter how good or bad these conditions actually are. Also, this concept allows situations in which some end-users might be satisfied with a particular PQ level and some others not, even if connected to the same power supply system.

The second concept is "specification-related" and defines PQ as a measure of conformance to the specifications and tolerance limits related to the operation of the service provider. With this approach, PQ is defined in an "absolute" sense because the quantification of PQ is performed against the specified requirements, and not relatively or with regard to the satisfaction of particular end-users. This concept simply assumes that the predefined requirements may indeed represent "good" power quality, i.e. allow normal and intended operation of both power supply system and end-user's equipment. The main problem with the second concept is that there are always situations in which these conditions cannot be controlled or maintained, meaning that by this approach PQ can only be graded on a "negative" scale. [3]

Common PQ Definitions

In existing standards and literature, PQ definitions have different formulations and therefore different interpretations. Even the basic term, "Power Quality", has different formulations. Power quality (or part of it) is also denoted as: voltage quality, current quality, quality of supply, service quality, electrical energy quality, electromagnetic compatibility, quality of consumption, etc. The most often used PQ definitions are given in Table 2.1 below.

General PQ Definition for this Thesis

The PQ definition cannot be limited to the characteristics of the supply system, but must include the requirements related to the end-user's equipment and neighbouring equipment, i.e. the entirety of the *electrical environment* in which both delivery and utilisation of electrical energy are performed. That concept of power quality is adopted in this thesis, where the following general PQ definition is proposed:

> ***Power Quality*** analysis is related to the theoretical and/or experimental assessment, characterisation and quantification of all relevant ranges of mutual interactions between the supply system and end-users' equipment, which may be expressed either as a measure of conformance to declared specifications and limits, or against the sets of (individual) end-users' requirements, formulated in addition to the basic specifications.

In that sense, and especially from the day-to-day practice point of view, PQ can be most closely described as the *system compatibility* or compatibility between a power supply system and the end-users' equipment connected to it [6].

---

3. All the power supply characteristics cannot always comply with the allowed limits and tolerances, and even when these limits are violated, there might still be some end-users that are not affected by these deviations. Practically, this reduces the second concept of the power quality to the first one.

Table 2.1: Two approaches/concepts used in PQ definitions.

"Relative" or User-related PQ Definitions	"Absolute" or Specification-related PQ Definitions
-Concept of powering and grounding sensitive electronic equipment in a manner that is suitable to the operation of that equipment (and compatible with the premise wiring system and other connected equipment [52] and [60]. **-Ability** of a device, equipment or system to function satisfactorily in its electromagnetic environment without introducing intolerable electromagnetic disturbances to anything in that environment (electromagnetic compatibility [63]). **-Any problem** manifested in voltage, current, or frequency deviations that result in a failure or misoperation of customer's equipment [65].	**-Set of technical parameters** defining the properties of the power supply as delivered to the user (in normal operating conditions) in terms of continuity of supply and characteristics of voltage (symmetry, frequency, magnitude, waveform, etc.) [61]. **-Characteristics** of the electricity at a given point on an electrical system, evaluated against a set of reference technical parameters [62]. **-Estimation** of the deviation from specified explicit or implicit values of electrical energy supply, or from the aggregate supply criteria ensured by an electrical system [64]. **-Supply** that is always available within voltage and frequency tolerance, with a pure, noise free sinusoidal wave shape [66].
PQ refers to the wide variety of electromagnetic phenomena that characterise the voltage and current during a specified time period and at a given location on the power system [52] ("neutral PQ definition").	
PQ refers to the measurement process, analysis and improvement of voltage at the point of common coupling (PCC) in order to maintain a sinusoidal waveform [67] and [68] ("absolute PQ definition").	
PQ refers to a set of electrical boundaries defined to allow power equipment to operate in its specified limits without significant loss of performance or life expectancy [69] ("relative PQ definition").	

2.3 Metrics for Quality of Supply

Various (sets of) indices and indicators are used for quantifying, benchmarking, comparing and exchanging the information on (reliability and power quality) supply system performance, after which targets can be set or adopted for the further improvement and analysis of different operating and loading conditions of the system.

Usually, the SQS indices are grouped in different classes, according to the area of interest and target applications. There are indices which are defined and applied for the analysis of individual customers, site indices for smaller areas of the system or BSPs, and system indices used for the analysis of the whole power system [70]. Some indices can be formulated to characterise all these classes (individual, site and system), while others can only be applied to a particular class. Different SQS indices can also be classified based on the type of considered events and phenomena, or based on the information they measure. This may include number of occurrences, duration, effects and characteristics, or the quantity/parameter they are describing, e.g. frequency, voltage, current, power or energy.

In existing literature and practice, several (sets of) indicators have been proposed for the assessment and evaluation of power system reliability, i.e. reliability of generation, transmission and distribution sub-systems, including the assessment of supply interruptions/outages of end-users. A more detailed description and associated expressions of typical security indices, both related to the system and end-load assessment, can be found in [15], [48] and [71].

Power supply companies and DNOs are required by the Regulators to provide annual reports presenting a specified set of reliability indices, usually those that can be used to directly assess the number and duration of customer interruptions. Unfortunately, this set of indices is not defined globally, and varies from one Regulator to another. An example is the EU area, where each country uses its own set of reliability indices. A report on quality of electricity supply [43] presented by the Council of European Energy Regulators (CEER) provides a comprehensive list of reliability indices used by EU countries. However, indicators with similar computation procedures and formulas sometimes receive different labels or names from local Regulators. This is the case of the UK, for instance, where the number of customers interrupted and the duration of interruptions reported to the Regulator practically follow identical computation procedures as the set of indices considered by the DNOs in Germany, Italy, Norway, US, Canada, etc., which calculate the reliability indices according to [33], but are entitled differently. In order to simplify the EU regulation procedures, the European Energy Authority (EEA) should propose a unified and unique set of clearly defined reliability indices as well as the transparent procedures for their assessment and further use in practical applications.

2.3.1 Reliability Indices

Failure Rate/Outage Duration

Reliability performance of a power supply system is usually assessed using basic probability indicators [72], such as *failure* or *fault rate* λ (expressed in failures/year), average *outage duration* r or *mean time to repair* $MTTR$ (in hours/failure) and *unavailability* U (in hours/year), which are allocated to all system components, and then used to assess the reliability (i.e. probability of outage) of a whole system, part of the system, individual BSPs or customers:

$$\lambda = \sum_{i=1}^{N} \lambda_i \tag{2.3}$$

$$r = \frac{\sum_{i=1}^{N} (\lambda_i r_i)}{\sum_{i=1}^{N} \lambda_i} \tag{2.4}$$

$$U = \lambda r \tag{2.5}$$

where: N is the total number of system components, which, when faulted, cause an outage of a considered part of the system, BSP or individual customers, and where each component is represented with the corresponding fault rate λ_i and $MTTR_i/r_i$.

Generating Capacity and Loss of Load: LOLE/LOEE/LOLP

Another set of reliability indices considers the effects of system outages and interruptions on the supplied load (frequency: how often the supply is disconnected, amount: what is the total disconnected load, and duration: for how long the supply is interrupted). This illustrates the importance of having accurate information on actual system loading conditions and using correct load models in simulations. For their calculation and assessment, a simple load model is used, usually given by the daily peak load for a whole year [15]. The daily peak loads (expressed in Megawatts (MW)) are arranged in descending order to form a cumulative load model known as the *daily peak load variation curve* (DPLVC). When the hourly load values are available (e.g. 24 average hourly load values for each day in a year), the *load duration curve* (LDC) [4] may be applied for reliability analysis. Figure 2.4 illustrates an example of a specific UK 33/11 kV substation supplying a rural area with an approximated demand of 8 Megavolt Amperes (MVA).

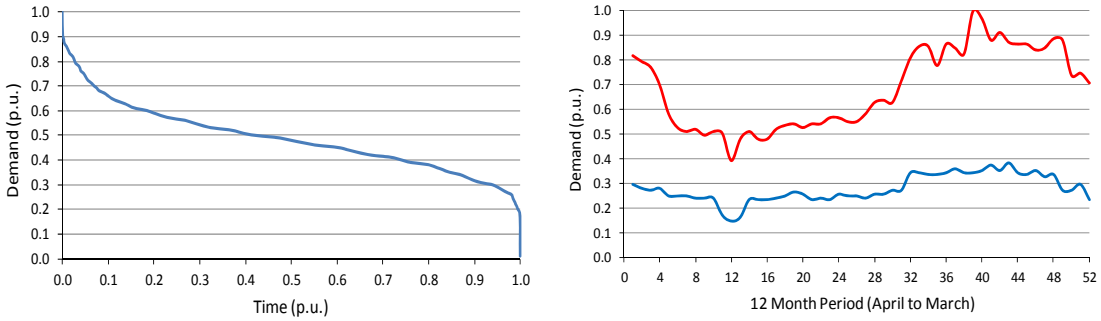

(a) substation load duration curve (LDC)

(b) substation maximum/minimum demand

Figure 2.4: Annual demand and LDC of a 33/11 kV substation in the UK [73].

The area under the load duration curve is the energy demand (in Wh) for a given time period. Whenever the active power (P) supplied by the system is lower than the required maximum demand, this difference will correspond to both the power not supplied and *energy not supplied* (ENS) over the considered time period.

Based on load/demand curves, two classical reliability metrics have been introduced in [11]. The first one is *loss of load expectation* (LOLE), which is defined in accordance with the DPLVC as the average number of days for which the daily peak load is expected to exceed the available system/generating capacity (plus primary generation reserve) given in MW. LOLE is obtained in days/year, but it can be computed in hours/year if LDC is available. Any outage of a generating capacity which is lower than available generation reserve (e.g. primary or running/spinning reserve) does not contribute to the computation of LOLE index, as the required demand will be supplied by the back-up generation within the minutes (for the UK,

4. **Demand at or above:** Demand level, in per unit (p.u.) of annual maximum demand. **Time:** Period of time during which the demand equals or exceeds the corresponding level, expressed in p.u. of one year (8760 h).

this primary reserve is set at around 1.32 Gigawatts (GW), while the peak UK demand is about 58 GW [74]).

The second loss of load-related index is *loss of energy expectation* (LOEE), expressed in MWh/year and based on the LDC. LOEE is defined as the expected ENS by the generating units, when the demanded P exceeds the available generating capacity in a given time period. *Expected energy not supplied* (EENS) and *expected unserved energy* (EUE) are equivalent variants to LOEE index [12] and [75], and are used in the literature with the same connotations.

Considering either DPLVC or LDC with the power demand W and the time T_k corresponding to the ENS_k by the available generation, LOLE and LOEE indices are given by [11]:

$$LOLE = \sum_{k=1}^{K} T_k p_k \tag{2.6}$$

where: K is the total number of time intervals T_k in which undelivered energy has been recorded, and p_k is the probability assigned to any k^{th} outage. This index provides the expectation of load loss in time units for a considered period of analysis. Similarly, LOEE only gives the expectation of energy loss:

$$LOEE = \sum_{k=1}^{K} ENS_k p_k \tag{2.7}$$

Accordingly, the *energy index of unreliability* (EIU) can be easily extracted:

$$EIU = \frac{\text{LOEE}}{W} \tag{2.8}$$

and then the *energy index of reliability* (EIR):

$$EIR = 1 - \text{EIU} \tag{2.9}$$

The main disadvantage of the LOLE metric is its inability to assess the severity of the outages, i.e. to distinguish between small or large load outages, and their corresponding frequency. Rather than being "load-weighted" in nature, instead, LOLE focuses on the loss of load duration. On the other hand, the available generating capacity considered in the calculation of LOLE and LOEE indices does not include the requirements of dynamic and transient system disturbances [76]. Instead, they measure the capability of the system to meet its load/demand requirements in a designated probabilistic state (i.e., including generating unit size, availability, load shape or uncertainty [15]). LOLE and LOEE are merely indicators which characterise a static state of a system, excluding from the analysis the dynamic behaviour of the power system.

Another probabilistic index is *loss of load probability* (LOLP) [12], which is defined as the probability that in a given time period, the available system generation, including the spinning reserve [77], cannot meet the actual load demand. When that happens, network operators must decide which loads need to be disconnected from the supply. For that purpose, well-defined load shedding schemes are usually recalled by DNOs and TSOs [78]. The actual load which must be shed is usually located on the distribution side of the system and is determined according to actual power flows, voltage profiles, overloading of system components and the required demand reduction needed to maintain system stability. For that purpose, DNOs sometimes intentionally reduce the supply voltage during an emergency condition, in order to cause undervoltage equipment tripping, and in that way perform an alternative voltage-regulation-caused load shedding (without physical disconnection of loads).

However, LOLP indicator does not provide information on the severity of an outage event, since it is not able to estimate what (amount of active) power is actually not supplied after the interruption [12].

Power Distribution: Sustained Interruption Indices

The reliability performance of power distribution systems can be evaluated using indices that estimate both frequency and duration of interruptions and outages. *System average interruption frequency index* (SAIFI) is one of such indices, defined as the average number of sustained interruptions (a type of long interruptions with a duration greater than 1 min [33]) per customer, recorded during a specific time period (e.g. a year). SAIFI is expressed in interruptions/customer/year as:

$$SAIFI = \frac{\text{Total number of customers interrupted}}{\text{Total number of customers served}} \tag{2.10}$$

Regarding the duration of outages, the *system average interruption duration index* (SAIDI) provides the average duration of interruptions in hours per customer during a designated time period (e.g. a year). SAIDI is expressed in hours/customer/year and is given by:

$$SAIDI = \frac{\sum \text{Customer Interruption Durations}}{\text{Total number of customers served}} \tag{2.11}$$

SAIFI and SAIDI can be directly compared with the failure rate λ and unavailability U respectively, when the total number of customers affected by all the considered interruptions is supplied by the same power equipment stated in an outage condition (e.g. all customers are connected at the end of a radial feeder with a series connected transformer). In this case, SAIFI and λ have the same value expressed in events/year, as well as SAIDI and U in hours/year.

Additionally, the *customer average interruption duration index* (CAIDI), in units of hours/customer interrupted, defines the average time required to restore the service:

$$CAIDI = \frac{\text{SAIDI}}{\text{SAIFI}} = \frac{\sum \text{Customer Interruption Durations}}{\text{Total number of customers interrupted}} \tag{2.12}$$

A variant of CAIDI is the *customer total average interruption duration index* (CTAIDI), as given by 2.12 for CAIDI, but where the customers with multiple interruptions are counted only once. Also, the *customer average interruption frequency index* (CAIFI) indicates the average frequency of sustained interruptions for customers affected by such interruptions:

$$CAIFI = \frac{\text{Total number of customers interrupted}}{\text{Total number of clusters interrupted}} \tag{2.13}$$

where: "clusters" represents a group of customers connected at the same point (PCC) and considered as concentrated loads. In this case, the customer is counted once regardless of the number of times interrupted, therefore CAIFI emphasises the number of recorded interruptions once each customer included in the analysis has been interrupted. However, this indicator does not distinguish among the "worst", "average" and "best" served customers.

The last sustained customer metric considered is the *average service availability index* (ASAI), defined as the time, in percentage, for which a customer has been supplied. ASAI can be calculated using SAIDI index:

$$ASAI(\%) = \frac{\text{Customer hours service availability}}{\text{Customer hours service demand}} = \frac{8760 - \text{SAIDI}}{8760} 100 \tag{2.14}$$

where: the customer is assumed to be connected 8760 hours a year. Otherwise, the number of hours the customer is connected to the supply system has to be specified.

SAIFI and SAIDI are usually applied for the reliability assessment of residential, commercial and industrial customers. However, these two indices present a disadvantage for differentiating between classes of customers (i.e. different load sectors, customers' load profile, etc.) or aggregate customers, where the aggregation has been done for the same type of customers. Accordingly, these indicators "weight" different customers equally, even though, for instance, one customer may represent a large industrial load (in the MVA region) and others may pose a small residential load (in a few kVA range). All customers, regardless of their size, are usually represented in the same way during the computation of SAIFI and SAIDI indices, as these indicators only compute the frequency and duration of power outages affecting all range of customers.

UK QoS Regulation: CI/CML

One of the main objectives of DNOs, particularly with respect to the requirements of the Regulators, is to reduce the number of CI and CML [79]. Interruption of customer supply can be caused by several factors, including automatic or manual actions to reduce the enhanced stress produced by system outages. The intentional automatic or manual tripping of a load or group of loads due to a lack of generating capacity or overloading of system components after a detrimental change that occurred in the power system (e.g. after a fault) is called *load shedding* [80]. Therefore, the adequate load shedding schemes can lead to improvements in the results of reliability indices like CI and CML. Different scenarios will be presented in this thesis in order to assess the potential benefits that load shedding and DSM schemes could bring to the reliability performance of electricity distribution networks.

The CI index, which is calculated per 100 customers, is the annual number of electricity customers affected by interruptions of the power supply longer than or equal to 3 minutes (long interruptions in the UK) [44]. The CI index excludes repetitive interruptions of the customers during the same incident, so these interruptions are counted as re-interruptions (RI) of the supply. Therefore, the number of customers interrupted per year can be calculated as in [45]:

$$CI = \frac{\text{The sum of the number of customers interrupted for all incidents}}{\text{Total number of customers}} 100 \tag{2.15}$$

where: the total number of customers includes all electricity customers whose supplies are connected to the DNO's distribution network. CI is calculated in the same way as SAIFI but expressed as the number of interruptions per 100 customers per year.

In addition, CML is the duration of long interruptions of power supply per year and is calculated as the average customer minutes lost per customer per year. CML has its similar equivalent in [52], namely SAIDI (given in hours), hence CML is given by [45]:

$$CML = \frac{\text{The sum of the customer minutes lost for all restoration stages for all incidents}}{\text{Total number of customers}} \tag{2.16}$$

Another metric is provided by [45] to quantify the number of customers re-interrupted per 100 customers per year:

$$RI = \frac{\text{The sum of the number of customers re-interrupted}}{\text{Total number of customers}} 100 \tag{2.17}$$

It should be noted that Regulators (e.g. OFGEM in the UK) often use CI and CML indices, or other indices with equivalent meaning and characteristics, to establish annual performance targets and the corresponding reward/penalty schemes for network operators. In the UK, cus-

tomers with a three-phase LV supply (i.e. voltage below 1 kV) are considered to be interrupted when one or more of the three phases is down. Moreover, for three-phase customers connected to high voltage (HV) levels (i.e. voltages between 1 kV and 20 kV) and experiencing one of the three phases disconnected, it is assumed that two-thirds of customers connected downstream of the point of disconnection had their supplies interrupted [45].

Load-based Indices

Generally, load-based indices provide a better representation of the frequency and duration of customer interruptions. The evaluation with load-based equivalents of SAIFI and SAIDI is performed using the *average system interruption frequency index* (ASIFI) and *average system interruption duration index* (ASIDI).

ASIFI is used to measure the performance of power systems in areas that serve a relatively low number of customers with a large concentration of loads (e.g. industrial or commercial customers). Moreover, ASIFI focuses more on the load rather than on the customers affected by interruptions.

$$ASIFI = \frac{\sum S_i}{S_T} \tag{2.18}$$

where: S_i is the apparent power of the load interrupted, expressed in kVA, and S_T is the total installed apparent power, in kVA, served by the network operator.

On the other hand, ASIDI, expressed in hours/year, provides a better assessment of the reliability for large customers, but it requires information on the customer's load rather than information on the number of customers affected by the interruptions:

$$ASIDI = \frac{\sum r_i S_i}{S_T} \tag{2.19}$$

where: r_i is the restoration time for each interruption, given in hours.

Momentary Indices

All previously discussed reliability indices are usually used to evaluate the system reliability performance for long interruptions/outages (longer than 3 min according to [44] and [45], and 1 min according to [52]). The customers' sensitive equipment (e.g. different power electronic devices) is also affected by short interruptions, voltage sags and voltage swells. The *momentary average interruption frequency index* (MAIFI) takes into account momentary interruptions that

may affect various types of loads. However, and similarly to previous indices, e.g. SAIFI, MAIFI weights all customers equally regardless of their size:

$$MAIFI = \frac{\text{Total number of customer momentary interruptions}}{\text{Total number of customers served}} \tag{2.20}$$

There is a variant of MAIFI called *momentary average interruption event frequency index* ($MAIFI_E$) expressed as:

$$MAIFI_E = \frac{\text{Total number of customer momentary interruption events}}{\text{Total number of customers served}} \tag{2.21}$$

where: momentary interruption event can be defined as an interruption with a duration limited to the period required to restore the supply by an interrupting device, according to [33], or a short-duration voltage variation (momentary interruption) with the duration in the range of 0.5 cycles and 3 s, according to [52].

$MAIFI_E$ is used to distinguish between one or more interruptions recorded for successive events. For instance, a fault cleared by a circuit-breaker is exemplified in [81] to establish the number of interruptions counted by $MAIFI$ and $MAIFI_E$. When an event is characterised by a series of actions such as trip-recloser-trip again, and then a recloser lockout, $MAIFI$ would count two interruptions and $MAIFI_E$ only one. Therefore, the choice of using either $MAIFI$ or $MAIFI_E$ depends on the policy of each utility or Energy Regulator.

In case when a customer experience more than one interruption, the index called *customers experiencing multiple sustained interruption and momentary interruption events* ($CEMSMI_n$) is applied [52]:

$$CEMSMI_n = \frac{CNT_{(k>n)}}{N_T} \tag{2.22}$$

with $CNT_{(k>n)}$ representing the total number of customers experiencing more than n interruptions, and N_T the total number of customers served.

Regarding the regulation of short interruptions (SI), MAIFI is used by several European DNOs (e.g. UK, France, Hungary, Italy, etc.) to report the frequency of those interruptions with duration of 3 min or less [43]. Thus, a confusion is created because momentary indices are included in the reliability analysis, but some definitions of momentary interruptions refer to both reliability and power quality concepts when, for instance, according to [33], a momentary interruption is defined as the single operation of an interrupting device that results in a zero voltage value. This definition corresponds to the concept of sustained interruptions, which are characterised by a zero voltage magnitude and a duration greater than 1 min, given by [52].

However, a momentary interruption is defined by [52] as an interruption with a duration between 0.5 cycles (10 ms) and 3 s, and a voltage magnitude less than 0.1 p.u. In addition, the confusion persists as momentary interruptions are considered by European Regulators to be all SI with a duration of 3 min or less. Therefore, this lack of concordance between different international standards (even the same institution, e.g. IEEE) should be eliminated and a straightforward definition for momentary interruptions be provided.

Characteristics of Reliability Metrics for Network Performance Assessment

Table 2.2 presents a general overview of the standard reliability indices which are most commonly used for assessing the performance of electricity distribution networks under different operating conditions. Considering the different characteristics and factors of measurement for each of the indicators (i.e. defined by letters from A to K at the bottom of the table), it provides a classification of QoS metrics into different sub-categories as a function of time. For each subcategory (e.g. momentary, sustained interruptions, etc.), the table provides different factors and network characteristics (e.g. magnitude, duration, frequency, etc.) considered and measured by each indicator.

Table 2.2: Characteristics of reliability metrics for network performance assessment.

INDEX	**INTERRUPTION**				
	Momentary $[0.5cycles - 3s]$	**Temporary** $(3s - 1min]$	**Sustained** $(T > 1min)$	**Short** $(T < 3min)$	**Long** $(T \geq 3min)$
CI	-	-	-	-	B,D,F,G
SI	-	-	-	B,F,G	-
CML	-	-	-	-	A,D,E,F,G
RI	-	-	-	-	B,E,F,G
LOLE	-	-	A,I,J	-	A,I,J
LOEE/EENS/EUE	-	-	C,I,J	-	C,I,J
LOLP	-	-	C,I,J	-	C,I,J
SAIFI	-	-	B,F,G	-	-
SAIDI	-	-	A,D,F,G	-	-
CAIDI	-	-	A,D,I	-	-
CTAIDI	-	-	A,E,I	-	-
CAIFI	-	-	B,D,I	-	-
ASAI	-	-	A,D,F,G	-	-
ASIFI	-	-	B,D,G,I	-	-
ASIDI	-	-	A,D,G,I	-	-
MAIFI	B,E,F,G	-	-	-	-
$MAIFI_E$	B,D,F,G	-	-	-	-
$CEMSMI_n$	B,E,F,G	-	B,E,F,G	-	-
Availability	-	-	A,F,G,H,J	-	A,F,G,H,J
Unavailability	-	-	A,F,G,H,J	-	A,F,G,H,J
Failure rate	-	-	B,F,G,H,J	-	B,F,G,H,J
Repair rate	-	-	A,F,G,H,J	-	A,F,G,H,J

A: duration	E: multiple interruptions counted	I: end-user
B: frequency (No. of occurrences)	F: whole system	J: generation
C: energy/power	G: subsystem	
D: one interruption counted	H: individual component	

2.3.2 New Available Reliability Concepts

Quantitative Reliability Metrics

A comprehensive evaluation of the system performance other than the conventional reliability-index analysis would make possible a reorganisation of the DNOs' strategies and policies on continuity of supply. The power and energy not supplied due to failures of the power components (PCs) are quantified as metrics which reflect the global state of the system.

The *power equipment not supplied* (PeNS), expressed in kW interrupted/failure/equipment, is defined as the ratio between the sum of the expected annual power interrupted by individual PCs and total number of PCs served by the DNO:

$$PeNS = \frac{\sum_{i=1}^{n} \frac{\sum_{k=1}^{m} P_{ik}}{m_i}}{n} \tag{2.23}$$

where n is the total number of PCs served, P_{ik} is the total active power expected to be interrupted when component i fails and m_i is the total number of failures experienced by PC i.

The *energy equipment not supplied* (EeNS), expressed in kWh interrupted/failure/equipment, is calculated as the ratio between the sum of the expected annual active energy interrupted by individual PCs and total number of PCs served:

$$EeNS = \frac{\sum_{i=1}^{n} \frac{\sum_{k=1}^{m} E_{ik}}{m_i}}{n} \tag{2.24}$$

where E_{ik} is the expected energy interrupted when PC i fails.

Moreover, the power and energy not supplied to individual or group of customers as a consequence of faults in the power system can be expressed by two quantitative customer-related indices. A first metric is *customer power not supplied* (CPNS), defined as the ratio between the sum of the total expected power not supplied due to customer interruptions and the total number of customers served by the DNO. *CPNS* is expressed in kW interrupted/failure/customer and is given by:

$$CPNS = \frac{\sum_{i=1}^{N} \frac{\sum_{j=1}^{w} P_{ij}}{w_i}}{N} \tag{2.25}$$

where N is the total number of customers served, P_{ij} is the active power expected to be interrupted to the customer i due to a failure in the system leading to the interruption j, and w_i is the total number of interruptions experienced by customer i.

The second customer-related index is the *customer energy not supplied* (CENS), expressed in kWh interrupted/failure/customer. *CENS* is calculated as the sum of the total expected energy not supplied due to customer interruptions divided to the total number of customers served:

$$CENS = \frac{\sum_{i=1}^{N} \frac{\sum_{j=1}^{w} E_{ij}}{w_i}}{N} \tag{2.26}$$

where E_{ij} is the energy expected to be interrupted to the customer i due to a failure that occurred in the system and led to the interruption j.

Annual Effective Time

A single metric, which combines the impact of the frequency and duration of momentary and sustained interruptions, is proposed in [82]. Practically it is a unified index which gathers different classes of interruptions including at the same time their frequency and duration. The effective time of each interruption experienced by a customer is therefore established. Accordingly, the *annual effective time* (AeT) of a single customer k experiencing n_k interruptions in a year is calculated as the sum of the effective times (T_e^i) of each interruption at a given location:

$$AeT_k = \sum_{i=1}^{n_k} T_e^i \tag{2.27}$$

The average value of the *annual effective time* of each interruption for a group of m customers is:

$$AeT = \frac{1}{m} \sum_{k=1}^{m} AeT_k \tag{2.28}$$

AeT index can be used instead of several reliability and power quality indicators as it provides the same information as e.g. SAIFI, MAIFI, SAIDI and CAIDI, but within a single value.

SAIFI/MAIFI Relative Cost Ratio

Regarding the economical assessment of power distribution systems, a cost model based on the relationship between the relative costs of momentary and sustained customer interruptions is introduced in [83]. The metric designated to represent the cost model is the *SAIFI/MAIFI relative cost ratio* (*SMRCR*). It expresses the estimated values of the ratio between the sustained interruption costs and momentary interruptions costs for various scenarios and time periods.

Furthermore, the combined *SMAIF* index, which quantifies economically both sustained and momentary interruptions, is given by:

$$SMAIF = SAIFI + \frac{MAIFI}{SMRCR} \tag{2.29}$$

SMAIF has been proposed to help the DNOs, based on the costs of momentary and sustained interruptions, at choosing the optimal operation for the several network protection schemes, for which 1 min or 3 min duration limit is relevant.

2.3.3 Power Quality Indices

As discussed before, the quality of the electricity supply at customer's PCC is characterised by two essential components: the supply continuity and the voltage quality (i.e. PQ), more precisely by the absence of deviation of a perfectly sinusoidal voltage source (constant frequency and amplitude) [47]. Therefore, power outages shorter than 1 min/3 min are also a problem of voltage quality, owing to the fact that they represent a reduction of its amplitude to zero. The associated problems can be divided into several categories: overvoltage, undervoltage, flicker, noise, transient, harmonic distortion and frequency fluctuations [84].

The indices described in the previous sections focus on reliability issues, where particular evaluation of short-duration variations (i.e. interruptions shorter that 1 minute, qualified as momentary interruptions) may result ambiguous. For example, a network fault may also result in voltage sags and SI occurring in the whole supply system, and thus being experienced by many end-users. The duration of these disturbances will be determined by the fault clearing times, and they may cause the tripping/malfunction of sensitive equipment, having the same or similar effects as the total disconnection of end-users.

Accordingly, a wide range of power quality metrics are used by DNOs for the assessment of voltage sags, voltage swells, SI, etc. (e.g. as in [85]). However, the QoS analysis in this thesis mainly focuses on the first component of the electrical energy quality: the continuity of supply at the consumer connection point, including some extra analysis on the relevant steady and transient PQ operating conditions of active distribution networks (provided in Chapter 4).

2.4 Security and Regulator-imposed Requirements for Supply Restoration Times

In addition to the analysis of planning, operation and maintenance of power supply systems, reliability and continuity of supply indices are also used for establishing regulatory targets, benchmarking and reporting system performance. For instance, the UK regulatory authority (OFGEM), considers the nature, frequency, duration and consequences (to the end-users) of supply outages in order to develop incentive scheme targets, i.e. penalty/reward schemes under the Guaranteed Standards (GS) [86] for the restoration of the interrupted supply.

In this way, the Regulator acknowledges a simple fact that the faults do occur in power supply systems, but it sets the standards and performance levels for dealing with them and for limiting their effects and impact on end-users. The GS require DNOs to compensate end-users in all cases when network reliability performance is lower than agreed, e.g. whenever the supply is interrupted to a higher number and/or size of customers for periods longer than the prescribed limits, considering also exceptional events such as severe weather conditions [87]. However, there are additional "per-event" requirements for the duration of each LI event resulting in

interrupted demands/customers, which DNOs have to satisfy according to the SQS legislation. These requirements are assumed to be part of the standard operating conditions of modern power supply systems, so DNOs do not get any reward for satisfying them, but may be penalized for failing to do so.

Accordingly, DNOs are rewarded when their overall/annual performance is above the agreed reliability levels, so the received incentives or penalties are based on the Interruption Incentive Scheme (IIS) when the network performance is improved or deteriorated. The proportion of revenue exposed under the scheme depends on each DNO's performance against their targets for CI and CML [88]. The annual targets specified by Regulators are based on historical reliability records and are related to the overall DNO performance with respect to all LIs and all affected customers in a given network. The minimum overall level of accuracy in the UK for reporting the number and duration of supply interruptions is set at 95% [45], allowing DNOs to omit from their reports the 5^{th} percentile of the worst served customers.

As each DNO's reliability performance and network characteristics (i.e. meshed or radial, urban or rural) strongly depend on the geographic location and supplied demand, the range of reliability indices reported by 14 UK DNOs (shown in Table 2.3 for year 2009) is used in the analyses presented in this thesis for the validation of the different reliability results. Accordingly, a highly meshed urban network will offer minimum values (increased reliability), while a radial rural system will present maximum values (poor reliability).

Table 2.3: Annual values of UK DNOs' reliability indices [27].

INDEX	UK DNOs' Reports		
	min	**mean**	**max**
SAIFI (interruptions/customer/year)	0.29	0.71	1.19
SAIDI (hours/customer/year)	0.57	1.09	1.84
MAIFI (interruptions/customer/year)	0.15	0.78	3.3

2.4.1 UK Security of Supply Requirements

After an interruption, the supply to electricity customers has to be restored within a specified period of time. Therefore, time limits are defined as maximum durations required by SQS legislation to restore at least a minimum group demand of customers. Accordingly, the network configuration, protection schemes and repair process of faulted network components are the main features which decide the duration of these interruptions.

Classes of supply are defined in [89] based on group demand ranges, for which the maximum allowed duration of interruptions is imposed, so that the minimum demand can be met. An example of how customers' supply should be restored within different periods of time is presented in Table 2.4 for the UK.

Six classes of supply (A to F) are defined on group demand (GD) ranges for which the max-

imum durations of interruptions and minimum demand that has to be met are specified. For example, if a group of customers with the power demand between 1 MW and 12 MW is interrupted, the supply must be restored to most of the customers in three hours' time. For the remaining interrupted customers within that group (with demand less than 1 MW), the power supply can be restored in accordance with the duration necessary to repair the faulted component which affected the customers (i.e. in repair time/MTTR).

Table 2.4: UK security of supply requirements for interrupted customers [89].

Class of Supply	Range of Group Demand (GD)	Minimum demands to be met after first circuit outage
A	GD$\leq$ 1 MW	In repair time: GD
B	1 MW<GD$\leq$ 12 MW	(a) Within 3 h: GD-1 MW (b) in repair time: GD
C	12 MW<GD$\leq$ 60 MW	(a) Within 15 min: minGD-12 MW; 2/3 GD (b) Within 3 h: GD
D	60 MW<GD$\leq$ 300 MW	(a) Immediately: GD-up to 20 MW (b) Within 3 h: GD
E	300 MW<GD$\leq$ 1500 MW	Immediately: GD
F	GD>1500 MW	According to transmission license security standard

Table 2.4 specifies the required limits for the supply restorations times, which are in most of the cases significantly shorter than the typical/published MTTR values of power components (see Section 2.5). It is important to note that each LI outside these limits (apart from exceptional events), and even though they do not accrue to specific penalties for DNOs, will progressively shift the overall network's reliability performance outside the specified annual targets.

The time-limit concept shown in Table 2.4 is used and presented in this thesis in order to quantify the effect of different network functionalities, such as the use of back-up supply or automatic/manual switching and reclosing. In addition, this methodology concept is fully transferable to e.g. a wide range of European countries with different SQS regulation and thus different supply restoration times to be met.

2.4.2 UK Regulator Requirements for Supply Restoration Times

The UK Regulator specifies additional requirements for the duration of customer interruptions in order to protect domestic/residential and non-domestic customers from excessive LI events. These requirements are introduced to protect those categories of customers that have no special contracts or agreements with DNOs regarding the duration of interruptions. The Electricity Standard of Performance Regulations [87] is the main UK statutory instrument which indicates the maximum admissible durations of interruptions for up to 5,000 customers and more than 5,000 customers. Table 2.5 presents these interruption time limits together with the corresponding penalties DNOs must pay directly to the customers (not to the Regulator), if supply is not restored within the specified period of time.

Table 2.5: UK regulator-imposed requirements for supply restoration times [87].

No. of Interrupted Customers	Maximum Duration to Restore Supply	Penalty paid to:	
		Domestic Customers	Non-Domestic Customers
Less than 5,000*	18 h	£54	£108
	After each succeeding 12 h	£27	£27
5,000* or more	24 h	£54	£108
	After each succeeding 12 h	£27	£27
*5,000 Customers correspond to about 12 MW Residential Load.			

2.4.3 Time to Restore the Supply After Temporary Faults

The classification of customer interruptions into SI and LI is not possible without, for instance, modelling the protection systems. A correlation between the type of faults, fault clearance times of the protection systems and applied network reconfiguration schemes is also required for a more accurate reliability assessment. For example, a permanent fault (LI) may result in a SI if the network can be reconfigured within three minutes (i.e. in Europe) to provide alternative supply to all customers, whereas a temporary fault (SI) may result in a LI when a manual/local intervention is required to restore the supply to the interrupted customers (e.g. to replace fuses at 0.4 kV busbars). Therefore, the calculated frequency of LI should also count temporary faults (SI) that result in LI due to the settings and characteristics of the protection systems.

The time to restore the supply to customers experiencing SI is estimated in this thesis based on the time settings of the protection and reconfiguration schemes applied for clearing temporary faults. Table 2.6 shows typical UK-based values of main network components [90, 91].

Table 2.6: Fault clearance times of typical UK protection systems [90, 91].

Network Component	Voltage Level (kV)	Protection System	Fault Clearance Time (s)
Overhead lines	11	Circuit breaker with auto-reclosing	10-120
	33	Circuit breaker with auto-reclosing	90
Cables	11	Circuit breaker with auto-reclosing	Up to 3
	33	Circuit breaker with auto-reclosing	90
Transformers	11/0.4	Fuse switches	Repair time
	33/11	Circuit breaker with auto-reclosing	0.15-10
	132/33	Circuit breaker with auto-reclosing	0.15-10
Busbars	0.4	Fuse switches	Repair time
	11	Circuit breaker	0.15
	33	Circuit breaker	0.15
	132	Circuit breaker	0.15

2.5 Power System Component Failure Rates and Repair Times

Reliability of a power supply system can be assessed statistically, based on the information on past system performance and use of historical data and records, or it can be assessed stochastically, based on a prediction analysis and use of probabilistic variables and parameters [92]. Therefore, the different procedures take into account available/collected data and records of outages (frequency, duration, causes, locations, consequences, etc.) that resulted in failures of system components and interruptions of supply to the end-users. This usually provides a clear identification of weak areas of a power supply system, what then can be used for reactive or proactive actions (e.g. system reinforcement or preventive maintenance).

Failure rates (λ) and mean repair times (i.e. MTTR) are two basic inputs of various procedures for reliability assessment. In available literature, reported values of these two input data vary in wide ranges (based on the type of network and type of component), which will have strong impact on the outputs of the applied reliability assessment procedures.

Accordingly, one of the first tasks of this PhD work was to identify physical parts of the modelled power systems (i.e. system components and their parameters), and to collect technical data and information necessary for their reliability analysis. Once this was available, a comprehensive database with failure/fault rates and mean repair times of all network components (e.g. overhead lines, power cables, transformers, switchgear, etc.) was created based on past recordings collected from two main sources: UK-related statistics (national aggregate data for five years) reported by the Energy Networks Association (ENA) [93] and statistics collected from the literature [94, 95, 96, 97, 98, 99, 100, 101]. Table 2.7 provides a complete sample of the processed data with statistics of λ and $MTTR$ values, which will be used for the reliability analysis of different distribution networks in this thesis. For those cases where data for specific power components is not provided in [93] (classified into 'urgent' and 'non-urgent' values), the corresponding values are taken from the literature data ('other sources').

Table 2.7: Failure rates and mean repair times for main network components [93, 94, 95, 96, 97, 98, 99, 100, 101].

Power Component	**Voltage Level** (kV)	**Failure Rate (λ)** (failures/km-year) for feeders (failures/PC-year) for other PCs		**Mean Repair Time ($MTTR$)** (hours)		
		ENA Report	**Other Sources**	**ENA Report**		**Other Sources**
				Urgent	**Non-Urgent**	
Overhead Lines	0.4	0.168	0.21	5.7		-
	11	0.091	0.1	9.5		-
	33	0.034	0.1	20.5		55
	132	0.0038	0.0104	19.1		55
Cables	0.4	0.159	0.19	6.9		85
	11	0.051	0.05	56.2	256.9	48
	33	0.034	0.05	201.6	338.4	128
	132	0.0277	0.022	222.7		128
Transformers	11/0.4	0.002	0.014	75	515.6	120
	33/0.4	0.01	0.014	205.5	542.6	120
	33/11	0.01	0.009	205.5	542.6	125
	132/11	0.0392	0.027	250.1		196
	132/33	0.0392	0.0193	250.1		116
	400/132	0.0392	0.0193	250.1		-
Buses	0.4	-	0.005	-		24
	11	-	0.005	-		120
	>11	-	0.08	-		140
Circuit Breakers	0.4	-	0.005	-		36
	11	0.0033	0.005	120.9	801.4	48
	33	0.0041	-	140	158.1	52
	132	0.0264	0.026	98.4		45
	275	0.0264	-	98.4		-
	400	0.0264	0.171	98.4		54
Switch Fuses	11	0.0004	-	35.3	385.4	-

2.5.1 Power Component Bathtub Curves and Models of Operation

Network components can be modelled in multiple ways for reliability purposes as they can often be broken up into different sub-components. For example, in the case of a single circuit breaker, it can also be regarded as several PCs, or different parts which can potentially cause a network outage (e.g. the measurement sensors, the electronic part which deals with control signals, or the mechanical part which opens the contacts). Therefore, one of the first requirements for network reliability modelling is to establish the choice for the power components to model.

Generally, the failure rate λ (and in the same context the repair time ($MTTR$)) over the expected lifetime of all network components follow the shape of a bathtub curve, as shown in Figure 2.5. The PC's failure rate and repair time are therefore higher during the "youth" and wear-out periods of the curve, showing the increased risk for a piece of equipment to be faulted when it is first put into operation, and then at the end of its lifetime (normally 40 years). The period in between is considered the useful life of the PC, characterised by intrinsic or random failures of the equipment.

In addition to the standard bathtub curve, Figure 2.5 presents a more detailed curve (i.e. the saw tooth bathtub) to represent the frequency of failures of a network component, as in this case the model represents an increased failure rate during the PC's useful life period. This is due to different periods of maintenance taking place in order to improve the network reliability performance. Accordingly, the standard bathtub curve is an approximation of the saw tooth bathtub curve, which models the average useful lifespan of the power component. This approximation is sufficient for most models, but a complete modelling must be adopted if different maintenance operations are included into the reliability analysis [47].

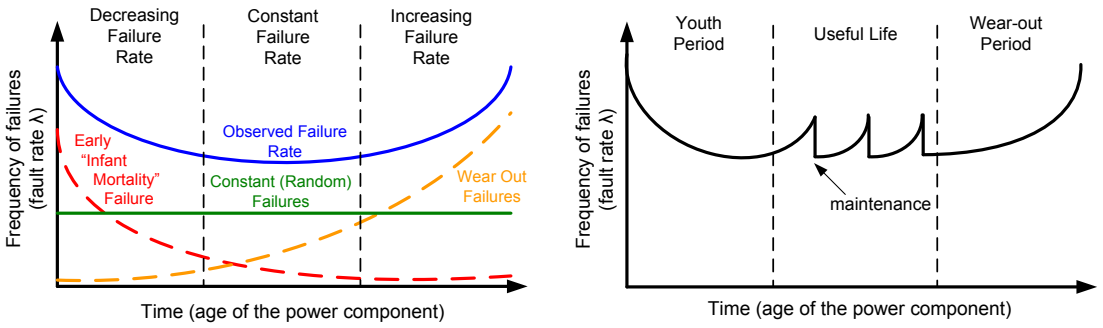

(a) Bathtub Curve

(b) Saw tooth bathtub curve

Figure 2.5: Bathtub curves for the risk of faults over a network component's lifetime [47, 102].

Also, in order to model the operation of the wide range of power components in the system, it is necessary to establish a model that represents the several operational stages of PCs (e.g. the simplest model is the one in two states). This concept is applied for the different reliability analyses presented in this thesis, and thus Figure 2.6 shows some examples of more complex models that can be employed with different classes of network components [49].

2.6 Analysis of Distribution Equipment Reliability Data

According to previous sections, one of the main efforts during this PhD work has focused on developing a complete database with component reliability data and its corresponding processing. However, the collection of data was characterised by significant variations in values from different power components, voltage levels (e.g. transmission or distribution part of the system), network location (i.e. load sectors ranging from metropolitan to rural areas), and even from the reliability performance of DNOs operating in the same or different country.

In order to better understand reliability data and their use for network performance assessment, this PhD work performed a detailed study and analysis of the existing component failure statistics and reliability performance of different European DNOs and TSOs. The studies show how utilities assess the performance of their electric power equipment. Accordingly, failure and interruption data have been collected and processed for the following DNOs/TSOs:

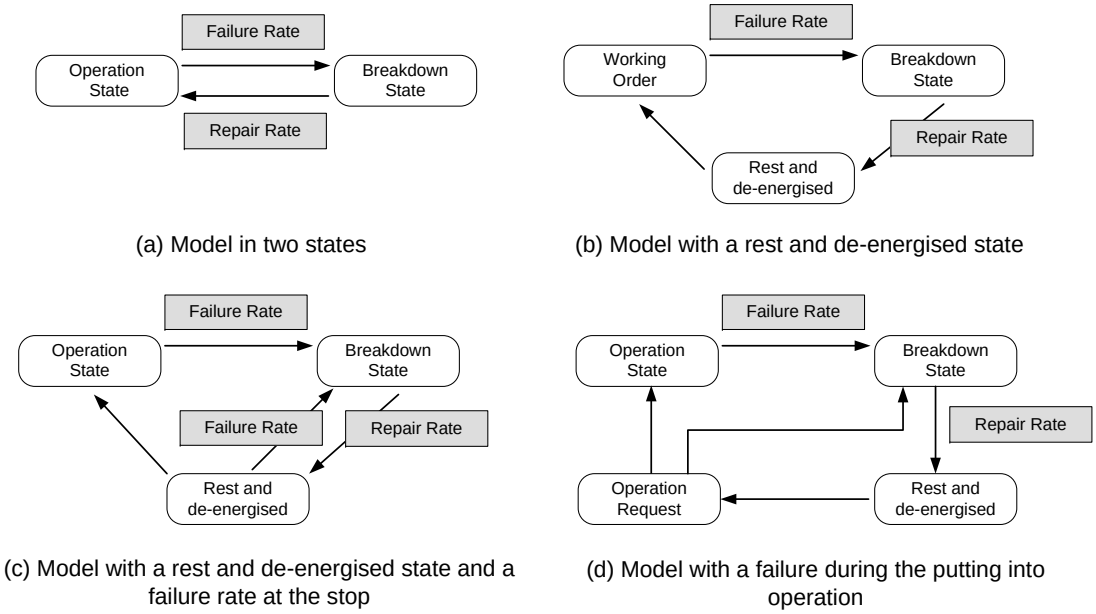

(a) Model in two states

(b) Model with a rest and de-energised state

(c) Model with a rest and de-energised state and a failure rate at the stop

(d) Model with a failure during the putting into operation

Figure 2.6: Operational models of power components [49].

- Swedish reliability performance - year 2010: 64 local networks;
- Scottish Power Energy Networks (SPEN) - Distribution reliability performance 2009/10;
- UK National Grid (NG) - Probability of faults and trips on the grid system - year 2012.

Nowadays, there is a need of providing a simpler and more efficient mechanism to show to electricity consumers how their DNO is performing, and consequently how it will address the new implementation of e.g. DG, ES and DSM functionalities within its distribution systems. Therefore, the aforementioned analyses provide a better understanding of how different electricity networks, for example operating in different countries or geographic areas (e.g. rural, sub-urban or urban sectors), present a significant variation on their reliability performance in terms of frequency and duration of customer interruptions. This comparison will enable to identify, considering differences in network design and environment, which DNO is performing over its maximum allowed limit of interruptions per year, and therefore should adopt a new policy for upgrading its network and provide a better quality of supply to customers.

The comparative data analysis is made on major categories of distribution equipment (e.g. power transformers, overhead lines, underground cables, etc.), main voltage levels, and also based on the type of outage causing customer interruptions (e.g. SIs, planned LIs, unplanned LIs, or even maintenance operations), which will derive into the overall reliability indicators annually reported by DNOs to the regulator. In this way, it is possible to identify what is the contribution from each factor to the total frequency and duration of interruptions. Due to the several influencing factors (including extreme weather conditions), component reliability data can exhibit significant variations. Thus, it is important to consider these influencing factors when estimating and using the reliability statistics for the risk analysis of distribution systems.

2.6.1 Reliability Case Study: 64 Swedish DNOs

This section provides a comparison analysis between the actual Swedish reliability data, published by the Swedish energy industry organization (Svensk Energi) to the national database (DARWin) in year 2010 [103], and the customer interruption recordings provided by 64 Swedish local DNOs. The data, which covers all system voltages (0.4 - 24 kV for distribution systems), is also divided into unplanned, planned and total long customer interruptions, with an additional section for short interruptions. In addition, the major distribution equipment categories are identified, including distribution lines and cables, transformers, fuse boxes, etc. Thus, this comparison serves as a good indicator of the aggregate customer impact.

Classification of Swedish DNOs into different network types

Once the annual interruption data from the 64 Swedish DNOs is processed (further details are provided in Appendix A), the resulting reliability indices (SAIFI, SAIDI and CAIDI) can be sorted from largest to smallest in order to roughly divide the 64 DNOs, according to their reliability performance, into three different network types. This classification is presented in Figure 2.7 below.

For this analysis, Table 2.8 provides past Swedish statistics, which are included in the last available version of the Swedish benchmarking report on continuity of supply [104, 105], covering a time period of ten years (1998 - 2008) for unplanned long customer interruptions in all local operating networks. Minimum, maximum and average values of the recorded reliability indicators over this period are used to classify the different DNOs into urban, sub-urban or rural networks. These limits have been accordingly included in Figure 2.7. As limits and average values for CAIDI index are not provided in the benchmarking report, they have been estimated using the values provided for SAIDI and SAIFI (e.g. $CAIDI = SAIDI/SAIFI$).

Table 2.8: Swedish regulator statistics for unplanned interruptions, sorted by load sector [105].

DNO Type	SAIFI (Interruptions/customer)			SAIDI (Minutes/customer)		
	Min	**Max**	**Average**	**Min**	**Max**	**Average**
Rural	1.00	2.08	1.65	101	1620	360
Sub-Urban	0.56	0.94	0.69	32	138	72
Urban	0.23	0.39	0.30	11	35	18
All Networks	0.58	1.29	1.00	54	890	194

There exists an overlapping in the maximum and minimum values for SAIDI indicator in the boundaries between network types (rural, sub-urban or urban). Therefore, a combination of minimum, maximum and average values has been considered in order to roughly classify the 64 DNOs provided. Regarding the use of CAIDI limits for network classification, average values are considered to establish the expected maximum thresholds, as no meaningful value was provided from maximum values for the classification.

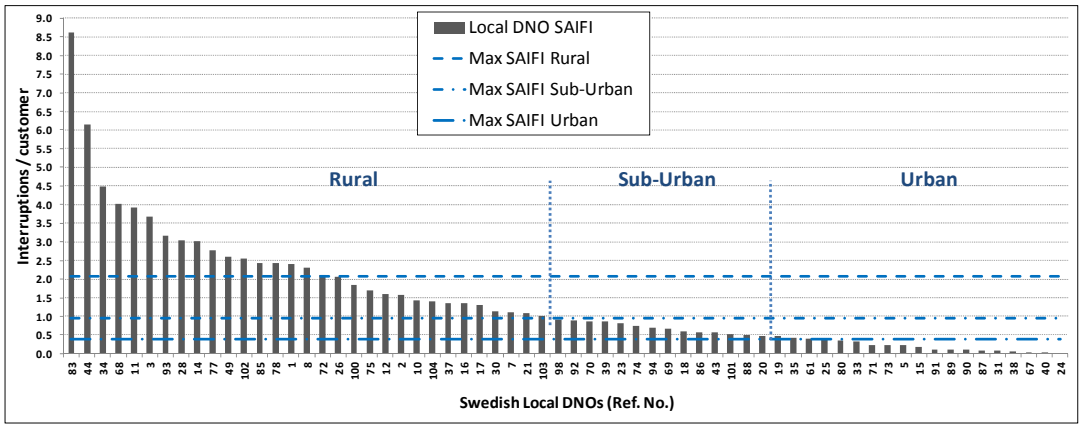

(a) Frequency of customer interruptions (SAIFI) per DNO – Year 2010

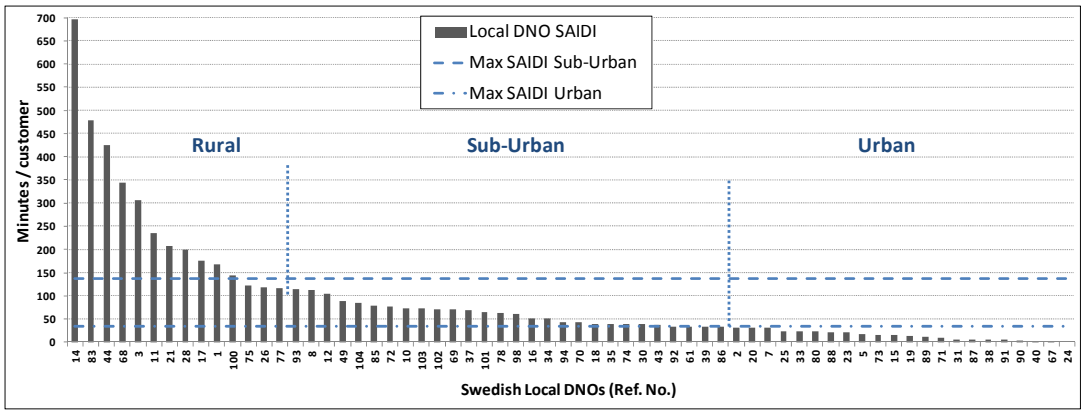

(b) Duration of interruption per customer (SAIDI) for each DNO – Year 2010

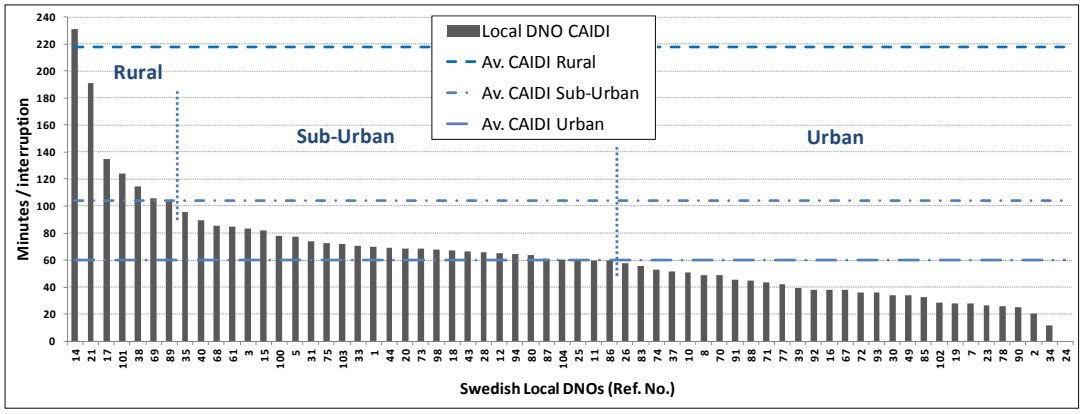

(c) Average duration of customer interruptions (CAIDI) per DNO – Year 2010

Figure 2.7: Classification of 64 Swedish DNOs into different load sectors.

For example, when one DNO is located within the rural limits in the three figures for analysis, there is a high certainty for the network to operate in a rural sector (the same analysis applies to sub-urban and urban sectors). This analysis can be effectively used by the Swedish DNOs

and Energy Regulator in order to compare and correlate each DNO's reliability performance with respect to the overall and own expected values. If for example, an urban network is operating with indicators within the limits of rural networks, that clearly means the DNO should improve its own performance and planning strategies. The same applies to DNOs, particularly those operating rural and radial networks, that see their annual reliability indices affected by extreme weather events and therefore cannot meet the maximum set reliability targets (as seen in Figure 2.7).

Further information and results on the Swedish DNOs' reliability assessment are presented at the end of this thesis, in Appendix A.1.

2.6.2 Analysis of SPEN Reliability Performance

As a prelude to the work presented in this thesis on network predictive fault performance (Chapters 5 and 6), in addition to a full database for load modelling, reliability data was provided by SP Energy Networks for the reporting year 2009-2010, covering the frequency and duration of customer interruptions in the Scottish electricity distribution system. This information was processed and directly correlated with the last 'Quality of Service Report' reported by OFGEM [27], in order to understand the configuration and linkage to the parts of the distribution networks where the incidents take place.

Part of the obtained results are presented in Figures 2.8 and 2.9, where a study of the reported number and average duration of unplanned LIs is provided, and Figure 2.10 with the corresponding CI and CML indices (sorted by voltage level and operating equipment) resulting from the raw reliability data provided. These results confirm the fact that the performance of MV and LV networks has a dominant impact on the QoS seen by end customers, and therefore affect the aggregate reliability indices reported annually to the energy regulator.

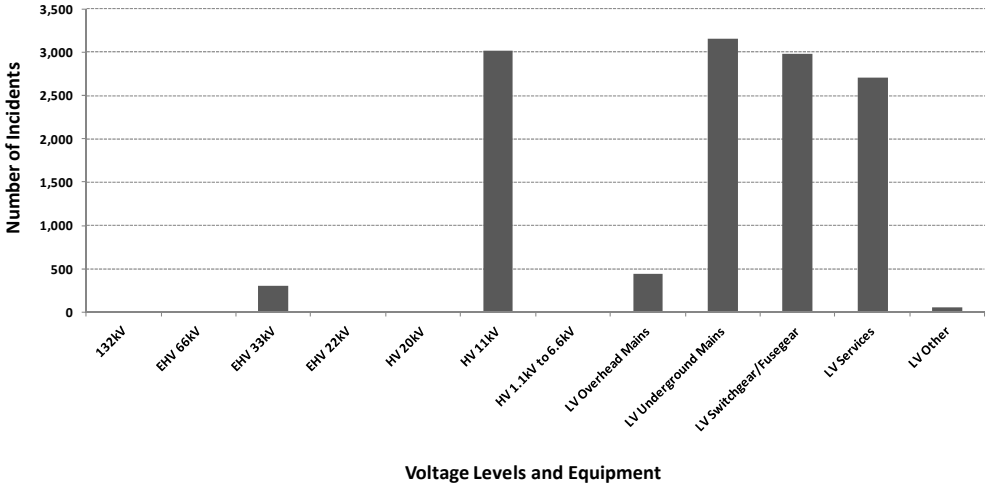

Figure 2.8: SPEN - Number of unplanned LIs by voltage level and equipment (09/10).

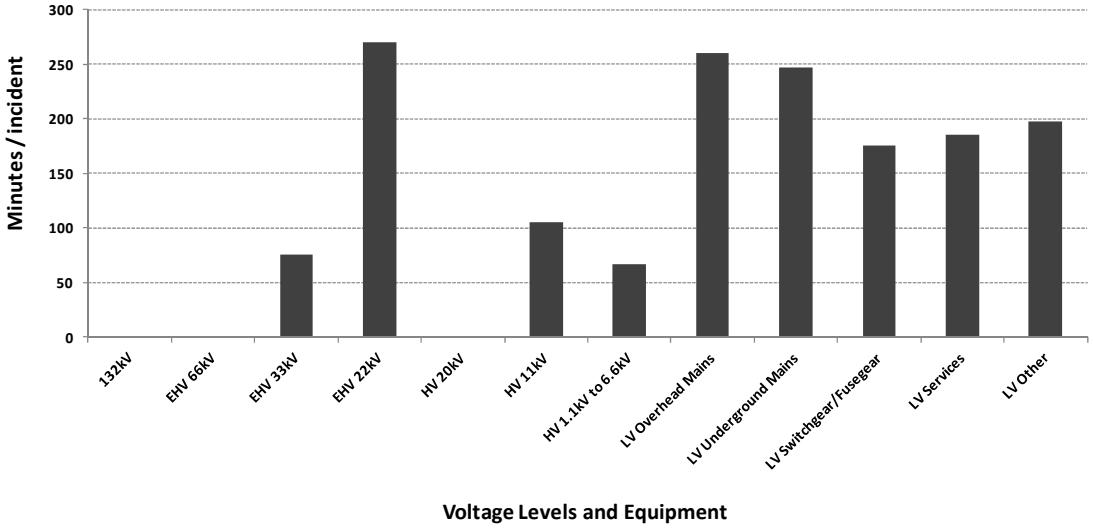

Figure 2.9: SPEN - Average duration of unplanned LIs (09/10).

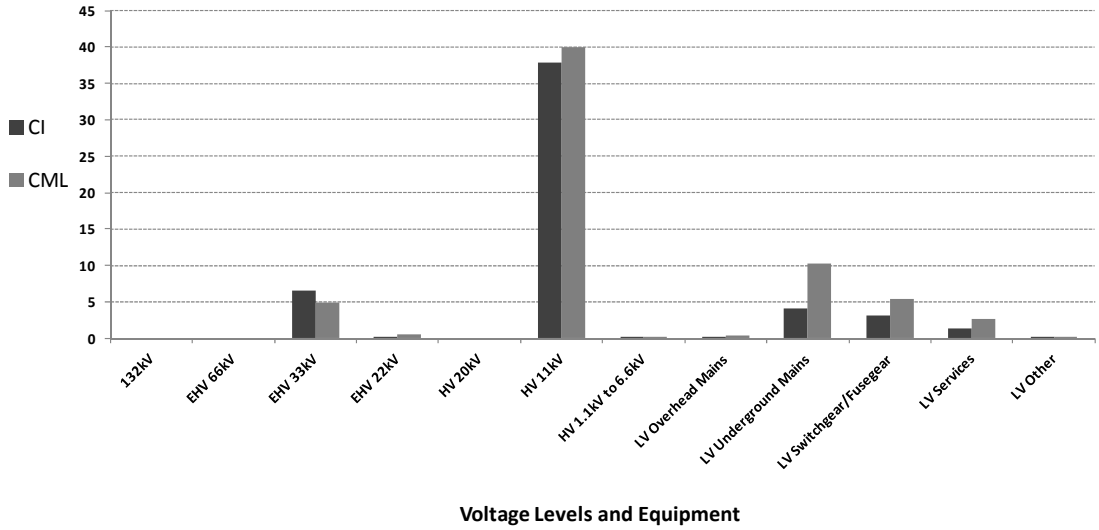

Figure 2.10: SPEN - Unplanned CI and CML by voltage level and equipment (09/10).

In addition, a probabilistic analysis of the duration of faults was also undertaken to assess the SPEN network behaviour, including the use of alternative supply and switching/restoration actions to meet the UK QoS requirements [87, 89]. According to Table 2.4 in Section 2.4.1, Figure 2.11 shows how the distribution networks are operated in order to restore the supply to customers in times under the specified limits (e.g. 15 min, 3 h, etc.) for the different group demands. However, not all the power outages are restored within these limits (e.g. due to unexpected events, severe weather conditions, etc.), thus the resulting probability density function (PDF) shows a certain probability of faults lasting longer than desired, and therefore accruing penalties for the DNO.

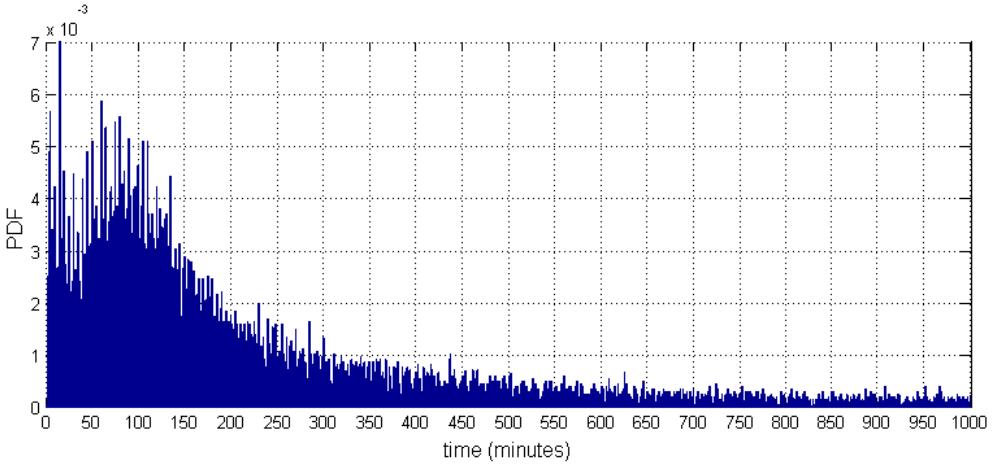

Figure 2.11: SPEN - Probability of duration of unplanned LIs (09/10).

Additional information and results, more specifically on the assessment of planned (i.e. pre-arranged) long interruptions in SPEN distribution networks, are provided in Appendix A.2.

2.6.3 Fault Probability Analysis of the UK Transmission System - NG

A collaboration work with the UK TSO, National Grid (NG), resulted in one of the NG internal reports in July 2012: *The Probability of Faults and Trips on the UK Grid System* [38]. The work's aim was to create a comprehensive database on the reliability and availability of the grid system, and undertake a corresponding data analysis as an input to the NG's reliability modelling work.

Considering NG's past statistics covering several years of network performance, the main objective was to estimate the risks of circuit unavailability, i.e. the risks that the circuit will suffer an unplanned trip and the risks that it will need to be outaged to repair a fault or defect in an asset. It was assumed that the risk of a spontaneous circuit trip, or a defect outage, is directly associated with an asset, and the risks were found by the overall number of incidents factored by the number of such assets on the transmission system. The assets involved were:

- Overhead lines: the risks were considered to be proportional to the length of the circuit;
- Cables: the risks were considered to be proportional to the length of the circuit [5];
- Transformers (including quad boosters);
- Protection and control equipment (including instrument transformers);
- Reactive compensation [6];

5. This assumption is not perfectly accurate, as many of the cable faults are associated with the cable sealing ends. Hence, it could be arguable that the risks are proportional to the number of sealing ends rather than the km length underground. However, the policy for this work was adopted as the best way of interpreting the available data.
6. No distinction was made between shunt capacitors, shunt reactors, static VAr compensators (SVCs) and series reactors. These statistics were included in the analysis, but it must be noted that one of these outages does not normally imply an outage of a circuit, as even a problem with a series reactor (between busbar sections) is likely to be resolved by a reconfiguration of the substation.

- Substation auxiliaries (faults associated with batteries, fire deluge systems, etc.);
- Telecommunications;

The analysis did not distinguish between different subclasses of assets. Also, no data was available to assess the effect of an asset condition (i.e. its age or its health assessment) on the risk that it suffers a trip/fault or a defect needing repair.

NG - Transient and Sustained Network Trips

The database covering urgent (i.e. unexpected) trips affecting the continuity of supply in the grid system provided data for the 6-year period between January 2006 and December 2011. During this time, there were 1,210 reported circuit trips, with an average of 4 trips per week [7]. Thus, the trips are categorised according to the component/asset which was considered as the primary cause of the fault.

Figure 2.12 shows the cumulative distribution functions (CDFs) representing the different probabilities for the duration of sustained circuit trips in the analysed system. It provides information for the wide range of power components; however, as the number of events for some assets is not high enough (i.e. statistically not significant), the distributions present a skewed nature and thus are shown on a logarithmic scale.

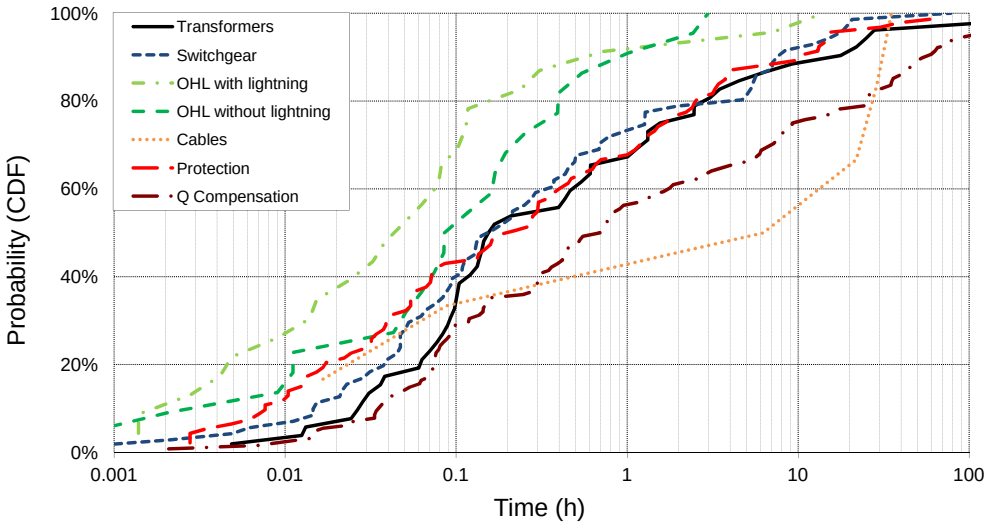

Figure 2.12: NG - Cumulative distributions of the duration of sustained circuit trips (6 years).

The modelling work is based on the arithmetic mean of the durations (implying the average time unavailable) shown in the table provided in Appendix A.3, which gives information on the overall statistics of transient, sustained trips (over 6 years) and planned outages (over 10

7. This is likely to be underestimated as, occasionally, a circuit will trip, be automatically restored, and then trip again shortly after (e.g. in a severe thunderstorm). Such incidents could then be reported as a single trip, so for the purposes of reliability analysis, be considered as only one event.

years). However, these statistics are disproportionately dependent on the few very long outages, and may be materially pessimistic.

For each type of power component, as shown in Figure 2.13 for overhead lines (OHLs), an attempt to fit an analytic function to these probability distributions was considered necessary, e.g. to establish the distribution of the duration of loss-of-supply events. Log-normal or Weibull distributions are considered the most appropriate for this purpose, therefore Figure 2.13 shows the quality of the "fit" likely to be possible. However, the "left-hand end" and "right-hand end" of the distribution would present different parameters for the model.

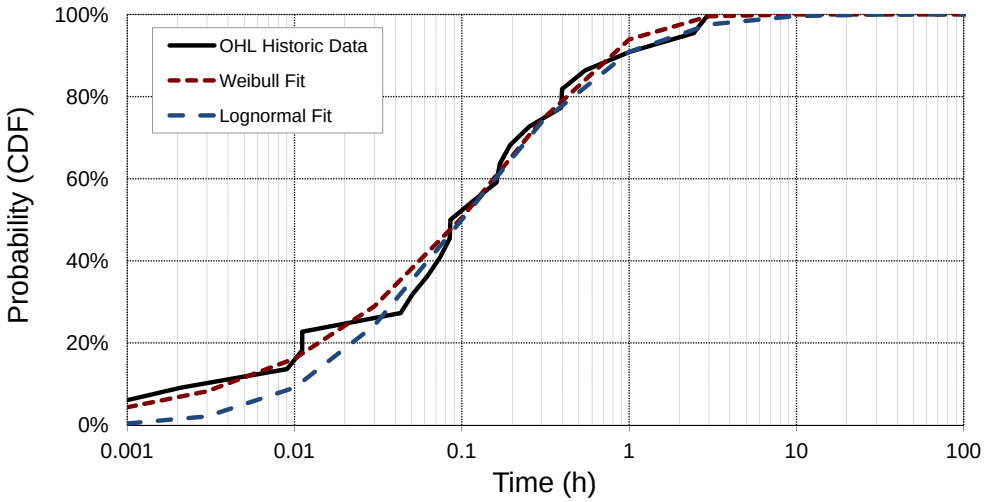

Figure 2.13: NG - CDFs of the duration of sustained trips of overhead lines (6 years).

The work was further developed to distinguish between assets at different voltage levels. For example, Figures 2.14 and 2.15 present the probability density functions (PDFs) and CDFs for different types of transformers operating in the transmission system. These results help to identify which type of transformers are more likely to fail during its lifetime, and what is the expected repair time for the outage.

As shown in the results, transformers operating in primary substations (e.g. EHV/66kV or EHV/33kV), and supplying GSPs down to distribution networks, experience a higher probability of faults than those operating at the top voltage levels (i.e. EHV for TSO) such as 400kV, 275kV, etc. For this particular case, Weibull distribution is also considered as an appropriate tool for fitting the empirical probability distributions. In addition, the probability distributions show a considerable similarity between the case which includes "All Transformers", and those of the type "EHV/132kV". This is due to the high population (i.e. statistically significant) of this type of transformers in the analysed transmission system, as compared to the other types of transformers.

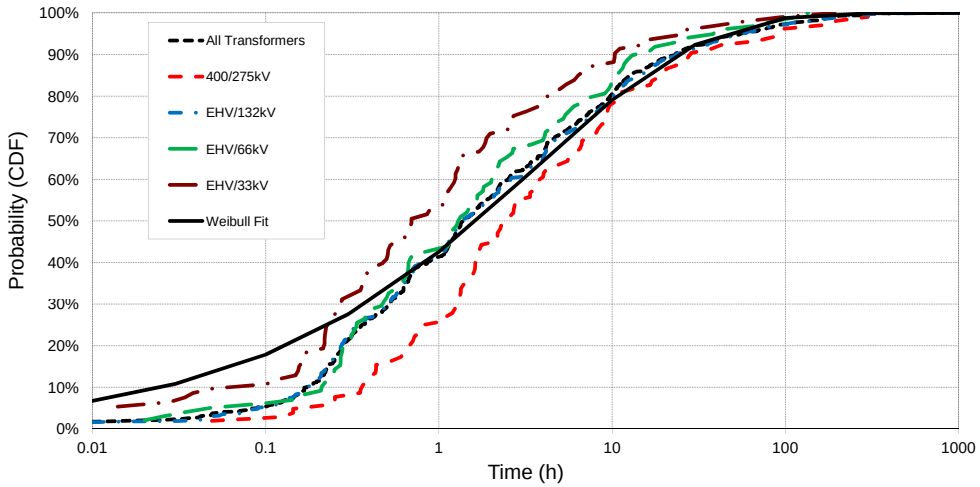

Figure 2.14: NG - CDFs of urgent events in different transformers (6 years).

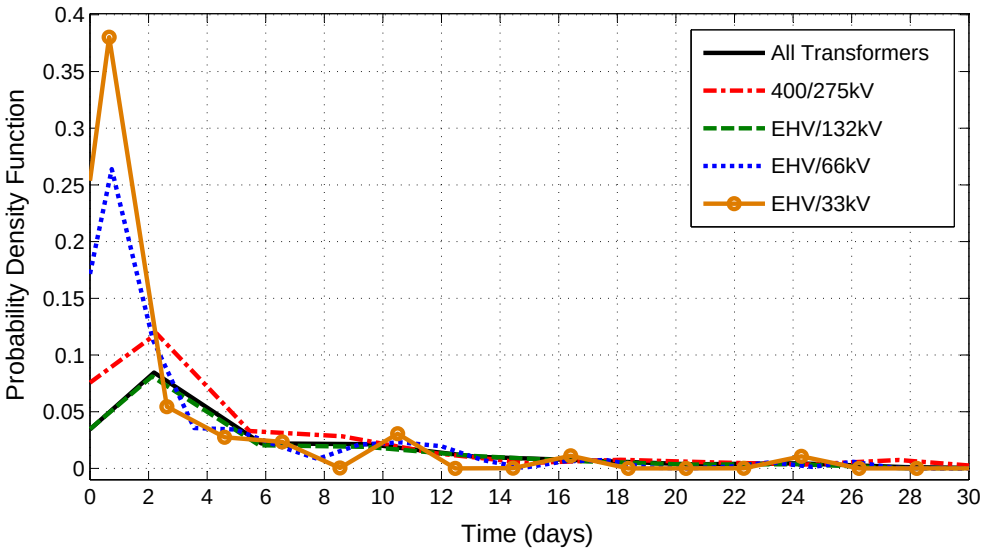

Figure 2.15: NG - PDFs of urgent events in different transformers (6 years).

Further probabilistic information studying the number and duration of outages for different types of transformers is provided in Appendix A.3. Finally, as an attempt to analyse the behaviour of the component's fault rate (λ) over the equipment lifetime (normally 40 years), Figure 2.16 shows the probability distributions of the outage rate for the wide range of power components. According to these results, there are some assets presenting a high probability of faults before the end of their lifetime, being the transformers, reactive compensation equipment, switchgear and cables the components with a higher risk of failure.

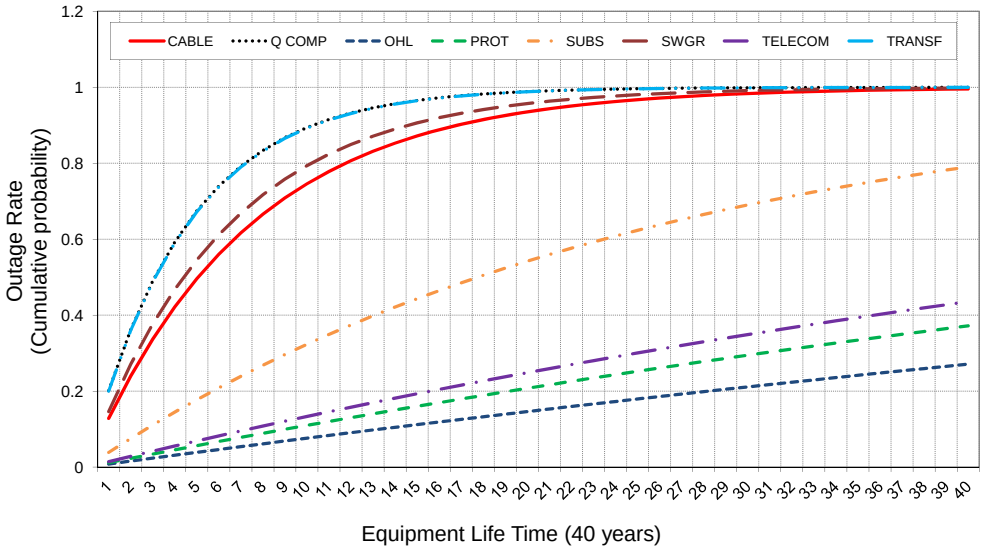

Figure 2.16: NG - Outage rate distributions for power components' lifetime.

NG - Planned Circuit Outages

Regarding the assessment of planned outages in the UK transmission system, a database was used with outages during the 10-year period between 2002 and 2011. This analysis was intended to distinguish between different planned interruptions (maintenance and repairs):

- planned outages for routine maintenance (considered to be systematic)
- planned outages to repair defects and faults in the assets

It was assumed that the number of defects, and hence the number of repairs, was proportional to the number of assets of that type involved. The corresponding results, average values, and probability distributions of the different types of power components resulting from planned outages in the grid system during the specified 10-year period are provided in Appendix A.3. As these interruptions are not considered as 'urgent', the values presented for the planned repair times are much higher than those for unexpected events (e.g. 1,000 h max. vs. 100 h max.).

2.7 Chapter Summary

This chapter has presented a general overview of the quality of supply assessment in power systems, including the most widely used reliability metrics and concepts. A review of security and regulator-imposed requirements for supply restoration times is also presented, in combination with a comprehensive database with failure rates and mean repair times of network components. Several reliability case studies are also provided with the analysis of actual component failure statistics and reliability performance of different European network operators.

Chapter 3

Modelling of Generic Distribution Networks

3.1 Introduction

The work presented in this thesis is mainly focused on the electricity distribution networks typically found in Scottish, wider UK and EU power delivery systems, while the main characteristics of the UK transmission network and its operation can be found in [74]. However, transmission and distribution of electricity must be analysed separately; the former is the bulk transport of electricity between power stations and load centres (typically constrained in the UK by limits on power flows from north to south), while the latter is the transport of electricity from primary and secondary distribution substations to customers. Therefore, this chapter initially focuses on the subtransmission and distribution parts of the power grid, which in the UK mostly takes place at 132 kV, 66 kV, 33 kV, 11 kV and 400 V three phase. The first voltage level (132 kV) is called the subtransmission network in Great Britain (GB), although in Scotland it is considered to form the transmission system.

It has to be taken into account that the structure of transmission and distribution system is different. The former usually takes a meshed arrangement, while the latter is normally radial, starting at a step-down on-load tap-changing (OLTC) transformer, or GSP, and feeding a number of lines which vary in length. Downstream, a series of transformers stepping the voltage down are spaced along the power distribution/delivery route, which may again take a meshed arrangement for the delivery of electricity to customers in urban or metropolitan areas.

For the initial purpose of this PhD research, in order to build typical distribution network models and to identify existing UK network arrangements and components, information on the distribution networks has been obtained from the different power utilities operating in the UK [73, 90, 91, 106, 107, 108, 109]. Figure 3.1 shows the licensed DNOs currently operating in the UK electricity market, where the assets connected at voltages under 132 kV account for more than 50% of the total network value in GB.

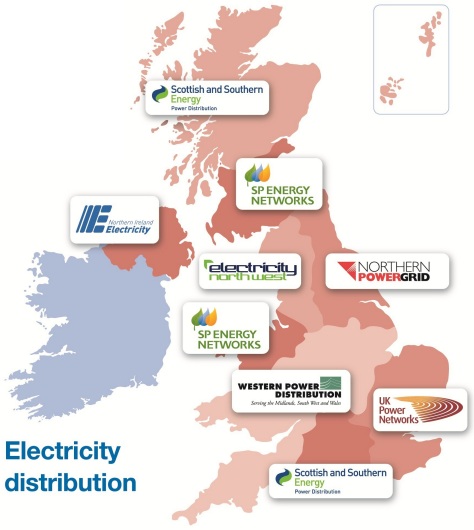

Figure 3.1: The UK context for electricity distribution [110].

3.1.1 Typical UK Distribution Networks

The first stage of this PhD research was the identification of typical network models and their equivalent representations. Therefore, existing and typical UK/EU network configurations were surveyed and identified (e.g. [111, 112]) in order to provide realistic results from the analyses presented in this thesis, allowing the comparison and correlation of the performance of different networks. These models were also verified using real configurations and measured data, provided by power utilities (e.g. SPEN) to ensure the validity of the calculated values.

Detailed information on all components of the "typical UK distribution networks" was assembled as a component database, where the required specifications, parameters, limits and settings were collected from several UK DNOs and manufacturers of power equipment, e.g. [113, 114]. In addition, the *UK Generic Distribution System* project [115] provides a set of generic models of distribution systems that are representative of UK networks, which can be used as a source of validation for the proposed network and software models. Furthermore, for the simulation and analysis of QoS in future electricity networks, typical strengths, fault levels and source impedances are also identified in this chapter.

3.2 Distribution Network Component Database

The built component database contains extended sets of data (electrical, mechanical and additional parameters) for transformers, overhead lines, cables, capacitors, generators and loads, as well as the typical settings of protection systems, voltage regulation, reactive power compensation and power conditioning equipment. Due to space restrictions, a sample of the component database, providing characteristics and parameters of those power components which are not included in the main body of the thesis, is provided in Appendix B.

The initial focus is on MV subtransmission and MV/LV distribution networks, covering mainly 132 kV, 66 kV, 33 kV, 11 kV and 0.4 kV levels. For every power system to be analysed, the required generation to meet the existing demand in the network is taken as a base for deciding the voltage level of the system. Consequently, this information is used to select the most appropriate ratings for every power component in the system. The proposed methodology to build the network component database, which covers every asset from generation to load, is illustrated in the diagram provided in Figure 3.2.

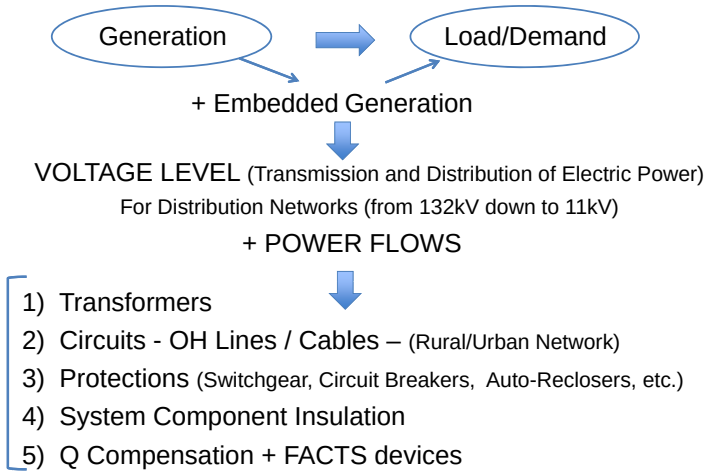

Figure 3.2: Methodology for building the MV network component database.

In that way, after identifying the typical distribution network configurations and topologies, any potential power system analysis will be fully documented. The idea behind this database tool is to choose particular components and their parameters from the list of most commonly used types, ratings and interconnections, and simply modify that selection for the purpose of different network studies and comparisons. This functionality was added to the several power system analysis software which has been used during this research (e.g. PSS/E, Matlab PS Toolbox), mainly focused on the steady-state assessment of balanced 3-wire systems, but also on unbalanced 4-wire LV networks for PQ-related studies.

3.2.1 Component Database Sample: Distributed Generation

This part of the component database provides information about the main types of DG currently connected to the UK electricity network, and also specifies the percentage of penetration of each technology. It also contains detailed parameters of existing embedded generation connections at different voltage levels, specifying installed MW capacity and fuel/plant type [73, 74, 90, 91, 106, 107, 108, 109]. Considering the need for modelling the wide range of DG technologies, this database will clearly help to identify the typical DG connections at different network locations and voltage levels.

For example, Table 3.1 provides extracted information [74] about all types of medium and small generation embedded within UK distribution networks up to year 2011. It also specifies all the DG technologies under operation of each DNO, according to their area of operation. Each DG technology is provided with the total installed capacity (in MW) and the most representative capacity (where available) of individual DG installations connected at GSP level, e.g. for Diesel type in Scottish Hydro Electric Power Distribution (SHE PD), it is 14/3 MW.

Table 3.1: Medium/small generation embedded within UK distribution networks [74].

Fuel/Plant Type	SHE PD	SE PD	SP Dist.	SP Manweb	NPG (NEDL)	NPG (YEDL)	ENW	WPD (East)	WPD (West)	UKPN (EPN)	UKPN (SPN)	UKPN (LPN)	WDP (S.West)	WPD (S.Wales)
	DG - Total installed capacity (MW) / Typical capacity of individual DG installations at GSP (MW)													
Biodiesel	0.14	-	-	-	-	-	-	-	-	-	-	-	-	-
Biomass	7	-	12.5	-	65	-	-	-	-	-	80	38	5.9/2.9	-
Diesel	14/3	30.7/9.6	-	12	6.4	28.4/8	36.7/6.6	-	23/8	7.1	19.6/5.6	29.1/6.4	5/2	-
Gas	0.23	177/10	-	-	125/50	185/10.5	141/10	-	156.1/10.5	46.4/5.7	20/10	-	10	-
Hydro	145/0.3	-	91.4/10	133.2/30	-	-	5.6	-	-	-	-	-	2.9	63.1/5.6
PV	0.02	-	-	-	-	-	-	-	-	-	-	-	-	-
Thermal	14.3/0.2	-	-	-	-	-	37	-	-	-	-	-	-	-
Waste	27/1	-	68.3/2.3	-	35	30.1/10	11.1	51.2/15	83.4/13	-	-	31	-	-
Wave	11/4	-	-	-	-	-	-	-	-	-	-	-	-	-
CHP	-	6	28.2/6.2	292/10	243/33.5	-	11.7	-	-	151/19	135.7/50	30	-	101.7/9.8
Crop	-	-	-	-	10	-	-	38	-	-	-	-	-	-
Waste Gas	-	-	-	-	10	-	-	-	-	-	-	-	-	-
Wind Offshore	-	-	-	180/90	3.8	-	289/100	180/90	-	155/60	90	-	-	-
Wind Onshore	117/0.9	-	328/15	259/13	101/5.5	80/2	346/5	119.4/16	12.2/0.2	183.6/1.5	59.8	3.8/0.22	76.5/6	133.6/3.9
Bio-gas	-	-	-	-	-	-	18.2/9.1	-	11	-	28.4/5.5	-	-	-
Gas CHP	-	16	-	98	-	41.5/10.5	149/16	90/14	63	-	254.2/56	116.1/5	-	-
Landfill Gas	-	7.5	-	19	-	-	11.4/6	-	-	74.2/11	-	-	23.5/2.6	19.7/2
Oil	-	-	-	-	-	-	28/10	24/10	5.5	151.7/17.6	-	-	-	-
Co-Firing Biomass	-	-	-	-	-	140/50	-	-	30	30	26	-	-	-
Diesel Engine	-	-	-	-	-	32/6.4	-	-	-	-	-	-	-	-
Gas/Steam	-	-	-	-	-	32	-	-	-	-	-	30.4/10.4	-	-
Steam	-	-	-	-	-	94.6/30	-	-	-	-	-	-	-	-
Steam Turbine	-	-	-	-	-	181.4/15	-	-	-	-	-	-	-	-
Steam/Waste /Diesel	-	-	-	94	-	-	-	-	-	-	-	-	-	-
Anaerobic Digest. CHP	-	-	-	-	-	-	-	0.75	-	-	-	-	-	-
Animal Biomass	-	-	-	-	-	-	-	15	-	41	-	-	-	-
Coal	-	-	-	-	-	-	-	30	17/8	-	-	-	-	-
OCGT	-	-	-	-	-	-	-	-	29	17	-	-	100/50	-
Gas Oil	-	-	-	-	-	-	-	-	-	40	-	-	-	-
Straw	-	-	-	-	-	-	-	-	-	31.3	-	-	-	-
Waste Incineration	-	-	-	-	-	-	-	-	-	55.6/13.8	-	-	-	5
Dual Fuel	-	-	-	-	-	-	-	-	-	-	-	55/22	-	-
Municipal Solid Waste	-	-	-	-	-	-	-	-	-	-	-	35	35	-
Diesel/Gas	-	7	-	-	-	-	-	-	-	-	-	-	-	-
Geothermal	-	7	-	-	-	-	-	-	-	-	-	-	-	-
Methane	-	30.6/6	-	-	-	-	-	-	-	-	-	-	-	-
Medium CHP	-	-	-	-	-	-	-	-	-	-	-	-	20.2/9.7	-

3.2.2 Component Database Sample: Transformers

The long term development statements (LTDS) provided by the UK DNOs and manufacturers data (e.g. ABB, Efacec-Portugal, etc.) were processed in order to create a database with the most typical transformer ratings. As an example result, Figure 3.3 shows the level of penetration for transformers operating at different voltage levels within UK distribution networks, in this case operated by Scottish and Southern Energy (SSE) [90] in the north of Scotland and south of England. Accordingly, it is possible to identify that the most typically used transformers for power distribution operate mainly at 33/11 kV (primary transformers) and 132/33 kV (BSP transformers). Although it always depends on the area of operation, this database provides information on the transformer parameters that should be selected when trying to model the "typical" UK power distribution network.

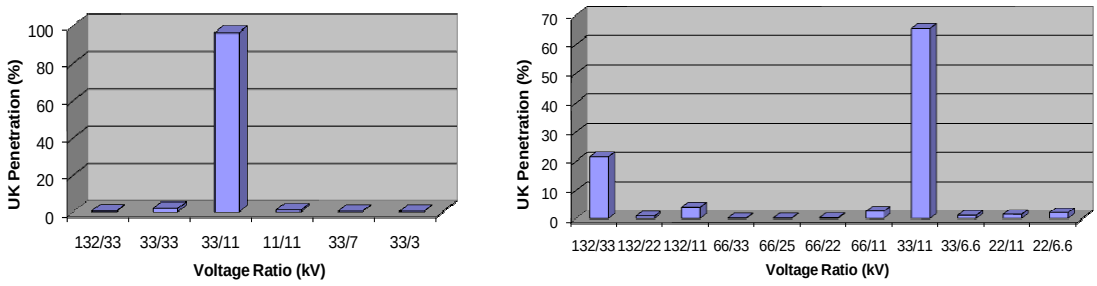

(a) Power Transformers (SHE – North-Scotland)

(b) Power Transformers (SE – South-Central England)

Figure 3.3: Comparison of typical UK transformer ratings.

For each voltage ratio considered in Figure 3.3, the database provides detailed information on the most typical parameters and characteristics of the power distribution transformers currently used in the UK:

- Power rating (MVA)
- UK level of penetration (%)
- Vector group
- Impedance value: R and X (p.u.)
- Zero sequence X (p.u.)
- Tapping range (number and % value of tap steps [73])
- Method of earthing [107] / Earthing impedance [106]
- Construction type (insulation) [107, 116]
- Additional information (overloading, thermal limits, cyclic rating capabilities, etc.)

Furthermore, information of typical transformers to be used by DNOs for future distribution network upgrading [73, 107] is also included in the database, providing general and complete specifications, transformer protections, typical arrangements, and also characteristics of typical three winding transformers [116]. For further reference, a complete report providing all the processed information for the transformer database is presented in Appendix C, as well as in

Appendix B.4, which provides a comprehensive table with a summary of the most common specifications of MV distribution transformers.

Following this methodology, the 'most typically used' power distribution transformer has been identified after processing all the data provided by DNOs (e.g. SSE). As specified in Figure 3.3, it operates at a voltage ratio of 33/11 kV (primary transformer), and it could be selected using one of the three main power ratings presented in Table 3.2.

Table 3.2: Selection of the 'most typically used' power distribution transformer in the UK.

Ranking	Power Rating	Site Penetration (%)	Area
1^{st}	15 MVA	30% (15% in each area)	Scotland + England
2^{nd}	30 MVA	25%	England
3^{rd}	10 MVA	20% (10% in each area)	Scotland + England

Therefore, the parameters of the most typical UK power distribution transformer (operating at 33/11 kV by SHE Scotland + SE England) would be as presented in Table 3.3:

Table 3.3: Typical 33/11 kV distribution transformers in the UK [90].

Nameplate Rating S (MVA)	Vector Group	Resistance R (p.u.)*	Reactance X (p.u.)*	R/X (p.u.)*	Zero Seq. X (p.u.)*	Tap Range		Method of Earthing
						Min	Max	
10	YY0	0.069	1	0.069	0.5	0.85	1.045	Resistance
15		0.06	1	0.06	5	0.8	1.05	
30		0.03	0.78	0.0385	4	0.8	1.04	

* on 100 MVA base

3.3 Development of Sub-Transmission Network Equivalents

Relatively small test network models (10-20 buses) are often used for the initial planning and testing stages of various researches, as well as for the communication of their final results and outcomes. These test networks, which may or may not be based on real power supply systems, should provide detailed information on all the modelled network components and relevant system operating/loading conditions. Among the test networks available in the existing literature, the IEEE 14-bus network [117, 118] was selected as the initial test network for analysis in the presented research work, as it is one of the most commonly used in a wide variety of power system studies. An internal survey was accordingly carried out on [119] in order to build a reference library, returning over 260 scientific papers and reports where the IEEE 14-bus network is used for power flow, security and power quality analysis, system state estimation, planning purposes, analysis of voltage stability, economic dispatch, optimal location of flexible ac transmission system (FACTS) devices, reactive power optimisation and many other studies.

Therefore, based on all the technical specifications and parameters gathered for the wide range of power components operating in UK/EU grids, the generic sub-transmission network proposed in this thesis is an UK variant of the IEEE 14-bus test system, as presented in Figure 3.4. The original IEEE 14-bus network represents a part of the 1960s Midwestern US supply system, and was intended for testing new power flow algorithms [117]. However, the available documentation for the original network model is quite old and does not provide sufficient and updated information on the network component values, required for the analysis of modern power supply systems with, e.g. DG or DSM functionalities. Therefore, the original IEEE 14-bus network is revised for the purpose of this thesis, in order to provide an updated specification for all network components, which will also allow for a full correlation with the previously published results in the literature. In addition, the updated model was used for several network reliability studies, considering 'smart grid' applications such as DSM schemes, as published by the author in [22].

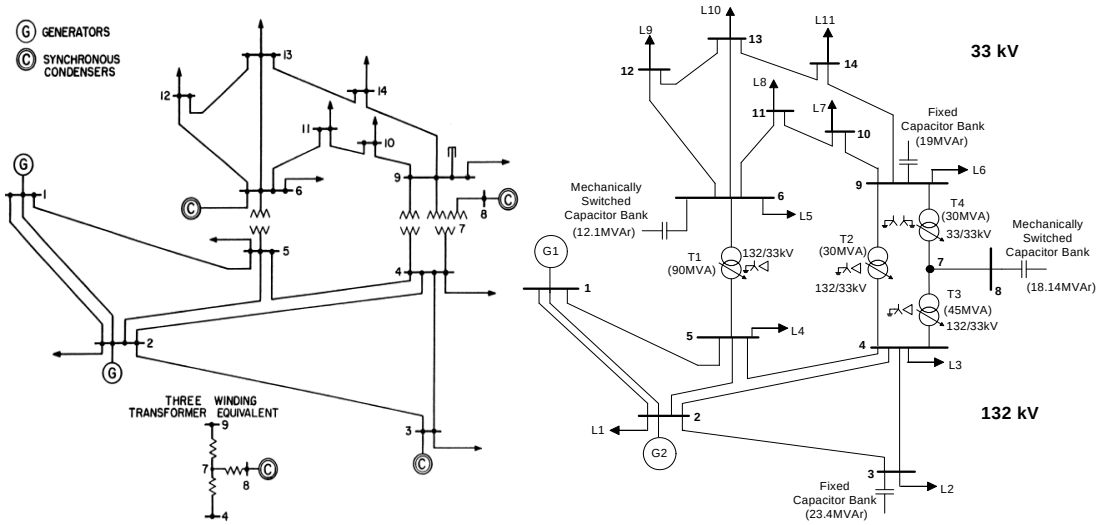

(a) Original IEEE 14-bus Network (b) Reference UK 14-bus Sub-Transmission Network

Figure 3.4: IEEE 14-bus network: original and UK revised variant.

All the base elements of the original IEEE 14-bus network have been maintained in terms of arrangement. Thus, the original configuration (number of buses and interconnecting lines) is preserved in the revised network, as well as the locations of system generation and system load. However, the adjustment of parameters for overhead transmission lines, transformer ratings, generation MW/MVAr capability (limits), automatic voltage regulation, load power factors, etc., will provide a more realistic set of results for an UK based sub-transmission network. In addition, as published by the author in [22], the revised version of the model is extended to consider the replacement of the synchronous compensators with capacitor banks at the 33 kV level, the connection of DG (one small-to-medium size at 11 kV, and one medium-to-large size at 33 kV), the addition of a power conditioning/FACTS device at 132 kV, as well as the categorisation of the original loads to represent different demand sectors and load mixes.

Considering the power flow through each line and the impedance values of the original IEEE-14 bus network to be matched, the results and specifications of the selected components for the UK version of the model are presented in Tables 3.4 and 3.5. The 'X/R' ratio of the original impedances has been considered as a key parameter in order to be matched with real transmission OHLs operating at 132 kV and 33 kV, as well as for 132/33 kV transformers typically used in the UK. For the selection of transformers, the power flow through each of the grid substations was also necessary to clarify what is their optimal power rating and operating voltage level.

Table 3.4: OHL specifications for UK sub-transmission network equivalent.

From Bus	To Bus	Voltage	Thermal Rating	Length	R	X	B	R_0	X_0	Type	Cross Section
		(kV)	(MVA)	(km)	(p.u. on 100 MVA)						(mm^2)
1	2	132	170.3	28.47	0.019380	0.060075	0.034637	0.042932	0.241087	ACSR*	242/39
1	5		125.7	93.8	0.053998	0.213306	0.077423	0.166696	0.628770		152/25
2	3		125.7	82	0.047205	0.186472	0.067683	0.145726	0.549671		152/25
2	4		82.3	67	0.051238	0.153254	0.033721	0.138402	0.433619		85/14
2	5		57.1	65	0.049709	0.148679	0.032715	0.134271	0.420675		42/25
3	4		48	71	0.064301	0.166844	0.034473	0.165488	0.432891		34/6
4	5		91.4	18	0.012754	0.040834	0.009154	0.027727	0.158946		89/52
6	11	33	12	7	0.091582	0.191339	0.002297	0.258699	0.722075		34/6
6	12		12	9.5	0.124290	0.259674	0.003117	0.351092	0.979959		34/6
6	13		22.8	4.2	0.066408	0.130396	0.000430	0.148800	0.591803		89/52
7	8		20.5	5.67	0.089651	0.176035	0.000581	0.200880	0.798934		85/14
9	10		12	2.7	0.032141	0.085922	0.000513	0.078162	0.360353		34/6
9	14		14.3	7.64	0.128604	0.272985	0.000309	0.231299	1.136162		42/25
10	11		12	5.6	0.082068	0.192406	0.000475	0.166419	0.807539		34/6
12	13		12	6.2	0.222427	0.201072	0.000937	0.321514	0.894288		34/6
13	14		12	10.5	0.169921	0.343964	0.001717	0.357364	1.414280		34/6

* ACSR: Aluminium Conductor Steel Reinforced

Table 3.5: Transformer specifications for UK sub-transmission network equivalent.

Transformer		Rating	Vector	R	X	X_0	Tap Range	
		(MVA)	Group	(p.u. on 100 MVA)			Min	Max
T1	(132/33 kV)	90	YD1	0.008	0.253	0.26	0.8	1.1
T2		30		0.016	0.333	0.333		
T3		45		0.014	0.267	0.269		
T4	(33/33 kV)	30	YY0	0.01	0.0413		0.81	1.04

A full correlation with the previously published results on the original IEEE 14-bus test system has been achieved for the UK variant shown in Figure 3.4. A steady state analysis, using the standard Newton-Raphson iterative method [120, 121, 122] with PSSE software package [123], has been performed with both versions of the test network in order to compare parameters such as bus voltages, power angles and active/reactive power flows transferred through transmission lines. Losses have also been considered to happen through resistances, reactances and shunt impedances in the power flow transmission. In addition, a correlation of the obtained results was done with additional software such as Matlab PowerSystem Toolbox and PowerWorld. The results obtained from the performance comparison between the original IEEE 14-bus network and its UK variant, presenting a small error between solutions, are presented in Figure 3.5.

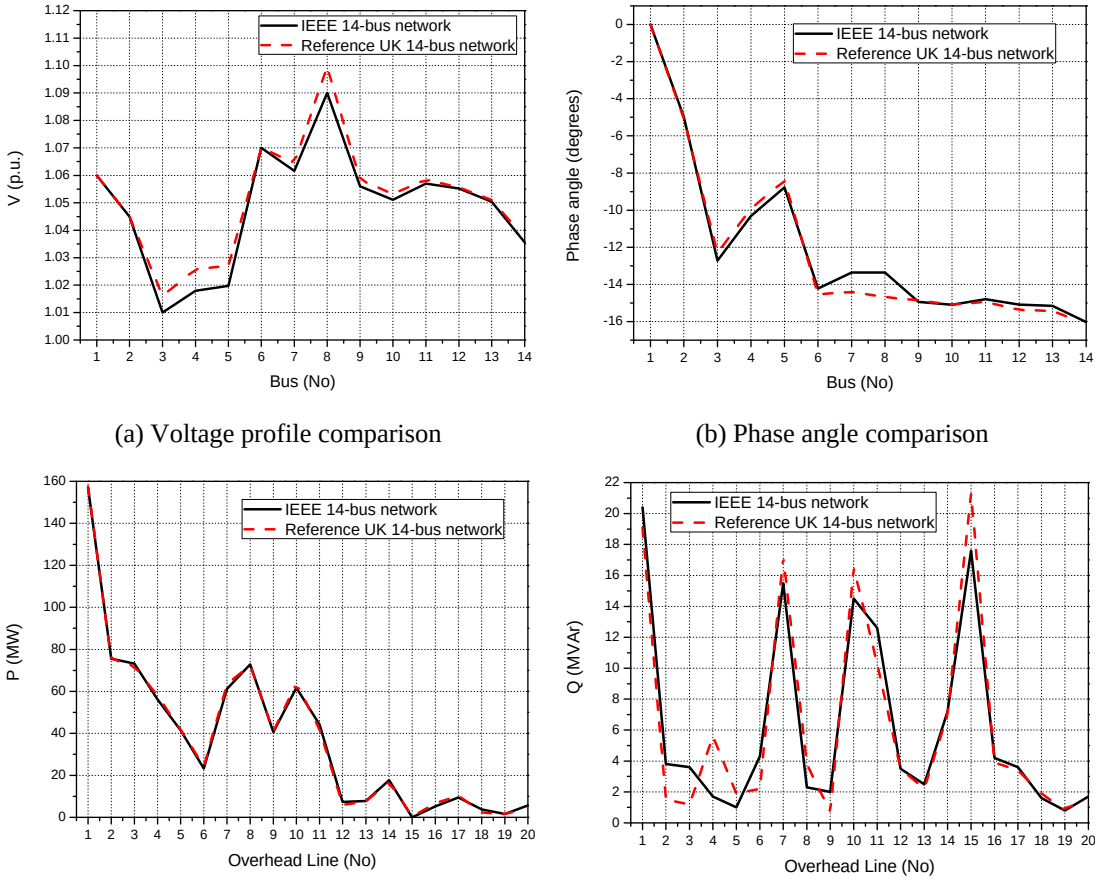

(a) Voltage profile comparison

(b) Phase angle comparison

(c) Active power flows comparison

(d) Reactive power flows comparison

Figure 3.5: IEEE 14-bus network vs. reference UK sub-transmission network.

For an overall sub-transmission and distribution network modelling, as published by the author in [22], either detailed or aggregate distribution network models (presented in this thesis) can be used to expand any of the BSPs at 33 kV (loads L5 to L11) in Figure 3.4. Considering the demand in the sub-transmission network equivalent, loads L5 to L11 could correspond to typical UK residential subsectors, such as highly-urban, urban or suburban, so they can be used to match the demand at the bulk loads with detailed/aggregate network configurations designated to supply residential customers.

3.4 Identification of Load Structure for Network Representation

Power distribution networks differ from each other in both characteristics and configuration, depending on location. This will determine important factors such as network strength, fault levels and source impedances, transformer ratings and feeder types/lengths, as well as the level of dedicated public/street lighting. In addition, geographic location, as well as time of the day and season of the year, have a strong influence on the electrical characteristics of the load/demand sectors, so these variations must be taken into account for the correct modelling of loads at the different voltage levels (HV, MV and LV). This information is required for the analysis of the network loading/operating conditions and assessment of network reliability performance in power system studies.

3.4.1 Load Modelling

The main purpose of a load model is to correctly represent the changes in active and reactive power demands of the modelled load as a function of variations of certain supply system parameters. Accordingly, the most frequently used load models can be described as a mathematical or analytical description of the changes in active and reactive power flows to a device, or group of devices connected to the power system, typically with respect to voltage and/or frequency.

Load models are traditionally classified into two main categories, static and dynamic. As this PhD research focuses on the steady-state analysis of power systems with very small frequency variations, there is no need to include neither dynamic nor frequency dependency in the static load models considered for analysis. Generally, static load models are commonly divided into three different categories [124]:

- **Constant Power:** Active and reactive power flow to the load is constant, irrespective of voltage. This is also referred to as the "Constant MVA" model.
- **Constant Current:** Active and reactive powers vary linearly with respect to voltage magnitude.
- **Constant Impedance:** Active and reactive powers vary in proportion to the square of voltage magnitude. Also described as the "Constant Admittance" model.

Figure 3.6 illustrates this graphically, showing the active power demand drawn by the three general load types, as a function of voltage. Typically, power system loads contain different proportions of each of the three load types, depending on the exact load mix at that network location. It is important to model this voltage sensitivity of aggregate loads correctly in many power system analysis applications [125].

The two most common methods of expressing this static load model analytically is through the exponential load model, shown in (3.1)-(3.2), and the polynomial load model (often abbreviated as "ZIP"), shown in (3.3)-(3.4).

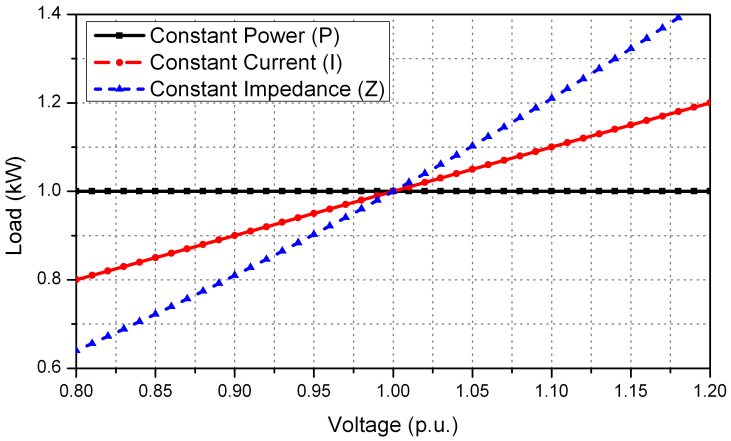

Figure 3.6: Active power demand created by 1 kW of each of the three load types, as a function of the supply voltage.

$$P = P_o \left(\frac{V}{V_o} \right)^{n_p} \tag{3.1}$$

$$Q = Q_o \left(\frac{V}{V_o} \right)^{n_q} \tag{3.2}$$

$$P = P_o \left[Z_p \left(\frac{V}{V_o} \right)^2 + I_p \left(\frac{V}{V_o} \right) + P_p \right] \tag{3.3}$$

$$Q = Q_o \left[Z_q \left(\frac{V}{V_o} \right)^2 + I_q \left(\frac{V}{V_o} \right) + P_q \right] \tag{3.4}$$

where: P, Q are the actual active and reactive powers drawn by the load, V is the actual supply voltage, V_o is the nominal supply voltage, P_o and Q_o are the nominal/rated active and reactive powers, n_p and n_q are the exponential model coefficients, and Z_p, I_p, P_p, Z_q, I_q, P_q are the polynomial, or "ZIP" model coefficients.

The exponential load model uses two coefficients (i.e. exponents), n_p and n_q, to define the relationship between the active and reactive power demands and the supply system voltage. When the coefficients equal 0, the load behaves as a constant power load; when the coefficients equal 1, the load behaves as a constant current load; and when the coefficients equal 2, the load behaves as a constant impedance load. The exponents may also take an arbitrary value, to more accurately represent power demand characteristics of the modelled load.

On the other hand, the polynomial "ZIP" model describes the load as the sum of the constant power (P), constant current (I) and constant impedance (Z) active and reactive power com-

ponents, as shown in (3.3) and (3.4). Generally, polynomial/ZIP models are able to provide a better representation of the characteristics of the modelled load, particularly in the case of non-linear load, when fundamental components of power demands are of the most interest. For this model, the polynomial coefficients are typically constrained according to (3.5) and (3.6):

$$Z_{p,q} + I_{p,q} + P_{p,q} = 1 \tag{3.5}$$

$$0 \leq Z_p \leq 1 \ , \ 0 \leq I_p \leq 1 \ , \ 0 \leq P_p \leq 1 \tag{3.6}$$

3.4.2 Aggregate Residential Load Model

Before attempting to build the different distribution network models, the first step is to define the load/demand on which all the calculations and design will be based. For this purpose, as the aggregate load models for residential and commercial sectors (i.e. as compared with industrial demand) are more widely available for use in power system analysis [41], the process of network planning and design presented in this thesis is mostly based on the UK residential load sector, which can be defined as dwellings whose sole purpose is to provide residency to the occupants. Accordingly, two sets of data are required: load curves (detailing how active/reactive power demands vary over the considered time period), and statistical information on the contributions of different load types to the total demand.

UK Residential Demand Curves

One of the most difficult aspects of this method is finding accurate statistical information on the load mix and load devices connected, and how this varies on a daily, weekly and seasonal basis. Some of this information is made publicly available, through published regional or national statistics on electricity end-use, such as in [126, 127, 128]. To illustrate the methodology, typical aggregate load curves of the UK residential load sector given in [128] are shown in Figure 3.7. This represents the overall UK residential sector demand. However, as the urban subsector accounts for more than 50% of residential demand [129], this subsector can be considered representative of the overall UK residential sector demand.

The curves for the three typical loading conditions in Figure 3.7 show the short and long-term temporal variations in power demand over the year. Therefore, each of them could be allocated to a specific season, such as the average loading conditions to the typical spring/autumn demand. However, the general profile between the three curves is similar, as user behaviour will not significantly vary throughout the year. The recorded seasonal variations are a result of changing contributions from physically-based loads, i.e. loads which respond to changes in the ambient conditions (through user response or internal thermostatic controls). Therefore, it is likely to expect increased/reduced contribution from lighting and electric space and water heating during the winter/summer seasons, respectively.

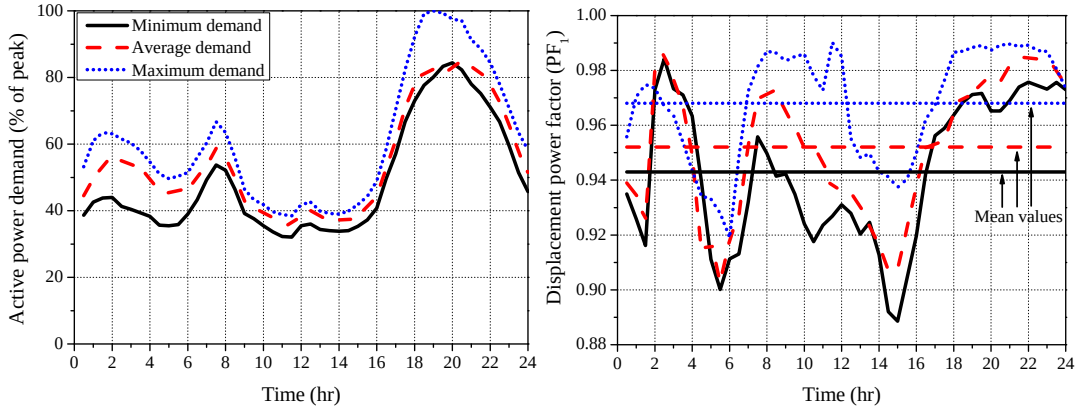

(a) active power [128] **(b)** displacement power factor

Figure 3.7: Typical aggregate daily load demand curves for the UK residential load sector for three characteristic loading conditions.

The available load demand curves often only provide information on the changes in active power demand, therefore a fixed power factor, typically around 0.95 - 0.98 (inductive), is often assumed for modelling purposes. The (fundamental) reactive power demands, which are represented by the displacement power factor PF_1 in Figure 3.7, are actually an output of the load modelling process in [41].

UK Residential Load Structure

A considerable amount of work has been carried out in developing and updating component-based load models based on UK load data, particularly focusing on the residential and commercial load sectors (e.g. [19, 21, 30, 31, 41, 124, 130]). Accordingly, the residential load mix varies depending on location and characteristics of the load. It has a time-varying nature, as the load structure changes depending on the time of the day, day of the week and season of the year. Therefore, one of the load profiles used for analysis represents the aggregate LV residential customers in the UK for average (i.e. spring/autumn) loading conditions, where maximum loading conditions (100% of the peak load) occur during the winter. Consequently, Figure 3.8 shows how the load curve is decomposed into different load types [128], which illustrates the contribution of the different electrical devices to the total demand during the 24 hours of the day. Additional loading conditions such as minimum (i.e. summer) or maximum (i.e. winter), as presented in [41], have also been considered for a different range of network analyses.

In Figure 3.8, the electrical devices and equipment found in the residential load sector are divided into the following types of loads: consumer electronics (CE) and ICT equipment; cooking load; 'wet' load; 'cold' load; direct and storage domestic hot water (DHW) load;

direct, storage and top-up space heating load; and lighting load. These are the most widely used load types for characterising residential load sector demand.

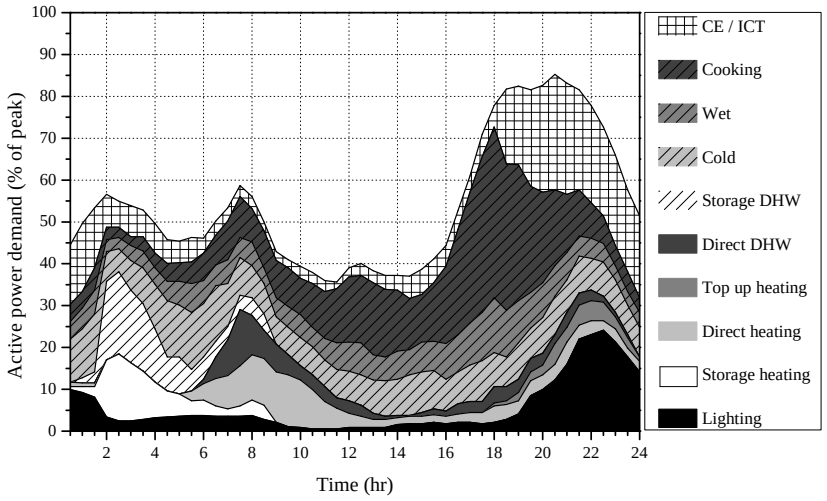

Figure 3.8: Decomposition of the UK residential load sector into load types for average loading conditions, using information in [128].

The load curve from Figure 3.8 is converted into a usable load model using the methodology presented in [19], where aggregation of loads is performed using five general load categories [41], based on the general electrical characteristics of the modelled residential equipment and devices. Each of these categories is then represented using a generic load model, which, based on their contributions to the total demand during the day, are combined to create the aggregate LV load model. Finally, the aggregate LV load model, which provides different polynomial/ZIP load coefficients and power factor values at each time-step (30 min) of the simulation, is connected to the corresponding network model of analysis.

For the purpose of distribution network modelling to be presented in the following sections, all demand is attributed to residential customer loads. Load demand figures produced by the Electricity Association data, presented in [131], show a minimum and maximum average demand of 0.16 kVA and 1.3 kVA respectively. However, the analysis in this thesis will consider an average demand per customer of 0.375 kW under minimum and 2.27 kW under maximum loading conditions, as proposed in [132]. This presents a 'worst case' scenario, enabling for a future upgrade of each network model, including new connections of customers, DG, etc. Therefore, each 11/0.4 kV substation will consider the maximum number of customers to be supplied (obtained from equal contributions of each customer, based on their corresponding "after diversity demands") in order not to overload the transformer rating capacity.

One major advantage of the component-based approach presented in [41] is that the resulting models are flexible, as the aggregate load models can easily be built to incorporate future or expected changes in the load composition by adjusting the contributions from each load type and load sector. In addition, they are particularly well suited to the modelling of DSM.

3.4.3 Residential Load Subsectors

The term "load sector" denotes an aggregation of loads from different load categories representing a typical structure and composition of electrical devices and equipment found in a specific end-use application, where similar activities and tasks are performed (e.g. residential, commercial or industrial load sectors). This usually results in inherent similarities in the characteristics and patterns of active and reactive power demands of end-users from the same load sector, allowing use of similar load models for the representation of their aggregate demands.

Although the purpose of every residential dwelling is identical and, generally, the individual loads used there will be similar, it is possible to divide this sector into four subsectors, based on the location, size and type of dwelling, as studied e.g. in [133]. The level of street/outdoor lighting will also be influenced by the location, and differences will also exist in terms of the size of renewable/distributed generation that is likely to be located in close proximity to the residential areas. Therefore, based on these general characteristics and parameters, the residential load sector can be divided into the following subsectors: highly-urban, urban, suburban and rural. These categories were also described and used in [19, 26, 30, 34].

Highly-urban (HU) residential load subsector

This subsector is represented by flat-type dwellings, usually found in large cities, in multi-storey and high-rise buildings and it is characterised by highly concentrated power demand. Three-phase motors may be used for elevators, pumps and central air-conditioning systems, which are usually not present in other residential subsectors. The number of rooms per dwelling is expected to be lower than in other subsectors, and there will be additional interior lighting load for illumination of communal areas. Dedicated public/street lighting is also greater than in other subsectors, due to the presence of parking spaces and higher required lighting levels in metropolitan areas.

Urban (U) residential load subsector

This subsector consists of house-type dwellings, ranging from one to few-storey buildings, located in city urban areas and it is characterised by medium to high concentration of power. As the average number of residents and rooms per household is greater than in the highly-urban subsector, higher power demands per household may occur. The public/street lighting in this sector is slightly reduced in comparison with the highly-urban subsector.

Suburban (SU) residential load subsector

This subsector is similar to the urban subsector, representing individual house dwellings located in city suburban areas and towns in close proximity to big cities. The load mix is similar to the urban subsector but the contribution from public/street lighting is likely to be slightly reduced. It is further characterised by medium power density.

Rural (Ru) residential load subsector

House-type dwellings in this subsector are one to few-storey buildings, located in more remote areas. Power density is low and some (smaller) three-phase motors may be used for agricultural works. Another notable difference is that no public/street lighting is present. Furthermore, the connection of larger DG is possible in this subsector.

3.4.4 Typical 'After Diversity Demand' Values per Residential Load Subsector

As previously discussed, in order to identify the typical demand behaviour of the residential load sector in the UK, the Electricity Association (supplied by Elexon Ltd) provides in [134] a full database with half-hourly electricity daily load profiles for standard UK profile class definitions (e.g. domestic unrestricted and domestic *Economy 7*), considering different days and seasons of the year. In the UK, the domestic *Economy 7* electricity tariff is a type of off-peak energy tariff which allows the customer to make use of several appliances (e.g. storage space and water heaters) at times of the day (i.e. night hours) when the overall demand and energy prices are lower. Therefore, the typical load curve for this type of customers will be totally different from the normal unrestricted (i.e. *Ordinary*) domestic customers. As these typical load profiles are provided for each season period (spring, summer, autumn and winter), they have been per-unitised from their peak value, and are shown in Figure 3.9 for both *Ordinary* and *Economy 7* customers.

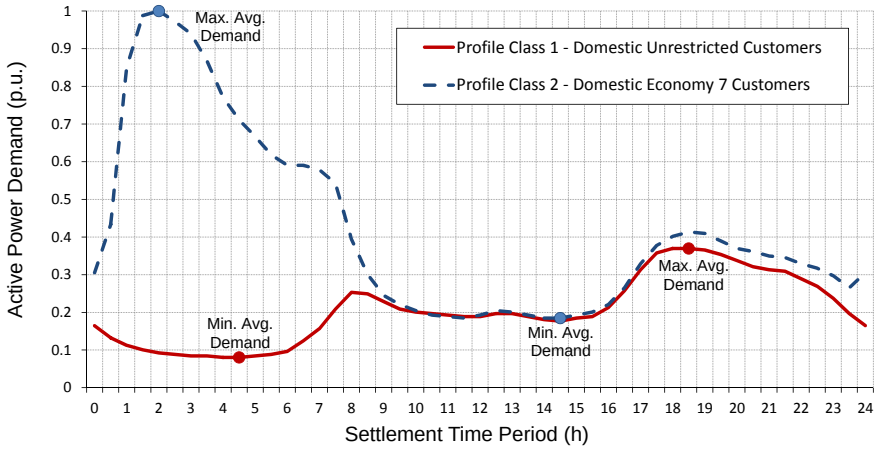

Figure 3.9: Typical UK domestic profile classes [134].

This part of the work aims to provide further demand references and different loading conditions (i.e. the max. and min. points highlighted in Figure 3.9) for the modelling and design of generic distribution networks supplying the four different load subsectors. As previously discussed, apart from the considered average demand per customer of 0.375 kW and 2.27 kW under minimum and maximum loading conditions respectively (in combination with power factor assumptions of Section 3.4.2), this research will provide correlated values of the 'after

diversity demand' (ADD) for both *Ordinary* and *Economy 7* customers, as well as for each season of the year. The demand estimation for the design of power distribution networks is usually based on diversity factors, such as the ADD concept, which can be defined as the minimum/maximum demand, per customer, as the number of customers connected to the network approaches infinity. This is usually derived from the minimum/maximum yearly nodal demand on the distribution network, divided by the total number of customers served. Further information and applications of this concept can be found in e.g. [135].

The proposed methodology uses measured load data provided by SPEN, covering one year of network operation (April 2009 to April 2010) at several GSP 132/33 kV substations. The recordings of active (MW) and reactive (MVAr) power demands at different SPEN network busbars over the one-year period are therefore used to calculate the total energy consumption, in MWh, for that particular year. Although the total aggregate demand may include demands from different load sectors (industrial, commercial, residential, mixed, etc.) depending on the location of each network GSP, the idea is to identify the total percentage energy consumption for each season of the year, with respect to the aggregate annual energy consumption. The calculated results are provided in Table 3.6, where as expected, a higher energy demand contribution takes place during winter (29% of the total), while the summer only contributes with 21% of the annual energy demand.

Table 3.6: Seasonal percentage contributions to the annual energy demand in SPEN networks.

Season/Year	Energy Consumption (MWh)	Load Contribution (%)	Days
Total (1 year)	19,208,960	100	365
Spring	4,333,436	23	91.25
Summer	4,086,898	21	91.25
Autumn	5,178,254	27	91.25
Winter	5,610,372	29	91.25

Sub-national electricity consumption statistics in [126], providing information on the average electricity consumption in different cities, areas, and even neighbourhoods in the UK, have also been processed in order to clarify the overall ratio of *Ordinary*/*Economy 7* customers over the total served electricity meters. Therefore, as the SPEN load measurements previously analysed refer to year 2009, the study focuses on statistics for energy consumption in that particular year [136], where it is possible to extract that around 27% of the total customers have an *Economy 7* tariff, so the rest (73%) of customers are billed according to an *Ordinary* tariff. This information, considering the total number of customers served, has been used to allocate a specific percentage of customers (73%/27%) to their corresponding load profile in Figure 3.9. In addition, as presented in Table 3.7, the information provided in [136] has been used to select a corresponding 'annual average consumption' per customer electricity meter, depending on location (i.e. HU, U, SU and Ru subsectors).

Table 3.7: Annual average domestic electricity consumption per meter in 2009 [136].

Load Subsector	**Average *Ordinary* Domestic Consumption** (73% of customers)	**Average *Economy 7* Domestic Consumption** (27% of customers)	**Total Average Domestic Consumption**
	(kWh)		
HU	3,185	4,795	3,500
U	3,594	5,411	3,950
SU	4,140	6,233	4,550
Ru	4,550	6,850	5,000

The data provided in Table 3.7 is based on the annual (i.e. 365 days) consumption per electricity meter, from which we already know what percentage corresponds to each season of the year (e.g. 23% over 91.25 days in Spring), as shown in Table 3.6. However, the timescale for the typical load profiles provided in Figure 3.9 for *Ordinary*/*Economy 7* customers is based on 24 hours. Thus, in order to estimate the average energy consumed per domestic customer in only one day (for each yearly season), the data in Table 3.7 has been divided by the corresponding number of days, either for annual (365 days) or seasonal calculations (91.25 days).

For each case (i.e. considering yearly seasons, load subsectors and classes of customers), once the daily average demand per customer is estimated in kWh, that energy amount is used to 'fill' the area under the per-unitised power curves presented in Figure 3.9. These curves represent the active power demand over the 24-hour time, thus by using the *Trapezoid* method as in [137], the power curve is divided in different time periods, each with a trapezoidal area representing the energy consumption within that period. In that way, it is possible to convert energy values (kWh) into active power demand, enabling to identify the ADD points (maximum and minimum average conditions in kW) for each case. These points have been put together in Table 3.8.

Table 3.8: After diversity demand (ADD) values per load subsector, class of customer and yearly season.

			SPRING (23% of total consumption)	**SUMMER** (21% of total consumption)	**AUTUMN** (27% of total consumption)	**WINTER** (29% of total consumption)	**ANNUAL**
			ADD (kW)				
HIGHLY URBAN	**Ordinary** (73% of customers)	**max**	0.61	0.56	0.72	0.77	0.66
		min	0.13	0.12	0.15	0.16	0.14
	Economy 7 (27% of customers)	**max**	1.2	1.1	1.42	1.53	1.31
		min	0.22	0.2	0.26	0.28	0.24
URBAN	**Ordinary** (73% of customers)	**max**	0.69	0.63	0.81	0.87	0.76
		min	0.15	0.14	0.18	0.19	0.16
	Economy 7 (27% of customers)	**max**	1.36	1.25	1.6	1.72	1.48
		min	0.25	0.23	0.29	0.32	0.27
SUB URBAN	**Ordinary** (73% of customers)	**max**	0.79	0.72	0.93	1	0.86
		min	0.17	0.15	0.2	0.22	0.18
	Economy 7 (27% of customers)	**max**	1.58	1.44	1.85	1.99	1.71
		min	0.29	0.27	0.34	0.37	0.31
RURAL	**Ordinary** (73% of customers)	**max**	0.87	0.79	1.02	1.1	0.95
		min	0.19	0.17	0.22	0.24	0.21
	Economy 7 (27% of customers)	**max**	1.73	1.58	2.03	2.18	1.88
		min	0.32	0.29	0.37	0.4	0.35

3.5 Modelling of Generic LV/MV Distribution Networks

After identifying the demand types and load categories for the different load sectors, the next step is to use typical/generic network models capable of representing the actual distribution systems connecting the several network GSPs with their secondary substations. In terms of network planning, the primary distribution system (11 kV or 6.6 kV in the UK) is typically a complex interconnected ring network containing many substations (indoor, outdoor or pole mounted), while the secondary distribution system (0.4 kV) is generally a radial network because of cost [138]. As previously discussed, each of them differs in arrangement and conditions depending on location. In cities, load density is high as compared to rural areas and therefore line lengths are shorter (typically less than 10km [139]), so underground cables are typically used to improve reliability of supply and for aesthetics. On the other hand, in rural areas the primary distribution is by means of OHLs and the substations are generally of the outdoor type, either pole mounted or switchgear type [139, 140].

Therefore, considering all the disparity in distribution network design, this PhD work presents a fully documented generic model for each of the load subsectors previously described, as well as for each voltage level commonly used for electricity distribution (LV and MV). Detailed and updated specifications for all power components and relevant system loading conditions are provided based on the database previously described. This information is considered essential for steady state network assessment, such as active/reactive power flows, system losses, voltage stability, etc., as well as for any network planning stage, where issues such as security and reliability of supply are of primary interest.

3.6 Detailed Representation of LV Residential Networks

Low-voltage networks typically operate at 415 V or similar voltage, after the primary distribution voltage is stepped down by means of 11/0.4 kV distribution transformers. Generally, these networks are operated radially, with a number of LV feeders starting from the LV busbars of the infeeding substation. These are main trunk feeders that may supply one or more lateral spurs and service connections, three-phase (3-ph) or single-phase (1-ph), which finally supply the customer's PCC and general protection panels. In terms of symmetry, the connection of multiple 1-ph consumers makes LV networks inherently unbalanced.

LV distribution lines can be in the form of underground cables or overhead conductors, depending on location and load density to supply. Thus, considering the network arrangement previously described, Table 3.9 provides line cross-sections typically used in the UK [131, 132, 139, 140, 141] for different LV distribution main feeders and spurs, as well as for each residential load subsector defined. As specified in Table 3.9, LV underground lines are mainly encountered in highly-urban and urban areas, while in suburban and rural areas it is most

common the use of OHLs. These were traditionally constructed by aluminium (Al) or copper (Cu) bare conductors [141], however ease of installation and environmental issues have led to the extensive use of bundled insulated overhead conductors over the last decades. Table 3.10 provides detailed information about typical configurations and parameters of LV lines used for electricity distribution in the UK [73, 90, 106, 107, 113, 114, 139, 140, 142, 143, 144, 145]. This table allocates an identification letter to each of the different LV lines in order to facilitate the modelling and classification of distribution feeders in the proposed LV network models.

Table 3.9: LV line cross-sections per residential load subsector [131, 132, 139, 140, 141].

Highly-Urban/Urban Underground network	
Interconnector	**Cross-sections (mm^2)**
Main trunk Feeder	$4 \times 300(Al)$; $4 \times 185(Al)$; $4 \times 120(Al)$
Lateral spurs	$4 \times 185(Al)$; $4 \times 120(Al)$; $4 \times 95(Al)$
Service connection	$4 \times 120(Al)$; $4 \times 95(Al)$; $4 \times 70(Al)$; $4 \times 35(Al)$; $2 \times 35(Cu)$
Suburban/Rural Aerial network	
Interconnector	**Cross-sections (mm^2)**
Main trunk Feeder	$4 \times 120(Al)$; $4 \times 95(Al)$; $4 \times 70(Al)$
Lateral spurs	$4 \times 95(Al)$; $4 \times 70(Al)$; $4 \times 50(Al)$
Service connection	$4 \times 70(Al)$; $4 \times 50(Al)$; $4 \times 35(Al)$; $2 \times 35(Cu)$; $2 \times 25(Cu)$

Table 3.10: Typical configurations and parameters of LV lines in the UK [73, 90, 106, 107, 113, 114, 139, 140, 142, 143, 144, 145].

LV Line Type		**Cross Sectional Area (CSA)**	**Positive seq.** Z_{ph}		**Neutral** Z_N	**Zero-phase seq.** Z_0		**Max. current**
Id.	**Configuration**		R_{ph}	X_{ph}	$R_{Neutral}$	R_0	X_0	Iz_{ph}
		(mm^2)	**(Ω/km)**					**(Amps)**
A	Underground Line (Cable) EPR or XLPE 0.6/1 kV 4x(CSA) Al / Cu (earth) CNE	300	0.1	0.073	0.168	0.593	0.042	465
B		185	0.164	0.074	0.168	0.656	0.05	355
C		120	0.253	0.071	0.253	1.012	0.046	280
D		95	0.320	0.075	0.320	1.280	0.051	245
E		70	0.443	0.076	0.443	1.772	0.052	205
F		35	0.87	0.085	0.87	3.481	0.058	156
G	Overhead Line Aerial Bundled Conductor (ABC) XLPE 4x(CSA) Al	120	0.284	0.083	-	1.136	0.417	261
H		95	0.32	0.085	-	-	-	228
I		70	0.497	0.086	0.63	2.387	0.447	195
J		50	0.397	0.279	-	-	-	168
K		35	0.574	0.294	-	-	-	148
L	Service Connection PVC or XLPE 0.6/1 kV 1x(CSA) Al / Cu (neutral / earth) CNE	35	0.851	0.041	0.9	3.404	0.03	120
M		25	1.191	0.043	1.26	4.766	0.03	100
N	Public Lighting PVC or XLPE 0.6/1 kV 1x(CSA) Cu / Cu (neutral / earth) CNE	25	1.18	0.043	0.9	4.72	0.03	100

Another important component of LV distribution networks is the secondary MV/LV substation, which typically comprises a single transformer with a rating of a few hundred kVA up to 1 MVA [146]. Table 3.11 provides full documentation of typical 11/0.4 kV transformers operating in the UK [73, 107, 146, 147], together with a direct correlation to the load subsector where each of them is typically used. The transformer's primary winding is usually connected in delta in order to isolate the earth fault on the secondary side and to ensure transformer stability, while the secondary winding is normally connected in star with an earthed neutral. This connection enables the supply of 1-ph loads operating at 230 V (loads connected between phase and neutral). Considering practical procedures from DNOs for network planning and arrangement in existing UK/EU LV distribution networks [145, 148], Table 3.12 shows the maximum distribution radius (i.e. based on maximum line lengths, etc.) an 11/0.4 kV transformer is typically designed to supply depending on demand type/subsector.

Table 3.11: Parameters of 11/0.4 kV secondary distribution transformers [73, 107, 146, 147].

Load Subsector	**Type**	**Rating (kVA)**	**Vector Group**	**Tapping Range**	**Basic Impulse Level (kV)**	**Load Losses at 75∘C (W)**	**No-Load Losses (W)**	**Z (%)**	**Model Parameters (Impedance on 2^{ary} side)**	
									R_{LV}	X_{LV}
									(p.u. on Transf. Rating)	
Highly Urban	Prefabricated substation	1500	Dyn11	± 5% in 2.5% taps	75	15810	1400	5	0.01054	0.048876
		1000				11000	1350	4.75	0.011	0.0462
		800				7410	1000	4.75	0.00926	0.04658
Urban & Suburban	Ground / Pad mounted	500				5100	680	4.75	0.0102	0.0464
		315				3420	580		0.01085	0.04624
		200				2900	540		0.015	0.045
Rural	Pole mounted	100				1750	320	4.5	0.0175	0.04145
		50				1100	190		0.02186	0.0393

In addition, as manufacturers of power transformers usually provide limited specifications, which is not enough for an accurate modelling of the transformers presented in Table 3.11, the full characteristics and specifications required to model secondary distribution transformers are provided in Appendix D. This includes all the phase constants and parameters of the transformer's equivalent circuit model, allowing for a full transient and dynamic network simulation, such as the study presented by the author in [21] and [31], where these models were particularly useful for the network implementation with Matlab Simulink software (i.e. SimPowerSystems Toolbox [149]). For each particular load subsector (HU, U, SU and Ru), the most typical/used secondary distribution transformer is selected in order to model the generic distribution networks proposed for analysis in this section.

Table 3.12: Maximum distribution radius of secondary distribution transformers [145, 148].

Load Subsector	**Max. Length (m)**
Highly-Urban	110
Urban	200
Suburban	300
Rural	800

Secondary distribution systems are always designed based on the criteria of current capacity and voltage regulation. Therefore, the LV network models presented in next sections have been designed accordingly. For each case (load subsector), the network diagrams provide information about the MV/LV substation, LV feeder lengths and cross-sections (as per Id. column in Table 3.10), number of LV consumers per load point, total demand, etc. They are intended to serve as study case networks suitable for different transient, steady-state simulations and reliability analysis, providing detailed characteristics of all the LV power components typically used in UK systems. The results from the performance analyses undertaken with these network models are presented by the author in next sections, as well as in [19, 21, 23, 25, 26, 28, 30, 31].

3.6.1 Highly-Urban Generic LV Distribution Network

In big cities (metropolitan areas), the LV network is typically an underground system with radial layout and 'heavy' loading conditions. Figure 3.10 provides a generic LV distribution model for the highly-urban residential subsector, which corresponds to an existing network operated by E.ON UK Central Networks [132]. The network has four three-phase trunk feeders which are supplied from the LV busbars of the infeeding 1 MVA 11/0.4 kV substation, supplying several branches with a total of 380 1-ph customers, i.e. individual households. Accordingly, the loads are represented as 19 load clusters, designated from HU1 to HU19. Furthermore, due to the relatively high load density, the length of all conductors is short to ensure that the voltage regulation does not breach performance specifications, i.e. +10/-6% [44]. In the event of a fault, the network may provide the possibility of closing an open link point, located at the remote end of one trunk feeder, to a feeder from another LV network in order to improve quality of supply. However, the network is considered to be 'radial' in normal conditions, and inherently unbalanced due to the number of supplied customers.

Excluding the 30 m long service cables used ('L' type lines in Table 3.10), the highly-urban LV network is 1,222 m long, with the following underground cables in use: 300 mm^2 (355 m), 185 mm^2 (601 m), 120 mm^2 (218 m) and 95 mm^2 (48 m). Detailed data are provided in Table 3.10. The total average load is measured at about 863 kW during maximum and 142.5 kW during minimum loading conditions.

Depending on the forecasted demand at each of the branches, the supplying trunk feeder can typically present either an input/output layout (if demand $\geq$ 50 kW), or a dedicated supply with 'T' layout (if demand < 50kW) [148]. In case of low demand, a minimum of one main feeder with an input/output approach will be required per 50 kW of maximum demand. The underground network models presented in this chapter consider multiple customers per load point (high/medium loading), therefore the distribution approach will be input/output in all cases. This arrangement provides selective protection through the use of LV disconnection boxes.

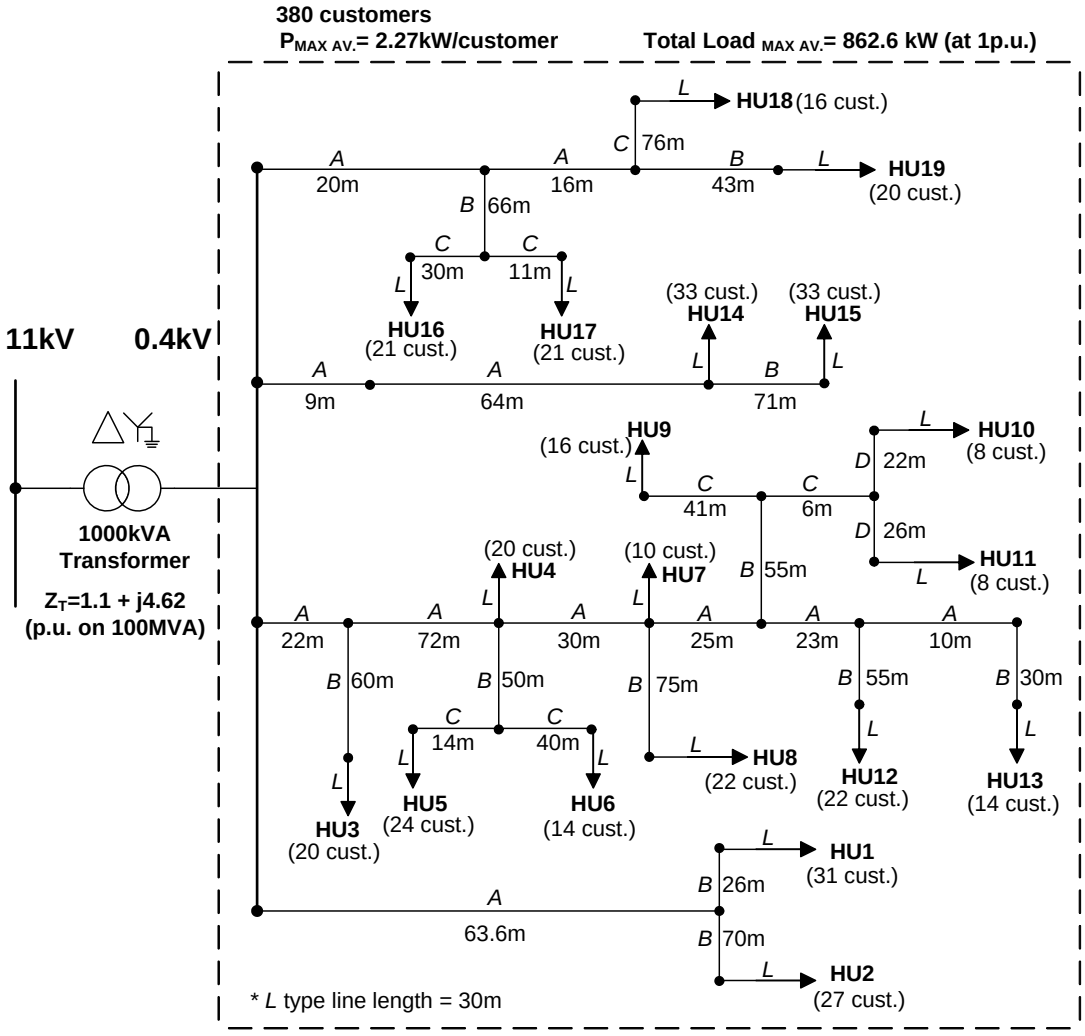

Figure 3.10: Highly-urban generic LV distribution network model.

3.6.2 Urban Generic LV Distribution Network

The LV network model provided in Figure 3.11 corresponds to the urban residential subsector (high loading), which also presents an underground arrangement operated radially. The typical 11/0.4 kV transformer used in the UK for this type of networks has a power rating of 500 kVA (Table 3.11), supplying a total of 19 load clusters (U1 to U19), with 190 1-ph customers. The urban LV network is 1588 m long, with the following underground cables in use: 300 mm^2 (122 m), 185 mm^2 (41 m), 120 mm^2 (62 m), 95 mm^2 (315 m) and 70 mm^2 (1048 m). Detailed data are provided in Table 3.10. In this model, the total average load is measured at about 431 kW during maximum and 71 kW during minimum loading conditions.

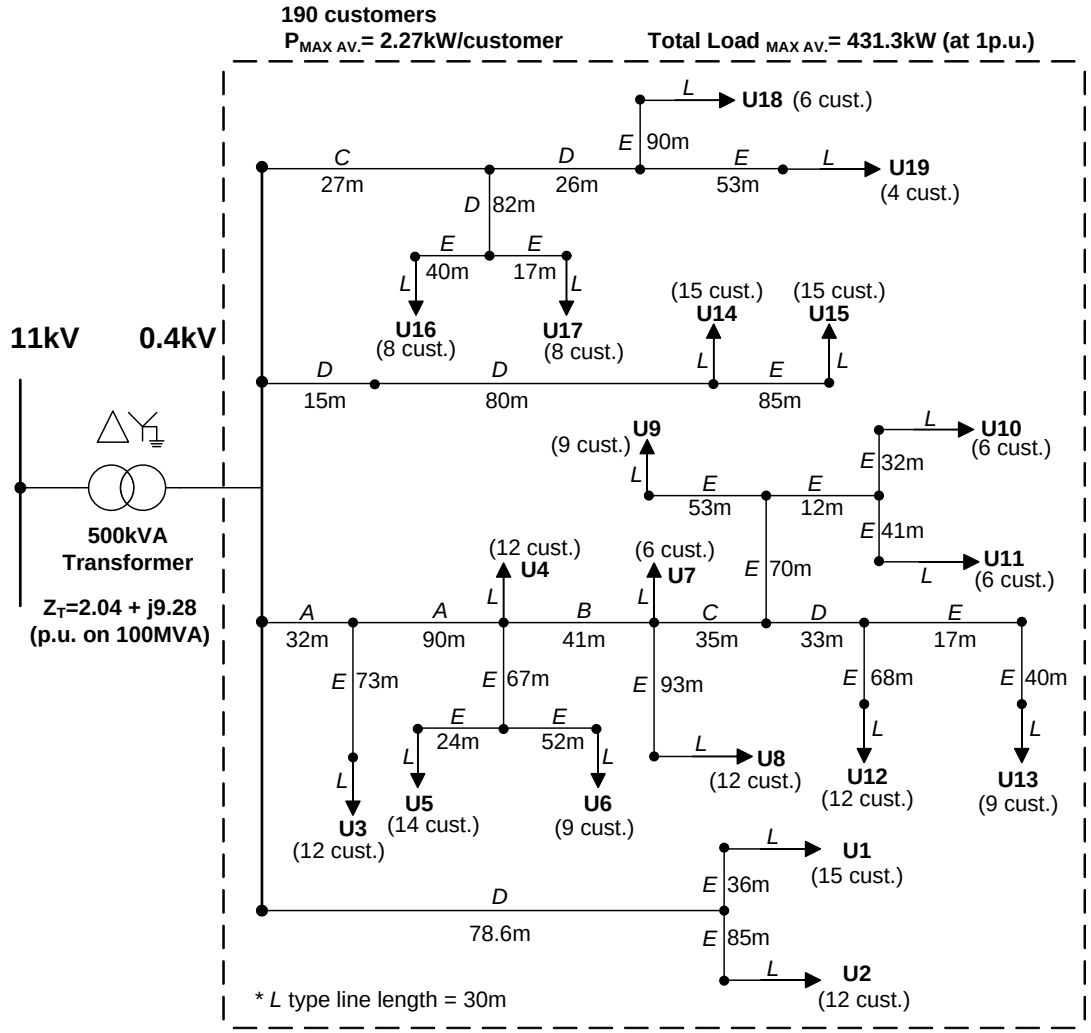

Figure 3.11: Urban generic LV distribution network model.

3.6.3 Suburban Generic LV Distribution Network

In smaller towns, where demand is considered as medium/low, the radial overhead system is used because of the lower capital costs. The typical network arrangement consists of several overhead distribution feeders (30 m of pole-to-pole distance), from which the service connection can be either OHL or underground cable. Figure 3.12 provides a generic model for the suburban residential subsector, where the infeeding 11/0.4 kV substation has a power rating of 200 kVA (Table 3.11), supplying a total of 9 load clusters (SU1 to SU9), with 76 1-ph customers. Excluding the service cables used, the suburban LV network is 840 m long, with a mixture of OHLs and underground cables in use: OHL 95 mm^2 (420 m), cable 95 mm^2 (150 m) and cable 70 mm^2 (270 m). Detailed data are provided in Table 3.10. The total average load is measured at about 172.5 kW during maximum and 28.5 kW during minimum loading conditions.

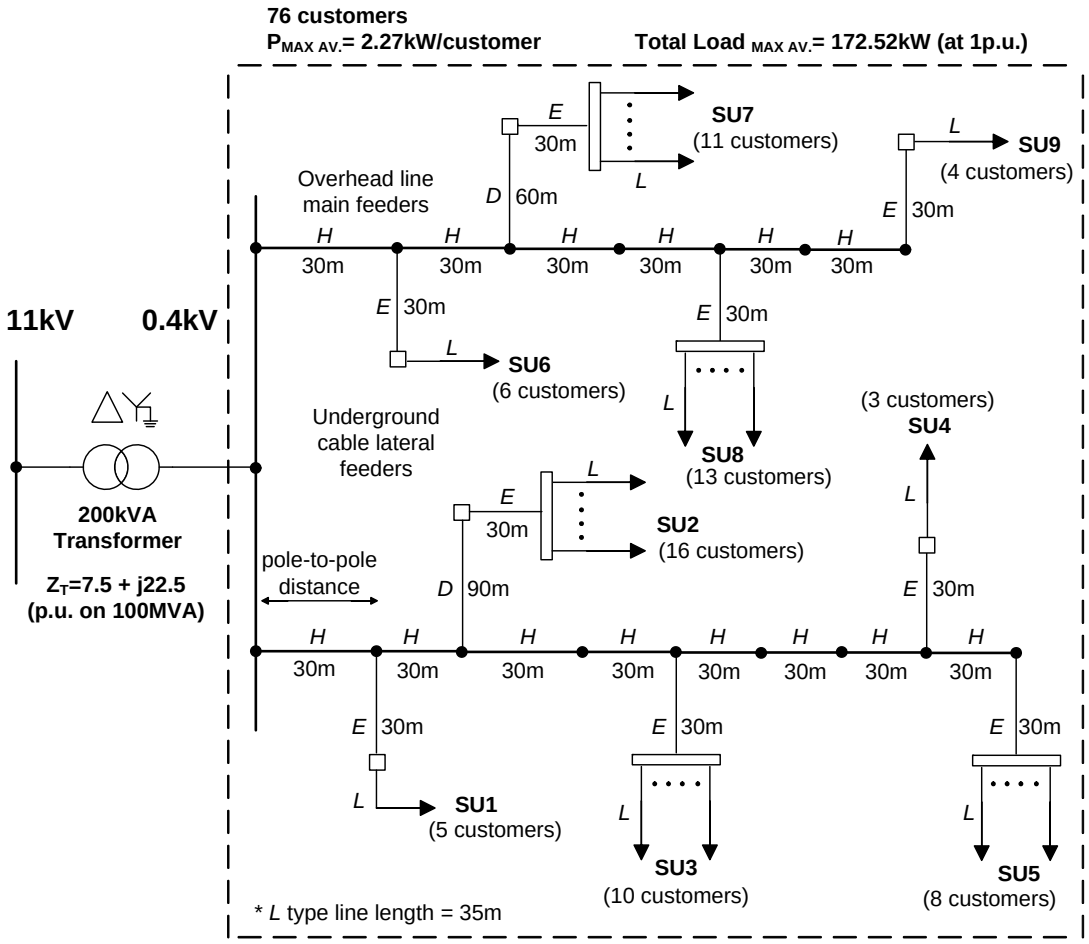

Figure 3.12: Suburban generic LV distribution network model.

3.6.4 Rural Generic LV Distribution Network

The network model provided in Figure 3.13 shows the typical network layout in rural residential areas with low loading conditions. In this subsector, the network also presents a radial arrangement and LV OHLs are typically used for electricity distribution. The pole-to-pole distance is 35 m, where each pole is used to protect (pole mounted fuses) and supply a single customer. In this model, the pole mounted 11/0.4 kV transformer presents a power rating of 50 kVA (Table 3.11), supplying a total of 19 1-ph customers (R1 to R19). Excluding the service cables used ('M' type), the rural LV network is 1235 m long, with the following OHLs in use: 50 mm^2 (665 m) and 35 mm^2 (570 m). Detailed data are provided in Table 3.10. The total average load is measured at about 43 kW during maximum and 7 kW during minimum loading conditions.

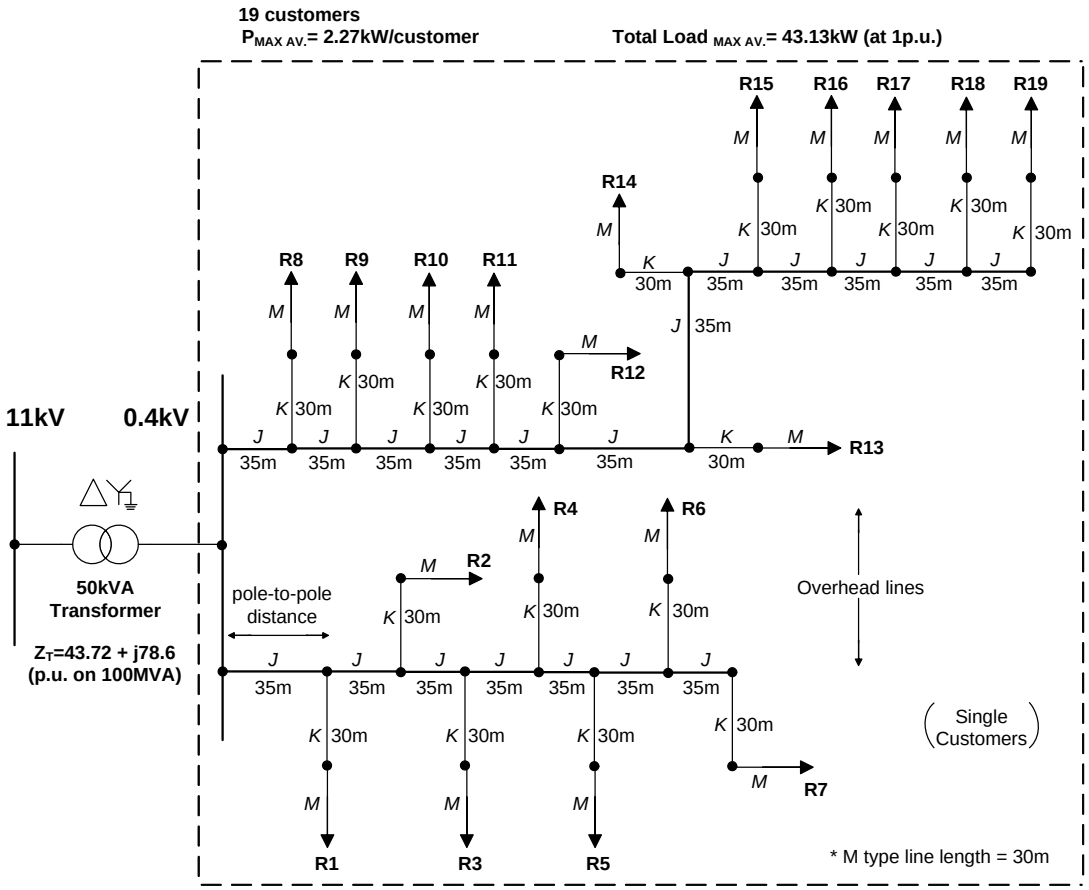

Figure 3.13: Rural generic LV distribution network model.

3.7 MV Distribution Network Modelling

Certain fundamental considerations must be considered prior to the identification and design of generic MV distribution networks. Some are technical and economic, such as the selection of conductor sizes for cables and OHLs, choice of switchgear current and fault ratings, transformer ratings and impedances. Others are regulation requirements related to the SQS [89], in particular permissible voltage variations, which directly affect performance conditions for DNOs. An important variable remains essential for the suitable choice of distribution network models, which is the variation in load density. Depending on location (i.e. load subsector), this will tend to result in different transformer ratings and conductor sizes, lengths and types (OHLs or underground cables). To quantify these effects, load density statistics, provided in [129] for the operating areas of each DNO in the UK, have been considered for the design of the generic MV networks proposed in this section.

The generic MV network models include a 33kV 3-ph source as a GSP, which is connected to a 33/11 kV substation. This substation, depending on the type of network, may contain one or two transformers equipped with OLTC in order to control the voltage at the secondary side within

the prescribed range of ±6% [44]. The 33/11 kV substation supplies several 11 kV outgoing feeders and each 11 kV feeder supplies a number of 11/0.4 kV distribution substations. The distribution network data used to build the MV generic models is provided in Tables 3.13 and 3.14. Table 3.13 provides detailed information about configurations and parameters of 11 kV distribution feeders typically used in the UK [91, 107, 111, 112, 113, 143]. This table also allocates an identification letter to each of the 11 kV lines in order to facilitate the modelling and classification of the presented network models. On the other hand, Table 3.14 provides full documentation of typical 33/11 kV transformers operating in the UK [90, 91, 111, 112] and the load subsector where each of them is normally used.

Table 3.13: Typical configurations and parameters of MV lines [91, 107, 111, 112, 113, 143].

11 kV Line Type		**Cross Sectional Area**	**Positive seq. Z_{ph}/km**		**Zero-phase seq. Z_0/km**		**Suscept. B/km**	**Max. current**
Id.	**Configuration**	**(CSA)**	R_{ph}**/km**	X_{ph}**/km**	R_0**/km**	X_0**/km**		Iz_{ph}
		(mm^2)	**(p.u. on 100 MVA)**					**(Amps)**
	Underground Line (Cable)							
O	-(3-core PICAS cable (screened, stranded Al)	300	0.09917	0.06322	0.69422	0.22128	0.0002698	525
P	-(3-core XLPE stranded/solid Al with	185	0.12271	0.06575	0.85896	0.23011	0.0002395	415
Q	95 or 70mm^2 Cu wire screen)	95	0.14403	0.06662	1.00824	0.23318	0.0001780	355
R	Overhead Line	150	0.11259	0.18363	0.39252	0.83701	0.0000842	490
S	-(AAAC (75∘C) 150 or 100 mm^2 Oak AL4)	100	0.14658	0.26189	0.30166	1.31330	0.0000122	395
T	-(ACSR 54/9 mm^2 11kV)	50	0.21626	0.20694	0.74174	0.99861	0.0000473	290

Table 3.14: Parameters of 33/11 kV primary distribution transformers [90, 91, 111, 112].

Load Subsector	**Rating (MVA)**	**Vector Group**	**Resistance R**	**Reactance X**	**Zero Seq. Reactance X_0**	**Tap Range (p.u.)**		**Tap Step**	**Method of Earthing**
			(p.u. on 100 MVA)			**Min**	**Max**	**(p.u.)**	
HU	30	Dyn11	0.03	0.78	4	0.8	1.04	0.0143	Resistance
HU & U	24		0.0291	0.7083	0.45	0.85	1.05		
	15		0.06	1	5	0.8	1.05		
U & SU	10		0.069	1	0.5	0.85	1.045		
SU & RU	7.5		0.095	1.08	0.52				Solid / Resistance
	5		0.14	1.3	0.8				
RU	2.5		0.3609	2.8	1.77	0.81	1.04		
where: HU - highly-urban, U - urban, SU - suburban, R - rural									

A generic MV model is presented in next sections for each of the four load subsectors defined in Section 3.4.3, representing four commonly used network topologies from UK distribution networks [97, 129, 138]. These have been designed based on the criteria of current capacity and voltage regulation [150], and provide detailed information to be accurately designed and modelled for steady state simulations. For each load subsector, the models present typical parameters of the 33kV GSP source, 33/11 kV substation, 11 kV feeder lengths and cross-sections (as per Id. column in Table 3.13), total demand, etc.

3.7.1 MV Underground Network Model Design

Underground systems are commonly used in highly-urban and urban areas due to the high power density of connected loads. At these locations, the MV distribution network is strong and meshed, and typical cable lengths are short in comparison to those operating in other areas. This will benefit the optimal voltage regulation due to the higher load density and proximity to the MV primary substation. Considering typical European networks, the 3-ph power distribution normally operates either with the neutral earthed or isolated [148], resulting in low values of the earth-fault current, equal to the system capacitance current [140]. The voltage between faulted equipment and earth is small, which improves safety. However, transient and power-frequency overvoltages can be higher than those with earthed systems.

Although underground MV networks present a meshed configuration, they normally operate radially with the support of another supply point, either a MV primary substation or a "reflection centre" in case of failure. A reflection centre presents a closed-loop arrangement that guarantees the supply of all feeders connected. Therefore, the distribution system will be capable of supplying the load (through all the feeders) from both ends of the network, and also capable of supporting itself in case of a n-1 failure. This is thanks to the cable '0', which is a feeder with no load in normal operation, connecting both ends of the network. In practice, due to voltage regulation and power capacity criteria, DNOs typically plan these networks considering a maximum of six 11kV feeders from the 33/11kV substation to the other end of the network [145, 148]. It is also normal practice to supply a maximum of ten 11/0.4kV distribution transformers from each 11kV feeder. Considering typical ratings of network components provided in Tables 3.13 and 3.14, 48 MW could be taken as an approximate value for the maximum demand supplied by underground MV networks, with a maximum supplied area of 1200 Ha (with low load density), 650 Ha (with medium load density) and 480 Ha (with high load density) [145, 148].

Due to unexpected events (faults) or planned maintenance operations, a connection/disconnection arrangement is also present in MV networks to avoid interruption of supply to customers. Typically, DNOs follow specific criteria for the location of tele-controlled circuit breakers (TCBs) in the 11kV feeders between both ends of the distribution network [145, 148]. When the installed power is less than 3 MVA, no tele-controlled points are normally required in between. However, when the installed power is between that value and 10 MVA, and the feeder's length is less than 10 km, at least one TCB is necessary for the automated protection of the system. On the other hand, if the installed power is higher than 10 MVA and the feeder's length is over 10 km, two TCBs are considered optimal. As for the location of fault-detection mechanisms, they will be installed between supply points or reflection centres and TCBs. They will also be installed between TCBs in case there is more than one in the circuit.

Considering all the previously described fundamentals for planning and design of MV underground networks, as well as the UK generic distribution network presented for analysis in [132]

and [129, 131, 151], Figures 3.14 and 3.15 present the proposed network models for highly-urban and urban load subsectors. These models, and different variants of them (including a mix of residential, commercial and industrial demands), have been used for several network transient and steady-state studies, as well as for reliability analysis as published by the author in [19, 21, 22, 24, 26, 30, 31, 35, 36], and therefore will be presented in next sections of this PhD thesis.

Highly-Urban Generic MV Distribution Network

As shown in Figure 3.14 and based on a high (i.e. 100%) residential demand, highly loaded 33/11 kV substations in the UK typically consist of two 24 MVA transformers (Table 3.14) operating in parallel and supplying an estimated total demand of 13,680 residential customers, based on a maximum level of ADD of 2.27 kW per individual household. A 33 kV source of 813 MVA strength is considered adequate for these conditions. The highly-urban MV network supplies a radius of approximately 2 km, with the following total lengths and cross sections of 11kV underground cables in use: 300 mm^2 (5.94 km) and 185 mm^2 (6.84 km). Detailed data are provided in Table 3.13. In this model, the total average load is measured at about 31 MW during maximum and 5.1 MW during minimum loading conditions. Considering that there are six incoming 11kV feeders from the MV substation, in normal operation each of them should not carry more than 83% of its power capacity, making possible the supply of the total load in case of a failure in one of the feeders (n-1 security criterion).

Urban Generic MV Distribution Network

A typical urban network configuration, which normally supplies a significant percentage of residential loads, is presented in Figure 3.15. Generally, this network has a slightly reduced strength, lower transformer ratings and longer cable lengths. Two 15 MVA 33/11 kV transformers (Table 3.14) supply the total load, of high/medium density, with an estimated demand equal to 9,120 residential customers. A typical 33 kV source strength of 543 MVA has been considered for these conditions. The urban MV network supplies a radius of approximately 3 km, with the following total lengths and cross sections of 11 kV underground cables in use: 185 mm^2 (9 km) and 95 mm^2 (9.9 km). Detailed data are provided in Table 3.13. The total average load is measured at about 21 MW during maximum and 3.4 MW during minimum loading conditions.

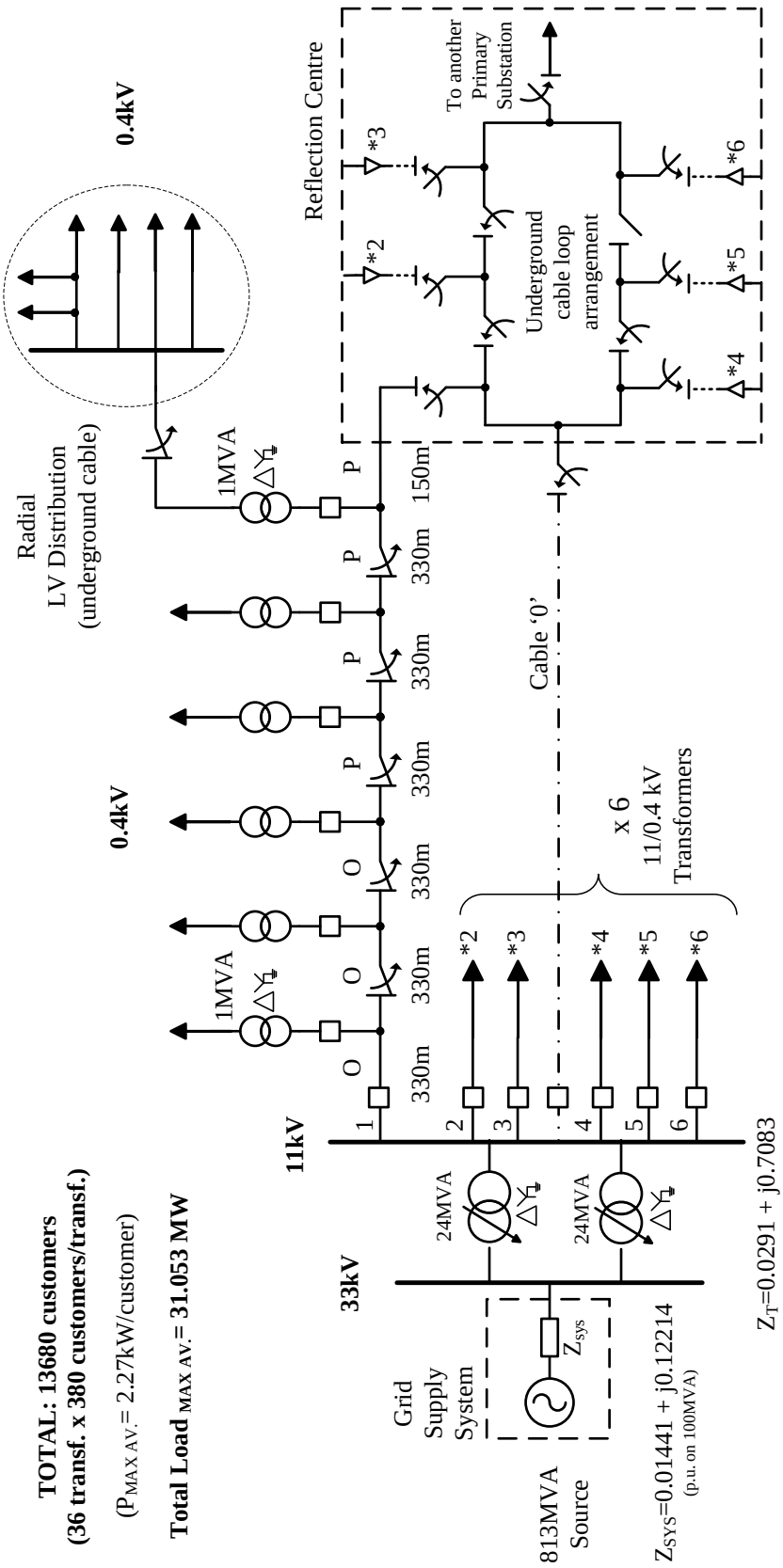

Figure 3.14: Highly-urban generic MV distribution network model.

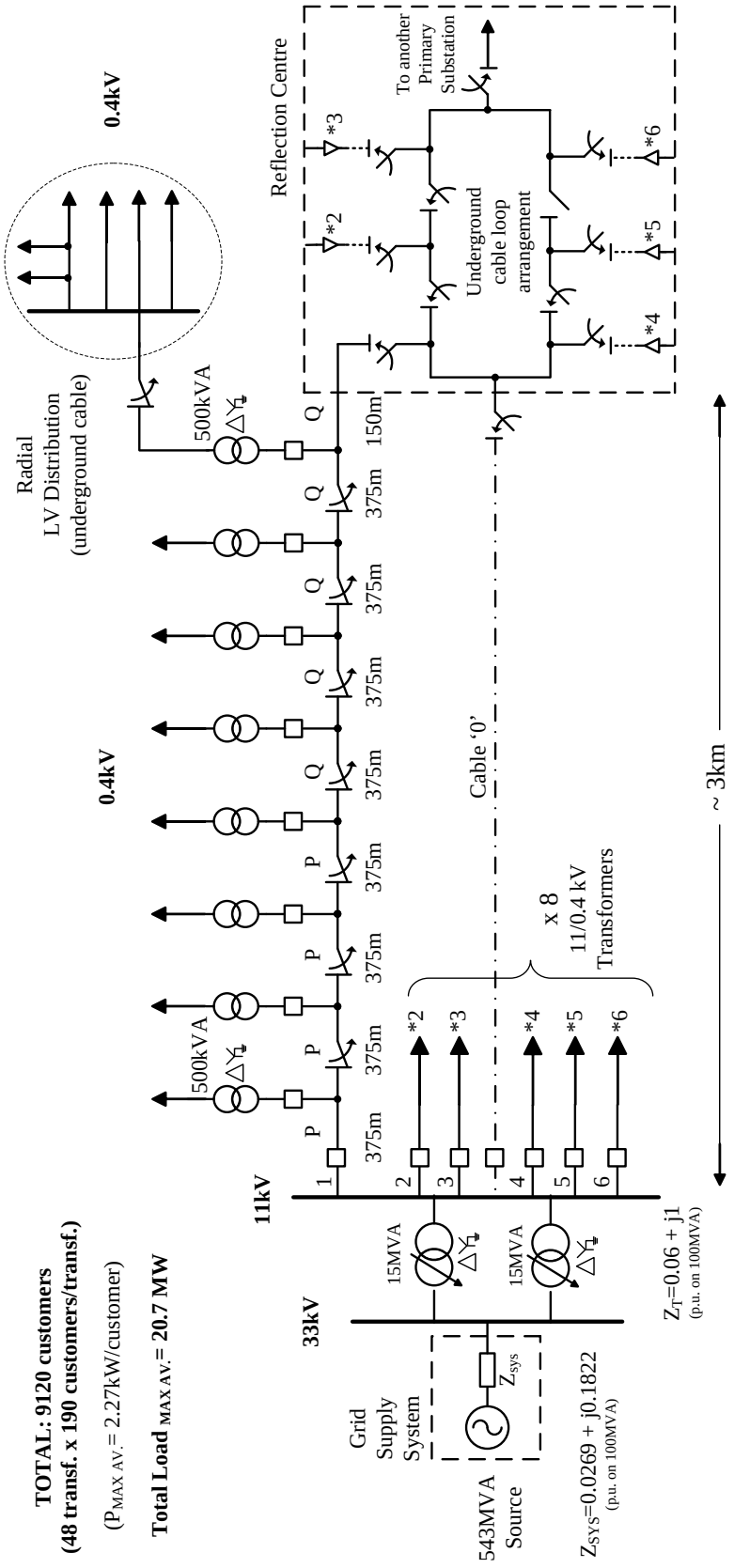

Figure 3.15: Urban generic MV distribution network model.

3.7.2 MV Overhead Network Model Design

Overhead MV distribution systems typically operate in suburban and rural areas due to the medium/low load density to be supplied. At these locations, the network is weaker than in highly populated areas and is generally not meshed. Feeder lengths are increased due to the lower density of housing and increased distance from the MV substation. Consequently, this will influence an optimal voltage regulation, resulting in a lower reliability performance. Overhead distribution networks also tend to operate either with neutral earthed or isolated [148], and include an automatic reclosing functionality in addition to the typical overcurrent protection (phase, neutral, homopolar).

MV overhead networks typically present an open arrangement. The distribution trunk feeder, which goes from the 33/11 kV substation to the boundary sectionaliser, presents a radial layout in normal operation, but is usually supported by another supply point (MV substation or reflection centre) in case of failure. The concept of 'reflection centre' in aerial distribution networks is similar to the one implemented in urban networks, however, with some differences. In urban networks it does not usually carry any load, but in aerial networks it is allowed to supply some load as long as it is capable of providing enough capacity margin to supply any of the other lines in case of a fault. The reflection centre does not necessarily have to present a concentrated arrangement, so the TCBs can be installed in different locations.

The 11 kV spur feeders, which are the OHLs off the trunk feeder, usually do not have any additional backup supply. Each spur feeder supplies several groups of 11/0.4 kV distribution transformers, and due to voltage regulation and power capacity, DNOs typically group no more than eight LV transformers together in a maximum radius of 4 km from the trunk 11 kV feeder to the furthest LV transformer [148]. The MV overhead network also presents a coordinated protection arrangement in order to maintain continuous supply to all customers, which is typically enabled through the use of TCBs, automatic sectionalisers, fixed disconnectors and auto-reclosing fitting.

Considering typical development criteria for MV overhead networks presented in [140, 148] and [129, 131, 151], Figures 3.16 and 3.17 provide detailed information in a generic overhead network model for both suburban and rural subsectors. These models, and different variants of them, have also been used for several network analyses presented by the author in [20, 23, 24, 25, 26, 34, 35, 36]

Suburban Generic MV Distribution Network

Figure 3.16 shows a typical configuration of a 33/11 kV distribution network supplying a suburban area, typically with a considerable proximity to the city, or smaller towns. In the proposed network model, considering a high (i.e. 100%) contribution from residential demand, the supplying MV substation consists of two 5 MVA transformers (Table 3.14) with an estimated total demand of 3,344 domestic customers. A 33 kV source of 423 MVA is considered appropriate for suburban locations. The overhead network model supplies a radius of approximately 6 km and is mainly designed with the following total lengths and cross sections of 11 kV OHLs: 150 mm^2 (11.8 km) and 100 mm^2 (17.2 km). Detailed data are provided in Table 3.13. In this generic network, the total average load is measured at about 7.6 MW during maximum and 1.3 MW during minimum loading conditions. The corresponding network protections and interconnection with adjacent MV substations are also indicated in the proposed network model.

Rural Generic MV Distribution Network

The rural MV generic network presented in Figure 3.17 generally presents a radial distribution arrangement with low-strength and long overhead feeder lengths. In rural networks, it is common to find only one 33/11 kV transformer operating in the MV substation, which directly affects the optimal reliability performance of the system. Table 3.14 provides further information of the 2.5 MVA transformer chosen for this generic model. Accordingly, the total estimated demand in this case equals to 646 residential customers, and a typical 33 kV source of 136 MVA has been considered adequate for these location. The rural generic network supplies a radius of approximately 9 km and is mainly designed with the following total lengths and cross sections of 11 kV OHLs: 100 mm^2 (16.5 km) and 50 mm^2 (19 km). Further data are provided in Table 3.13. For this network model, the total average load is measured at about 1.5 MW during maximum and 0.25 MW during minimum loading conditions.

3.8 Chapter Summary

This chapter has presented the generic models of typical sub-transmission and power distribution systems, providing their equivalent representations at different network locations and voltage levels. First, the work focuses on the development of a comprehensive component database for network modelling, which provides a wide range of specifications and parameters of actual power equipment. Moreover, this chapter reviews the main principles of load modelling for power system analysis, identifies typical load structures at different residential subsectors, and proposes an aggregate residential load model for an accurate network design and operation.

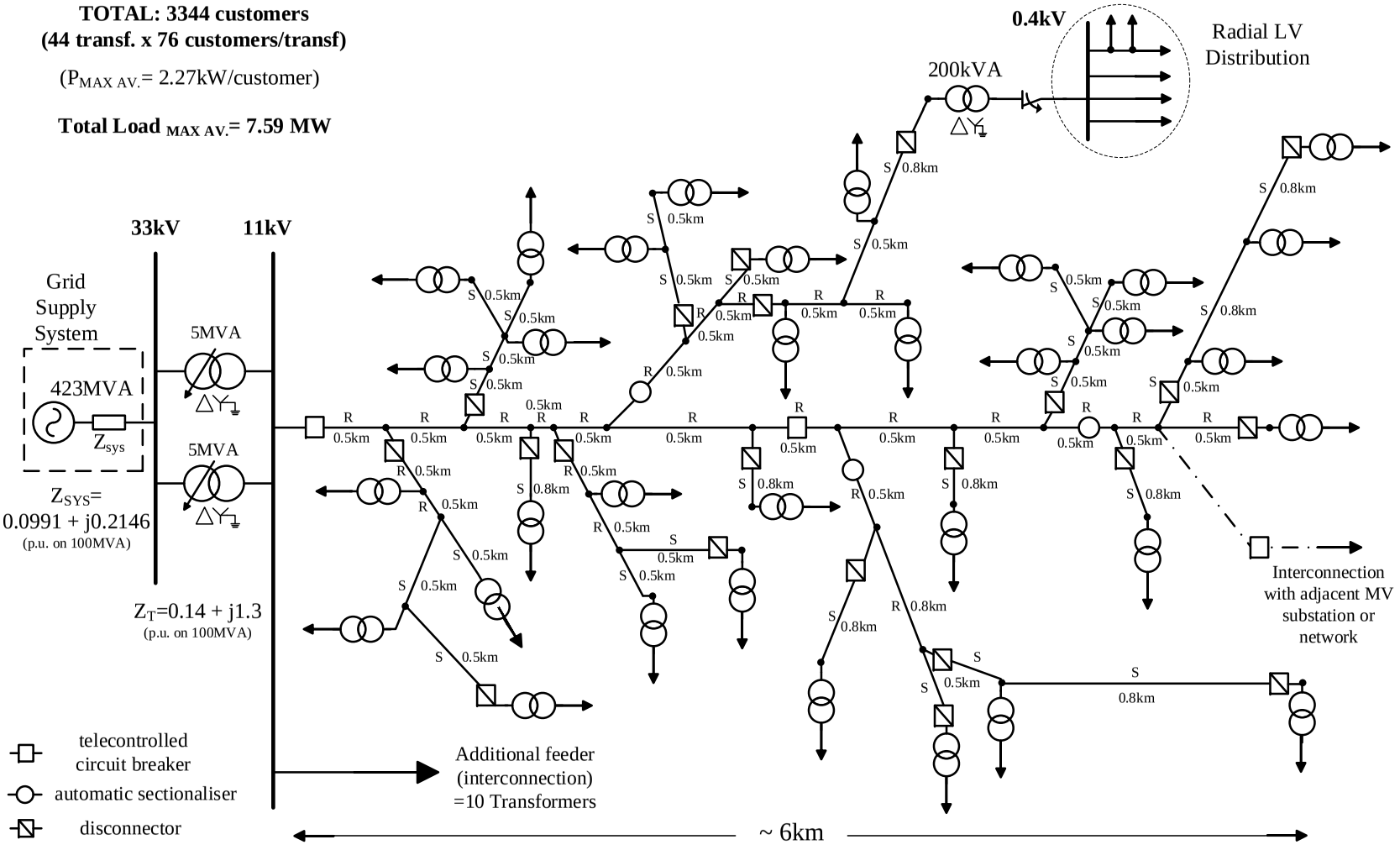

Figure 3.16: Suburban generic MV distribution network model.

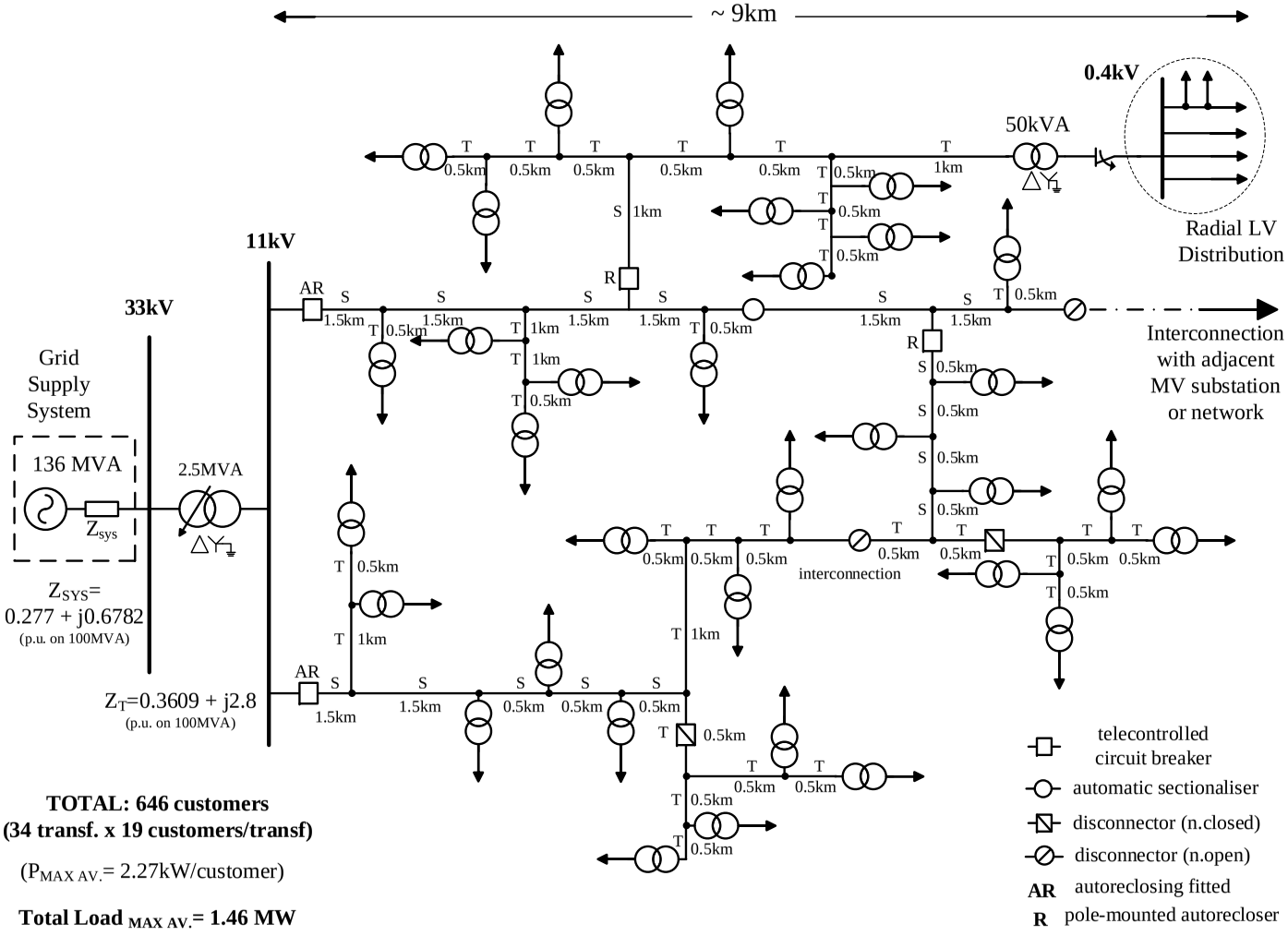

Figure 3.17: Rural generic MV distribution network model.

Chapter 4

Distribution System Equivalents: Aggregation Methodology and Network Analysis

In this chapter, the modelling, aggregation and network analysis of distribution system equivalents is discussed. The aim of this part of the research is to determine an appropriate model for accurate estimation of LV system supply impedances, and to provide a methodology for aggregating LV and MV distribution networks for the correct assessment of quality of supply at bulk supply points, including microgeneration models and distributed generation/storage functionalities. Accurate electrical and reliability equivalent models are therefore formulated for different distribution networks and load subsectors.

4.1 Analysis and Calculation of LV System Supply Impedances

A primary distribution system is designed based on power flows, voltage regulation, power losses and system fault levels. Consequently, the last factor, i.e. fault levels, has been used as the starting point for a proposed methodology to calculate reference impedances and public supply network impedances at different points of the MV/LV distribution system.

This has been done by extracting information from UK DNOs [73, 90, 91, 106, 107, 108, 109] about system fault levels at the secondary busbar of 33/11 kV primary substations, and from this value, calculating the upstream 3-ph system impedance (Z_{SYS}) at that point of the distribution network. Then, using the MV and LV power component database created (Chapter 3), the different impedances of all system components encountered along the route (transformers, MV/LV feeders, etc.) down to the end-user premises (LV supply), have been added up in order to calculate realistic values of public supply network impedances. As primary and secondary distribution configurations vary depending on location and load to supply, in order to decide which components to consider (transformer rating, feeder type/length, etc.), the four different subsectors defined in Section 3.4.3 have been used for these calculations: *Highly-Urban* (metropolitan areas/city centre), *Urban* (city suburbs/bigger towns), *Suburban* (towns) and *Rural* (small villages).

The aim of this work is to provide a wider range of reference supply impedances and network fault levels than those provided in the technical report IEC/TR 60725:2005 [152], which proposes a different methodology for the calculation of public supply network impedances for use in PQ-related analyses. The IEC report [152] provides information and collected values of the supply system impedance (up to the PCC with other LV consumers) from different countries. Therefore, it has been considered as the source of validation for the typical UK values calculated in this section. However, the information provided in the IEC report is not considered appropriate enough, as the impact from the MV system upstream the PCC is neglected. If, for example, the LV network is supplied from a MV circuit of considerable length, e.g. rural areas, the system design may allow for a voltage drop in the MV circuit, which the IEC report does not consider. Therefore, the proposed methodology will provide reference impedance values considering the different network arrangements typically used at the four defined subsectors (from rural to metropolitan areas).

4.1.1 Supply Impedances: Typical Residential Premises

Because there exists a variety of statutory supply voltages, permitted variations and the specifications used by supply authorities for power system plant and equipment, a specific UK analysis with particular service capacities was considered essential. Three-phase, four-wire, distribution systems are used worldwide to supply LV consumers, with nominal voltages in the region of 230/400 V; however, there are considerable variations in the way in which the supplies to individual consumers are connected to 3-ph systems. In the UK, it is unusual to take more than one phase into a residential consumer's premises; consequently, both large loads less than 15 kVA (i.e. $\leq$75A per phase) and lighting circuits are supplied 1-ph (i.e. between line and neutral at 230 V). Accordingly, the typical network arrangements considered for overhead and underground LV power distribution are illustrated in Figures 4.1 and 4.2.

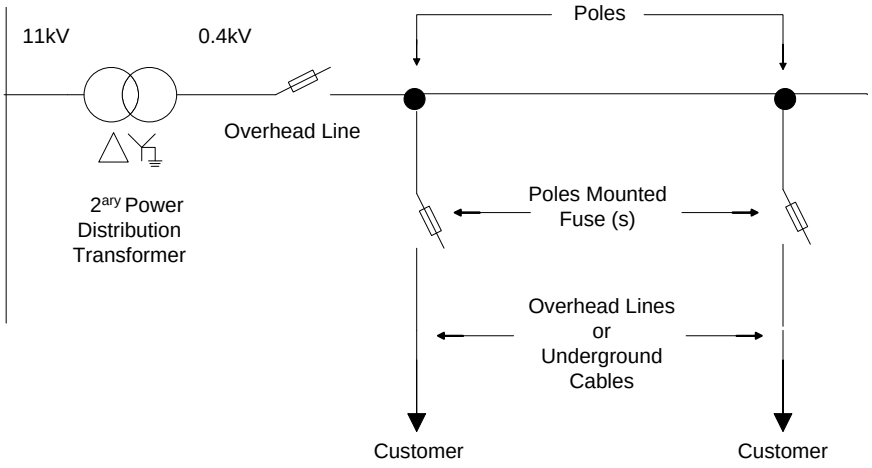

Figure 4.1: Typical arrangement for overhead LV distribution systems [139].

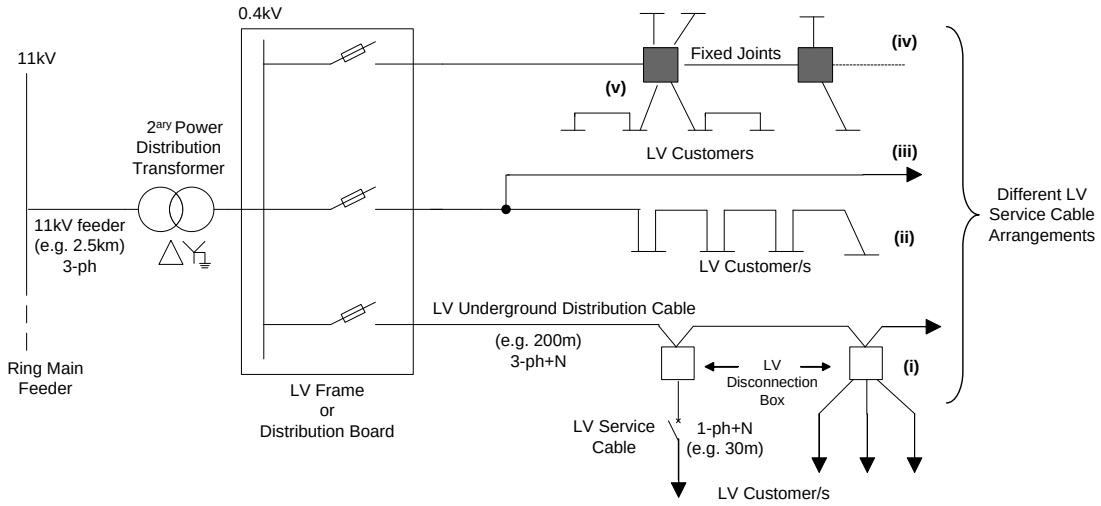

Figure 4.2: Typical arrangements for underground LV distribution systems [139].

Where, in Figure 4.2:

(i) One cable supplies a number of disconnection boxes with fuses, similar to the OHL, so several customers can be supplied from one box;

(ii) Cheaper arrangement owing to the linking connections between customers, but do not permit such individual good protection facilities as the LV disconnection boxes;

(iii) Arrangement for individual large or remote customers, i.e. "dedicated supply";

(iv) Situation with fixed underground joints, which are much cheaper than cable disconnection boxes or cabinets although the selective protection facility is not possible;

(v) Arrangement proved to be cost effective where each customer in a terraced house has his/her own service and this simple arrangement meets the local safety regulations.

4.1.2 UK Case Study: MV/LV Fault Levels and Supply Impedances

The supply system impedance associated with the supply to the premises of a typical residential consumer is determined by the average value of maximum power demand of all the consumers connected to a typical network and the steady state voltage drop at maximum load used to design the system [152]. Therefore, for the different calculations above, four specific UK locations have been selected: Birmingham city centre (highly-urban), Aberdeen (urban), Oban (suburban) and Glencoe (rural). Each location will present different network configuration and characteristics (i.e. underground cable or OHL system), and may not be representative of other similar areas therefore the results obtained should be considered as an indicator for the direct comparison of system impedances and fault levels at different locations in the UK, as well as for the study of the less favourable case, in comparison with the values presented in Table 1 of the IEC report [152].

In order to illustrate the methodology undertaken for the four residential subsectors, the analysis presented in this section focuses on the urban subsector, where several meshed underground

distribution networks operated by SHEPD [90] were selected at different metropolitan areas of Scotland. More particularly, the existing urban network arrangements in three Scottish cities were considered for comparison: Aberdeen, Dundee and Inverness. When comparing the 3-ph system impedances at different 11 kV busbars of these networks (with 100 MVA base), it was important to note the similarity in terms of X/R ratios, fault levels and supply impedances:

-Aberdeen: Z_{SYS}=0.0569 + j0.6822 p.u. (X/R = 12)
-Dundee (LOCHEE): Z_{SYS}=0.0414 + j0.6636 p.u. (X/R = 16)
-Inverness (RAIGMO1A): Z_{SYS}=0.0638 + j0.6889 p.u. (X/R = 10.8)

As the Aberdeen 11 kV busbar presents values around the average X/R ratios in urban areas, it was selected as the case study for the urban subsector. In particular, as shown in Figure 4.3, the 11 kV busbar 'QUEENS1A' at the primary substation 'Queens Lane North' from the Woodhill 33 kV BSP was selected. At that network location, apart from the supply impedance Z_{SYS}, a fault level of 141 MVA was extracted from the system characteristics provided:

Short circuit currents:

3-ph peak make: 22 kA
3-ph rms break: 7.4 kA

Circuit breaker ratings:

3-ph make: 46.9 kA
3-ph break: 18.4 kA

Therefore, the fault level, or 'short circuit apparent power' (S_{SC}) is calculated by applying:

$$S_{SC} = \sqrt{3} \cdot U \cdot I_{3ph-rms-break} = \frac{U^2}{|Z_{SYS}|} = 141MVA \tag{4.1}$$

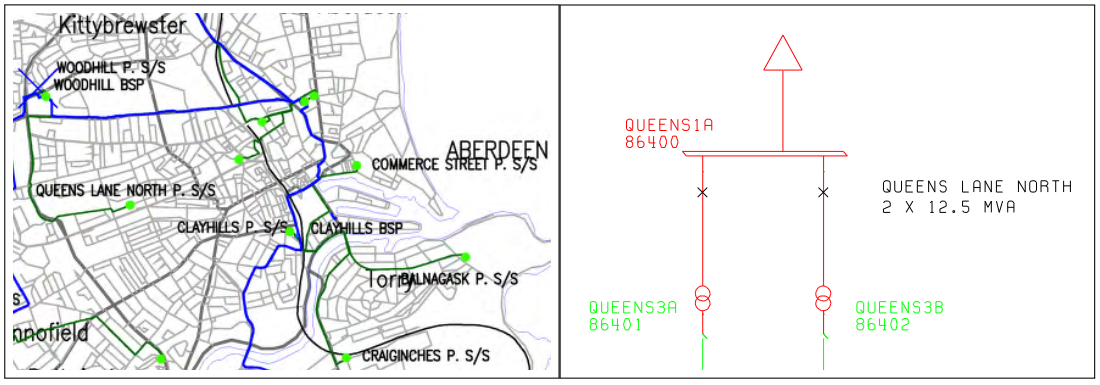

(a) Network map of Aberdeen (Scotland, UK) **(b)** Selected 11kV busbar of Woodhill 33kV system

Figure 4.3: Existing urban network arrangement considered for system fault level analysis (SHEPD) [90].

Once the system fault level and supply impedance are known, the different power components encountered along the route down to the LV supply (PCC) must be included in the analysis. For this purpose, the typical configurations and parameters of MV/LV transformers and distribution lines provided in Sections 3.6 and 3.7 for the four different subsectors were used. In this case, according to the network arrangements presented in Figures 3.11 and 3.15 for the urban subsector, the underground circuit path leading to the end-user premises is composed of:

- 11 kV feeder circuit with high/medium capacity: *185mm^2 3-core XLPE stranded aluminium* (Table 3.13);
- 11/0.4 kV 500 kVA distribution transformer (Table 3.11 and Appendix D.2);
- 0.4 kV mains distribution cable with high/medium capacity: *EPR or XLPE 0.6/1 kV 4x185 Al/Cu (earth)* (Table 3.10);
- 0.4 kV service cable: *PVC or XLPE 0.6/1 kV 1x35 Al/Cu (neutral/earth)* (Table 3.10).

In terms of distribution and cable lengths, the less favourable case has been considered taking the maximum values provided in the network models and Table 3.12. The maximum distribution radius of a 500 kVA transformer in an urban area is approximately 200 m, thus the analysis is based on those residential customers located farthest from the MV substation and trunk feeder (i.e. worst served customers). Figure 4.4 shows the single-line network model for the calculation of different fault levels and supply impedances in a typical UK urban area.

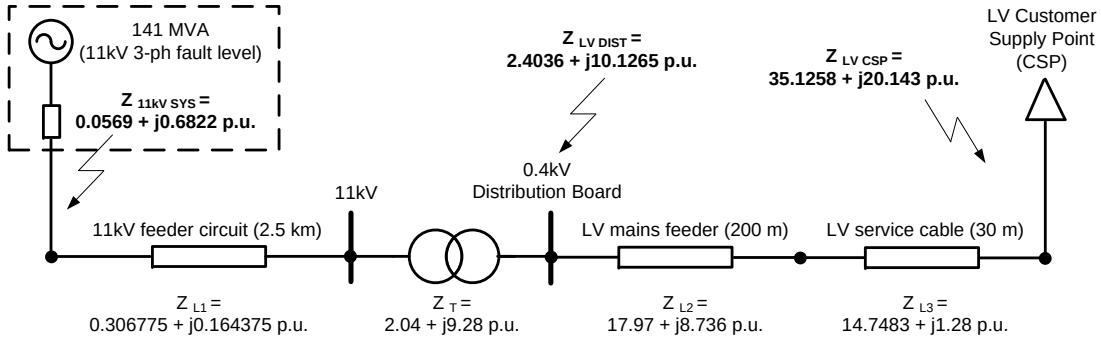

Figure 4.4: Network model for determining MV/LV system fault levels and supply impedances in urban areas.

Finally, as primary and secondary distribution configurations vary depending on the load subsector supplied (e.g. underground or overhead arrangement), Table 4.1 provides the reference results obtained at different points of the distribution system for each subsector. These are fault levels and supply impedances calculated at 11 kV level, i.e. at the secondary busbar of the infeeding 33/11 kV substation, and 0.4 kV level, i.e. at the LV distribution board and customer supply point (CSP). Accordingly, the results obtained at the LV CSP level (last columns in Table 4.1) are directly comparable against the range of values provided for the UK in Table 1 of the IEC report [152], which are provided in Table 4.2 in the form of maximum percentiles (e.g. 98%). Thus, these 'maximum' thresholds are now classified according to network type.

Table 4.1: Comparison of MV/LV system fault levels and supply impedances.

Type of Network	MV (11kV Supply)					LV Distribution Board (0.4kV Supply)					0.4 kV Customer Supply Point (CSP)				
	Fault Level (3-ph)	System Impedance (3-ph)				Fault Level (3-ph)	System Impedance (3-ph)				Fault Level (3-ph)	LV Public Supply Network Impedance			
		R	X	R	X		R	X	R	X		R	X	R	X
	(MVA)	(p.u. on 100 MVA)		(Ω)		(MVA)	(p.u. on 100 MVA)		(Ω)		(MVA)	(p.u. on 100 MVA)		(Ω)	
Highly-Urban	209	0.0290	0.4763	0.035	0.5763	18.71	1.27	5.191	0.00239	0.00973	3.29	27.93	12.07	0.0524	0.0226
Urban	141	0.0569	0.6822	0.0688	0.8255	9.61	2.404	10.127	0.00451	0.01899	2.47	35.13	20.14	0.0659	0.0378
Suburban	112	0.1691	0.8646	0.2046	1.0462	3.84	8.402	24.674	0.01575	0.04626	1.18	73.50	41.53	0.1378	0.0779
Rural	28	0.6379	3.4782	0.7719	4.2086	1.05	45.740	84	0.08576	0.15749	0.28	327.31	127.31	0.6137	0.2387

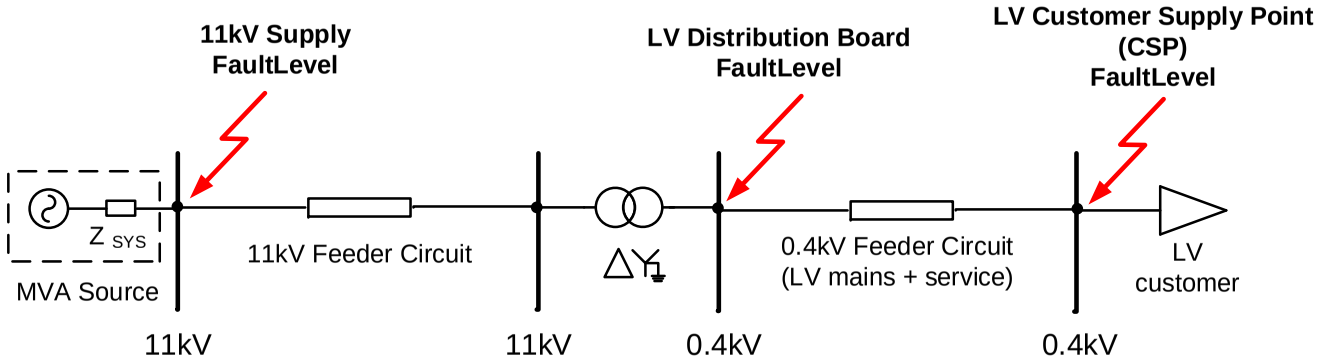

Figure 4.5: Single-line circuit diagram for MV/LV fault levels calculated.

Table 4.2: UK residential consumers' complex supply impedance, in ohms, for 1-ph connections at 50 Hz (IEC/TR 60725:2005) [152].

Country	Percentage of consumers having supply impedances equal to or less than the listed complex values			
	98 %	95 %	90 %	85 %
United Kingdom	0.46 + j0.45 Ω	-	0.25 + j0.23 Ω	-

4.2 Network and Load Aggregation Methodology

Due to their volume and complexity, LV and MV distribution networks are often represented by lumped aggregate models in order to reduce computation times in power system analysis. These aggregate load models, which often provide only information on active and reactive power demands downstream from the point of aggregation (GSP), represent highly dispersed loads and, as the load aggregation proceeds from lower to higher voltage levels, more and more network components should be included, but are typically neglected. In addition, as most of the ES, MG/DG and DSM resources are connected at LV levels, this may have a strong impact on the possible benefits these could have on the QoS, as system functionalities within the lumped parts of the network are usually inaccurately assessed. For the analysis of new 'smart grid' functionalities, these should be correctly represented in the aggregate models.

Accordingly, this work implements a new methodology for the aggregation of system loads at LV and MV level, allowing for the ongoing and anticipated changes in the load structure and the supplying networks to be directly incorporated in the network analysis. As explained in Section 3.4, this part of the thesis builds on previous work in [19, 21, 30, 31], where component-based LV load models are built using the measurements, statistical information, and other available data on the active/reactive power demands. Figure 4.6 shows a "flow chart" illustrating the aggregate load modelling approach used in this thesis [19, 30]. This methodology also includes the connection of LV MG, which is discussed in the following sections. In addition, these load models can be modified to examine the impact of any changes in the load mix, e.g. due to the implementation of specific DSM schemes [21, 31].

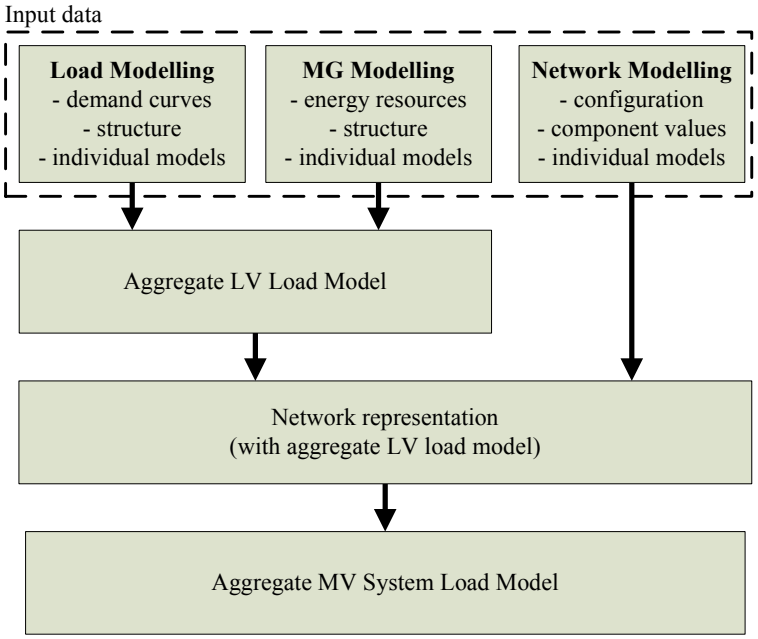

Figure 4.6: Overview of the aggregation methodology [41].

4.2.1 LV/MV Distribution Network Equivalents

After identifying and developing the generic models of LV and MV distribution networks, as well as their typical individual components in Sections 3.6 and 3.7, their aggregated representations (same-type and mixed-type aggregates) have been derived for each load subsector (i.e. HU, U, SU and Ru) in order to build a network aggregation methodology, capable of providing accurate and flexible network equivalents for a comprehensive steady state QoS analysis. For the purpose of investigating the aggregate network and load model characteristics, the level of detail afforded by the networks in Sections 3.6 and 3.7 is not necessary, therefore these network models may be reduced to a single-line equivalent impedance Z_{eq} in order to reduce system complexity and calculation times.

The proposed network aggregation methodology was developed drawing on work described in [132] and [153], where a technique for reducing a radial network into a single line equivalent impedance was developed for fast computation of load-flow calculations and voltage stability analysis of radial distribution networks. Using the power component impedances from the LV and MV generic networks presented in previous sections, the aggregation method presented in this thesis is applied in reverse order, as it starts aggregating individual network components from the point of consumption up to the supplying primary (MV) or secondary (LV) substation.

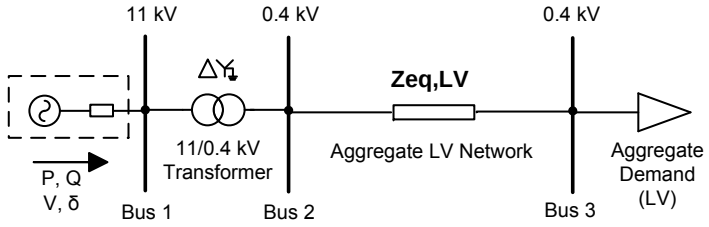

(a) lumped LV distribution network: equivalent impedance (Zeq,LV)

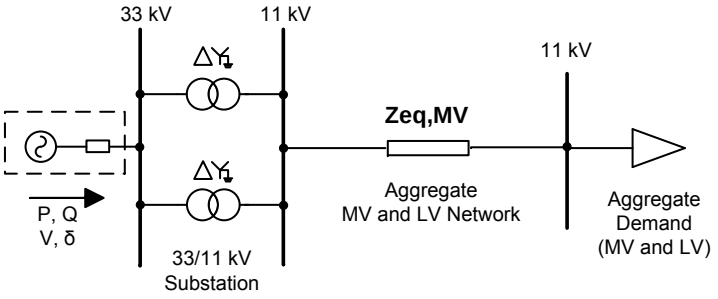

(b) lumped MV/LV distribution network: equivalent impedance (Zeq,MV)

Figure 4.7: MV and LV equivalent network configurations.

Figure 4.7 shows the equivalent network schematics for both MV and LV distribution systems, where the equivalent impedances $Z_{eq,LV}$ and $Z_{eq,MV}$ represent their overall network impedance.

For each load subsector, as the characteristics of the MV distribution network strongly depend on the supplied LV system, the first step was to calculate the aggregate network equivalents for the generic LV distribution systems presented in Section 3.6. Thus, the resulting $Z_{eq,LV}$ represents the overall LV network impedance and the aggregate demand is equal to the sum of all residential LV loads in the lumped system. The different values of $Z_{eq,LV}$ for each load subsector are therefore used in combination with their corresponding MV network parameters (Section 3.7) to derive $Z_{eq,MV}$ in each case.

The established technique can be summarised in two steps:

1. Calculate the equivalent impedance at every load location in the network. This is the summation of all impedances up to the network location (i.e. series/parallel feeders), and can include multiple customers at the same bus. This is expressed by (4.2).
2. Determine the overall network impedance by summing all equivalent impedances calculated in Step 1. This step is described by the equation in (4.3).

$$Z_{location}(i) = \sum_{n=1}^{N} Z_{customer}(n) \tag{4.2}$$

$$Z_{eq} = R_{eq} + jX_{eq} = \sum_{i=1}^{I} Z_{location}(i) \tag{4.3}$$

where: $Z_{customer}(n)$ is the network impedance up to customer n at location i, $Z_{location}$ is the sum of all customer impedances at location i, N is the number of customers, I is the number of network locations and Z_{eq}, R_{eq} and X_{eq} are the equivalent impedance, resistance and reactance.

All the detailed network models presented in this thesis, both LV and MV, have been tested and modelled using PSSE software for steady state analysis (active and reactive power flows, voltage stability, etc.). Therefore, this serves as a strong basis to prove that the network equivalent impedances provide the same results when modelled for identical purposes. As shown in Figure 4.7, particular attention has been given to steady state conditions at the system supply point (Bus 1), in order to make sure that power flows, voltage magnitude and power angle remain unchanged from the detailed network models. Therefore, the fundamental steady-state network characteristics are preserved when the aggregation methodology is applied.

Table 4.3 provides the calculated values of the equivalent impedances for the LV (0.4 kV) and MV (11 kV) networks in each load subsector. These aggregate network models, which effectively reduce required computation times in power system analysis, were used to develop improved MV aggregate load models considering different contribution from residential and commercial demand [19, 29, 30, 32]. The procedure starts with component-based models of main load categories at LV level, and then incorporates the typical LV/MV network configurations to obtain accurate representation of the aggregate demand at higher voltage levels (e.g. 11 kV or 33 kV). In addition, the aggregation methodology also served to analyse the impacts of different DG, MG and DSM scenarios on network QoS performance [21, 29, 31, 32].

Table 4.3: MV and LV equivalent network impedances per load subsector.

Subsector	LV distribution network		MV/LV distribution network	
	$Z_{eq,LV}(0.4kV)$		$Z_{eq,MV}(11kV)$	
	$R(p.u.)$	$X(p.u.)$	$R(p.u.)$	$X(p.u.)$
	(on 100 MVA base)			
Highly-Urban	1.079	0.628	0.075	0.155
Urban	3.337	0.915	0.137	0.225
Suburban	8	2.164	0.484	0.775
Rural	12.665	1.624	2.008	2.962

4.2.2 Validation of Equivalent Network Methodology

In order to check that the fundamental steady-state network characteristics are preserved with the proposed aggregation methodology, an additional validation of the equivalent network impedances is undertaken for load modelling purposes. A comparison of the MV load characteristics (i.e. at Bus 1 - Figure 4.7(a)) using the detailed network models, presented in Sections 3.6 and 3.7, and the equivalent network impedances from Table 4.3 was performed. For this analysis, the urban generic LV network model proposed in Figure 3.11 is used for validation against the equivalent LV network configuration shown in Figure 4.7 (a). Accordingly, the detailed LV network (Figure 3.11) is populated with different load models in order to simulate the 24hr stochastic variations of individual households, i.e. detailed ZIP models capturing the user behaviour with a 10min resolution (1440 points per day). These residential load models, based on the information provided in Section 3.4, were developed in research undertaken out of the scope of this thesis, so do not require detailed explanation, as its only purpose to this research is to validate the network aggregation methodology, i.e. to allow for the connection of the aggregate LV load model to the equivalent network impedance. Further details of the load modelling approach for individual households is available in [41, 154].

On the other hand, as the supplied demand of the equivalent LV network (Figure 4.7 (a)) is only represented by one load point, its aggregate load parameters (composed of all individual households in the system) are represented according to the aggregate LV load model introduced in Section 3.4.2. For both networks of analysis, the supply voltage magnitude is varied in the range of 0.8-1.2 p.u. at each simulation time step, and the active and reactive power responses are measured to calculate the resulting load model coefficients. The more detailed polynomial/ZIP representation of load is used to directly compare the two sets of load model parameters obtained. The values in Figure 4.8 confirm the ability of the equivalent network impedance to retain the performance of the detailed network model. This is an important result for this research, as it allows for the direct connection of an aggregate LV load model to the equivalent network impedance, which significantly reduces the modelling effort without introducing an error, and allows for performing complex reliability analysis in a more effective way.

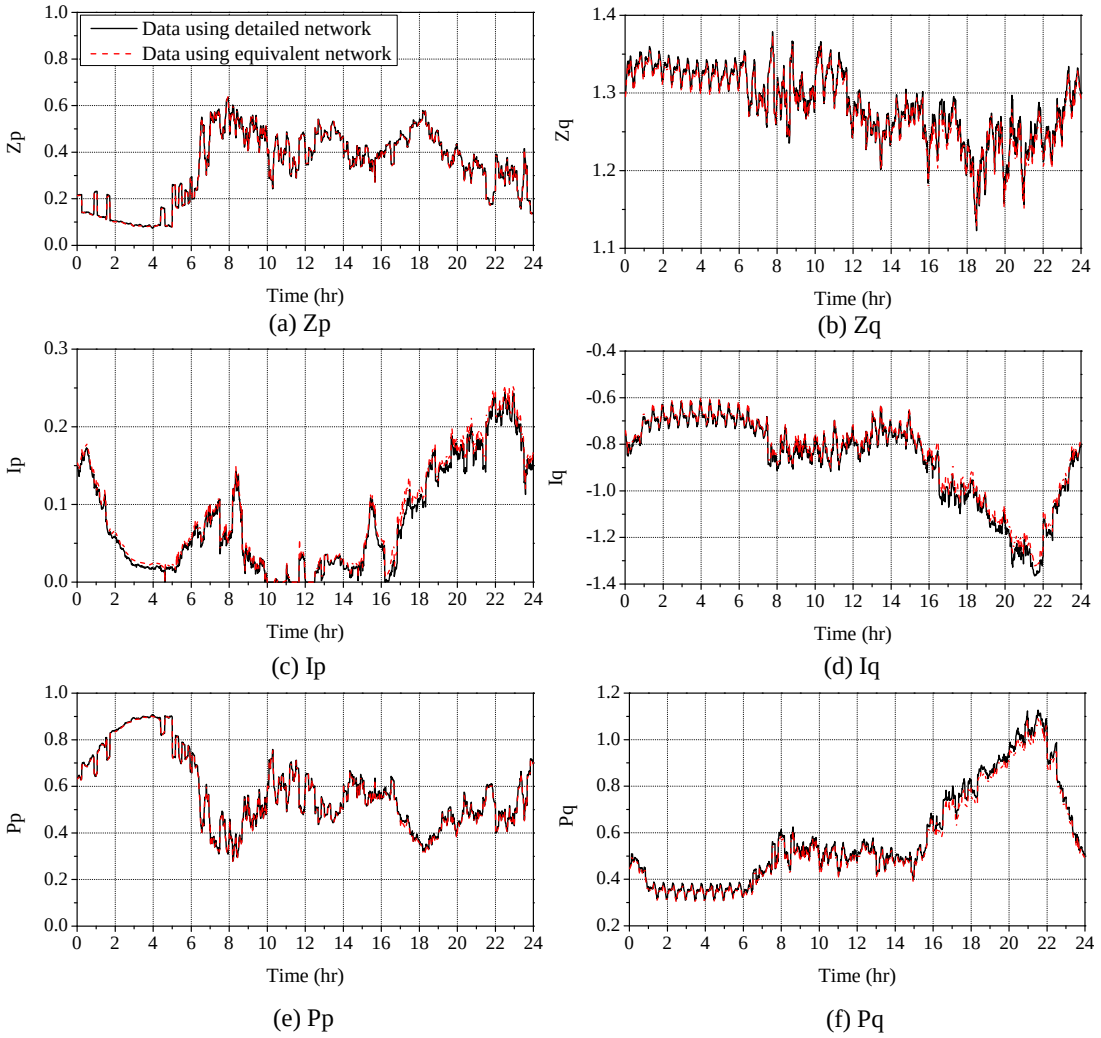

Figure 4.8: Comparison of example MV polynomial/ZIP load model coefficients obtained using detailed and equivalent network models.

4.2.3 Network Influence on Aggregate Load Model Parameters

When developing the MV load model, the electrical behaviour of the aggregate MV load will be a combination of the actual load and the network. As current flows through the network impedances, the corresponding changes in active and reactive power flows are attributed to the network elements. For steady-state analysis, the current flow in the network, and, therefore, the aggregate MV model, is influenced by the connected LV load. For dynamic analysis, which is not considered in this thesis, the network effect will be more complex due to the operation of the various control and protection devices.

To illustrate the effect of the network on the load model as the point of reference moves from LV to MV, a simple case study is presented. In the following examples, the reactive power characteristics of the load models are used to demonstrate the network contribution to the MV

load model, as the changes are more pronounced for reactive power than active power, due to the large reactance of the secondary distribution transformer. A voltage sweep is performed at the MV side and the values of reactive power at Bus 1, 2 and 3 (as denoted in Figure 4.7 (a)) are recorded, with the network influence being obtained as the difference between the values recorded at Bus 1 and Bus 3.

The most simple scenario is if the load is constant impedance type ($n_p = n_q = 2$). In this case, the whole system (network plus load) will also behave as the constant impedance type of the load. This is shown in Figure 4.9 (a), with additional values of exponential coefficients for all the considered load scenarios included in Table 4.4. If the LV load connected at Bus 3 is constant current type ($n_p = n_q = 1$), the current in the network is constant and, as the network components have a constant impedance, the network behaves as constant power type ($n_p = n_q = 0$). As the aggregate MV model includes both the influence of the network and the LV load, the corresponding exponential coefficient will lie between 0 and 1, depending on the percentage contribution of network and load to the total demand. If the LV load at Bus 3 is constant power ($n_p = n_q = 0$), the network current is inversely proportional to the network voltage and the network components behave similar to constant impedance type with negative characteristics (i.e. n_p and $n_q \approx -2$) as larger than 1 p.u. currents will be demanded by the constant power load type for supply voltages lower than 1 p.u., resulting in an increase of network losses. Therefore, the resulting MV load model will have exponent between 0 and -2.

Table 4.4: Values for example of network influence on the aggregate MV load model.

Bus	Connected load			
	Z	I	P	Mixed
1	2.00	0.84	-0.56	0.79
N	2.00	0.00	-2.37	-0.12
3	2.00	1.00	0.00	1.00

where: N represents the combined effect of the supply network and transformer.

Finally, when the LV load is composed as a mix of the three general load types, as is often the case in reality, the network components will behave as a mixture of constant impedance (with positive and negative characteristics) and constant power types. Therefore, when a mixed LV aggregate load is connected, the effect of the network components is to generally reduce the values of the exponential coefficients of the MV aggregate load model. In this example, the mixed load is taken with an equal contribution of the three load types, therefore the aggregate LV characteristic is effectively that of the constant current load. However, the values in Table 4.4 shows that the network influence is not the same as for constant current loading condition, and the aggregate MV load model coefficient value is also lower for the mixed load scenario.

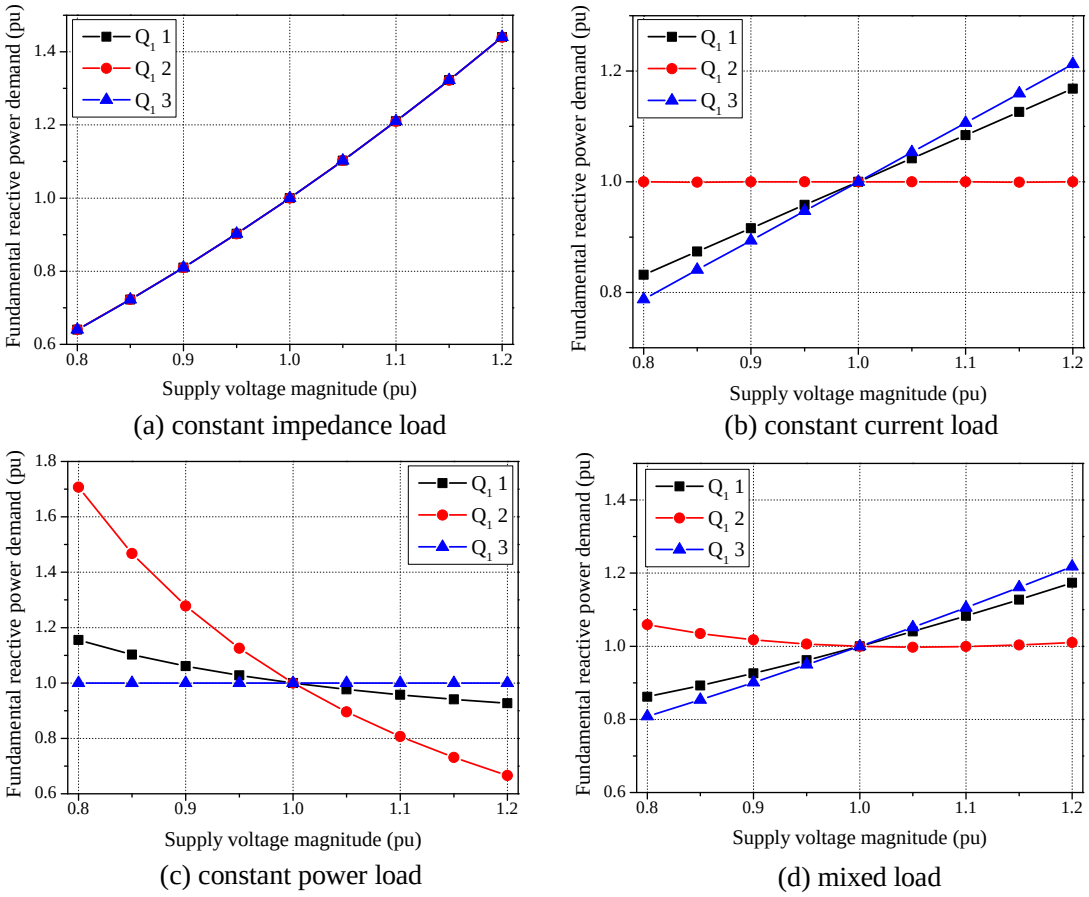

Figure 4.9: Network influence on MV aggregate load characteristics (reactive power).

4.2.4 MV Aggregate Load Model

The LV aggregate residential load model, whose characteristics and details were previously specified in Section 3.4.2 for average loading conditions, is connected to the urban aggregate network in order to obtain the MV (11 kV) load model. This is done by using the supply transformer to instigate a step changes in voltage. Further details for this approach, as well as for the methods used to develop measurement-based load models, can be found in [19, 41, 155].

Accordingly, a comparison between the aggregate LV and MV load characteristics is shown in Figure 4.10, with model values presented in [19, 41]. The influence of the network is clearly visible on the MV load representation, where a reduction in model exponential coefficient values at the higher voltage level is observed. As expected, the effect on reactive power coefficient is more pronounced because of a relatively large reactance of the network components (primarily the reactance of the supply 11/0.4 kV transformer). The effect on active power coefficient is small, as the resistive/active power losses in the network are low in comparison with the active power demand. The network influence will also reduce the displacement power factor of the load, as viewed from the MV level, which is attributed to the reactance of secondary distribution transformer and is most pronounced during the evening peaks.

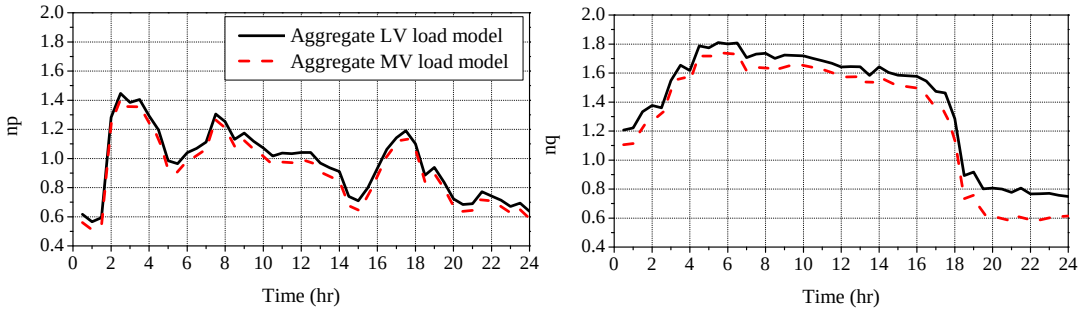

(a) active power **(b)** reactive power

Figure 4.10: Comparison of MV and LV aggregate load models for UK urban load subsector example, expressed in exponential form.

4.3 Modelling and Aggregation of the MV and LV Networks

When the network aggregation methodology is applied up to the 33 kV system level, i.e. the interface GSPs between the transmission and distribution networks, the total demand contribution at each of these GSPs is a combination of residential, commercial and industrial load sectors (along with other load types with a smaller contribution to the overall demand, such as transportation, street lighting, agriculture, public administration etc.) depending on node location. Therefore, in order to build an accurate equivalent representation of the aggregate network model at each GSP, a load identification methodology was required to disaggregate the electrical demand data at the GSPs into different load sectors. Full details of the modelling approach applied for the load identification methodology and its validation are not reproduced here, instead, the reader is referred to [40], where the MV/LV network aggregation methodology is used to identify the portion of the load at each GSP node potentially available for DSM studies. For this purpose, the analysis uses the aforementioned component-based models of typical residential and commercial UK loads [19, 41]. Accordingly, this combined research and its outputs were also jointly presented by the authors in [26, 29, 32].

In order to build an equivalent representation of the aggregate network and load at the 33 kV level, this work analyses electrical demand data measurements, recorded at all of the 33 kV GSPs in the SPEN network region in the form of half hourly measurements of active and reactive power demands, over the course of one full year [1]. The different aggregate ZIP/exponential model representations will be calculated at all the 33 kV GSPs, which are illustrated by the red squares in Figure 4.11, showing the distribution network in the Edinburgh city area [2].

1. The recording year used by the DNO runs from 1^{st} April to 31^{st} March.
2. The overall network area used in the study is much larger, comprising of 89 GSPs across the entire Central and Southern Scotland region.

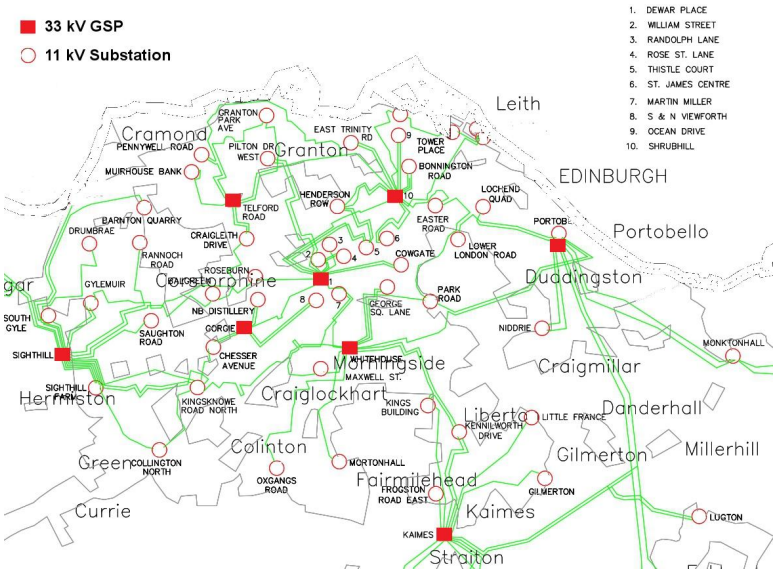

Figure 4.11: Map illustrating the 33 kV distribution system in the Edinburgh city region [91].

As it is not feasible to fully model the distribution network at each GSP due to the modelling and computing effort necessary, instead, for each of the 89 GSPs in the SPEN system, the supplying network was classified according to the four distribution network subsector equivalents defined in Section 4.2.1 of this thesis (i.e. HU, U, SU and Ru).

4.3.1 Definition of Supplying Network Subsectors

The classification of GSPs is based on the MVA ratings of the primary distribution transformers, using the data given in the SPEN Long Term Development Statement [91]. The primary transformer ratings (33/11 kV, or less commonly, 33/6.6 kV in UK systems) are used for the classification since, of all the distribution network parameters, these provide the best indication of the capacity and ratings of the downstream MV and LV network components and connected load. For this purpose, the typical parameters and MVA ratings of 33/11 kV transformers per load subsector, provided in Table 3.14, are used.

In all of the analysis shown, the classification of subsector (HU/U/SU/Ru) was made at the GSP level. The following simplifying assumption was made: at each GSP, all feeders were assigned the subsector load type. In reality, however, individual GSPs often serve a mixture of subsectors.

Table 4.5 shows an example of one GSP in the SPEN system, Govan (GOVA), where there is a mixture of HU, U and SU feeders. The median value of the transformer MVA rating at all feeders was used to classify the GSP. In the case of GOVA, the median rating is 15 MVA, so it is assumed that the GOVA GSP (and therefore, all connected feeders) have urban-subsector characteristics. This simplification greatly reduces the complexity of the calculation of the

MV network equivalents. The results of this subsector classification for all nodes in the SPEN system are provided in Table E.1, Appendix E.

Table 4.5: Example of MV system classification at GOVA bus [91].

Primary substation	Secondary substation	Tx	From	kV	To	kV	Vector Group	Transformer Rating (MVA)
Govan	CARDONALD	1	CARDT1	33	CARD10	11	DYN11	11.5
	CARDONALD	2	CARDT2	33	CARD20	11	DYN11	11.5
	ELIZ. ST	1	ELIST1	33	ELIS10	6.6	DYN11	10.0
	ELIZ. ST	2	ELIST2	33	ELIS20	6.6	DY11	10.0
	HELEN ST	1	HELST1	33	HELS10	6.6	DYN11	20.0
	HELEN ST	2	HELST2	33	HELS20	6.6	DYN11	20.0
	LINTHOUSE	1	LINTT1	33	LINT10	11	DYN11	7.5
	LINTHOUSE	2	LINTT2	33	LINT20	11	DYN11	7.5

The equivalent impedances for LV and MV networks per load subsector, provided in Table 4.3, can be applied directly in the analysis. In the GOVA example, the Urban $Z_{eq,LV}$ can be used to represent the LV supplying network (i.e. 0.4 kV components), and the Urban $Z_{eq,MV}$ to represent the MV supplying network (i.e. the secondary transformer, and all other 11 kV or 6.6 kV components downstream).

4.3.2 Modelling the Interconnecting 33 kV Networks

A similar classification procedure was used to find equivalents for the interconnecting 33 kV networks. These interconnecting networks typically consist of several 33 kV feeders running from the GSP to the 33 kV/11 kV (or in some cases, 33 kV/6.6 kV) primary transformers. Figure 4.12 shows a typical urban interconnecting 33 kV network (Govan GSP).

Generally, highly-urban and urban 33 kV networks serve sizeable loads and hence have high ratings, with a large proportion of underground cables. On the other hand, suburban and rural 33 kV networks are composed mostly of OHLs with smaller capacities. Rather than modelling all of the 33 kV networks throughout the SPEN system, four "characteristic" nodes on the SPEN system were selected to represent the interconnecting networks for each of the four subsector classifications:

- Highly Urban (HU): WGEO - West George St.
- Urban (U): GOVA - Govan
- Suburban (SU): KAIM - Kaimes
- Rural (R): NETS - Newton Stewart

These 33 kV networks, including OLTC primary transformers, were built in detail using PSSE software, in order to quantify the typical effects of the MV network on real and reactive power losses at the four load subsectors. This approach is based on the assumption that the selected sample nodes for each subsector (HU/U/SU/Ru) are representative of all other nodes in the

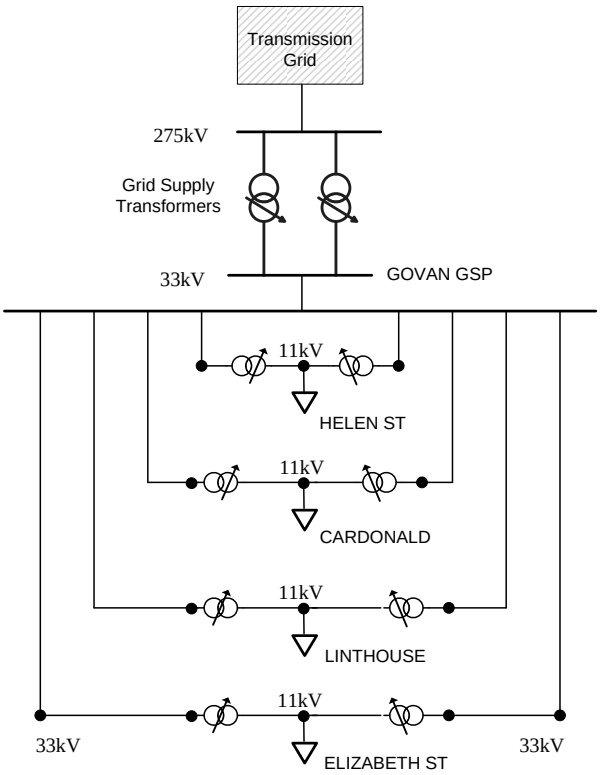

Figure 4.12: Govan GSP 33 kV network [91].

system with the same classification, e.g. all other urban loads have similar characteristics to the selected GOVA node.

This greatly reduces the modelling effort required, as only the four "characteristic" (i.e. generic) nodes are simulated in detail. The modelling of the interconnecting networks incorporates the action of the primary OLTC transformers (33/11 kV), which regulate the substation voltage within the specified $\pm 6\%$ range. Accordingly, the results obtained at each time step in the simulation are taken after any automatic adjustments of the transformer taps was performed (any necessary OTLC adjustments are typically carried out within timescales of tens of seconds to several minutes).

4.3.3 Aggregation of 33 kV Networks

The load components, along with the interconnecting networks are aggregated at the GSP level to produce a simplified, aggregate load model at each HV network bus, which fully incorporates DSM loads. This load model can be reproduced throughout the network as required, and is flexible, since the component-based approach allows for changes in the load structure and composition, e.g. due to a DSM action, to be implemented easily in the network analysis.

The end result of the aggregation is that the component-based load models (expressed in polynomial ZIP form), the LV and MV equivalent impedances, and the interconnecting 33 kV

network are replaced by a single aggregate ZIP/exponential representation at the GSP, for each time step in the simulation. Figure 4.13 illustrates the general methodology in a flow diagram.

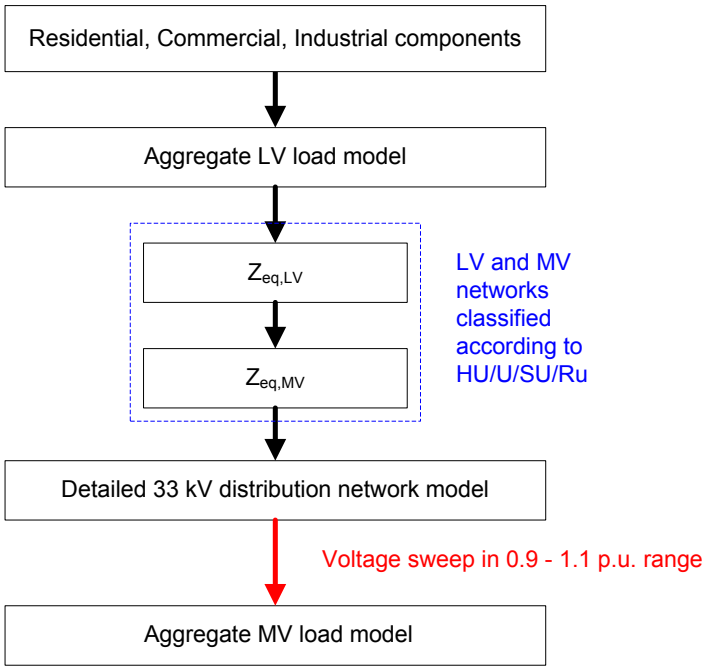

Figure 4.13: GSP load aggregation methodology.

The method applied for finding aggregated ZIP/exponential model coefficients is similar to that used in [19]. The main steps carried out for each network node can be summarised as follows:

- According to the contribution of each of the main demand sectors (i.e. residential, commercial and industrial) identified in [40], the aggregate LV load models for each sector are combined;
- The appropriate detailed network model is selected from one of the four subsectors HU/U/SU/Ru;
- The LV ZIP load models, along with the equivalent impedances, $Z_{eq,LV}$ and $Z_{eq,MV}$ are connected at the secondary substations;
- A voltage sweep in the range of 0.9-1.1 p.u. is carried out by adjusting the voltage at the GSP in increments of 0.025 p.u. and calculating the power flow;
- The active and reactive power flows at the GSP are recorded for each voltage increment;
- The exponential and polynomial ZIP coefficients at the 33 kV node are found by least squares estimation fitting of the active and reactive power results.

4.3.4 Aggregated Polynomial and Exponential Load Models Incorporating Network Effects

The load aggregation methodology outlined in Figure 4.13 describes the load characteristics and their composition variations over the course of the day, expressed in the form of polynomial or exponential load models (see Section 3.4.1). For the first output form, the analysis is carried out at each half-hourly interval, resulting in a time-varying set of ZIP coefficients which incorporate the actual effects of the network:

$$P_n = P_{o,n}\left[Z_{p,n}\left(\frac{V}{V_o}\right)^2 + I_{p,n}\left(\frac{V}{V_o}\right) + P_{p,n}\right] \quad for \quad n = 1,...,48 \tag{4.4}$$

$$Q_n = Q_{o,n}\left[Z_{q,n}\left(\frac{V}{V_o}\right)^2 + I_{q,n}\left(\frac{V}{V_o}\right) + Q_{q,n}\right] \quad for \quad n = 1,...,48 \tag{4.5}$$

where: P_n, Q_n are the actual active and reactive powers drawn by the load at each time step n, V is the actual supply voltage, V_o is the nominal supply voltage, $P_{o,n}$ and $Q_{o,n}$ are the nominal/rated active and reactive powers, and $Z_{p,n}$, $I_{p,n}$, $P_{p,n}$, $Z_{q,n}$, $I_{q,n}$, $P_{q,n}$ are the polynomial, or "ZIP" model coefficients. The ZIP coefficients are constrained so that they must sum to unity in both the active and reactive cases.

In order to illustrate an example of the outputs from the aggregation process, the active and reactive power ZIP coefficients obtained from the aggregate 33 kV load model at one selected node (Bathgate - BAGA) are shown in Figure 4.14.

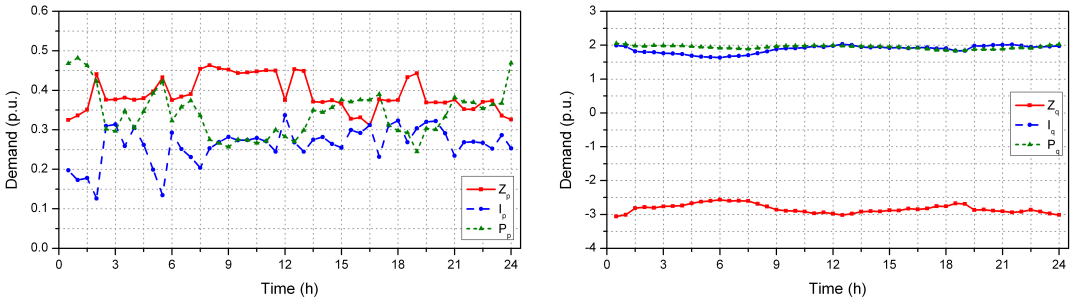

(a) Active power **(b)** Reactive power

Figure 4.14: Polynomial ZIP model coefficients calculated at BAGA 33 kV node.

For the purposes of displaying and comparing the load models in a graphical format, the exponential load models ((4.6) and (4.7)) are often preferred, since these make the results of the analysis easier to visualise. The exponential models are also fitted using least squares estimation, after carrying out the voltage sweep at 33 kV, and are illustrated for the BAGA node in Figure 4.15.

$$P_n = P_{o,n}\left(\frac{V}{V_o}\right)^{n_{p,n}} \quad for \quad n = 1,...,48 \tag{4.6}$$

$$Q_n = Q_{o,n}\left(\frac{V}{V_o}\right)^{n_{q,n}} \quad for \quad n = 1,...,48 \tag{4.7}$$

where $n_{p,n}$ and $n_{q,n}$ are the exponential model coefficients. Figure 4.15 shows the resulting n_p and n_q values for loading conditions corresponding to the maximum winter day. These aggregated 33 kV GSP load models have been applied in transmission network analysis, which is not the scope of this PhD thesis, thus the reader is referred to [29, 32, 40].

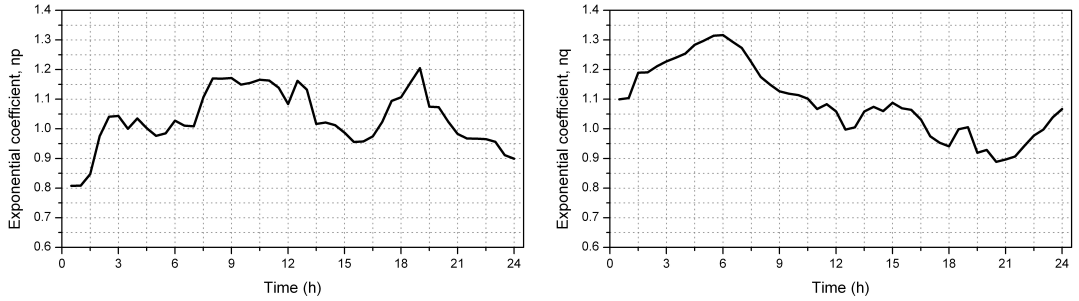

(a) Active power **(b)** Reactive power

Figure 4.15: Exponential coefficients calculated at BAGA 33 kV node.

4.4 Inclusion of Micro-Generation Models in Network Aggregation Methodology

As already discussed, current distribution systems are designed such that performance of the MV and LV networks have a dominant impact on the quality of service seen by the end customers. A potential solution to this problem, which will allow the deferral of capital investment for network area reinforcement, is the end use of renewable-based micro and small-scale generation technologies, connected in parallel to LV networks. Solar-photovoltaic (PV) and small-scale wind turbines (WTs), which are the most common in the majority of European countries [3], will be analysed in this research in combination with energy storage (ES) applications. It is estimated that the installed capacity of small-scale wind generation in the UK could be as high as 1.3 GW by 2020 [156], and the European Union has recently set a target of 400 GW of installed PV capacity by 2020 [157].

As these technologies will be installed and operated in parallel with the LV network load, they will have an impact on the performance of the LV network and will alter the aggregate electrical characteristics (as viewed from the MV load supply point). This clearly indicates the

3. Combined heat and power (CHP) systems will not be considered for analysis in this research

importance of including MG effects in the development of MV aggregate network/load models. Moreover, when MG systems are present in high numbers, e.g. in a large residential area, or as an aggregate representation at a MV BSP, the aggregate effects and potential benefits of MG on network reliability and supply quality can be significant [132, 158].

Therefore, as presented in the flowchart in Figure 4.6, this work studies the inclusion of MG within the network/load aggregation methodology. As one of the aims of this research is primarily interested in the development of aggregate and equivalent network models for power system analysis, only brief details of the MG modelling effort are included here (full details are available in [39]). It is shown that even a modest MG penetration of 10% may have a considerable impact on the electrical characteristics of the aggregate load/demand in which it is included.

4.4.1 Modelling of Micro-Generation

Correct assessment of renewable-based MG should take into account high levels of temporal and spatial variations of renewable energy resources (RER), which change on both short-term scale (e.g. minute-by-minute, or hourly variations) and medium to long-term scale (e.g. daily, weekly, or seasonal variations), as well as from one geographic or network location to another. Three datasets are required to include MG in the aggregate model development process:

- MG energy resources: which specifies the available primary energy resources (e.g. wind) for conversion to power generation.
- MG structure and composition: which specifies the contributions of different MG technologies to the total installed MG capacity and their actual outputs.
- Generic models of MG: representation of the installed MG technologies in a form suitable for use in power system analysis.

These datasets, covering a wide range of MG technologies (i.e. small-scale wind and PV generation systems), are fully described in [39] and are used in this thesis for different power system analyses in combination with the proposed generic networks. Although the installed MG technology will be determined by the locally available resources, the effect of MG on the electrical characteristics of the aggregate network/load are investigated using only small-scale wind energy systems, defined as less than 2.5 kW [39], in this research. This MG technology was selected to allow for collaboration with parallel research in [28].

Assessment of Input Renewable Energy Resources (RER) and MG Power Outputs

Daily and seasonal variations of available RER, measured at several locations in the city of Edinburgh, Scotland, are used to identify ranges of input wind and solar energy resources for a typical day in spring season (21^{st} of March), corresponding to average system loading conditions. For the chosen day, wind speed measurements, taken for the previous 14 days and subsequent 14 days, are processed to determine the expected variations of available wind

resources at the given location. In the case of solar irradiance, measurements are taken to cover a range of 3 months (21^{st} of March - 21^{st} of June). Accordingly, based on the described resource assessment, the corresponding power outputs from the considered MG technologies (micro and small PV and wind-based systems) are calculated following the methodology presented in [31] and [39], and are illustrated in Figure 4.16. The analysis uses aggregate models of micro/small WTs described by (4.8), which are based on four generic WT models developed in [28].

$$P_{WTagg} = -10.3v + 3.83v^2 - 0.11v^3 \tag{4.8}$$

where, v is the input wind speed in m/s and P_{WTagg} is the power output of the aggregate wind-based MG model at a given wind speed (for $v \geq 3$ m/s), in W/m^2 of the WT swept area. In addition, PV systems are represented by an equivalent generic aggregate model, also presented in [31] and [39], and described by (4.9).

$$P_{PVagg} = 0.127\left(1 - e^{-0.008(S_{irr}-60)}\right) \tag{4.9}$$

where, S_{irr} is the input solar irradiance (W/m^2) of the PV panel and P_{PVagg} is the electrical power output (given in W_e/m^2) of the aggregate PV MG model at a given solar irradiance (for $S_{irr} \geq$ 60 W/m^2). This approach simplifies the problem of aggregating WT/PV MG systems by using only one equation that depending on either the input wind speed or solar irradiance can provide the corresponding power output. Thus, the modelled PV systems will reach maximum power output (1 p.u.) for an input solar irradiance of 1 kW/m^2 (keeping it constant for higher values), while the WT systems generate rated power for wind speeds greater than 12 m/s. For further analysis, the same RER assessment was also applied [39] to calculate minimum, maximum and average power outputs of aggregate WT/PV MG systems for the rest of yearly seasons (i.e. Summer, Autumn and Winter), corresponding to different loading conditions.

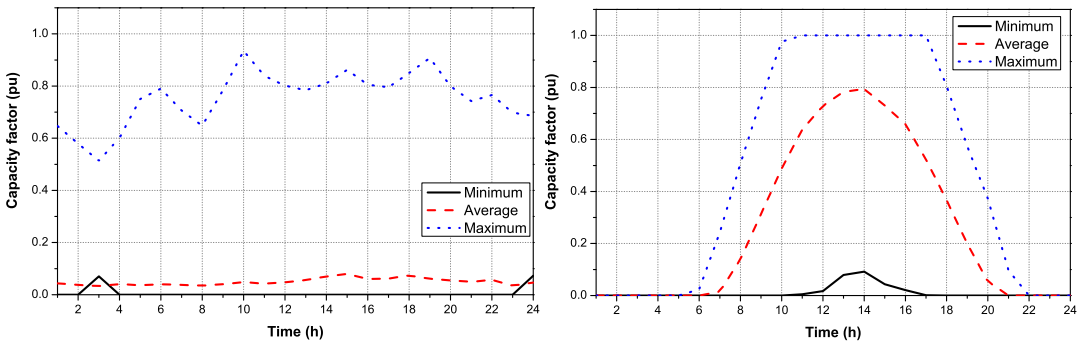

(a) wind-based MG systems **(b)** solar-PV MG systems

Figure 4.16: Estimated minimum, maximum and average power outputs of aggregated wind and solar-PV microgeneration systems for Spring.

Both wind and PV MG systems are connected to the grid via an inverter interface, allowing the control of generated active and reactive power, which are the most important factors for use in the network aggregation methodology. The inverter's power electronic conversion efficiency (typically 91%) is obtained from manufacturer's specifications in [159]. This work assumes MG systems to operate with 0.95 leading power factor and are, therefore, capable of supplying both active and reactive power to the grid, as stipulated in [160]. For the purpose of this research, it is also assumed that the system supplies an ideal sinusoidal waveform, with no harmonic content, to the local grid. This effectively makes the MG act as a negative load within the LV network, which is adequate for the development of MV aggregate steady-state network/load models with low MG penetration levels.

Aggregate LV Micro-Generation Model

In order to undertake an initial analysis of the impact of MG on residential load, the power outputs from the wind-based MG systems (i.e. the generic WT model developed in [28, 39]) are subtracted from the demand curves to examine the effect on the active and reactive power demand of the residential load sector. This does not include the effect of interactions between the MG, the connected load and the supply network, e.g. reduction in network losses, which is considered further in the following section.

In this example, the assumed penetration of small-scale wind-based MG is taken as 10% of the peak load (i.e. maximum winter demand). Although the penetration is small, the maximum possible load which may be offset can reach up to 30% of the actual power demand. Figure 4.17 shows the resulting effects for maximum loading conditions. For this initial analysis, the MG devices are assumed to operate at unity power factor, so there is no ability to provide reactive power support to the network. This will lower the value of displacement power factor of the aggregate load, as the local supply of active power will reduce the power imported from the distribution network, while the reactive power demand will remain unchanged.

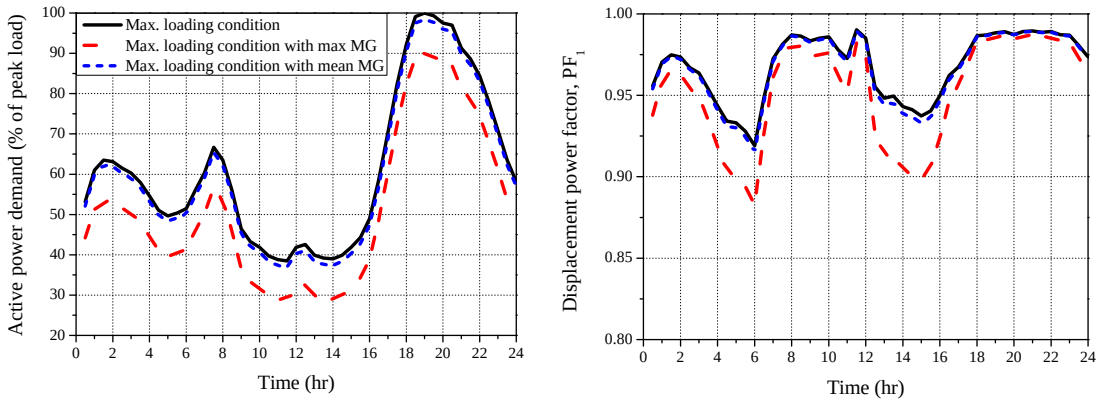

(a) active power (b) displacement power factor

Figure 4.17: Impact of aggregate LV wind-based MG model for maximum residential demand.

4.4.2 Aggregate Network and Load Characteristics with Micro-Generation

Apart from the changes on the power demands, the overall effect of MG on the electrical characteristics of the aggregate network/load model requires further validation. To quantify this, the effect of the network must be taken into consideration. In this example, the detailed LV urban network (presented in Figure 3.11, Page 71) is again used to provide comparison of the presented results. MG is assigned at each load point of the network, as indicated by the black circles in Figure 4.18. A 10% MG penetration roughly equates to one MG of rated power 2.25 kW per load group. All other network properties are unchanged.

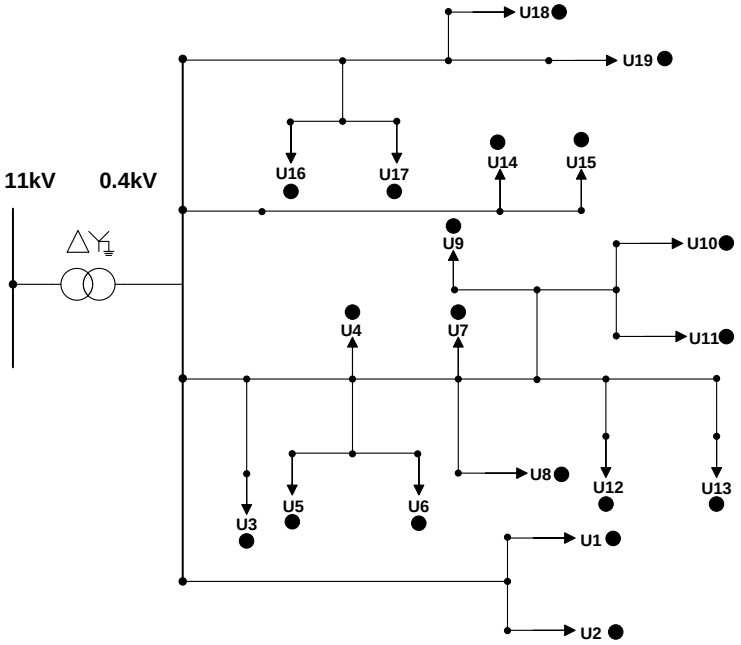

Figure 4.18: Urban network with connected microgeneration.

Because the network operation will change due to the connection of MG units, the network aggregation methodology presented in Section 4.2.1, which allows for the representation of the entire LV network by a single equivalent impedance, will need further validation for the new proposed MG scenario. The output from all MG units is connected in parallel with the aggregate LV load and supplied from the equivalent network impedance, as shown in Figure 4.19.

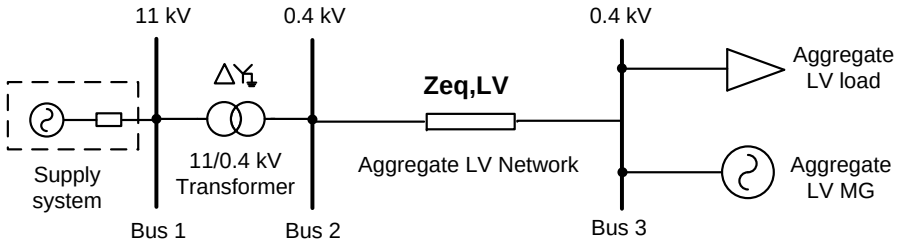

Figure 4.19: Equivalent network configuration with connected microgeneration.

Figure 4.20 compares the active and reactive power at the MV level for V = 0.8 pu and V = 1.2 pu, i.e. the maximum and minimum supply voltage magnitude considered in this research for load model development, for the detailed network and equivalent network configurations with MG. There is negligible difference in the characteristics at the 11 kV busbar with the results obtained using the equivalent network impedance model with MG, therefore, the equivalent network can again be used for the development of aggregate MV load models, which include the effect of MG. It should be noted that it is unlikely that the MG units will remain connected for sustained under/over-voltage conditions of such severity. However, this hypothetical scenario provides a similar validation as the developed load models for the simulated network.

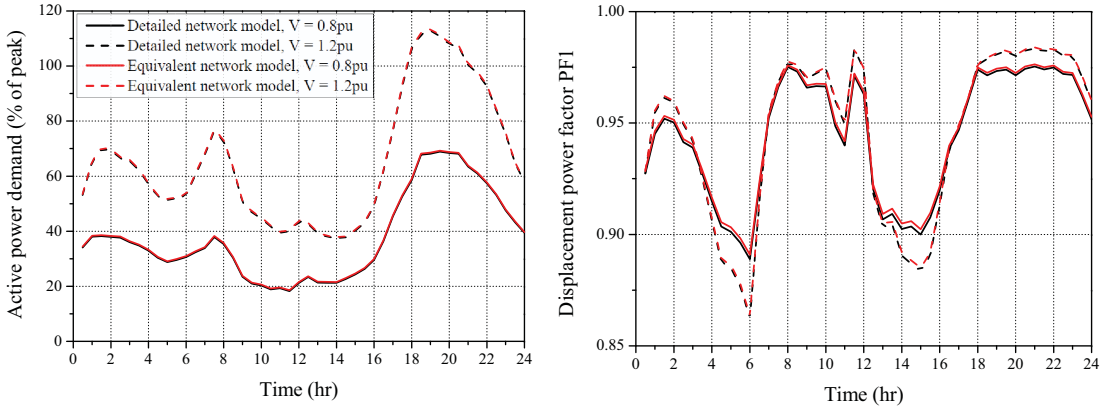

(a) active power demand (b) displacement power factor

Figure 4.20: Comparison of active and reactive power flows at 11 kV aggregate load supply point for detailed and equivalent network models for maximum loading conditions.

Due to the inverter interface, the MG units are modelled as a constant active power source, i.e. the device will output only active power, based on the available wind resources, regardless of the voltage in the LV network to which it is connected. Therefore, when operated in parallel with the LV load, it will act to reduce the demand of the constant power loads within the aggregate, even though the actual MG unit will supply all locally connected load. In the resulting mathematical derivations of the load model coefficients, this will resolve to raise the contribution of the constant impedance and constant current loads within the aggregate mix. This is confirmed by the simulation results in Figure 4.21, which shows an increase in the MV aggregate load model coefficient with locally connected MG units.

Although the installed MG is not participating in reactive power support within the LV network, it will still have a small effect on the reactive power characteristics at the MV level due to the participation of the supply network on the aggregate load characteristics. By supplying some local load, the power supplied from the MV network will reduce. The lower value of current flow through the network impedances will change the contribution of the network to the aggregate load, which, for this case, partly unloads the secondary distribution transformer and reduces the influence of this network component on the aggregate MV load characteristics.

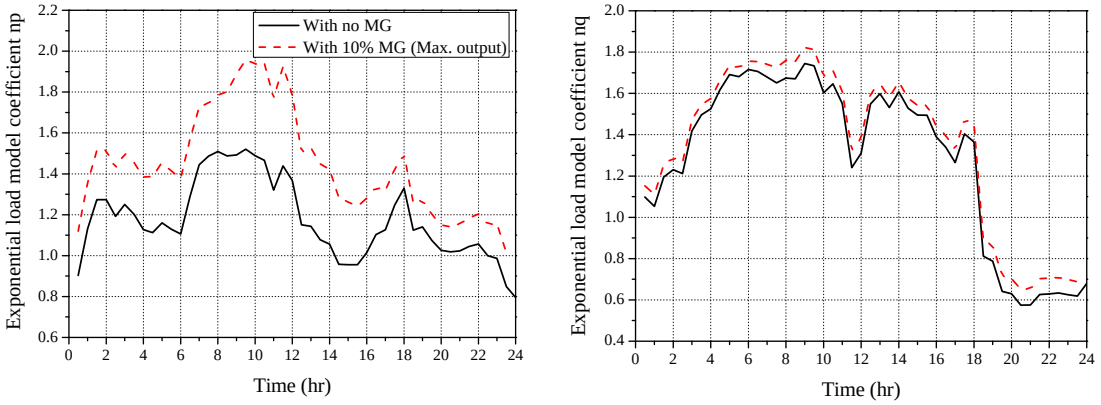

(a) active power (b) fundamental reactive power

Figure 4.21: Exponential load model interpretation of MV aggregate load for maximum loading conditions with installed microgeneration.

The results obtained in this case study show an extension of the aggregation methodology to include the effect of MG within the MV aggregate network/load model. Although the assumed penetration of MG is modest, it is shown that it may still have a significant impact on the steady-state load model coefficients of the aggregate load representation. This indicates that, if the penetration of LV MG increases in the future, it will be even more important to consider their impact and effects on all aspects of power system analysis.

4.5 Impact of DSM and Distributed Generation/Storage on Network Performance

One of the main contributions of this thesis is in the development of detailed and equivalent network models, and, consequently, in their combined analysis with aggregate load models, as well as in their implementation in power system studies (i.e. steady-state and reliability analysis). Accordingly, this section introduces two case studies within the DSM and energy storage (ES) area, in order to demonstrate the applicability of the equivalent networks and aggregate load models (including MG systems) for the performance assessment of future ”smart grids”.

Advanced monitoring, sensing, communication and control aspects of smart grids (realised through, e.g. smart meters, or active/flexible network management), will allow DNOs to have a much better and more direct control of their networks, including control of distributed demand, generation and storage resources of residential customers. Particularly, DSM of residential loads is expected to play an important role, as this demand is higher than in any other load sector (e.g. 32% of the total UK electricity consumption [127]). However, the majority of these customers are deeply embedded within the LV networks, and DSM will require coordinating large groups of customers to achieve the volume of demand required to make a significant contribution to network support. For this purpose, the aggregate network models presented in

this thesis can be of value, as they allow for improved representation of these LV BSP loads, without significantly increasing the simulation time or complexity of simulations.

Accordingly, the proposed case studies consider the effects of several 'smart grid' scenarios within the LV network, and the propagation of changes from the LV load up to the GSP on the primary winding side of the 33/11 kV distribution transformer. The purpose of this analysis is to highlight the ability of the equivalent network/load models to perform an accurate assessment of future 'smart grid' functionalities (i.e. DSM, MG and ES) on the performance of two distribution networks with diametrically opposed characteristics. Because the assessment of 'smart grid' functionalities and scenarios requires a large number of network simulations, further analyses have been carried out in combined research by the author in [20, 21, 30, 31]. In addition, some of the 'smart grid' scenarios proposed in this section will be further analysed for reliability purposes in the next chapters of this thesis.

4.5.1 Case Study: Smart Grid Applications in an Urban Residential Network

For this study, the generic LV urban network (Figure 3.11, Page 71) is extended to include the 11 kV distribution network (Figure 3.15, Page 78) up to the GSP on the primary winding side of the 33/11 kV transformer. The combined network diagram is schematically displayed in Figure 4.22, where the 33/11 kV transformer is the only component operating with active voltage control and uses an OLTC to regulate the voltage at the secondary side of the transformer within the prescribed range of $\pm 6\%$. The 11/0.4 kV transformer is manually adjusted for expected seasonal variations in loading conditions, which is taken as a 1:1 ratio for the average loading conditions in this example.

The network model was built in MATLAB/Simulink software and populated with the previously developed generic load models. This software was chosen to allow for correct connection of the circuit-based load models, and also for the connection of inverter interfaced MG models. This model allows for a PQ-related analysis of changes in active/reactive power flows, system losses, voltage profiles and propagation of harmonics as a result of different 'smart grid' scenarios. Accordingly, the reader is referred to the results obtained from this PQ-related research in [21, 31].

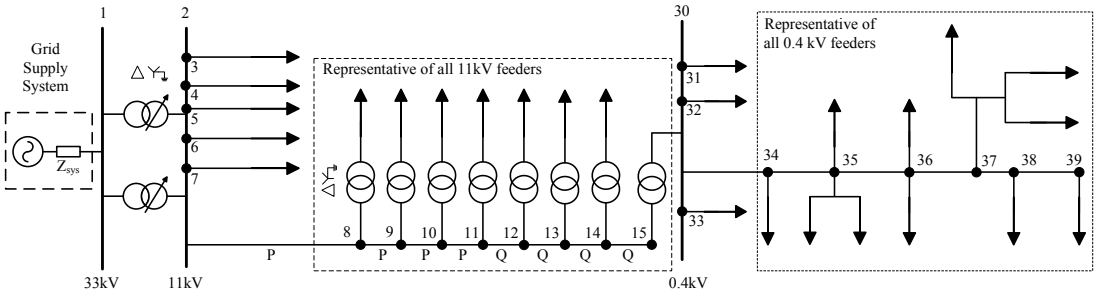

Figure 4.22: Typical UK network configuration supplying urban residential load.

Identification of DSM Scenarios

The availability of residential loads for DSM is determined by the characteristics of individual loads and consumer routines. Many loads are unsuitable for even short-term load shifting due to their role in modern life, e.g. lighting, PCs, TVs and cooking appliances. The remaining load is generally suitable for DSM, but some load types offer more potential to DSM schemes than others. Due to the cyclical nature of operation, 'cold' loads (e.g. fridges and freezers) are suitable for only a short-term deferral, while storage heating loads are mostly already used with off-peak tariffs [126]. Therefore, this example assumes that 'wet' loads (e.g. washing machines and dishwashers) are the most likely available for residential DSM schemes ([30] provides further discussion).

The selection of the best/optimal DSM scheme will depend on the amount of load required for a particular corrective or preventive action. This case study considers a simple DSM scheme in which an arbitrary amount, taken as 40% of all 'wet' loads present during the peak loading period (18:00 - 22:00 hour, Figure 3.8, Page 61), is controlled. The load is reconnected in the same manner it was removed, i.e. the DSM portion of the load is simply delayed until a specified time. Therefore, this four-hour DSM load block can be reconnected at either: 22:00 (DSM 1), 02:00 (DSM 2), 06:00 (DSM 3), 10:00 (DSM 4) or 14:00 (DSM 5) in the daily load profile, as shown in Figure 4.23. More sophisticated reconnection schemes may aim to improve system performance by evenly redistributing the DSM load; however, reconnecting the load in blocks can be considered as a 'worst-case' scenario and may simply create new peak loading conditions. This will also demonstrate the possible range of operating conditions across the entire 24 hour period.

As well as the current load mix (i.e. 'present' scenario), the wholesale substitution of general incandescent lamps (GILs) with compact fluorescent lamps (CFLs), an expected near future change in the residential load sector, is also analysed. This 'near future' scenario is important to consider, as lighting load is responsible for about 18% of the total active power demand in the residential demand [21]. In the near future scenario, the lighting demand is proportionally reduced to reflect the expected savings based on current replacement of GIL with CFL light sources, while the contribution of all other loads is kept constant. Further details are provided in [21, 41].

System Losses

Changes in active and reactive power demands due to the devised DSM scenarios will influence changes in current flows and associated losses in the system. Accordingly, there is a noticeable reduction in the total (daily) energy supplied by the 33/11 kV substation between the 'present' and 'near future' scenarios (Table 4.6), resulting in a slight reduction in system losses at both MV and LV in the 'near future' scenario, Table 4.7. In this table, it is also important to note the high contribution of the LV (0.4 kV) part of the network to the total system losses (i.e. between

5% and 9% of the total energy supplied), in comparison with the MV (11 kV) feeders, which contribute with less than 0.5%.

Table 4.6: Comparison of total daily energy supplied for two urban network scenarios.

"Present" scenario		"Near future" Scenario			
active Energy	'reactive' Energy	active Energy		'reactive' Energy	
(MWh)	(MVArh)	(MWh)	(%)	(MVArh)	(%)
262.14	99.31	244.94	93.44	93.69	94.34

where: "near future" is shown as percentage of "present" scenario

Table 4.7: Comparison of daily system energy losses for two urban network scenarios.

Voltage (kV)	"Present" scenario				"Near future" Scenario			
	active Energy		'reactive' Energy		active Energy		'reactive' Energy	
	(kWh)	(%)	(kVArh)	(%)	(kWh)	(%)	(kVArh)	(%)
11	807.0	0.31	422.5	0.43	703.7	0.27	368.5	0.37
0.4	14123.7	5.39	8887.4	8.95	12322.2	4.70	7753.6	7.81

where: the losses are shown as a percentage of the "present" scenario;
Note: transformers losses are not shown.

Power Flows

A comparison between the aggregate active and reactive power demands at the 33 kV bus (Bus 1 in Figure 4.22) for the 'present' scenario is shown in Figure 4.23. The shaded area in the results plots corresponds to the difference between the base case of each scenario to the resulting value after removal/reconnection of 40% of 'wet' load. A 3.3% and 7.7% reduction of peak active and reactive demands are recorded when the devised DSM scheme is implemented. During that period (18:00-22:00 hours), the total active energy demand is reduced by 4.4% and reactive energy demand by 14.5%. When the DSM load is reconnected in Region 1, the peak will essentially be shifted until 22:00 hours, and the displacement power factor will reduce due to the motor load component of the 'wet' load.

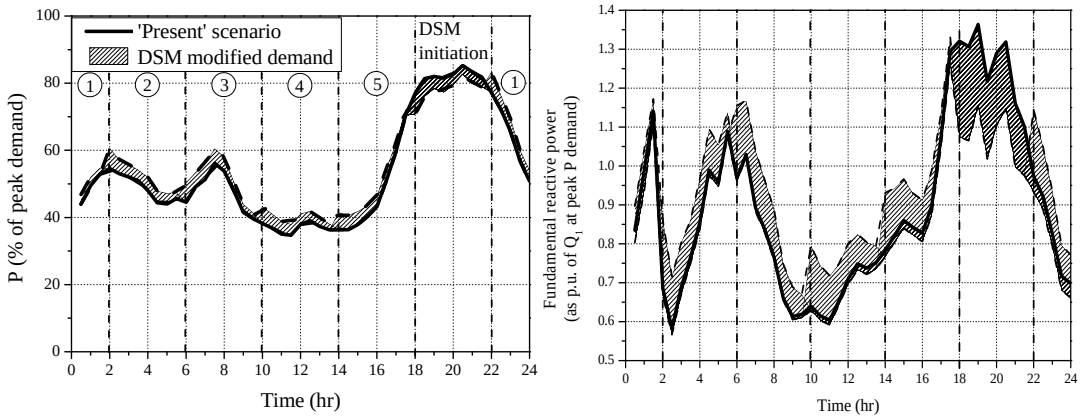

(a) active power: 'present' scenario **(b)** fundamental reactive power: 'present' scenario

Figure 4.23: Comparison of aggregate active and fundamental reactive power demands with devised urban DSM schemes.

Voltage Profiles

The operation of the 33/11 kV OLTC transformer regulates the voltage at the secondary winding (i.e. Bus 2, Figure 4.22), in order to maintain the voltage of all LV customers within the prescribed limit of +10/-6% of the nominal voltage. Considering the expected voltage drop, the OLTC transformer will react every time the voltage of the last supplied LV customer is about to breach the constraints. Accordingly, the changes in daily LV network voltage profiles are shown in Figure 4.24 for the first and last (Bus 30 and Bus 39, Figure 4.22) supplied LV customers. Reducing the active power demand by DSM action will actually increase the number of tap-change operations. There is very little effect of reconnection, as the voltage profile is generally within the limits without the need for OLTC action. However, reconnection of the DSM load in the night time hours (DSM 2), actually improves the voltage profile, despite the increased load, as a result of the additional operations of the OLTC transformer.

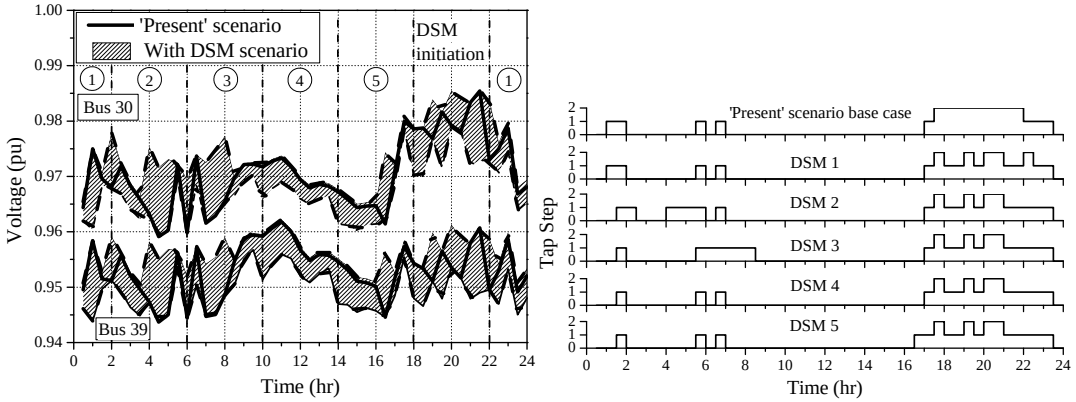

(a) voltage profile: 'present' scenario **(b)** OLTC tap settings: 'present' scenario

Figure 4.24: Comparison of LV voltage profiles and transformer tap settings with devised urban DSM schemes.

4.5.2 Case Study: Smart Grid Applications in a Suburban Residential Network

The test system in Figure 4.25, which was proposed in Section 3.5 as a typical UK residential suburban distribution network, is modelled with PSSE software for analysis in this section. For this study, the generic MV suburban network (Figure 3.16, Page 81), including the supplying GSP at 33 kV level, is extended to include the generic LV suburban systems (Figure 3.12, Page 72) with the interconnection of renewable-based MG units at the end customers' load points. Due to its radial configuration and tree-like structure of lateral feeders, this network is more suitable for the impact assessment of 'smart grid' functionalities (i.e. MG, ES and DSM) on network QoS performance than a typically meshed urban network. Again, some of the 'smart grid' scenarios analysed on the suburban distribution network were further analysed for reliability purposes as presented in [20, 23, 25], with additional details provided in next chapters of this thesis.

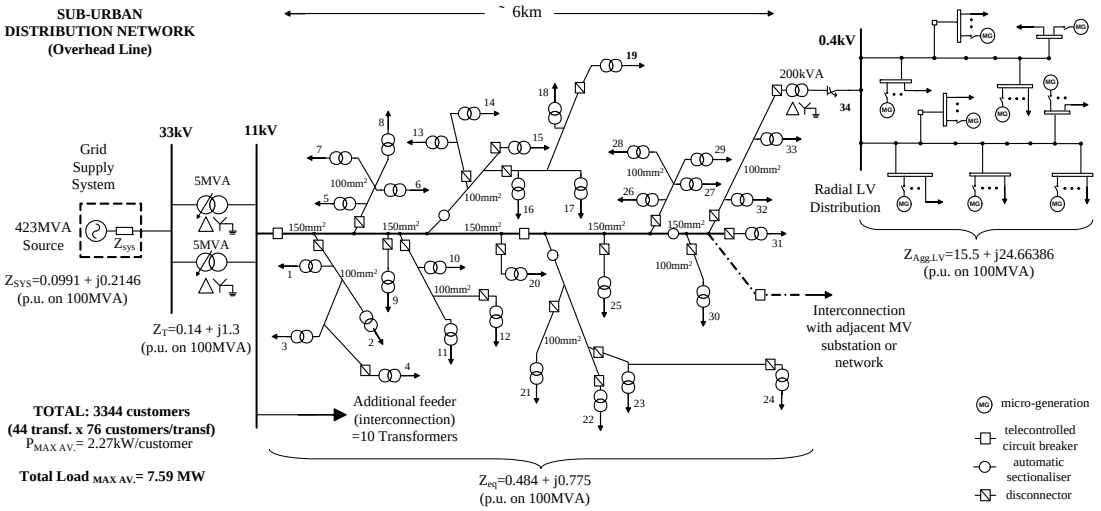

Figure 4.25: Typical UK network configuration supplying suburban residential load.

Definition of 'Smart Grid' Schemes

A set of different 'smart grid' scenarios is proposed in this section to improve overall network performance. These scenarios include separate and combined implementation of DSM, MG without ES (i.e. 'uncontrolled MG' scenario) and MG/DSM with ES applications. Accordingly, based on the RER assessment and power outputs from the considered aggregate MG models (solar-PV and wind-based systems) previously described in Figure 4.16, this analysis assumes an equal contribution/installed capacity for both PV and wind MG systems, whose combined power outputs are shown in Figure 4.26 for a "typical" day in spring season (corresponding to average system loading conditions). Three 'smart grid' scenarios are discussed and implemented, based on the load profile identified for the UK residential sector and classification of residential consumption into several load categories (Figure 3.8, Page 61).

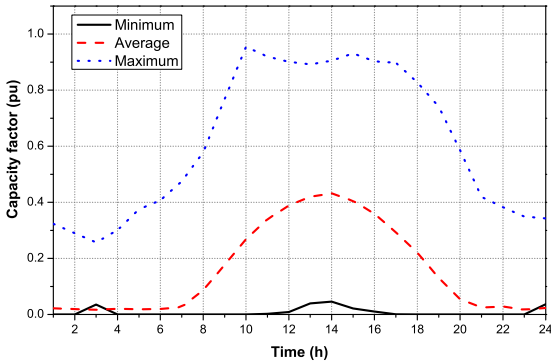

Figure 4.26: Combined power outputs of solar-PV and wind-based microgeneration systems.

- 'Uncontrolled MG' Scenario:

A relatively low penetration of the aggregate PV/wind MG in the LV networks is assumed: 10% of the peak residential demand, where 1 p.u. in Figure 4.26 corresponds to 10% of the peak

residential demand. This scenario uses daily MG outputs for average solar/wind energy inputs from [31], which are not controlled for any energy storage implementation (Figure 4.27). The MG systems will decrease the total demand and, therefore, reduce the loss of supply due to fault-caused interruptions experienced by residential customers.

- 'DSM + Energy storage' Scenarios:

If one of the supplying 33/11 kV 5 MVA transformers in the primary substation (Figure 4.25) fails when demand is greater than the power rating of the other operating transformer (i.e. 2/3 of the peak load), all customers may still be supplied if an intelligent DSM scheme is adopted by the DNO. During this contingency, one transformer could only be able to supply the load for a limited period of time, due to possible overloading conditions. Therefore, the additional use and coordination of energy storage (ES) from connected MG could further help to supply the excessive loads until the normal supply is established.

These scenarios introduce a combined application of DSM, MG and ES control, which firstly shift a moderate amount of 40% of all 'wet' loads present during the evening peak hours (18:00 - 22:00) to late night hours (02:00 - 06:00). This is a typical DSM scheme for reducing peak load, marked as 'DSM' in Figure 4.27. As all LV customers are represented by the same aggregate demand profile, the load reduction is assumed to be equally shared. Secondly, the coordinated operation of MG with ES is used to supply part of the demand locally (at LV). By using ES as a backup supply (i.e. to decrease peak loading), the frequency and duration of customer interruptions may be reduced in the event of an interruption. Thus, apart from the load shifted due to the DSM action, all MG outputs stored during the day (calculated at 3.67 kWh per domestic customer) are used in coordination with the devised DSM to further reduce the evening peak load (18:00 - 22:00 hours), marked as 'DSM + Energy Storage' in Figure 4.27.

Power Flows

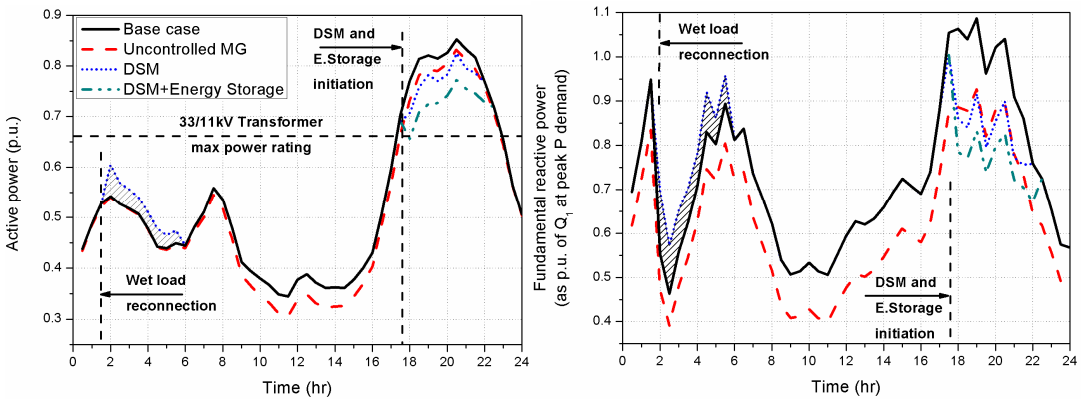

(a) active power **(b)** fundamental reactive power

Figure 4.27: Comparison between aggregate active and reactive power demands for the implemented suburban DSM scenarios.

A comparison between the aggregate active and reactive power demands at the 33 kV bus is shown in Figure 4.27, for the base case, 'DSM', 'uncontrolled MG', and 'DSM + Energy Storage' scenarios. The fundamental reactive power is normalised using the value of reactive power at the peak active power demand for the maximum loading conditions (i.e. winter peak demand).

Voltage Profiles

As significant levels of two-way communication between the DNOs and (individual) customers are not yet implemented through smart metering in the existing networks, OLTC transformers control voltage at the secondary side taking into account the expected loading conditions. This is to ensure that the voltages at the farthest away (i.e. the last supplied) LV customer is still within the regulated limits (0.94-1.1 p.u) [161]. Accordingly, the changes in daily LV voltage profile are shown in Figure 4.28(a) at the secondary side of the 11/0.4 kV substation. The applied DSM scheme has improved the voltage profile during the night-time hours, due to the changes in OLTC tap setting (Figure 4.28(b)). In the evening, the voltage magnitude oscillates around the base case voltage, which is again due to the increased number of tap changing operations. Additionally, the effects of MG outputs increase the LV voltage profile to almost 1 p.u., resulting in less OLTC transformer operations.

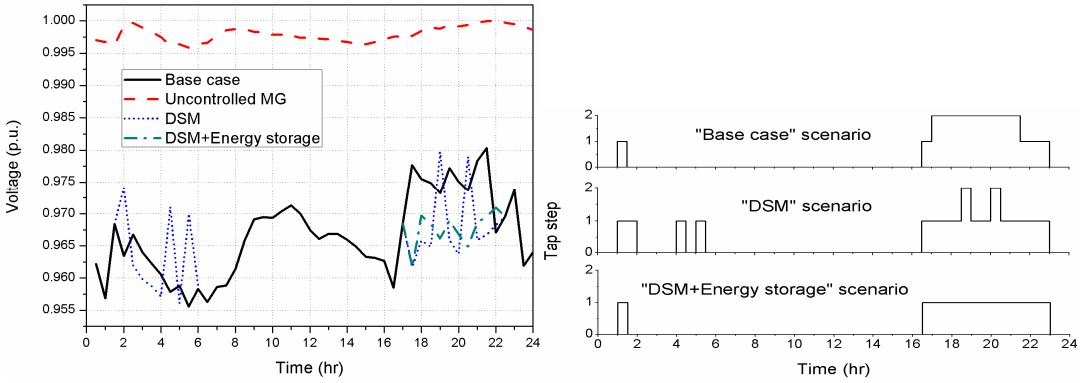

(a) voltage profile at 2^{ary} of 11/0.4 kV transformer **(b)** 33/11 kV OLTC transformer tap settings

Figure 4.28: Comparison between LV voltage profiles and transformer tap settings for the implemented suburban DSM scenarios.

4.6 Reliability Equivalents of LV and MV Distribution Networks

As previously discussed in Section 2.3, Page 19, a set of system reliability indices, which in the UK measure customer interruptions (CI) and customer minutes lost (CML), are annually reported by the DNOs to quantify the level of reliability in their distribution networks. Therefore, the correct assessment of network reliability performance is an important, but difficult and time-consuming task. However, the network modelling approaches often taken by DNOs may not be completely adequate, as they might introduce high levels of uncertainties and, therefore,

big errors between the estimated and actual reliability indices. This has been confirmed in most of the reliability performance studies of large power supply systems, in which LV and MV parts (i.e. 0.4 kV, 11 kV and 33 kV networks) are simply represented by an aggregate/bulk load, due to the complexity of calculation.

Reliability indices calculated with that approach are often inaccurate, as failures of the power components (PCs) in the part of the system represented by the bulk load cannot be modelled correctly. However, if correct failure rates and repair times are allocated to a bus or substation where bulk load is connected, a more accurate reliability equivalent model can be formulated, allowing to simplify the model of the analysed large network and reduce the simulation times. Therefore, by using the network equivalent models presented in this chapter, this section presents a general methodology for the calculation of accurate reliability equivalent models for each MV/LV distribution network and load subsector (HU/U/SU/Ru) presented in Section 3.5. Figure 4.29 illustrates the resulting aggregate LV and MV network models after the inclusion of reliability equivalents.

The proposed methodology is based on recorded failure rates, λ, and mean repair times (i.e. MTTR), d, of the PCs in the equivalent part of the system and relevant UK SQS requirements, as presented in Table 2.4, Page 33. The analytical approach proposed for reliability analysis of radial networks in [162] is extended in this section, in order to correctly analyse modern meshed distribution networks with alternative supply points, for which supply restoration times are empirically determined. Accordingly, the accuracy of some of the calculated reliability equivalent models has been verified by applying different reliability studies on the generic distribution networks, as published by the author in [24, 25, 34].

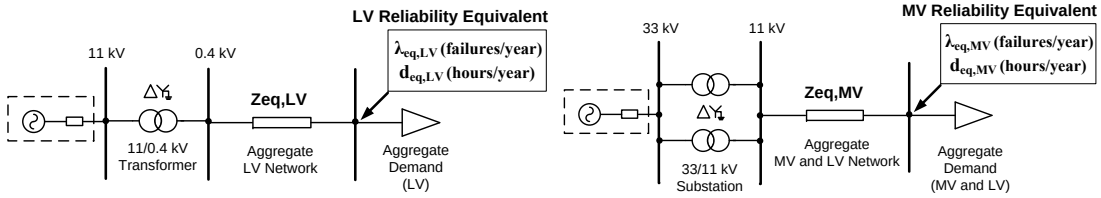

(a) LV network model **(b)** MV network model

Figure 4.29: Aggregate LV and MV network models, with equivalent network impedances and reliability equivalent model parameters.

4.6.1 Input Data for Reliability Equivalent Models and Analysis

Failure rates (λ) and mean repair times (d) are two basic inputs for reliability assessment, specially for Monte-Carlo simulation (MCS), which first identifies all the PCs in the modelled network and their reliability characteristics. Thus, the equivalent failure rate (λ_{eq}) and equivalent repair time (d_{eq}) of the LV and MV buses, where the aggregate load points are connected, are derived from the known λ and d values, provided by the full database previously built in Table 2.7 (Page 36), for all relevant PCs in the aggregate part of the system.

Therefore, based on the analytical approach described in [162], the equivalent failure rate, λ_{eq}, of the buses where the aggregate demand is connected can be calculated as the sum of the failure rates of all power components (i.e. N number of PCs) in the LV or MV network:

$$\lambda_{eq} = \sum_{i=1}^{N} \lambda_i \tag{4.10}$$

For instance, if the lumped system consists of 20 transformers, the equivalent transformer will have a λ_{eq} given by the sum of the λ_i of all 20 transformers. The process is repeated for all PCs within the analysed system and in the end a single equivalent failure rate is obtained to represent the aggregate LV or MV network for reliability analysis. On the other hand, the equivalent repair time, d_{eq}, of the buses where the aggregate demand is connected can be calculated as the average value of all power components' mean repair times:

$$d_{eq} = \frac{1}{N} \cdot \sum_{i=1}^{N} d_i \tag{4.11}$$

Each reliability equivalent (λ_{eq} and d_{eq}) considers the reliability performance of every PC (e.g. lines, transformers, buses, protections, etc.) downstream the point of aggregation (i.e. LV or MV aggregate buses in Figure 4.29) and thus can be used for determining the frequency and duration of interruptions (reliability assessment) within the aggregated network.

4.6.2 Reliability Equivalent Parameters with Alternative Supply

According to the UK SQS regulation [89] previously discussed and presented in Table 2.4, Page 33, the proposed methodology is fully applicable to those PCs which interrupt a supplied group demand (GD) less or equal than 1 MW, as these interruptions are not required to comply with any SQS requirements, and thus can be restored within the corresponding component repair time (i.e. MTTR values provided in Table 2.7, Page 36, [NAFIRS]).

However, further attention should be allocated to those PCs in the network which are capable of interrupting GDs of more than 1 MW, as SQS legislation requires customers with high power demands to be supplied with at least one backup supply point. The duration of customer interruptions will strongly depend on actual configuration of power supply systems, thus highly-urban/urban meshed networks will have a lower duration of supply interruptions than suburban/rural radial systems. Therefore, before calculating a reliability equivalent model for each distribution network and load subsector (HU, U, SU and Ru), an empirical study of the detailed systems (Section 3.5) is required in order to determine the input repair time for each type of MV/LV BSP substations where the aggregate networks/loads are connected.

Depending on the interrupted bulk-supplied GD, different restoration times are required to restore supply after the first circuit outage (e.g. 15min, 3h, etc, according to UK SQS in

Table 2.4). Therefore, the alternative supply concept is introduced in the calculation of the equivalent repair time (d_{eq}, 4.11) for each subsector by allocating a SQS value to those PCs causing faults in the network which interrupt a demand higher than 1 MW, 12 MW, etc, [89]. Instead of considering MTTR values to calculate the equivalent duration of interruptions of bulk loads by simply applying (4.11), the 'time to restore supply' (TTRS) concept is introduced to correctly assess the duration of supply interruptions in the equivalent systems.

Accordingly, Table 4.8 shows the calculated input parameters for the aggregation of generic residential LV networks (presented in Section 3.6) to be connected at the LV BSP in Figure 4.29(a), as well as for the MV part of the distribution networks (presented in Section 3.7), and the combination of both of them (from 33 kV down to 0.4 kV) to be connected at the MV BSP as shown in Figure 4.29(b). Security of supply requirements are also provided for each type of distribution network considered.

Table 4.8: Reliability equivalent parameters per network and load subsector.

Reliability Equivalent Model Parameters		**FAILURE RATE (as in (4.10))** λ_{eq} **(failures/year)**	**REPAIR TIME (as in (4.11) and [89])** d_{eq} **(hours/year)**	**Security of Supply Requirements [89]**
LV Distribution Networks (residential demand)	HU	4.31	16.6	(GD $\leq$ 1 MW) to be met: in Repair Time
	U	2.51	17.5	
	SU	1.21	18	
	Ru	0.87	22	
MV Distribution Networks (from 1^{ary} to 2^{ary} substations)	HU	1.63	42.5	(GD > 1 MW and $\leq$ 12 MW) to be met: within 3 h and (GD > 12 MW and $\leq$ 60 MW) to be met: within 15 min
	U	2.26	45.9	
	SU	4.09	67.9	
	Ru	4.33	74.4	
Combined MV / LV Distribution Network (aggregate group demands)	HU	156.6	41.7	
	U	122.5	45.1	
	SU	57.1	67.4	
	Ru	33.7	74.2	

The calculated values in Table 4.8 clearly provide a comparison between the different SQS network performances to be expected from rural to highly-urban subsectors, and from LV to MV power distribution systems. This is shown, for example, as values of d_{eq} increase from highly urban to rural areas, due to longer restoration times required in radial systems. On the other hand, the higher demand concentration in metropolitan areas and the higher number of installed PCs in meshed networks, specially in LV networks, make the values of λ_{eq} and so their fault probabilities to behave oppositely. However, this trend on the λ_{eq} value is not particularly applicable to the MV (11 kV) part of the distribution system (from 1^{ary} to 2^{ary} substations), as the increased length of the operating OHLs (in comparison with more reliable underground cables) make the final failure rate (λ_{eq}) to increase from HU to Ru areas.

If these equivalent values are used as the input data for the reliability assessment of aggregate LV and MV distribution networks (Figure 4.29), the calculated reliability indices, e.g. CI and CML, will have a small error (about 2%, as proved through a detailed analysis by the author

in [24]) when compared against the results calculated for the detailed systems. Using the correct reliability equivalents will help to both avoid the underestimation of the reliability performance of the aggregate networks connected at LV/MV BSPs, and to reduce system complexity, as the electrical and reliability models of all PCs do not need to be represented in detail.

4.7 Conclusions

In this chapter, the modelling, aggregation and network analysis of distribution system equivalents have been discussed. Accordingly, the main analysis of this chapter was based on the generic network models presented in Chapter 3, which can easily represent the wide range of actual sub-transmission and distribution systems supplying a mix of different demands (mostly residential customers). A network aggregation methodology is built from these detailed models to enable an accurate and flexible power system's reliability assessment. These generic models and distribution network equivalents maintain the technical characteristics of real operating networks, whereas, at the same time, they reduce their complexity to allow efficient modelling and simulation of the existing and future distribution network functionalities. In addition, part of this research was focused on the calculation of LV system supply impedances at four different network subsectors (highly-urban, urban, suburban and rural), providing reference impedance values for different voltage levels (LV and MV) and typical network arrangements.

Regarding the expected 'smart grid' functionalities to be applied in future power distribution systems, the LV and MV network equivalent models also incorporate capabilities for the integrated assessment of microgeneration models, demand-side management and distributed generation/storage functionalities on network steady-state quality of supply performance.

Moreover, this part of the research proposes a methodology for calculating reliability equivalent models, capable of representing LV and MV parts of large power supply systems (i.e. 0.4 kV, 11 kV and 33 kV networks), which are normally modelled by an aggregate/bulk load due to the complexity of calculation. The proposed methodology, for each MV/LV distribution network and load subsector (HU/U/SU/Ru), is based on recorded failure rates and mean repair times of all the power components within the aggregate part of the system. The analysis also includes relevant security of supply requirements, in order to correctly analyse modern meshed distribution networks with alternative supply points, for which supply restoration times are empirically determined.

Chapter 5

Risk and Reliability Modelling of Power Supply Systems

This chapter presents the main reliability criteria and techniques used in this thesis for the calculation of system and end-users' reliability indices. As methods currently used for network reliability assessment must be adapted for the correct assessment of the expected 'smart grid' functionalities (e.g. DG, ES or DSM), the application of Monte Carlo Simulation method is proposed in this chapter, as it provides a powerful tool for modelling complex systems.

The following sections discuss the inclusion of actual load profiles in reliability analysis, the use of different input probability distributions, as well as the impact analysis of time-varying failure rates of network components. The uncertainty and convergence of the resulting reliability indices is also discussed, in combination with a study of multiple-fault occurrence.

Finally, a new theoretical interruption model is introduced for assessing more accurately the moment in time when interruptions of electricity customers are likely to occur, which can be used in a wide range of applications related to planning and operation of power supply systems. Different reliability applications of the integrated Monte Carlo Simulation procedure presented in this chapter have been published by the author in [20, 22, 23, 24, 25, 34, 35, 36].

5.1 Reliability Criteria and Techniques

5.1.1 General Overview

Over the last decades, the concept of reliability assessment evolved into a comprehensive approach for evaluating various engineering strategies, typically linked to system planning and operation studies. The meaning of reliability concept, which was initially expressed as the ability of a component to operate without interruptions during its lifetime, as specified by the manufacturer, has been generalised and now receives different connotations in engineering applications. A significant change in the reliability concept is emphasised by the context in which this term is nowadays used in power system reliability analysis. Instead of assigning the reliability analysis to each individual component in terms of frequency and duration of its failures, the reliability concept is now extended and typically refers to the performance assessment

of a whole system, subsystem, or part of a system supplying electricity customers. For instance, in the UK there is a general standard for Security and Quality of Supply (SQS) [50], which includes both reliability and continuity of supply aspects in the overall system performance assessment.

Before the liberalisation and privatisation of the electricity sector, the reliability performance of power systems had been assessed as a whole for the entire system. Three distinctive papers [12], [13] and [14] show the procedures which can be followed to evaluate the reliability of a power system on three hierarchical levels, including respectively the generation subsystem, both generation and transmission, and finally, the third hierarchical level including all subsystems of generation, transmission and distribution as a whole. Since the introduction of this methodology was considered as an early forthcoming classification for the liberalisation process, the analysis has been divided into three different network subsectors to highlight that the generation, transmission and distribution of energy are not under the same entity and that any reliability-related analysis has to be done independently for each part of the system.

Nowadays, the attention is focused on the way the distribution systems perform with respect to interruptions to customer supply. This is how the reliability concept evolved and became more related to the continuity of supply assessment. There is, however, a boundary defined when DNOs quantify the performance of their power supply systems. This boundary is established through the limits defined by the load points at the MV level. Neglecting some events, which occur in the LV networks, leads to unrealistic performance reports on continuity of supply. Therefore, further investigation is required to correctly represent the LV customers, with respect to MV ones, when the reliability performance of distribution systems is carried out.

5.1.2 Approaching Reliability Analysis

Analytical vs. Probabilistic Techniques

Several techniques have been developed over past years in order to reduce the compromise between economic constraints and reliability performance of distribution networks. Among them, an analytical approach is often used for practical applications, such as the planning of network's capacity, i.e. the *N-1* or *N-2* security criterion, that the system must comply with when it loses one or two major power components (PCs) respectively. However, analytical methods do not consider the stochastic or probability nature of system's behaviour, demand or PCs' faults. Although many power system analyses currently use an analytical approach, the need for probability techniques has been widely recognised in several studies (e.g. [15]).

Accordingly, one of the key aspects in a probabilistic analysis is the complete comprehension of the system. By using the different probability tools, it is possible to estimate the network's future probable behaviour. However, some major difficulties are encountered for an accurate probabilistic modelling:

- *lack of input data*: statistical databases on failure rates and mean repair times of PCs are based on several years of recordings and monitoring of electricity networks, which are often incomplete or contain errors (specially applicable to new technologies);
- *modeling probabilistic phenomena*: the probabilistic models of failures and malfunctions of power equipment are complex and difficult to represent;
- *modeling system's response*: the probabilistic models must be able to simulate the behaviour of the system for a large number of operating conditions, which requires substantial computational resources for a correct validation of results.

In spite of all these disadvantages, probabilistic analysis has become a key factor in decision-making processes for planning and design of power systems. Moreover, in order to reduce the limitations of calculation resources, the reliability analyses presented in this thesis are based on the comprehensive database with failure rates and mean repair times of all types of network components (previously presented in Section 2.5, Page 35), which was built from the past recordings in UK networks, covering a five-year period.

Reliability Assessment Methods

Analytical methods and simulation techniques [15] are two basic approaches that can be used to assess the reliability performance of power supply systems. The analytical approaches are based on mathematical models, which characterise the analysed system and allow for probabilistic combinations of different states of the system, in order to find appropriate numerical solutions for several reliability indicators. The outputs of the analytical procedures are limited to average values and standard deviations, providing thus only a general characterisation of the analysed parameters. As this information is not always sufficient or adequate to estimate, plan or operate properly the power supply systems, simulation techniques are used instead of analytical methods, by using as input recordings and statistics related to the analysed system. Both approaches have advantages and disadvantages:

- the analytical approach generally simplifies the system, making the model to become completely unrealistic in some cases. On the other hand, the simulation approach is able to include and reproduce all the characteristics and functionalities of the analysed network;
- computation times offered by analytical techniques are relatively short, while simulation techniques require a more time-consuming computation;
- analytical models always provide the same results for the same system, model and input data, while simulation methods are dependent on the precision imposed at the start of the simulation;
- simulation techniques enable to perform a more comprehensive evaluation, in which output reliability indices are expressed as probability distributions rather than simple average values and standard deviations.

One of the most often used simulation methods for assessment of reliability performance of power supply systems is the Inverse Transform Method [163, 164, 165], also known as Monte Carlo Simulation (MCS) procedure. Non-sequential (or random) and sequential simulations are two additional variants of MCS technique often used in power system studies [48, 166, 167, 168]. The non-sequential MCS methods consider the time as an independent variable, neglecting the transitions between the different states of the system. On the other hand, sequential MCS methods, which are applied for the reliability analysis in this research, are characterised by the chronological or time-sequence transitions of network components from one state to another (i.e. between "normal operation" states and "faulted" states). For both variants of MCS method, its effectiveness strongly depends on the input data, i.e. the more comprehensive the database with past recordings, the more accurate the results from MCS.

In the same way power flows define the electrical properties of the network in steady-state conditions, the reliability model predicts the dysfunctional behaviour of the system. Therefore, the model must be able to accurately quantify the annual frequency and duration of interruptions for each supplied load in the system. However, several factors have been identified as possible reasons for the reliability underperformance of the methods used by DNOs for the estimation of frequency and duration of customer interruptions. Linear regression methods, which rely on extrapolation of past network performances, should be avoided and replaced by MCS based approaches. Although the MCS procedure is quite difficult for implementation in complex and large networks, it generally provides more accurate results than linear regression methods. However, attention is required as any neglected information or incorrect input data could lead to significant errors in the estimated reliability metrics.

5.2 Application of Monte Carlo Simulation Procedure

Several MCS-based studies have been reported in the literature on the reliability performance of power supply systems, e.g. [169, 170, 171, 172, 173, 174, 175, 176, 177, 178, 179, 180]. The Monte Carlo method, in a broad sense, is defined as a technique based on the use of random or pseudo-random numbers [181]. The random numbers are stochastic variables which are uniformly distributed in the interval $[0, 1]$ and present a stochastic independence, meaning that the variables can take any value between 0 and 1 with the same probability.

Once the reliability characteristics of all the PCs in the analysed system are identified, the system states are established to define operating and failure stages of individual components through the use of a random generator. Accordingly, the random numbers generated are assigned to an inverse distribution function (e.g. exponential, Weibull, Rayleigh, Gamma, etc.) in order to convert the component failure rates (λ) and mean repair times (i.e. MTTR) into system states (i.e. time to fail (TTF) and time to repair (TTR)) based on the operating and failure stages of individual power system components.

The adequate period of time allocated to power system reliability analysis is usually one year [15] and, for the analyses presented in this thesis, it is assumed that an initial period of simulation of 40 years corresponds to the maximum operating lifetime of all network components. The period of simulation of 40 years has been introduced as an intermediate (inner) simulation loop firstly to capture the frequency of failures experienced by the network components during their lifetime and secondly to mitigate the variations that usually occur in the results of a single iteration, which is used to model one year of operation [15]. In addition, the simulations are repeated for a desired number of years (e.g. 1000) through an outer loop as illustrated in Figure 5.1, resulting in the calculated probability distributions of failures of each network component. Every time a component fails to operate, a power flow algorithm is run to check and quantify which individual customers, or group(s) of customers, are affected by the fault.

Once the frequency of supply interruptions is quantified, the next step in the MCS procedure is to establish the duration of customer interruptions. Then several reliability indices can be derived for the whole system, parts of the system or individual load points. The main steps of the MCS approach used in this research, which is shown in detail in Figure 5.1, can be summarised as following:

1. assign failure rates and repair times/security of supply time limits/protection settings to all network components within analysed system;
2. establish probability distributions to model initial conditions;
3. convert probability failure rates in time values based on a random number generator;
4. determine faulted components;
5. for all faulted components, transform their associated random variables into time values corresponding to the moment in time when the failure occurs;
6. run power-flow algorithm after the failure of each network component;
7. establish interrupted customers;
8. calculate the duration of each interruption;
9. compute reliability indices (e.g. ENS, SAIFI, SAIDI, MAIFI, etc);
10. estimate the error (precision);
11. reduce the variance (not applied in this thesis) - a method to reduce the variance of the estimated results, to reduce the computation time necessary for a given precision.

5.2.1 Classification of Long and Short Interruptions

The network model and failure rates (λ values from Table 2.7, Page 36) are used to assess the frequency of the customer interruptions by faults that occurred within the system. Moreover, the duration of long interruptions (LIs) is obtained based on the MTTR values (Table 2.7, Page 36) of faulted network components, whereas the times corresponding to the protection settings (provided in Table 2.6, Page 34) are used to calculate the duration of short interruptions (SIs). Once the frequency and duration of interruptions are achieved, the reliability indices can further be calculated and different planning and QoS strategies can be adopted.

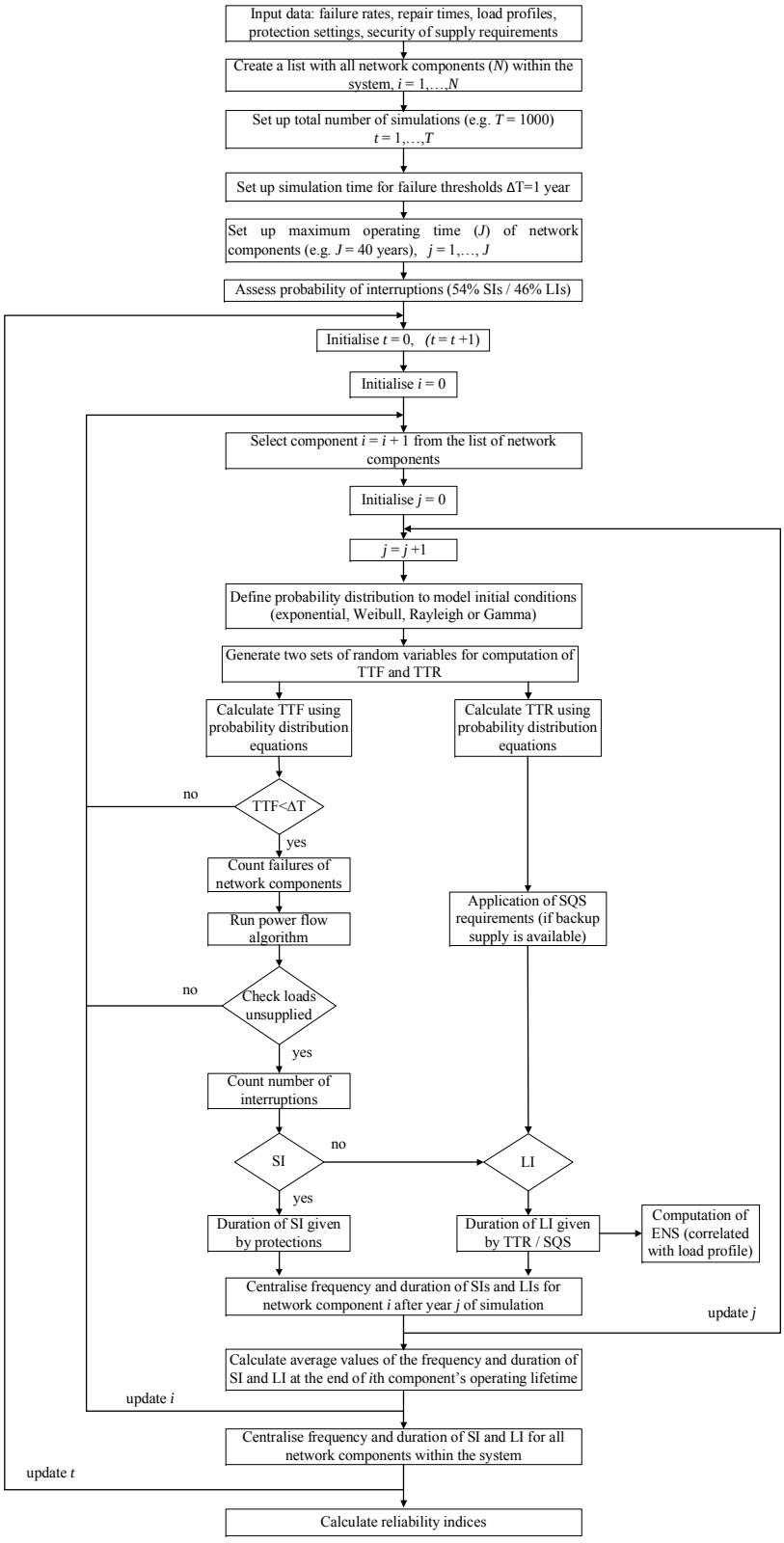

Figure 5.1: General algorithm of the applied MCS procedure.

A simple way to make distinction between short and long interruptions of customer supply is to refer to data gathered from real systems and to allocate a certain percentage of the simulated failure states to SI class and another percentage to LI class. For that purpose, past recordings collected from 14-UK DNOs between 2005 and 2009 are analysed [27], identifying that 54% of the fault events are temporary and 46% are permanent.

Time to Restore Supply After Permanent Faults

Security of supply requirements forces DNOs to reconsider the way the customer interruption process is assessed and managed, as the corresponding penalties could affect their income. A correlation of the time values given in these requirements (provided in Table 2.4, Page 33) with the repair times of faulted network components is used in this work to establish the duration of interruptions. These requirements, depending on the type of network analysed in each case, are typically satisfied by reconfiguring the network to provide alternative supply.

Every time a permanent fault occurs, the time to restore supply (TTRS) to the interrupted customers is given by the duration limit(s) specified for the corresponding group demand(s). However, for the rest of interrupted customers within that group, the repair times (i.e. MTTR values) of PCs from Table 2.7 should be applied, as their supply can be restored after the faulted component has been repaired. In other words, the analysis considers applying the MTTR values from Table 2.7 only when "in repair time" value is stipulated in Table 2.4. Instead of a fixed time limit, regardless of the time value (i.e. either MTTR or TTRS) applied to restore supply to interrupted customers, these values are modelled in the MCS procedure as the mean value of the selected probability distribution (e.g. exponential, Weibull, Rayleigh, Gamma, etc.).

In addition, this thesis proposes a straightforward methodology for assessing the reliability performance of power supply systems regarding the targets which are imposed by Regulator to protect domestic and non-domestic customers from extremely long durations of interruptions. For that purpose, in addition to the corresponding protection schemes and UK SQS requirements, Regulator-related legislation (Table 2.5, Page 34) is included in the reliability analysis. Accordingly, the risk of having interruptions longer than the specified targets is one of the main outputs of the proposed methodology.

5.2.2 Inclusion of Actual Load Profiles in MCS

Actual demands at the load supply points are used as the additional information for a more realistic assessment of customer interruptions. For example, load profiles of commercial or residential customers (presented in Section 3.4) are used to establish whether a fault in the network will result in an interruption of customer's supply. This is a further step to the classical sequential MCS analysis in which, after establishing the probability states of the system, redundant solutions to the faulted PCs are searched to finally conclude whether the loads are interrupted or not. In conventional MCS analysis, the loads are usually represented by bulk/lumped

models characterised by rated powers. Hence, any fault resulting in customer interruptions will interrupt maximum load, although for most of the time the actual demand is lower than the maximum, and only part of the customer loads (or no load) will be disconnected. Accordingly, a better correlation between the moment in time when a fault occurs in the system and the actual demand interrupted will significantly improve, for instance, the calculation accuracy of power/energy reliability indices (e.g. ENS index). The linkage of empirical load models (e.g. Figure 3.8, Page 61) to the MCS procedure will result in a more accurate assessment of customer interruptions, and will enable for an appropriate assessment of potential DSM/ES schemes for analysis.

The case of a 33 kV GSP group demand supplied by two parallel transformers, each with a rated power lower than the peak load (typically 70%-75% of the peak demand) is an example of the latter discussion. When one of the two transformers fails to operate, all power demand will still be met by the other transformer, as long as the demand is maintained below the transformer's rated capacity. Figure 5.2 shows how important it is to accurately predict the moment when the fault occurs, as any error could influence the results. All customers are supplied (i.e. there is no interruption) when one of two parallel transformers fails and power demand (black solid line) at the moment of failure is below the rated power of a single transformer (black dashed line).

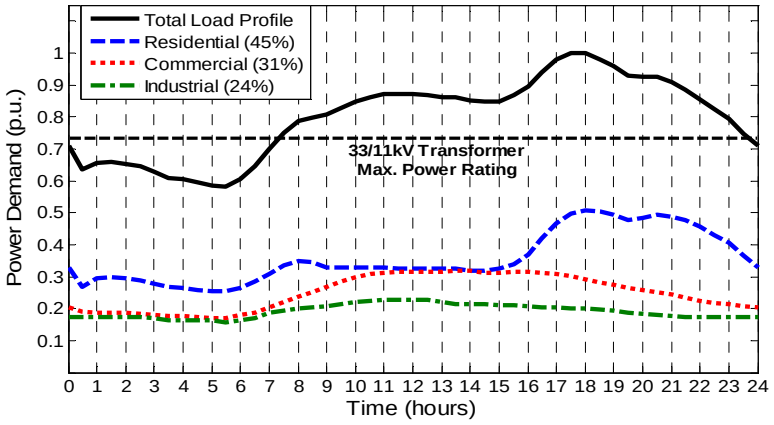

Figure 5.2: Demand identification of a mixed load profile at 33 kV GSP.

At the GSP level (33 kV), the total demand contribution is generally a combination of residential, commercial and industrial sectors/loads depending on node location. For this analysis (Figure 5.2), the GSP substation load profiles are first identified, where the aggregate demand is decomposed from the average daily contributions of about 45% residential, 31% commercial and 24% industrial customers at a monitored primary substation [91]. The "typical" daily load curves for the three main load sectors were found by selecting GSP demand measurements which were made up almost entirely of a single load sector for the selected day [40].

5.2.3 Assessment of Input Probability Distributions

The initial conditions of component failure rates (λ) and repair times (i.e. MTTR) can be modelled with a series of probability density functions (PDFs). Exponential, Weibull, Rayleigh and Gamma distributions are first considered in this thesis to calculate 'time to fail' (TTF) and 'time to repair' (TTR) values for the system components. In addition, the use of Beta distribution as an input tool for the MCS model is also analysed. The expressions (5.1), (5.2), (5.3), (5.4), and (5.5) provide general characteristics and parameters of the considered PDFs as input for MCS, which apply the inverse transformation method to convert random numbers into TTF or TTR values. Further details regarding the probabilistic development of these expressions, as well as their fundamental variables and corresponding scale/shape parameters, can be found, for example, in [49] and [182].

$$\text{Exponential: } TTF(or\ TTR) = inv\{1 - exp(-\lambda t)\} \tag{5.1}$$

$$\text{Weibull: } TTF(or\ TTR) = inv\left\{1 - exp(-t/\delta)^{\beta}\right\} \tag{5.2}$$

$$\text{Rayleigh: } TTF(or\ TTR) = inv\left\{1 - exp(-0.5(t/\sigma)^2)\right\} \tag{5.3}$$

$$\text{Gamma: } TTF(or\ TTR) = inv\{\gamma(k,\theta t)/\Gamma(k)\} \tag{5.4}$$

$$\text{Beta: } TTF(or\ TTR) = inv\left\{\frac{B(x;\alpha,\beta)}{B(\alpha,\beta)}\right\} \tag{5.5}$$

Other probability distributions have also been considered to model the initial conditions of the MCS procedure, but the obtained results suggested that these PDFs cannot be adopted in reliability analyses of power supply systems. For instance, the results that Normal distribution would provide are likely to contain negative values, which would make the assessment of the customer interruption process unrealistic. Further analysis regarding the distributional variation associated with reliability indicators for power distribution systems is presented in [72].

Preliminary Assessment of Input PDFs for Modelling Fault Repair Times

Prior to full deployment of MCS, an initial analysis is required to select the most appropriate PDFs for modelling the initial conditions (i.e. TTF and TTR values) of PCs. First, a simple study of a 33 kV bus is undertaken to compare the functionalities that different PDFs offer when modelling the TTR values of that particular bus. In this case, the analysis focuses on the use of several PDFs to convert the input value of MTTR = 140 hours into the corresponding

TTR values (considering a simulation of 1000 years), while the bus failure rate: $\lambda = 0.08$ faults/year, is modelled only through exponential distribution in all cases, in order to maintain the frequency of faults in the analysed bus. For a typical 33 kV busbar, λ and MTTR values are taken from the sample database previously presented in Table 2.7, Page 36.

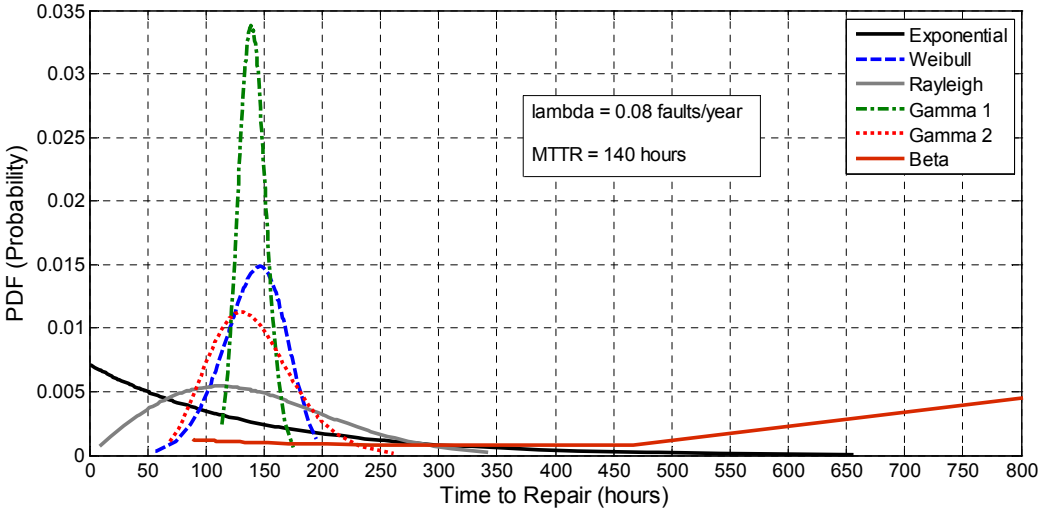

Figure 5.3: Input probability distributions for modelling the fault repair time of a 33 kV bus.

In order to make an accurate estimation, the very same set of random variables is applied to each different PDF, thus the same number of faults (79 in this case, for a 1000-year simulation based on 0.08 faults/year) will occur for the assessment of different PDFs. As shown in Figure 5.3, for each fault in the system (out of 79), the corresponding duration times are modelled through the application of the inverse transform method to exponential, Weibull ($\beta = 6$), Rayleigh ($\beta = 2$), two different versions of Gamma PDF ($\theta_1 = 1$ and $\theta_2 = 9.5$), and Beta ($\alpha = \beta = 0.5$) distributions. The resulting probability distributions in Figure 5.3 clearly suggest the need for a correct selection of the PDF representing the input data for MCS, as each of them provides completely different results for the expected TTR values of a 33 kV bus. Table 5.1 shows the analytical parameters resulting from each PDF, providing a comparison of the mean, standard deviation (from mean), minimum and maximum expected values.

Table 5.1: Comparison of input analytical parameters for modelling the fault repair time of a 33 kV bus (MTTR = 140 hours).

Probability Density Function	Mean value	Standard Deviation	Minimum value	Maximum value
	(hours)			
Exponential	131.58	139.91	0.41	656.56
Weibull	136.86	29.19	57.03	195.24
Rayleigh	133.30	75.88	8.53	342.10
Gamma 1	141.33	12.68	113.63	174.83
Gamma 2	144.34	39.65	68.58	261.46
Beta	147.36	127.71	89.17	827.31

Considering the resulting PDFs from the above example, it is clear an opposite behaviour from mean and standard deviation values in Table 5.1, affecting also the minimum and maximum limits of the TTR values. Some distributions provide TTR values very close to the mean (e.g. Gamma 1, Gamma 2, or even Weibull), offering a very low standard deviation. However, these PDFs will neglect the long tail of the resulting distribution required to cover TTR values from very long interruptions, but also faults with shorter duration (i.e. closer to SI values), which are more realistically covered by exponential or Rayleigh PDFs. Therefore, the latter ones, i.e. exponential and Rayleigh (variant of Weibull) distributions, are considered among the best options for modelling fault repair times in MCS. Regarding the use of Beta distribution, due to its nature, it may provide unrealistic results as the conversion of input reliability data into TTR values will never provide fault duration values in the range close to zero (i.e. SIs), and also accounts for a very high standard deviation due to its steep ends.

According to previous assumptions, in most of the analyses of this research, the times of failure (λ values) are considered to follow an exponential distribution, while repair times (MTTR values) are modelled through Weibull's distribution, with the two corresponding scale/shape parameters (Rayleigh PDF) according to [49, 182]. Further analysis, comparisons and results will be provided for the wide range of PDFs in next sections of this thesis, including assessment of the most appropriate PDFs for modelling failure rates (i.e. TTF values) of PCs.

5.2.4 Impact of Time-Varying Failure Rates on Distribution Reliability

Most distribution reliability studies treat failure rates (λ) as constant values over network components' lifetime, which are then converted into TTF values with the corresponding PDF in each case. However, it has been widely shown (e.g. [102, 183, 184]) that failure rates of PCs change according to several conditions, such as the type of asset (with different aging patterns), geographical location, operating characteristics, weather conditions, etc. Also, DNOs' experience has demonstrated that most components follow a certain time-varying pattern in their life cycle, such as the previously introduced bathtub curve (Section 2.5.1). Accordingly, PCs will present a high failure rate following installation (i.e. 'youth' period), then λ decreases and settles to a nearly constant value during the functional period of the PC, and finally, the failure rate tends to increase (i.e. wear-out period) until the component fails or is replaced. As specified in Section 2.5.1, maintenance operations could also be included in the analysis with the saw-tooth bathtub curve. However, these are not considered in this work in order to simplify the analysis.

The goal of this preliminary study is to examine the effects of changing failure rates on distribution system reliability. By applying MCS to a network test model, a reliability assessment using time-varying failure rates will be compared with one using constant failure rates.

Bathtub Scaling Factor

In order to incorporate a change in the failure pattern into the reliability assessment, a time-varying scaling factor following a bathtub (Beta) distribution can be used. The scaling factor defined in this analysis, $\alpha(t)$, is a function of time, varying throughout the expected lifetime (EL) of each PC:

$$\lambda(t) = \alpha(t) \cdot \lambda_c \tag{5.6}$$

where, $\alpha(t)$ is the time-varying scaling factor and λ_c is the constant failure rate normally used for modelling the faults in PCs [183]. The scaling factor can be modelled using different PDFs in order to match the different stages of the bathtub curve. For example, studies presented in [102] or [183] divide the bathtub periods by using linear, exponential or parametric models, which will obviously result in different sets of results. In this analysis, instead of varying the normally constant failure rate only during the break-in and wear-out periods (e.g. by using decreasing/increasing exponential distributions), the input fault rate (λ) is considered as the mean value of the time-varying Beta distribution [182], which is derived considering its fundamental parameters α_B and β_B = 0.5. Then, the model expression for the scaling factor becomes:

$$\alpha(t) = Beta_{PDF} = f(t, \alpha_B, \beta_B) = f(t, 0.5, 0.5) = \frac{1}{\Pi\sqrt{t(1-t)}}, \text{ for } t \in [0,1] \tag{5.7}$$

As in (5.7) the scaling factor $\alpha(t)$ is restricted within the range [0,1], those values are thus extrapolated to the realistic lifespan of every PC in the network model (i.e. 40 years). The applied procedure is shown in Figure 5.4, as an example of a 33 kV bus with a λ_c=0.08 faults/year and a expected lifetime (EL) of 40 years. Instead of building the selected PDF by converting a constant failure rate of λ_c=0.08 faults/year (red dashed line), different time-varying values $\lambda(t)$ are now selected (blue line) over component's lifetime (i.e. 40 years).

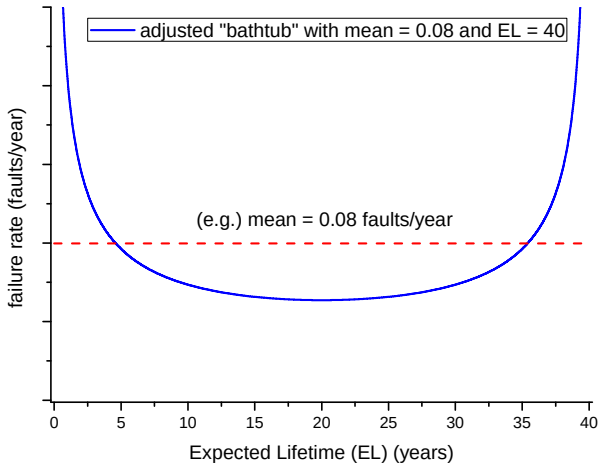

Figure 5.4: Example application of Bathtub (Beta) distribution for the expected lifetime of a power component.

Test Network and Time-Sequential Simulation

The reliability performance of the test network in Figure 5.5 is used as a benchmark study to assess any reliability benefits from the use of time-varying fault rates ($\lambda(t)$). In order to ease the validation of results, the analysis is focused on a specific area of a typical suburban distribution network, as previously detailed in Section 3.7 of this thesis. The test system represents a radial MV overhead feeder supplying 10 secondary transformers, which serve a maximum average load of 1.82 MVA (760 residential customers, i.e. loads L1 to L10) and are represented with their corresponding load profiles and load mix as previously specified in Figure 3.8, Page 61. Security of supply requirements are also included in the analysis for the calculation of restoration times (TTR values) for this type of radially operated networks. In total, the network model is composed of 134 PCs, including transformers, buses, OHLs, circuit breakers, fuse switches, etc. A commercial load (L11) is also included in the model, which is supplied from the primary 33/11 kV substation with an installed demand of 2.2 MVA. However, the commercial loads will not be considered for analysis at this stage.

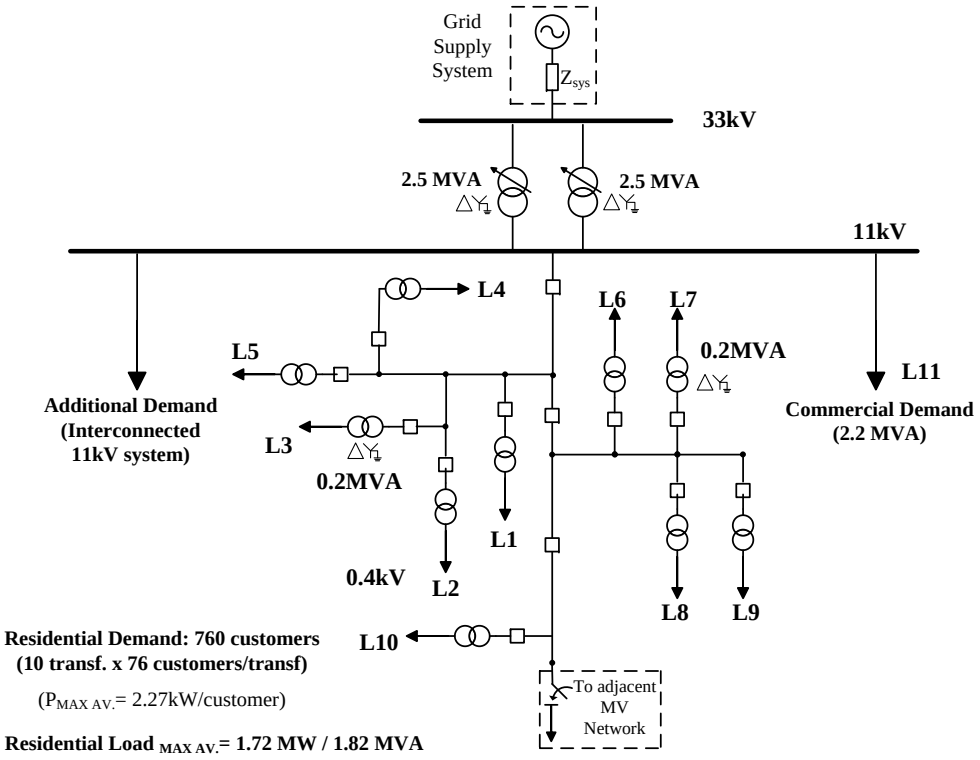

Figure 5.5: Suburban test distribution network (residential + commercial load).

A time-sequential MCS is performed to assess the effects of time-varying fault rates, which will be compared with the results obtained using constant failure rates (λ_c). By applying the time-varying scaling factor ($\alpha(t)$), the failure rate ($\lambda(t)$) is updated and the resulting TTF value is obtained accordingly. The simulation is incremented on a year by year time frame (in 40-year lifetime cycles) and stopped when convergence is met or 1000 years have passed.

For this preliminary study, the PCs are assumed to be new when the simulation starts, which means their initial age is zero. However, a more detailed analysis (e.g. [102, 183]) would be required for the correct assessment of the impact that different aging, environmental or operational conditions would have on each PC over the network's lifetime. Also, the method of component replacement is another important factor to consider, as the assumption of replacing all the PCs after they reach the end of their useful life may not be accurate enough for specialised analyses on network management.

Table 5.2 provides the results of the MCS analysis, with a comparison of the average reliability indices as a result of modelling the PCs' failure rate with both constant and time-varying characteristics. Some analyses (e.g. [102]) apply the constant fault rate (λ_c) to the time period corresponding to the PC's useful life (i.e. out of the break-in/wear-out periods) and then increase λ probability during these high-risk periods, thus frequency-based indicators (i.e. SAIFI and MAIFI) computed with this assumption will experience an increase in their final values, as compared to the constant fault rate (λ_c) over the 40-year time. However, as the analysis presented in this section applies the component fault rate to the mean of the bathtub curve, about the same number of faults are still expected to take place over the 40-year simulation, according to the values of SAIFI and MAIFI indicators in Table 5.2. However, now the interruptions are occurring at different times over the PC's lifetime, stressing the network operation differently, interrupting different power demand values (due to the time-sequential simulation), thus duration-based reliability indicators (i.e. SAIDI, CAIDI) and ENS are now computed with different values.

Table 5.2: Comparison of average reliability indices for constant and time-varying failure rate.

Failure Rate (λ) Distribution	**SAIFI** (int/load/year)	**MAIFI**	**SAIDI** (h/int/year)	**CAIDI** (h/load int.)	**ENS** (kWh/load/year)
Constant λ	0.22	0.25	3.89	12.05	401.6
Time-Varying λ	0.21	0.26	3.4	11.22	349.3

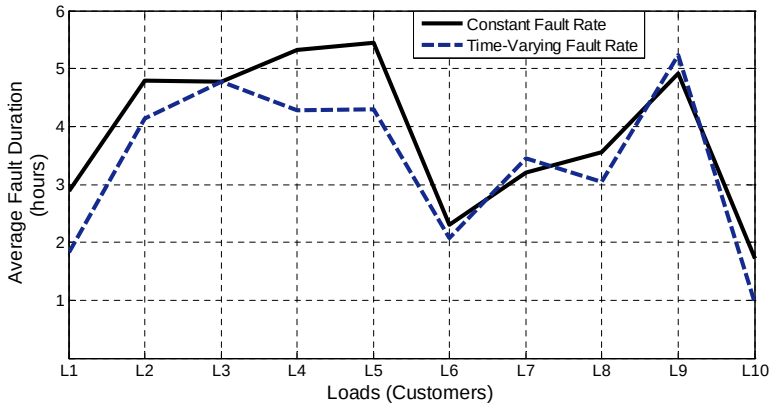

Figure 5.6: Comparison of average duration of interruptions per network load point.

Regarding the average results provided in Table 5.2, the reliability values calculated with the 'constant λ' approach present an overestimation of the reliability performance of the analysed network, specially on the duration and energy-based values of SAIDI, CAIDI and ENS indices. As shown in Figure 5.6, the average duration of the expected customer interruptions at the different load points in the network are more accurately assessed if the 'bathtub time-varying λ' approach is applied in the MCS. These effects are obviously expected to change depending on different network characteristics, arrangements, operating conditions, etc. However, the time-varying failure rates may result in a more accurate representation of actual system reliability.

5.2.5 Integrated Code for Monte Carlo Simulation

For further reference and details, Appendix F presents a detailed example of the main Matlab code used in this research for modelling, by applying an integrated approach, all the aforementioned functionalities of MCS. The code is divided in different sections, including the probabilistic processing of input failure rates and repair times, acknowledgment of time-varying fault probabilities and load profiles, inclusion of backup supply for classification of outages into LIs and SIs, as well as details on the adjustment of simulation accuracy (e.g. 1000 years in 30 min time-steps) for a time-sequential MCS analysis. Several variants of this base code have been developed during this PhD work in order to obtain simulation results.

For each simulation case, the output data (obtained from the process in Matlab) are used as input parameters for representing the stochastic behaviour of the network, by applying risk assessment and power flow analysis. The algorithm is implemented in Python code, using PSSE software [123] to model the analysed distribution network and solve the power flows at each iteration. According to the previously discussed assumptions, the network simulation stage considers all the characteristics of the load models, including ZIP coefficients, load profiles, and different mix of demand sectors (e.g. residential, commercial, etc.), which will also be used for application of several DSM/ES schemes for analysis in the next chapter of this thesis. In addition, by modelling the network reconfiguration and corrective capabilities (i.e. backup supply and reconfiguration actions), it is possible to accurately assess the frequency and duration of customer interruptions, which will be used for computing the final reliability indicators representing end-users and overall system's behaviour.

5.3 Precision Estimation of Monte Carlo Method

As time-sequential MCS used for network reliability analysis is a highly-demanding computational method, the accuracy of results depends on the number of samples in the simulation and variance of the estimate. Therefore, MCS needs many trials to obtain a reasonable accuracy in the obtained results. This section describes the modelling effort during this research in order to estimate the precision of reliability indices calculated by applying the proposed MCS method.

5.3.1 Uncertainty Assessment of MCS

Precision is generally used as a criterion to stop the process of stochastic convergence in MCS method. Therefore, the aim of the analysis in this section is to assess the "natural" behaviour of the time-sequential MCS without applying any technique for variance reduction or acceleration methods (out of the scope of this thesis). Instead, the problem was solved through the parallelisation of calculations by using multiprocessors and several computers. Accordingly, before applying the method to further and more complex analyses, the reliability assessment is firstly applied to the radial test network in Figure 5.5. However, this time the use of alternative supply (i.e. backup action) is not included in the simulation. This is basically to avoid any intrinsic influence of this functionality on the resulting TTR values (i.e. there is no modification, by using "natural" MCS) for computing the final reliability indices.

Coefficient of Variation

The coefficient of variation ε (or precision) of an estimator is a measure of relative dispersion, corresponding to the ratio between the standard deviation and the average [48], with $\sqrt{var(x)}$ being the standard deviation, $\bar{x}$ the average, and N the number of results (i.e. years/samples of simulation):

$$\varepsilon = \frac{\sqrt{var(x)}}{\bar{x} \cdot \sqrt{N}} \times 100(\%) \tag{5.8}$$

MCS steps must be repeated until the coefficient of variation (ε) of the selected reliability index becomes lower than the level of tolerance imposed. For example, a typical tolerance level imposed (e.g. as in [49, 185]) is 7% for the interruption frequency (i.e. SAIFI and MAIFI) and 12% for the unavailability (i.e. SAIDI, CAIDI and ENS). On the other hand, a maximum number of samples N can be imposed as a criterion for stopping the convergence process of MCS. However, the number of samples depends on the variance and the minimum coefficient of variation imposed:

$$N = \frac{var(x)}{(\varepsilon \cdot \bar{x})^2} \tag{5.9}$$

To accelerate this process (i.e. decrease number of samples), by keeping the same precision and not affect the result, solutions must be found to reduce the variance. Five main techniques (not applicable in this analysis) are used in power system analysis to accelerate the MCS [48, 181], which imply the substitution of "natural" sampling with a more sophisticated sampling.

MCS Uncertainty

In order to understand the expected uncertainty (or coefficient of variation ε) from the reliability indices obtained with the proposed MCS method, four different sets of network simulations are undertaken and compared in this analysis. Firstly, three different and totally independent sets of 1,000-year simulations (in 30 min time-steps) are applied to the test network of Figure 5.5, which will serve to assess the randomness of the MCS process by repeating the same number of iterations in different simulations and comparing the outcome. However, as the accuracy of

these simulations might be limited due to the restricted number of samples to 1,000 years, an additional simulation set is proposed, assessing the network reliability for an extended period of 34,000 years, in 4 h time-steps. This will help to clarify whether an extremely long and heavy-loaded simulation is able to provide a much better accuracy (i.e. lower uncertainty by increasing number of samples) when predicting the stochastic behaviour of the tested network.

As a result of these simulations, Figure 5.7 shows how the uncertainty (i.e. coefficient of variation ε) varies over the simulation time, up to 34,000 years, for four different reliability indices. This curve demonstrates a better accuracy as long as the simulation proceeds in time, as compared to simulations limited to e.g. 1,000 years. In addition, Table 5.3 provides a comparison of the resulting uncertainties (in % to the final value) at the stopping time of each simulation, which again demonstrates the most precise results from longer simulations. The 34,000-year simulation decreases the uncertainty to values around 1%, as compared to 5-7% from the 1,000-year simulations. This is mainly due to the higher number of considered outage events (>100,000), making the relative dispersion of results to get closer to the final average value. It must be noted that all the considered results lay within the commonly used tolerance limit of 7% for the interruption frequency and 12% for unavailability.

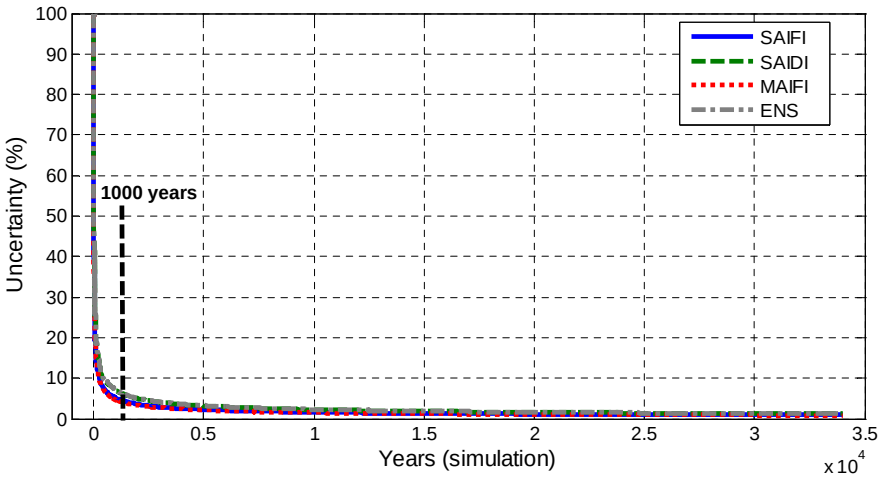

Figure 5.7: Uncertainty distribution of reliability indices over simulation time.

Table 5.3: Uncertainty evaluation of Monte Carlo simulation method.

No. Years Simulation	No. Events (LIs)	Uncertainty (%)			
		SAIFI	MAIFI	SAIDI	ENS
1,000 (set 1)	2,980	5.03	4.89	7.34	7.36
1,000 (set 2)	2,895	5.20	4.74	7.53	7.54
1,000 (set 3)	2,996	5.14	4.75	7.12	7.13
34,000	102,590	0.88	0.82	1.23	1.25

Apart from the uncertainty of the MCS method on its own, it is possible to compare how this affects the final average results for the system reliability indices. Table 5.4 presents a comparison of results for the different sets of simulation.

Table 5.4: Comparison of average reliability indicators for uncertainty analysis.

SIMULATION Results	Avg. No. (LIs/year)	Avg. No. (SIs/year)	SAIFI	MAIFI	SAIDI	CAIDI	ENS (MWh)
1,000 years (set 1)	2.980	3.426	0.2980	0.3426	31.0381	35.4218	3.2684
1,000 years (set 2)	2.895	3.507	0.2895	0.3507	30.3855	36.6470	3.2011
1,000 years (set 3)	2.996	3.624	0.2996	0.3624	29.5304	34.7074	3.1085
34,000 years	3.017	3.464	0.3017	0.3464	30.5143	35.7127	3.1007

There is no big difference in the final values between the simulations with 5-7% tolerance (1,000 years) and the 34,000-year simulation with uncertainty of about 1%. This validates the maximum tolerance levels suggested in [49, 185], and indicates that a simulation of 1,000 years with the proposed MCS method should be enough to provide accurate results for the average reliability indicators. It is important to note that any difference in the final values of SAIFI and MAIFI (frequency of interruptions indices) between sets of the same type (1,000 years) is not due to a variation in the MCS uncertainty, but due to the randomnes of the MCS process, making different number of outages (LIs and SIs) to occur over the simulation time. If the simulation time is not long enough (e.g. 1000 years), power components of, for example, 0.001 faults/year might not be allocated any fault within that time. Therefore, the accuracy in the frequency of interruptions analysis depends on the initial stage of MCS, where random numbers are applied to a PDF for obtaining TTF values. This problem can be solved by increasing the number of samples (e.g. 34,000 years) and thus decreasing the uncertainty of MCS.

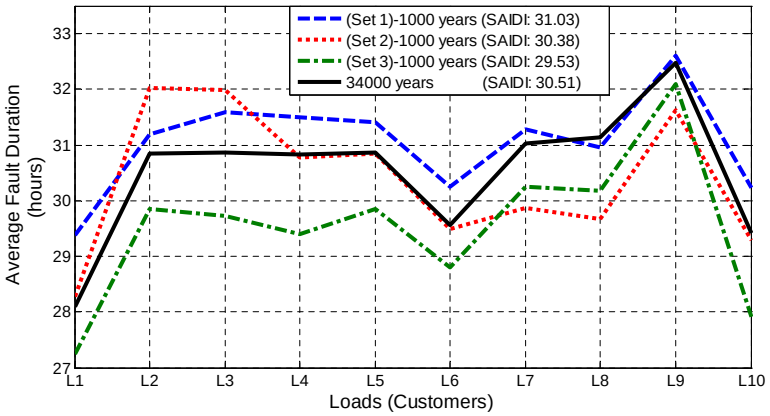

Figure 5.8: Comparison of average duration of load interruptions for uncertainty analysis.

As for the variation in average values of the indices measuring duration of interruptions (SAIDI, CAIDI, ENS), the origin of this problem is in the PDF used to transform the MTTR value of each power component (e.g. exponential, Weibull, Rayleigh, etc., as discussed in Section 5.2.3) and the fact that each new simulation will use a different set of random numbers that will generate a different set of final TTR values. However, if an appropriate number of sample years is simulated, the input PDF used to transform MTTR values will provide a more "complete" set of LIs values as the output from MCS, covering the whole range of interruption values and,

therefore, building a complete PDF with more accurate results. Again, due to a lower uncertainty, the black curve in Figure 5.8 (corresponding to 34,000 years of simulation) provides a more reliable solution to the average values of LIs at each load point of the test network.

All previous assumptions might be accurate enough for computing average values of reliability indices, as well as for representing their resulting PDFs (for each different case) in terms of shape and probability values. However, if the effect of extremely long interruptions (with very low probability of occurrence) on network reliability performance needs to be analysed, longer simulations are required, as there exist a considerable difference in the tail's length of the resulting PDFs when comparing the 1,000 and 34,000-year simulations. For example, from the obtained results, the 34,000-year simulation is able to represent interruptions longer than 650 h, however the three sets of 1,000 years only result in outages within the range of 320 h and 530 h. These are maximum outage times considering the lack of alternative supply in the test network of analysis. Therefore, if a higher accuracy is desired (for the risk assessment of very long interruptions), the MCS uncertainty must be improved by increasing the samples/years of simulation.

5.3.2 Multiple/Simultaneous Fault Analysis

Another important factor, which is normally less researched in risk and reliability modelling of power systems, is the occurrence of multiple simultaneous faults in the networks. These cases, which are consequence of several power components tripping simultaneously, or after a cascading effect (e.g. due to overloading conditions), stress the network up to its $N-1$ or $N-2$ security limits, and thus result in customers experiencing very long times of supply interruptions. Therefore, it is important to understand what is the probability of these faults happening in distribution networks, and also what is their estimated contribution to the total down-time of the overall network per year. As multiple/simultaneous faults have a big impact on the computation of final reliability indicators, they considerably affect DNOs annual income through the payment of penalties to the energy regulator.

Accordingly, through the stochastic applicability of MCS, a detailed analysis has been carried out to identify the number of single and multiple (i.e. double, triple, etc.) faults/trips of power components within the radial test network of Figure 5.5, for the different sets of simulation. As no backup action is included in the model, the resulting proportion of single/multiple faults can be considered as representative of the "natural" reliability behaviour of this type of radially operated distribution networks. For this analysis, two different sets of 1,000 years are compared against the 34,000-year simulation. Their results are compared in Tables 5.5 and 5.6 below, where absolute (i.e. total) and relative (i.e. per-year) values are provided respectively. The identified outage events are classified into permanent (i.e. LIs > 3 min) and transient (i.e. SIs < 3 min) faults, providing their frequency and duration over the simulation time.

Table 5.5: Comparison of absolute values for multiple/simultaneous fault analysis.

Multiple Fault Analysis (Absolute values)	Frequency (No.)						Total Outage Duration (over simulation time)	
	Permanent Faults (>3min)			Transient Faults (<3min)				
	Single	Double	Triple	Single	Double	Triple	Single	Double
Set 1 (1,000 years)	576 (99.14%)	5 (0.86%)	-	703 (99.57%)	3 (0.43%)	-	5.227 years (99.68%)	6.021 days (0.32%)
Set 2 (1,000 years)	584 (99.65%)	2 (0.35%)	-	696 (99.71%)	2 (0.29%)	-	5.027 years (99.96%)	9.5 hours (0.04%)
34,000 years	19,589 (99.6%)	79 (0.4%)	-	22,905 (99.47%)	121 (0.53%)	1 (0%)	174.67 years (99.8%)	123.5 days (0.2%)

Table 5.6: Comparison of relative values for multiple/simultaneous fault analysis.

Multiple Fault Analysis (Relative values)	Frequency (No.)						Total Outage Duration (over simulation time)	
	Permanent Faults (>3min)			Transient Faults (<3min)				
	Single	Double	Triple	Single	Double	Triple	Single	Double
Set 1 (1,000 years)	0.576 /year	0.005 /year	-	0.703 /year	0.003 /year	-	1.907 days /year	8.64 min /year
Set 2 (1,000 years)	0.584 /year	0.002 /year	-	0.696 /year	0.002 /year	-	1.834 days /year	0.57 min /year
34,000 years	0.576 /year	0.0023 /year	-	0.673 /year	0.0035 /year	≈ 0 /year	1.875 days /year	5.23 min /year

As shown in tables above, there is a consistency in the frequency and duration of single and double faults for the three different cases (even for the 34,000-year set). Only in this latter case, with such a long time of simulation, a transient triple fault is captured. Accordingly, for a more extensive analysis of the effects from multiple/simultaneous faults on network reliability, the percentages provided in Table 5.5 for single, double and triple faults could be interpreted as the standard deviation values (σ, 2σ and 3σ) from the mean of a non-standard normal distribution, by modifying the standard normal PDF (e.g. Figure 5.9).

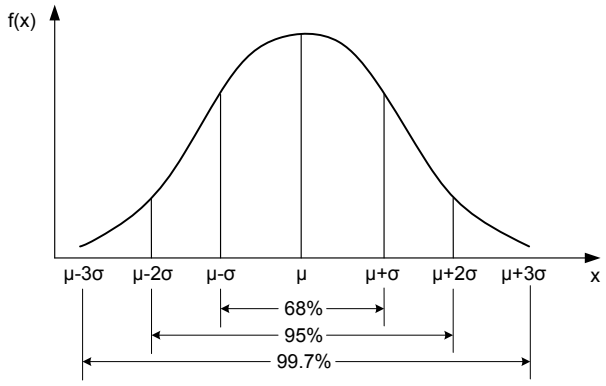

Figure 5.9: Standard deviation and probabilities associated with a normal distribution.

Again, due to the variability of input PDFs and random numbers in MCS, the most detailed results are those provided by the 34,000-year simulation, as more double (and even triple)

faults are captured within the simulation time. Therefore, the 79 permanent double faults that take place within 34,000 years of simulation (Table 5.5) have been analysed and presented in Figure 5.10. After processing the empirical results on double fault probability, Figure 5.10 shows the kernel (probability) density function representing the most probable durations for this type of multiple faults in the system (without applying any corrective backup action).

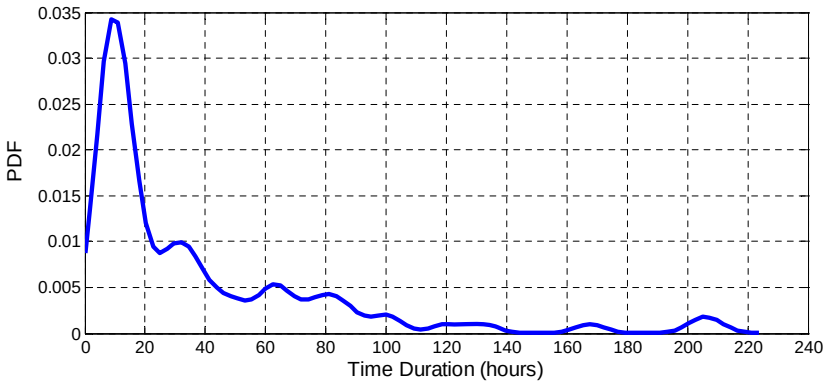

Figure 5.10: Kernel density function of permanent double faults after a 34,000-year simulation.

5.3.3 Convergence Analysis of MCS

Considering that the uncertainty criteria proposed in Section 5.3.1 for stopping Monte Carlo simulation might not be enough in some cases, an additional criteria based on convergence is developed in this section. As long as the simulation is run for a minimum number of samples (years), it has been proved that there are not big differences in terms of mean values and PDFs between sets of, for example, 1,000 and 34,000 years. However, if 1,000 years (with 5-7% uncertainty) is considered not accurate enough, and taking into account the high computational demand of a 34,000-year simulation (<1% uncertainty), an additional criteria could be formulated for stopping MCS with a high enough level of accuracy.

Accordingly, by considering again the sets of simulation discussed before, i.e. 3 sets of 1,000 years and another of 34,000 years, applied to the radial test network of Figure 5.5, the results provided in Figures 5.11 and 5.12 below present the calculated convergence of the mean values for the reliability indices measuring frequency of interruptions (i.e. SAIFI and MAIFI). First, Figure 5.11 provides a comparison of how the mean value of SAIFI index converges as the simulation proceeds for the three different sets of 1,000 years, while Figure 5.12 shows how the convergence behaves with the possibility of increasing the precision of results by extending the number of samples (years) in the simulation. Therefore, this analysis could help to develop and additional criteria for stopping MCS with some confidence. The final mean values (i.e. SAIFI and MAIFI at the stopping time of MCS) for the different sets of simulation are those previously shown in Table 5.4, where the uncertainty of MCS was discussed.

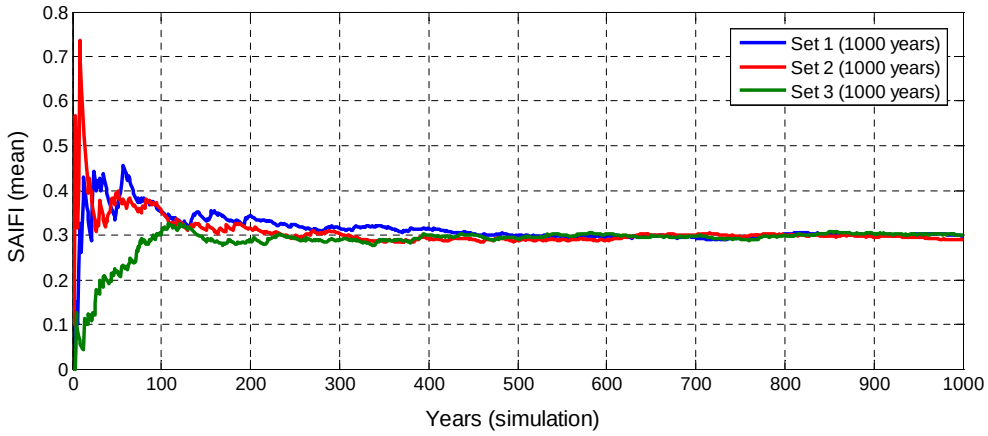

Figure 5.11: Convergence of SAIFI mean value for three different 1,000-year simulations.

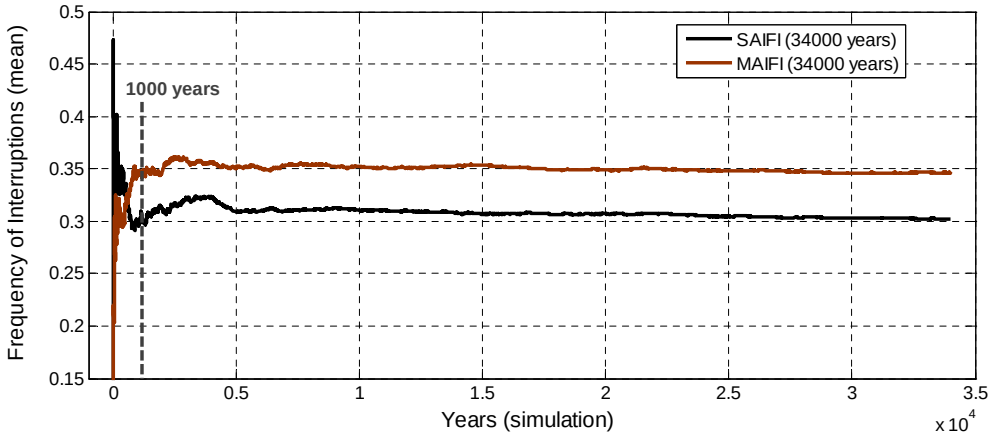

Figure 5.12: Convergence of mean value of frequency of interruptions (SAIFI and MAIFI indices) over a 34,000-year simulation.

Convergence Criteria for Stopping MCS

Again, as it happened with the coefficient of variation ε (i.e. uncertainty) discussed before, the convergence tolerance (based on the standard deviation concept) must be set to a desired threshold, more or less accurate. The new convergence criterion is based on the results presented in the Figures 5.11 and 5.12, where the mean values of different indicators progressively converges to the final value. Therefore, the absolute difference between consecutive mean values (e.g. x_1, x_2, etc.), measured in %, is tracked along with the simulation and used as the criteria to stop MCS when it is below a certain limit, i.e. a tolerance (τ) of 0.1% for example:

$$\tau = \left| 1 - \left(\frac{x_2}{x_1} \right) \right| \times 100(\%) < 0.1\% \ (\textit{to be set}) \tag{5.10}$$

This criteria is firstly applied to one of the indicators obtained before (SAIFI, from Set 1 of 1,000 years) as shown in Figure 5.13 below. The convergence tolerance is measured and

compared against the ±0.1% limits over the simulation time, but for such a small number of samples (1,000 years) it does not provide any additional criteria for stopping MCS. There exist a convergence of the tolerance approximating to values around 0.1%, but they keep oscillating up to the end of the simulation, so the stopping time of 1,000 years would not be conclusive enough for the set tolerance of 0.1% (maybe for a higher one).

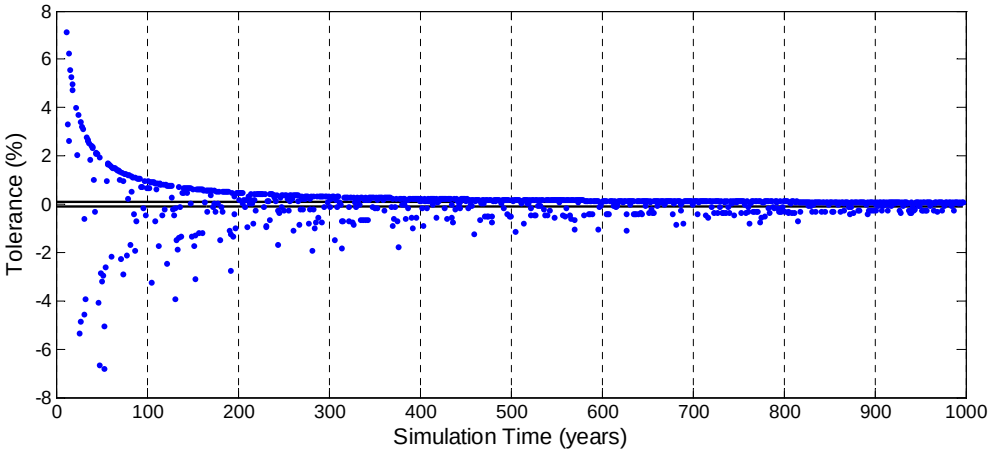

Figure 5.13: Convergence tolerance of SAIFI index over a 1,000-year simulation.

Therefore, the same method is applied to the 34,000-year simulation, as shown in Figure 5.14 below, in order to identify any optimal point for stopping the simulation somewhere between 1,000 and 34,000 years.

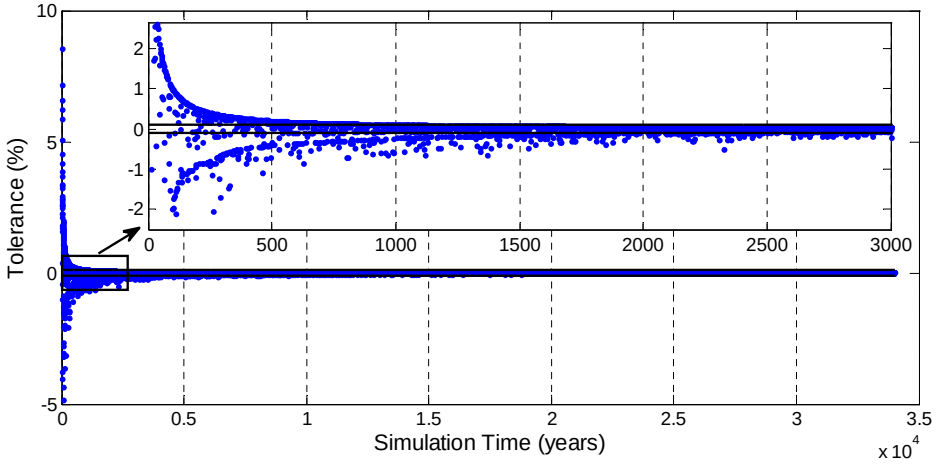

Figure 5.14: Convergence tolerance of SAIFI index over a 34,000-year simulation.

In Figure 5.14, the tolerance values start to converge and fall within ±0.1% values from very early samples (i.e. 1500 years), however their oscillation around the set thresholds does not provide the required accuracy in the results. Therefore, a possible criterion for stopping MCS could be based on searching for the last sample where the tolerance is out of the desired limits (>0.1%). In this particular case, as shown in Figure 5.15, the last year in which there is a

difference bigger than 0.1% between mean values is in year 9,235. Hence, that could be one possible criterion for stopping the simulation, as it was checked that further sampling will fall within the 0.1% limits, and would not provide more accurate results for the desired accuracy.

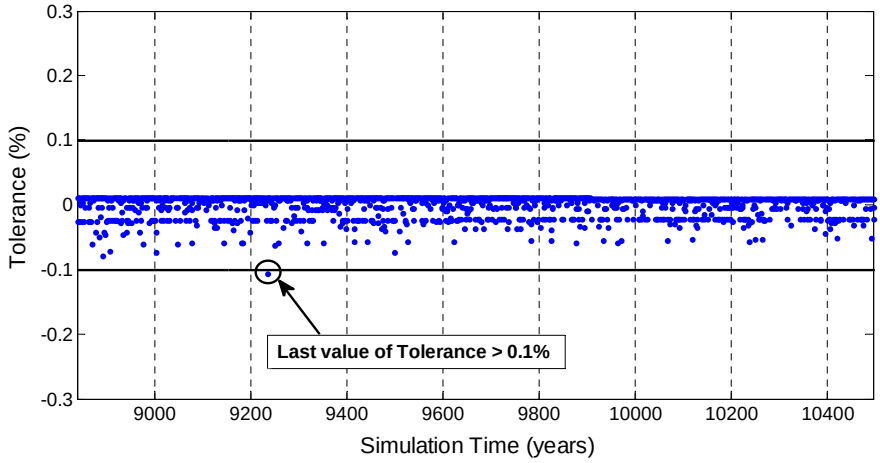

Figure 5.15: Zoom into the convergence tolerance of SAIFI index over a 34,000-year simulation.

In order to speed up the simulation process, another possible option would not be as accurate as searching for the last value to fall out of the limits, but would require a maximum number of occurrences within a specified range of samples. For example, for every consecutive 500 years of simulation, MCS would not stop until the number of tolerance values (τ) to fall out of the limits is less than a specified percentage (%).

5.4 Empirical Model for Customer Interruption Process

This section describes a theoretical interruption model for assessing the customer interruption process in power supply systems, enabling to establish more accurately the moment in time when both SIs and LIs occur. For this purpose, past recordings of SIs and LIs from two DNOs are used to define the empirical time-distribution of the interruption process, and develop the corresponding theoretical interruption model. The estimation of the exact time when network outages occur can be improved if a realistic interruption probability model, derived from real measurements, is used during the analysis. Instead of using values of interruption times obtained from the conversion of failure rates (λ) into TTF values (which result in a uniform distribution regardless of the input PDF selected to model the failure process of network components), an empirical interruption model should be employed in the MCS procedure.

Two-year recordings from two European DNOs were processed for this analysis to determine hourly distributions of SIs and LIs (i.e. time of the day when interruptions occurred). Accordingly, only the interruption times of the outage recordings were selected for analysis. After

the interruption times were classified into different groups of hours, the number of interruption occurrences for each hour (from 0 to 24 h) was counted, allowing to transform these values into probabilities by dividing the frequency of hourly interruptions to the total number of recordings. Figure 5.16 shows the probability profiles of SIs and LIs, together with the aggregate load profile at the GSP level (33 kV), which considers a mixed load of residential, commercial and industrial demand, as previously specified in Figure 5.2, Page 127. There exist a close correlation between the SI/LI interruption profiles and aggregate load profile, confirming a higher probability of occurrence of both SIs and LIs when demand is higher (i.e. between 8:00 and 19:00 hours).

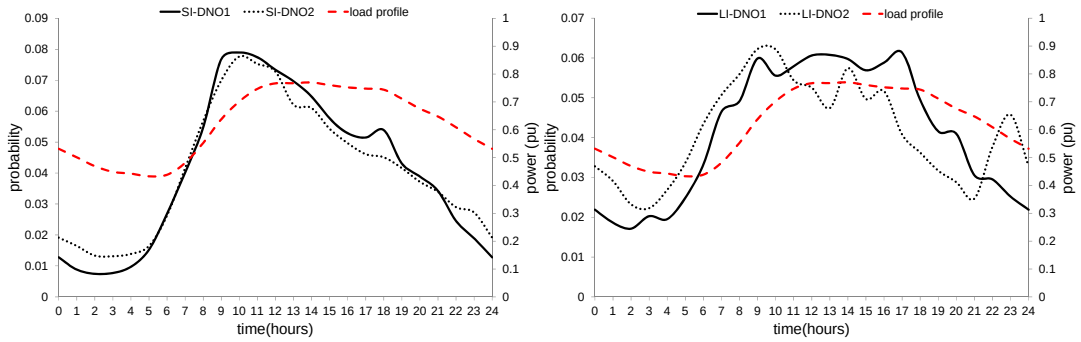

(a) SI Profile **(b)** LI Profile

Figure 5.16: Daily probability distributions of short and long interruptions.

In order to provide additional material for the work on network predictive fault performance, Appendix G provides further probabilistic analysis of the outage data provided by Scottish Power Energy Networks (SPEN) for the reporting years 2009 and 2010, covering permanent/-long and temporary/short interruptions in their electricity distribution systems. Accordingly, in this appendix the fault recordings are used to determine the (daily, seasonal, etc.) probability distributions of both unplanned and planned long and short interruptions of customers.

5.4.1 Theoretical Interruption Model

In order to make the proposed outage model applicable when recordings/statistics of both SIs and LIs are not available for the analysed system, this section introduces a theoretical model that matches the empirical PDFs of network interruptions. In Figure 5.16, the recordings used to build the two empirical interruption probability profiles follow a similar pattern, even though they correspond to two completely different supply systems in Europe. Therefore, the profiles of SI and LI distributions, which can be used in the MCS procedure for a better estimation of reliability performance, can be approximated with a multi-zone theoretical interruption model. Accordingly, the two SI and LI distributions from Figure 5.16 are averaged and used to create the theoretical interruption model shown in Figure 5.17, in which four zones represent different probabilities of occurrence at different times of the day.

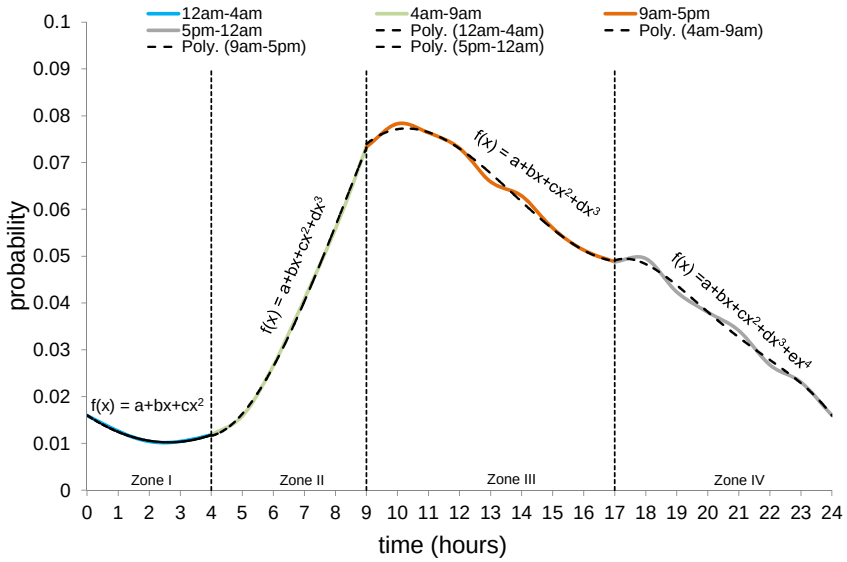

a) Polynomial approximation for SI profile.

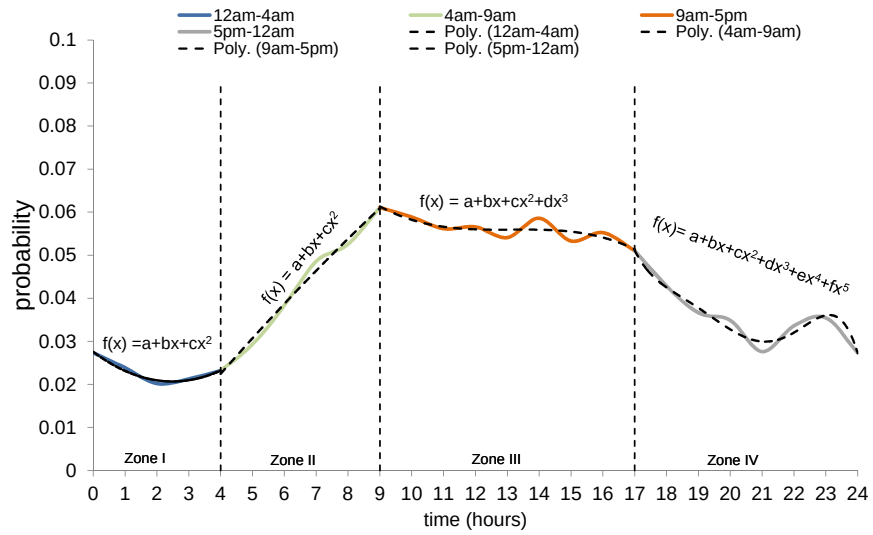

b) Polynomial approximation for LI profile.

Figure 5.17: Theoretical model approximation of the average empirical distributions.

In Figure 5.17, 'Zone I' corresponds to night hours (between 12 am and 4 am) and interruptions within this period can be modelled as a second degree polynomial function for both SIs and LIs. 'Zone II' is allocated to morning hours (between 4 am and 9 am), where interruptions occurring during this time can be approximated by a third degree polynomial function for SIs, and a second degree polynomial function for LIs. 'Zone III' corresponds to day hours, giving the probability of SIs and LIs occurring between 9 am and 5 pm as a third degree polynomial function. Finally, 'Zone IV' is defined for evening hours (between 5 pm and 12 am), which is modelled as a fourth order polynomial function for SIs, and fifth order polynomial function for

LIs. In this way, the empirical interruption probability model can be represented in reliability analyses by the theoretical interruption curves of SIs and LIs, illustrated in Figure 5.17 with black dashed lines. The analytical expressions of the theoretical approximations are given by the polynomial coefficients 'a' to 'f' in Table 5.7 for both SI and LI curves. It should be noted that for an accurate reproduction of the empirical values, the polynomial coefficients must be used in simulations with a significant number of decimals.

On the other hand, if a more general approach is required to reproduce the empirical values of fault probabilities, a simplified approximation was published by the author in [34], where the multi-zone theoretical interruption model is derived as a combination of uniform and linearly increasing/decreasing probability distributions.

Table 5.7: Polynomial coefficients of theoretical interruption curves - SI and LI approx.

Int. Type	Hour Interval	Polynomial Coefficients					
		a	$b \cdot X$	$c \cdot X^2$	$d \cdot X^3$	$e \cdot X^4$	$f \cdot X^5$
SI	**0-4**	0.0160072425	-43.922667E-4	8.351203E-4	-	-	-
	4-9	0.0794654623	-0.0396454157	67.473557E-4	-2.689127E-4	-	-
	9-17	-0.2951633646	0.0903534231	-70.098141E-4	1.697450E-4	-	-
	17-24	-8.3078087319	1.6335357513	-0.1188044458	38.161714E-4	-4.58276E-5	-
LI	**0-4**	0.0275694530	-55.420851E-4	11.136680E-4	-	-	-
	4-9	-0.0135739431	95.794898E-4	-1.445445E-4	-	-	-
	9-17	0.2362372821	-0.0413568955	31.590979E-4	-8.03559E-5	-	-
	17-24	158.581766979	-39.979245586	4.0231665614	-0.201873857	50.491682E-4	-5.03459E-5

5.4.2 Application and Effectiveness of the Outage Model

The proposed theoretical interruption curves can have a strong impact on several engineering applications related to interrupted customers and the computation of system and end-users' reliability indices, such as the estimation of energy not supplied (e.g. ENS index). In order to emphasise the differences between estimated results with the theoretical interruption model and those obtained with the conventional MCS procedure, a simple example can be drawn by considering a (BSP) load point supplied through a simple system as illustrated in Figure 5.18.

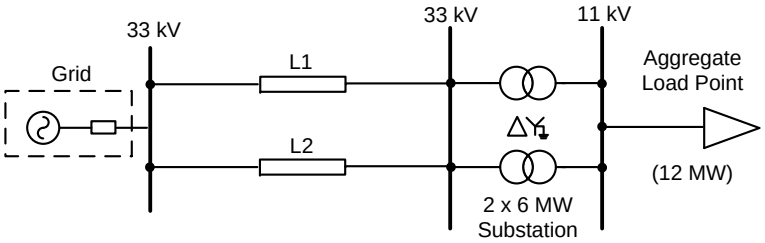

Figure 5.18: Simplified MV system supplying aggregate load point.

For this analysis, the initial conditions of failure rates (λ) and repair times (MTTR) are modelled by either exponential, Weibull, Rayleigh or Gamma distributions ('real' distributions). Accordingly, the CDFs of the theoretical interruption curves (black (LI) and grey (SI) solid

lines) and the CDFs of the real distributions, which are the result of simulating the interruption time occurrence for the large system analysed in next chapter, are shown in Figure 5.19 together with the power profile of the aggregate mixed load (red dashed line). Regarding the CDFs of real distributions, similar CDF profiles are obtained for both SI and LI simulations, therefore Figure 5.19 only illustrates one set of CDFs for the real distributions (i.e. the LI's one).

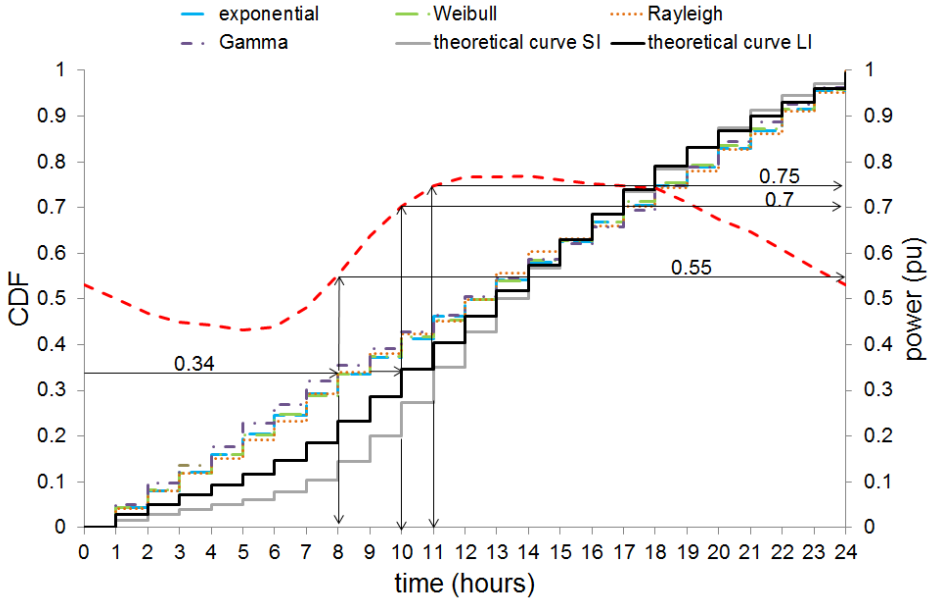

Figure 5.19: Moment of interruption modelling for real distributions and theoretical CDFs.

The process of developing the CDFs of the real distributions is a straightforward approach derived from the reliability analysis. The interruption times obtained from the conversion of failure rates (λ) into TTF values are extracted from the MCS results and included in a common data vector, which is defined separately for every distribution assumed to model the initial conditions of MCS. Once the vector of all interruption times is available, the CDF is calculated for each considered distribution. On the other hand, the theoretical CDFs of SIs and LIs are calculated from the probability values given by the polynomial coefficients in Table 5.7. It is noticed that the exponential, Weibull, Rayleigh and Gamma CDFs overlap and can be approximated by a unique CDF. Also, if a Kolmogorov-Smirnov test [186] is performed, it can be concluded that the results of the real distributions match the uniform distribution:

$$f(t) = \begin{cases} \frac{1}{b-a} & a \leq t \leq b \\ 0 & t < a \text{ or } t > b \end{cases} \tag{5.11}$$

where, t is the analysed variable, $f(t)$ is its PDF, a and b are the extremes of the time interval in which data fall into. In this analysis, the variable t is any given hour within the 24-hour day interval, with $a = 0$h and $b = 24$h.

If, for instance, the MCS procedure generates an input random variable of 0.34, the time when the interruption occurs is different for the real distributions and theoretical curves, and consequently the power interrupted changes. In the case of real distributions, the interruption occurs at 8 am with a corresponding power of 0.55 p.u., while the theoretical curves show that the customer would be interrupted at 10 am (for LI) and 11 am (for SI), with an interrupted power of 0.7 p.u. and 0.75 p.u. respectively. This simple example demonstrates that an error in the initial modelling assumptions results in unrealistic results, and that the theoretical model obtained from recordings increases the accuracy of the reliability estimations.

The energy not supplied (ENS) to the BSP in the basic system of Figure 5.18 can be quantified by running the simulation algorithm with and without the proposed theoretical curves. Four types of loads, residential, commercial, industrial and mixed load having the power profiles as in Figure 5.2 (Page 127), are used to model the analysed BSP. In addition, the estimations achieved with the theoretical model are compared against those given by the real distributions and the differences between them are shown in Table 5.8. It should be noted that even though the theoretical model is employed in the simulation procedure, this is only used to determine the moment in time when interruptions occur and not to completely replace the distributions used to model the initial conditions. More specifically, failure rates (λ) and repair times (MTTR) are modelled using either exponential, Weibull, Rayleigh or Gamma distributions, and instead of considering that the interruptions occur at the moment given by the results of those distributions (which fit the uniform distribution as seen in Figure 5.19), the values resulted from the theoretical model are used.

Table 5.8: ENS results with real distributions and theoretical model for different load types.

Probability Distribution		ENS (MWh/yr)	Type of Load			
			Residential	Commercial	Industrial	Mixed Load
Exponential	real distribution	mean	23.44	19.47	21.68	22.34
		std.	20.58	17.44	19.74	19.96
	theoretical curve	mean	19.33	14.11	17.69	18.93
		std.	16.72	14.98	15.57	18.34
	difference between real and theoretical distrib.	mean	4.11	5.36	3.99	3.41
		std.	3.86	2.46	4.17	1.62
Weibull	real distribution	mean	32.05	27.83	31.91	29.06
		std.	43.07	42.04	42.5	42.89
	theoretical curve	mean	30.32	19.73	26.2	26.04
		std.	41.38	26.52	37.15	35.4
	difference between real and theoretical distrib.	mean	1.73	8.1	5.71	3.02
		std.	1.69	15.52	5.35	7.49
Rayleigh	real distribution	mean	43.67	30.52	27.57	18.61
		std.	28.19	18.5	16.26	39.95
	theoretical curve	mean	32.87	20.61	24.83	29.24
		std.	19.82	11.27	17.11	16.33
	difference between real and theoretical distrib.	mean	10.8	9.91	2.74	-10.63
		std.	8.37	7.23	-0.85	23.62
Gamma	real distribution	mean	19.09	15.72	17.08	16.78
		std.	8.54	7.07	7.75	7.91
	theoretical curve	mean	19.79	16.48	17.65	17.53
		std.	8.71	7.34	7.75	7.93
	difference between real and theoretical distrib.	mean	-0.7	-0.76	-0.57	-0.75
		std.	-0.17	-0.27	0	-0.02

The simulation results presented in Table 5.8 confirm a significant discrepancy between the results of the real distributions and those of the theoretical model. Although the theoretical interruption model only changes the considered time at which system faults are computed over the day (instead of uniformly distributed), it obviously affects the final values of ENS index, due to the daily variation of the power which is interrupted in each case (i.e. residential, commercial, industrial or mixed demand curves). In addition, there exist considerable differences, for example, among results obtained from different real distributions (even for the same load profile). This is due to the fact that each PDF, with different probabilistic nature, has a different effect on the frequency (i.e. counted number of system faults) and duration of interruptions, which therefore has an impact on SAIFI and SAIDI indices, and also on the final values of ENS index.

For exponential, Weibull and Gamma cases, the highest difference between the real distribution and theoretical model results is recorded when the load point is represented by a commercial customer (i.e. 5.36, 8.1 and 0.76 MWh/year), whereas in the Rayleigh case it seems that the residential load followed by the mixed power profile leads to significant discrepancies in the estimations (i.e. 10.8 and 10.63 MWh/year, respectively). At this stage, it can be concluded that the theoretical model contributes significantly to the ENS estimations, however it cannot be decided which of the four real distributions is the most suitable to accompany the theoretical model in similar studies. This will be assessed in the analysis presented in next Chapter, where the reliability performance of a realistic supply system will be compared against reported figures by UK DNOs.

5.5 Conclusions

In this chapter, an integrated approach for reliability modelling of power supply systems has been discussed. Accordingly, this chapter presents the main reliability criteria and techniques used in this thesis for the calculation of system and end-users' reliability indices. Regarding the essential considerations for the study of distribution system's reliability, the focus was on the expected changes in this type of networks and on the new challenges they introduce to quality of supply studies.

As the methods currently used for network reliability assessment must be adapted for the correct assessment of the expected 'smart grid' functionalities (e.g. DG, ES and DSM), the application of Monte Carlo Simulation (MCS) method is proposed in this chapter, as it provides a very powerful tool for the modelling and resolution of complex systems. Although its main disadvantage is represented by its demanding computation time, due to its nature, the solution time can be reduced by the use of parallel calculation. In addition, the MCS procedure can be easily combined with analytical equivalents, which enable the aggregation of customers and sections of the network, depending on desired level of detail and available computation speed.

Several applications have been introduced in this chapter for the correct modelling of MCS methodology and the correct classification of long and short customer interruptions. Accordingly, the inclusion of actual load profiles in the procedure is discussed, as well as the assessment of different input probability distributions, and the impact of time-varying failure rates on distribution reliability. The precision estimation, i.e. the study of uncertainty and convergence of the resulting reliability indices, is also discussed in combination with a study of the expected multiple/simultaneous faults within a distribution network's lifetime.

Finally, a new theoretical interruption model is introduced for assessing more accurately the time of the day when interruptions of electricity customers are likely to occur. Recordings of short and long interruptions from two power supply systems are analysed, and the similarity between their patterns is identified and then used to introduce a general interruption probability distribution model, defined in stages as multi-zone theoretical curves. For an accurate reliability assessment of future distribution networks (i.e. with new 'smart grid' functionalities), ENS index must always be considered as one of the main measuring indicators due to the dependency of network fault probabilities on the aggregate load profiles over the day.

Chapter 6

Integrated Reliability Analysis of Active Distribution Networks

This chapter evaluates the applicability of the proposed Monte Carlo simulation algorithm, in combination with different network functionalities and equivalent models, for an integrated reliability analysis of actively-managed distribution networks. The effectiveness to model the initial MCS conditions of the previously developed theoretical interruption model is also assessed in this chapter by applying the method to a 'realistic' distribution system.

The following sections discuss the application of different reconfiguration, switching, and security of supply schemes to the MCS procedure, in order to assess the network stochastic behaviour and evaluate the impact of different network functionalities on the accuracy of reliability performance results. Moreover, a deterministic reliability algorithm is developed, in order to acknowledge the protection of electricity customers from extremely long outages.

Finally, this chapter analyses the influence of distributed energy resources on reliability performance of active networks (i.e. "smart grids"). The integrated time-sequential MCS methodology is used to assess the potential improvements that different demand-side management and energy storage schemes will have on the frequency and duration of customer interruptions.

6.1 Reliability Performance of a Real Power Supply System

Considering all the reliability criteria and techniques presented in Chapter 5 for the correct calculation of system and end-users' reliability indices, this section expands the validation of the applied MCS procedure (i.e. algorithm in Figure 5.1) by testing the effectiveness of the proposed theoretical interruption model in a more realistic distribution network configuration, consisting of about 15,000 residential electricity customers. In Chapter 5, results obtained from a basic BSP system demonstrated that the theoretical interruption model contributes significantly to the ENS estimation, as it enables to capture the exact time when supply interruptions take place in the network. Therefore, the analysis presented in this section will also compare the reliability results against reported figures of reliability indices (by UK DNOs), which will determine the most suitable PDF that shall be used to model the initial conditions of MCS and accompany the proposed theoretical model throughout the simulation process.

The test system used in this section to illustrate the integrated reliability assessment methodology, and validate the proposed theoretical interruption model, is based on the typical/generic MV distribution networks previously defined and analysed in Section 3.7 for different load subsectors. Accordingly, the test system in Figure 6.1 represents typical configurations of highly-urban and suburban residential and small commercial distribution networks. The total load supplied in the highly-urban/meshed network is 36 MVA, with an alternative supply point at 11 kV, whereas the suburban system is operated with radial configuration, serving 4 MVA of load and with the support of a backup supply point at the end of the radial trunk feeder. For example, the meshed configuration of the highly-urban network allows to efficiently isolate faults on 11 kV main and lateral feeders, therefore the presence of alternative supply points is analysed with particular attention, as it is important for the operation of modern distribution networks and for satisfying security and reliability-related requirements.

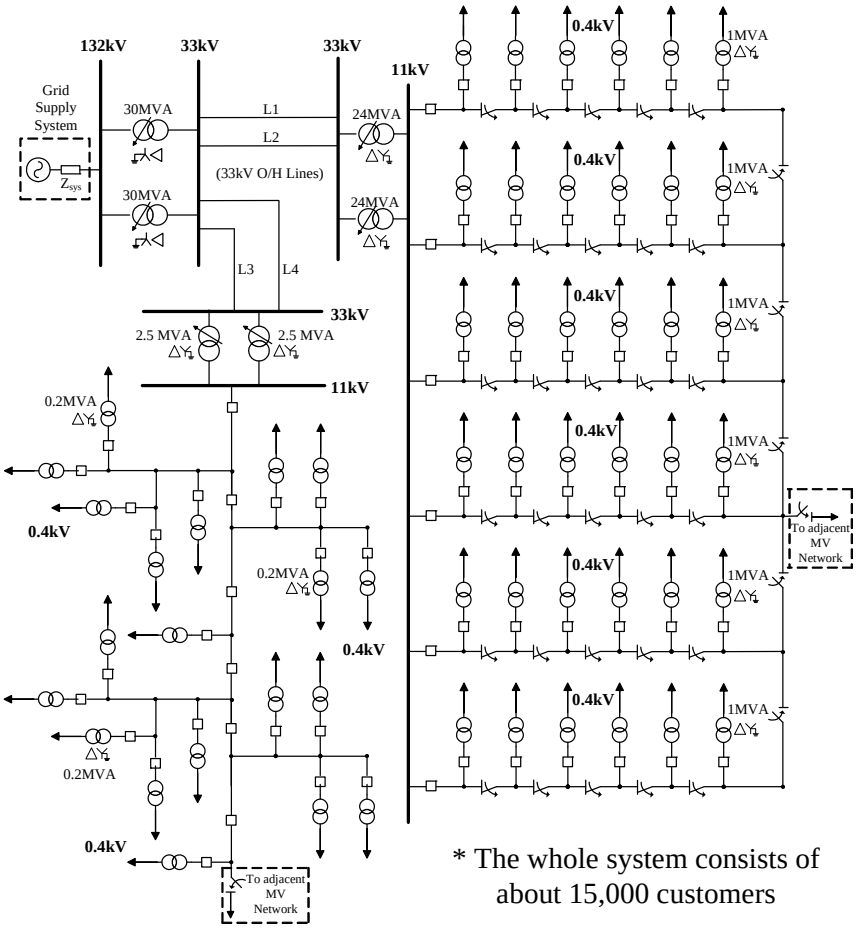

Figure 6.1: Distribution system with typical highly-urban and suburban configurations.

For both network configurations, the frequency of customer interruptions is determined by analysing faults which occur in the system based on failure rates assigned to all network components. However, the considered scenarios change in terms of duration of supply inter-

ruptions due to the differences in network configurations and the use (or not) of alternative supply. Accordingly, the values of failure rates (λ) and repair times (MTTR) implemented to model the initial conditions of the test system in Figure 6.1 correspond to collected reports in Table 2.7 (Page 36) for each network component and voltage level. After a fault occurs, the customers will be interrupted for a certain period of time in accordance with applied protection schemes and required time to repair (TTR) the faulted power component(s), (PCs). Therefore, data presented in Tables 2.4 and 2.6 (Section 2.4) are used for modelling security and quality of supply (SQS) requirements and protection settings, respectively. The time to restore supply (TTRS) is equal to the repair time (i.e. MTTR value from Table 2.7) of faulted PC/s when the fault is permanent and it is not possible to reconfigure the network due to its radial structure. On the other hand, the duration of interruptions within the meshed parts of the system is determined by the protection schemes (i.e. TTR values) for some of both temporary (SIs) and permanent faults (LIs), when the reconfiguration of the system is possible.

6.1.1 Assessment of Energy Not Supplied (ENS)

The same approach, as the one previously applied to the aggregate BSP case in Section 5.4.2, has been employed to the test distribution network in Figure 6.1 to determine the ENS index (presented in Figure 6.2) under 'real' distributions and theoretical model assumptions.

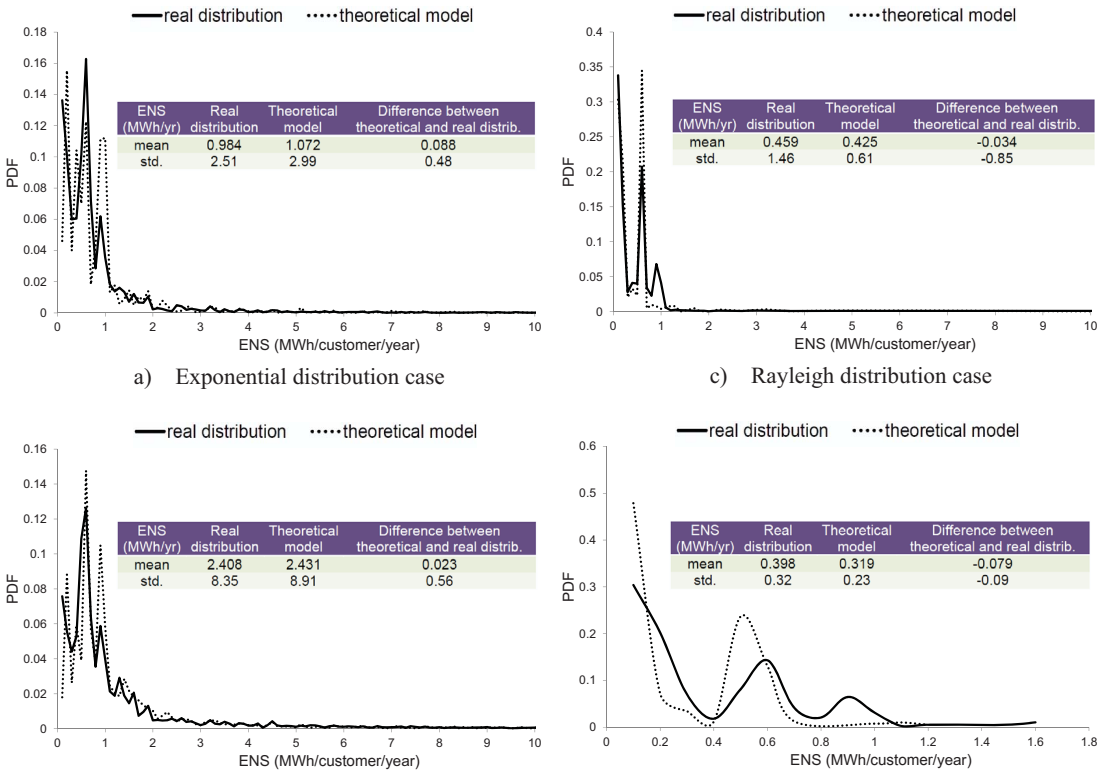

a) Exponential distribution case

c) Rayleigh distribution case

b) Weibull distribution case

d) Gamma distribution case

Figure 6.2: Estimations of ENS index for several probability distributions.

For the calculation of ENS PDFs in Figure 6.2, the estimations for the real distributions are obtained following the steps given by the MCS algorithm in Figure 5.1, whereas the theoretical model outputs are in accordance with the steps included in Section 5.4 of the last chapter. Accordingly, the PDFs assumed to model the initial conditions of the simulations show different results for the ENS index. The values obtained for the exponential distribution are on average about 1 MWh/year for the entire system; Weibull distribution leads to energy not supplied values of 2.4 MWh/year, whereas Rayleigh and Gamma distributions limit the results to significantly lower values (300-400 kWh/year) compared to previous two cases.

Regardless of the distributions considered to model the initial conditions of the simulation procedure, the results confirm the findings reported in Section 5.4.2 for the system supplying a single aggregate load point: errors affect the estimations if the theoretical model is not implemented to assess the interruption times. The differences between theoretical and real distribution results are not significant when reported for the whole system, presenting difference mean values within the range of 23 to 88 kWh per year, for Weibull and exponential distributions respectively.

However, the difference between the comparisons increases sharply if ENS is quantified for individual customers or group of customers instead of for the whole system. For example, differences in the calculated ENS between real distributions and theoretical model for the worst served customer within the analysed system are over 1.2 MWh per year (i.e. with Weibull distribution). For Weibull PDF, this difference represents up to 52 times the difference mean values obtained for the whole system (e.g. 23 kWh). This can be explained by the diversity within the system reliability. Some customers are supplied by grid connections characterised by a lower reliability than others. Thus, there is a cancellation (i.e. averaging) effect between customers with high amount of interrupted power and those which have a history of both low frequency and duration of interruptions. The load profile associated to each customer point also has its contribution to this cancellation effect.

6.1.2 Estimation of Conventional Reliability Indices

The theoretical interruption model influences the estimation of ENS index, both for the whole system, and even more for individual customers. However, the expected impact on the results from the application of real distributions depends on the level of system reliability, as for highly reliable systems these changes are not significant in comparison to systems featuring lower degrees of reliability. Therefore, in order to establish which PDF is most suitable for modelling the initial conditions of MCS procedure in combination with the theoretical model, i.e. most specifically the conversion of component failure rates (λ) into 'time to fail' (TTF) values (as the conversion of repair times (MTTR) into 'time to repair' (TTR) values through different PDFs was already discussed in Section 5.2.3), three reliability indices, SAIFI, SAIDI and MAIFI, are calculated for the supply system in Figure 6.1 and compared against figures gathered from annual reports submitted by all 14-UK DNOs to OFGEM (Table 2.3, Section 2.4).

The results for the three reliability indices are illustrated in Figure 6.3 for exponential, Weibull, Rayleigh and Gamma distributions by applying the proposed theoretical curves in a 1,000-year simulation. Furthermore, their mean values and standard deviations are listed in Table 6.1 together with the DNOs' reported numbers. As previously discussed, the theoretical interruption model estimates more accurately the time of the day at which system faults are computed, affecting the resulting values of ENS index. However, for the calculation of SAIFI, SAIDI or MAIFI indices, no major deviations are obtained in the results provided by either the theoretical model or the conventional method (i.e. by using real distributions), thus, results are only presented for the theoretical model in this case. Again, it is possible to see considerable differences in the resulting PDFs of Figure 6.3, which clearly suggest that some PDFs will need a higher number of simulation samples in order to maintain and provide the expected (i.e. realistic) frequency and duration of interruptions.

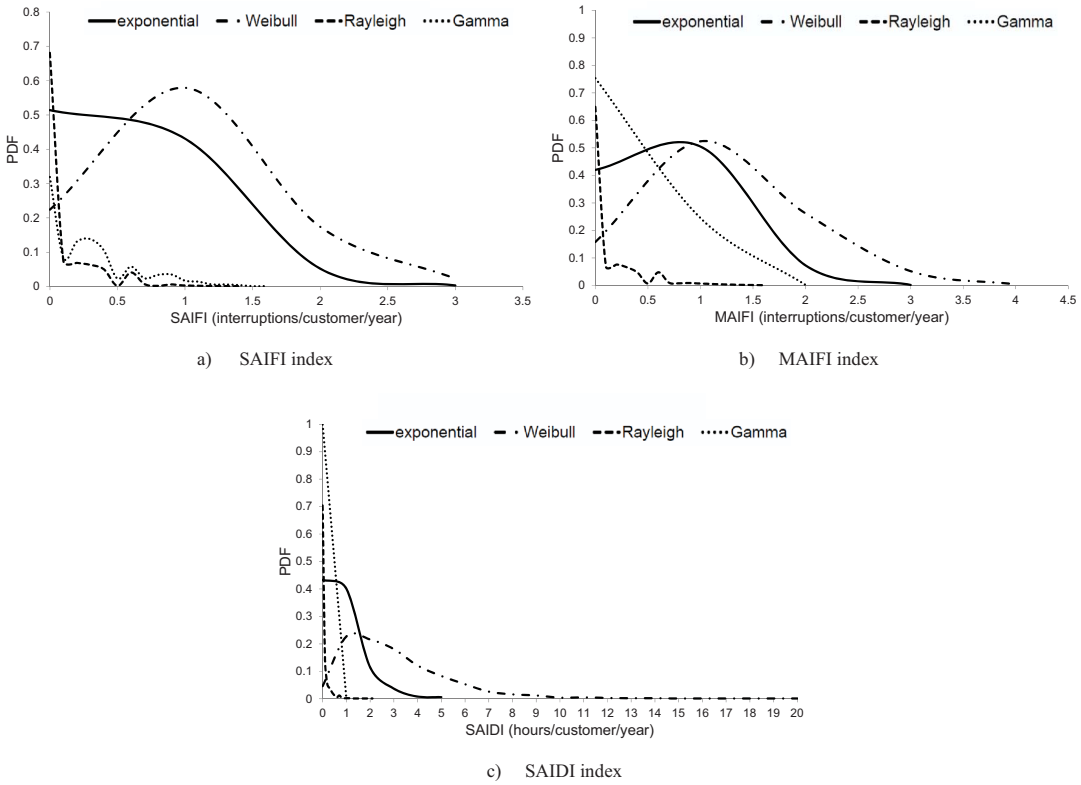

a) SAIFI index

b) MAIFI index

c) SAIDI index

Figure 6.3: Probabilistic estimations of reliability indicators for different PDFs.

The obtained results for SAIFI, SAIDI and MAIFI indices are limited to values close to zero when Rayleigh and Gamma distributions are used to model the initial failure conditions of MCS procedure. Table 6.1 confirms that the mean values obtained with these two distributions are on or far below the lower limits reported by DNOs. However, a direct comparison with the overall reported QoS values [27] must be carefully considered, as they account for the entire DNOs' distribution system (covering from radial networks in rural areas to underground meshed systems in metropolitan areas) and therefore consider every single PC and part of their

Table 6.1: Comparison of mean values and standard deviations of estimated reliability indicators with different probability distributions.

Probability Distribution		SAIFI (int/customer/yr)	SAIDI (h/customer/yr)	MAIFI (int/customer/yr)
Exponential	**mean**	0.60	0.85	0.70
	std.	0.48	0.84	0.50
Weibull	**mean**	1.02	3.06	1.21
	std.	0.61	2.35	0.71
Rayleigh	**mean**	0.10	0.08	0.13
	std.	0.19	0.18	0.23
Gamma	**mean**	0.30	0.001	0.32
	std.	0.31	0.03	0.33
UK DNOs' Reports [27]	**min.**	0.29	0.57	0.15
	mean	0.71	1.09	0.78
	max.	1.19	1.84	3.30

networks contributing to the overall average index. These must be considered only as a general reference when validating the results obtained for a test system like the one in Figure 6.1, as it only represents part of a general distribution system, however it still offers a mixture of typical highly-urban and suburban systems for an overall UK network simulation.

Regarding the other PDFs, exponential and Weibull distributions seem to cover a wider range of outcomes. The disadvantage of Weibull distribution is that it has a long tail towards infinite, which makes the mean values to be higher (i.e. SAIDI is 3.06 hours per interruption and customer, while the upper reported limit is 1.65 hours). Also, exponential is the only distribution which provides results falling within the lower and upper limits reported by DNOs for all reliability indices. Moreover, the mean values provided by exponential PDF are close to the reported average values: the simulated SAIFI is 0.6 interruptions per customer and year, and the reported value is 0.71 interruptions; simulated SAIDI is 0.85 hours and reported 1.09 hours; and simulated MAIFI is 0.7 interruptions and reported 0.78, respectively. Overall, it can be concluded that exponential distribution shall be considered in similar surveys to model together with the proposed theoretical model the initial failure conditions (TTF values) of MCS procedure, as it provides the closest match to the reported numbers. Weibull distribution can also be used, but it is likely to overestimate the indicator values. On the other hand, Rayleigh and Gamma distributions tend to shrink the results within the vicinity of zero.

6.2 Risk Assessment of Interruption Times Affecting Customers

As previously specified in the definition of reliability indices (Section 2.3.1), in the UK, three system-related metrics [45] are annually reported by DNOs to the Regulator (OFGEM) in order to reflect their reliability performance: customer interruption (CI), customer minutes lost (CML) and short interruption (SI), are used to quantify the frequency and duration of long and short interruptions, in accordance with SQS requirements [89]. Even though all three

metrics are reported to Regulator, targets are only imposed for the CI and CML indices. Besides these SQS obligations in the UK, which are specified by the corresponding 'TTRS' times and interrupted group demands provided in Table 2.4 (Page 33), DNOs must also satisfy additional requirements related to the duration of long interruptions for customers that are not protected by special contracts/agreements (i.e. residential and small commercial). Therefore, for those customers that correspond to unprotected category, DNOs should restore interrupted supply within a given period of time, otherwise penalties are applied [87]. No rewards are specified in this case and penalties are paid directly to affected customers and not to Regulator. Therefore, an efficient planning strategy, which may lead to reported reliability indices below the targets and avoid unprotected customer-related penalties, requires accurate upfront analyses.

This section proposes a methodology for assessing the performance of power supply systems in relation to targets imposed by Regulator to protect domestic and non-domestic customers from extremely long durations of interruptions. For that purpose, apart from the protection (Table 2.6) and SQS requirements previously defined, Regulator-related legislation should be included in the reliability analysis. Accordingly, the penalty conditions/thresholds defined by the UK Energy Regulator, which were discussed and presented in Table 2.5 (Page 34), are used as criteria to quantify the penalty risk that DNOs are exposed to.

The proposed methodology is again applied to the typical UK distribution system presented in Figure 6.1, Page 152, consisting of two 11 kV highly-urban and suburban configurations, with about 15,000 domestic and non-domestic customers. Regarding the reliability analysis approach, the initial conditions of network component failure rates and repair times are considered to be exponentially distributed.

6.2.1 Deterministic Algorithm for Customer Interruption Risk Assessment

If the duration of interruptions is reduced for individual groups of customers in accordance with the thresholds given in Table 2.5 (18 h for up to 5,000 customers and 24 h for more than 5,000 customers), the system-related index CML will be decreased and thus the targets for the latter are more likely to be met. Therefore, this section proposes a deterministic algorithm to be used in combination with the MCS procedure for estimating DNOs' risk of experiencing interruptions with duration above the imposed targets.

Let us consider that N is the total number of group demand (GD) classes specified in the SQS requirements (Table 2.4) and that customer group vector $c = [c_1, c_2, ..., c_n]$ consists of $n \leq N$ customer classes (e.g. 6 for UK SQS regulation). For each group of customers c_i, $\forall\, i = 1, ..., n$, a time vector $t = [t_1, t_2, ..., t_n]$ can be defined so as to contain the time classes t_i which represent the durations required to restore the supply according to SQS values. Time class t_i can take more than one value when the supply is restored in stages (i.e. classes B, C and D in Table 2.4). Furthermore, time thresholds τ_j, $\forall\, j = 1, ..., v$ as specified in Table 2.5 for domestic and non-

domestic customers are used to define a time threshold vector $\tau = [\tau_1, \tau_2, ..., \tau_v] \; \forall \; v \leq V$, where V is the total number of Regulator-imposed duration limits for restoring supply.

Both vectors t and τ are incorporated in the MCS procedure to model the reconfiguration of the system after an event (i.e. restore the supply to interrupted customers within 15 min in the case of customer class C) and DNOs' response to failures, which require the replacement of faulted component, when the risk of being penalised is estimated in accordance with the time threshold targets τ_j instead of MTTR values. Thus, every time "In repair time" is given in the SQS requirements (e.g. class A), the value of t_i (=MTTR) is replaced by the time thresholds τ_j, only when these thresholds are violated by the faulted component's MTTR (i.e. MTTR $> \tau_j$).

The MCS procedure presented in Section 5.2 changes slightly during the risk assessment with the time thresholds τ_j. An initial stage is required to determine the components whose failures lead to customer interruptions and for which the supply is not restored unless the faulted components are repaired within the time given by the MTTR values in Table 2.7 (e.g. there is no alternative supply for network reconfiguration). Firstly, two lists L_1 and L_2 are created: $L_1 = 1, ..., k, \forall \; k = 1, ..., K$ with all network components K within the system and $L_2 = 1, ..., m$, $\forall \; m = 1, ..., M$ with all customers M served by the system. Then, both lists are arranged in ascending order of their network components and customers' identification number. The first component is selected from L_1 and a power-flow simulation is run to establish the group of customers affected by its failure. All interrupted customers are identified in L_2 and assigned to their corresponding customer class c_i. Once the customer class is determined, its power range (i.e. GD value) is selected from the second column of Table 2.4. The time required to restore supply to interrupted customers is identified as the time corresponding to the customer class affected by the failure. The procedure is carried on with the selection of the second network component from L_1, etc., thus the labelling process is repeated until all components are addressed, all customers are assigned to classes and the list L_1 becomes empty.

At this stage, the outage duration corresponding to failure of each network component within the analysed system is known, leading to the need of reconfiguration actions, alternative supply or repair in case of failure. The next step of the proposed deterministic algorithm is to replace the time values of those network components, which must be repaired within the time given by MTTR so as to restore the supply to interrupted customers, with the time thresholds τ_j and then run the MCS procedure. Thus, the reductions in the estimated penalty risk are quantified when the system's reliability performance response to targets is addressed.

A summary of the proposed methodology is provided in the following:

1. count the number N of group demand (GD) classes (e.g. 6 for UK SQS regulation);
2. define vector c with customer groups;
3. define vector t with security of supply (SQS) durations;
4. define vector τ with time thresholds for domestic and non-domestic customers;
5. create a list L_1 with all network components;

6. create a list L_2 with all customers served;
7. sort the contents of L_1 and L_2 in ascending order;
8. select first faulted component from L_1 and check interrupted customers from L_2 affected;
9. identify interrupted customers and assign them to corresponding class c_i;
10. establish power range the interrupted customers fall into;
11. identify time to restore supply (TTRS) to interrupted customers in SQS requirements;
12. repeat process until list L_1 becomes empty;
13. replace MTTR values with time thresholds τ_j;
14. run MCS procedure;
15. assess the risk associated with duration of interruptions.

6.2.2 Duration of Interruptions Assessment

Planning the response process to customer interruptions should consider strategies that include the risk of facing penalties if supply is not restored within the time thresholds imposed by Regulator [87]. This risk is addressed in this section for the test distribution system in Figure 6.1 (Page 152). In the proposed methodology (i.e. MTTR vs. Time thresholds), instead of restoring the supply to interrupted customers within the time given by MTTR, the time thresholds τ_j are engaged into analysis. By employing the deterministic procedure, it is found that all electricity customers supplied through the distribution system in Figure 6.1 demand about 40 MW of power, which cover the first three customer classes c_1, c_2 and c_3 defined in the SQS requirements. Accordingly, the risk analysis for the duration of interruptions is carried out for each customer class, which is illustrated in Figure 6.4 with the corresponding PDFs. In addition, Table 6.2 gathers all calculated risk values of having interruptions above the penalty threshold.

The risk of having interruptions above the time threshold of 18 h decreases significantly with the increase of customer class power demand. This reduction is explained by the ability of the system to find alternative supply through system reconfiguration when faulted components disconnect large amounts of load. In case estimations are obtained based on MTTR values, the penalty risk given by the probability of having interruptions above the threshold of 18 h is about 37% for customers within class c_1, dropping to zero for customer classes c_2 and c_3, respectively. On the other hand, the duration of interruptions assessment against targets indicates a penalty risk of about 11% for class c_1. This suggests the penalty risk can be reduced sharply if average values of imposed targets are considered to restore supply instead of long repair times.

Table 6.2: Penalty risk for durations of interruptions above Regulator-imposed time thresholds.

Customer Class	Risk (%) results for	
	MTTR inputs	Time thresholds inputs
Class 1	36.8	10.9
Class 2	0.2	0.1
Class 3	0	0

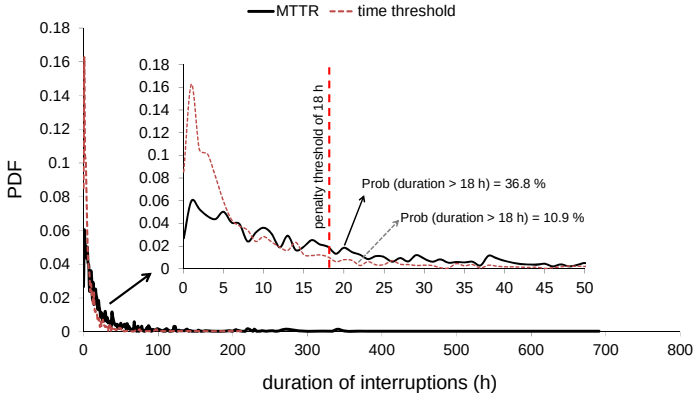

(a) customer class c_1 with interrupted power up to 1 MW

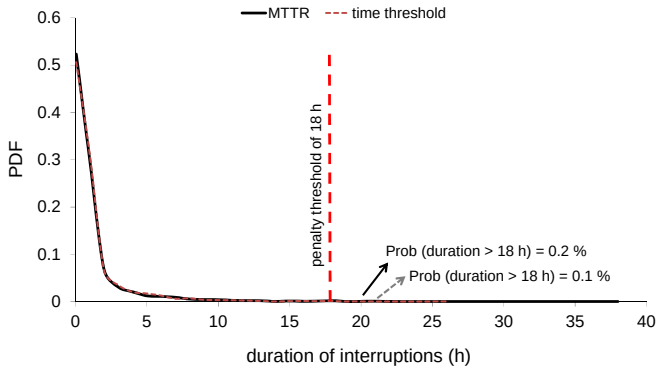

(b) customer class c_2 with interrupted power between 1 MW and 12 MW

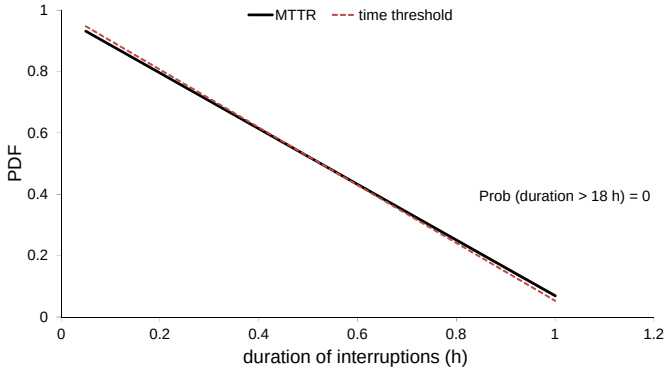

(c) customer class c_3 with interrupted power between 12 MW and 60 MW

Figure 6.4: Estimated durations of interruptions for different customer classes in a typical UK distribution system.

6.2.3 Reliability Indices Reported to Regulator

The system's reliability response to penalty targets, which protect domestic and non-domestic customers from long durations of interruptions, are compared in Figure 6.5 against the results obtained for MTTR inputs. The proposed deterministic algorithm has only influence on the results of the duration-related index CML (Figure 6.5(c)). An average value of 118 minutes per

customer and year represents the performance of the system if supply is restored within the repair time (MTTR), whereas 50 minutes per customer and year is the system's performance response with penalty time targets. A 58% reduction in the CML index suggests a more accurate penalty-risk assessment could help DNOs' planning for an improved reliability performance.

On the other hand, the frequency-related indices shown in Figures 6.5(a) and 6.5(b), do not change significantly when the deterministic procedure is implemented. Average values of CI and SI are, for both analysed cases, about 60 and 70 interruptions per 100 customers and year.

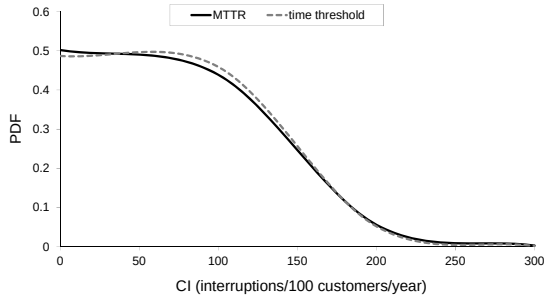

(a) CI index

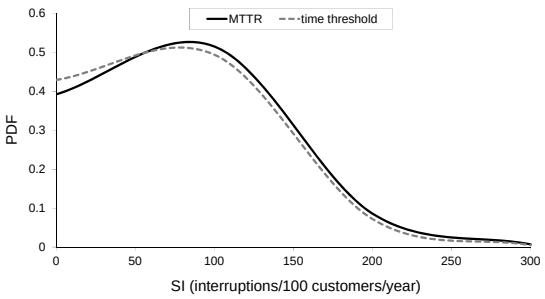

(b) SI index

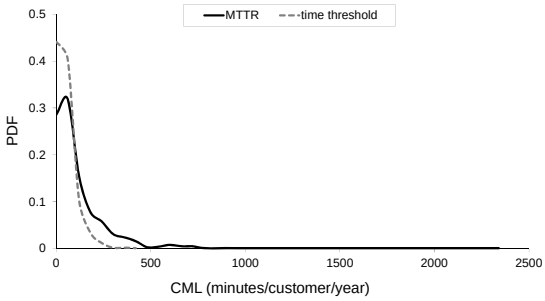

(c) CML index

Figure 6.5: Probabilistic comparison of reliability indices with SQS and repair time thresholds.

Overall, reductions are only significantly visible for those indices quantifying the duration of interruptions after the repair times have been replaced with regulatory-based targets. However, the time thresholds considered for analysis in this case are UK-specific. Similar regulatory environments exist in other countries, i.e. with time-based penalties applied to DNOs for post-fault restoration. Therefore, it must be noted that the proposed methodology is also applicable in other systems/regulatory environments, by applying their corresponding time thresholds and penalty/reward incentives.

6.3 Quantification of Network Functionalities through Monte Carlo Simulation

The aim of this section is to assess and evaluate, by using different approaches, the impact of several network actions on the accuracy of reliability performance results. A typical urban distribution network, consisting of a meshed underground configuration (as previously presented in Figure 3.15, Section 3.7) is modelled in PSSE software in combination with the previously discussed time-sequential MCS procedure. The methodology has also been applied to a typical radial distribution network, such as those operated in suburban areas (e.g. Figure 3.16, Section 3.7), in order to compare the impact of network functionalities on systems with different characteristics. However, only the results from the former one (i.e. urban network) are presented for discussion in this section of the thesis.

A comparison is provided after analysing the same network conditions and scenarios using time-sequential MCS first, and secondly using an analytical contingency approach as an attempt to fully match the mean values of the resulting reliability indices. Evidence will be provided to argue that these two methods cannot be directly compared, as the second one lacks important data and network characteristics at the time of producing results for the optimal network reliability performance. This concept, which was introduced in Section 5.1.2, is shown by comparing the different scenarios and additions to the simulation procedure, up to the final state in which all the possible network conditions are considered for an accurate and integrated network reliability assessment.

Input Data and SQS Requirements for Network Reliability Assessment

The network model for analysis is shown in Figure 6.6 overleaf, which is a MV/LV urban distribution network typically operated within the UK interconnected grid system. Although underground MV networks present a meshed configuration, they normally operate radially with the support of another supply point, either a MV primary substation or a reflection centre offering a closed-loop arrangement that guarantees the supply in case of a *N-1* failure. Due to unexpected or planned maintenance operations, an automated protection arrangement is also deployed to avoid the interruption of supply to customers.

Apart from network configuration and design, the protection schemes and repair process of faulted components (according to SQS legislation [89]) are the main features which will decide the final duration of interruptions. Accordingly, the classes of supply (i.e. A, B, and C) based on group demands (Table 2.4) interrupted by different components/parts of the network are highlighted in the model of Figure 6.6. Any fault in those areas of the network should be restored according to the SQS time thresholds of Table 2.4 (i.e. 'In repair time', 3h and 15min). Moreover, the additional (UK) regulatory requirements (time thresholds) to protect customers from excessively long interruption events (Table 2.5) are also included in the MCS analysis.

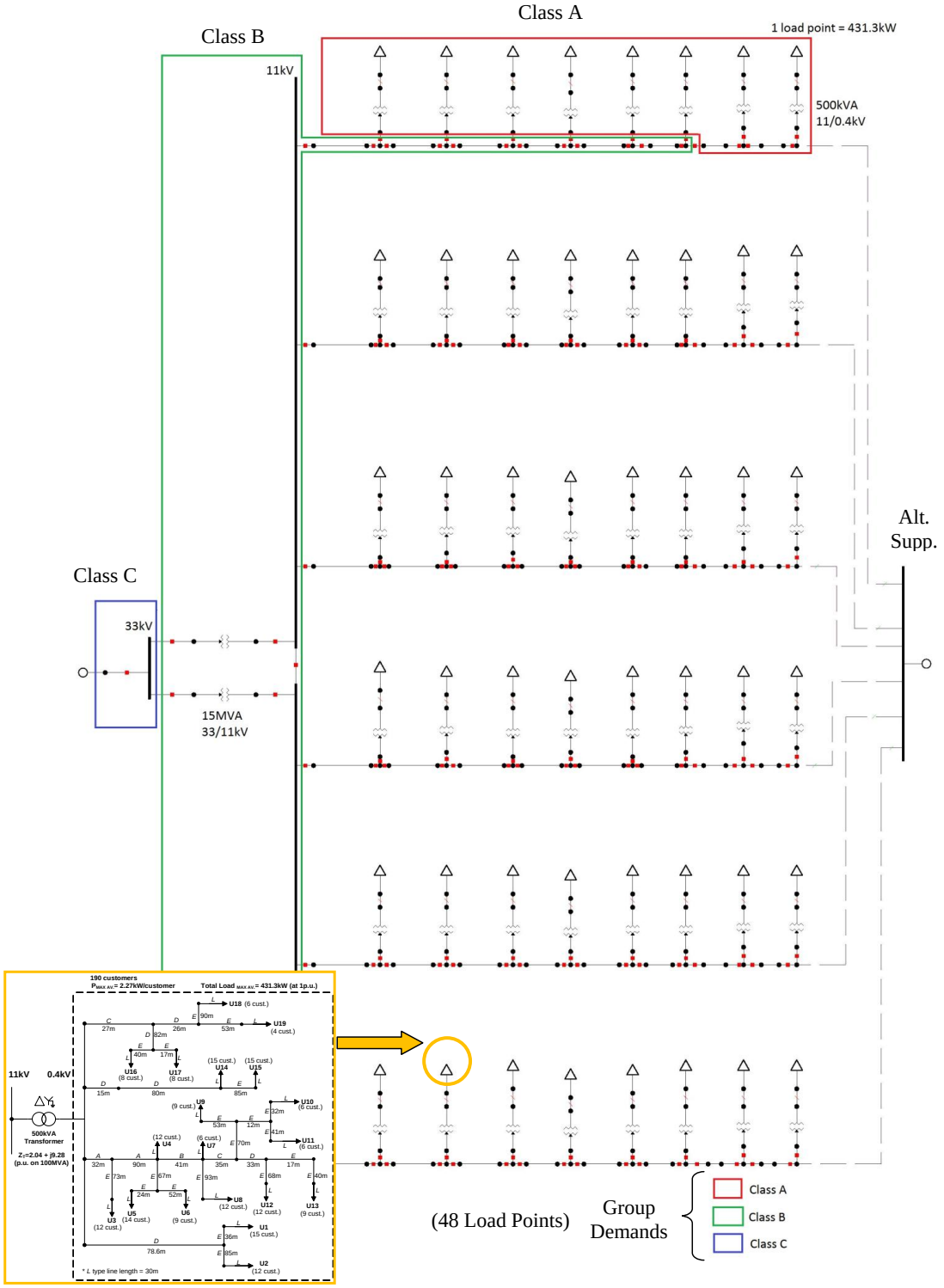

Cases 1.c), 2.c) and 3.b): with Aggregate LV Networks

Figure 6.6: Typical MV/LV urban distribution network with underground meshed configuration (divided in group demand classes).

6.3.1 Reliability Equivalents of Aggregate LV Networks

Initially, the analysed MV network model in Figure 6.6 supplies a total of 48 load points, each of them supplied by a secondary substation (11/0.4 kV transformer), and therefore representing the total aggregate load of the equivalent LV networks connected at those nodes. The first set of proposed scenarios will consider only the power supplied to these 48 aggregate loads (48 x 431.3 kW); however, neglecting the events which occur within the LV networks will lead to unrealistic performance reports on continuity of supply. Therefore, the following scenarios will also consider the detailed model of urban LV networks (presented in Figure 3.11, Section 3.6) as an attempt to improve the accuracy of reliability results. Figure 6.6 illustrates this process by representing the detailed LV network model (purely residential demand) which is used to expand each LV BSP in the system (cases 1.c, 2.c and 3.b, to be presented in next section).

As each LV network supplies a total of 19 load points (points of common coupling for LV residential customers), now the total number of load points to track adds up to 912 (48 MV nodes x 19 LV nodes), which will directly impact the final reliability indices, as the increased number of served customers will change the normalised values of the resulting indices.

Regarding the system modelling approach, the calculation of reliability indices using the LV network equivalent models could lead to inaccurate results if failure rates (λ) and repair times (MTTR) of all components in the aggregate LV network are not used to assess the quality of supply of the buses where the bulk load is connected. Therefore, this analysis considers a more accurate reliability equivalent model (previously presented in Table 4.8, Section 4.6) providing the equivalent failure rate, λ_{eq}, and equivalent repair time, d_{eq}, for the buses where the aggregate LV demand is connected:

$$\lambda_{eq} = \sum_{i=1}^{N} \lambda_i \ , \qquad d_{eq} = \frac{1}{N} \cdot \sum_{i=1}^{N} d_i \ . \tag{6.1}$$

where, N is the total number of power components within the LV network. According to the calculated values in Table 4.8 (Page 118), the input parameters for the aggregation of urban LV networks are λ_{eq} **= 2.51 failures/year**, d_{eq} **= 17.5 hours/year**.

This change will pose a big impact on the total number of customer interruptions experienced per year, as the LV part of the system has a dominant impact on the quality of service seen by end customers. As a direct comparison of this concept, for those scenarios where the equivalent LV networks are not considered in the reliability analysis, the failure rate (λ) and repair time (MTTR) for a single LV bus are directly taken from Table 2.7 (Page 36), which are equal to λ = 0.005 failures/year and d = 24 hours/year. The considerable difference in the failure rate (λ) (now considering the whole LV system with λ_{eq}) will therefore lead to a more realistic assessment of the resulting reliability indicators.

6.3.2 Network Scenarios for Reliability Assessment

***Scenario 1*: Inherent reliability of network components, modelled with their MTTR values (no back-up action)**

Scenario 1 does not consider the action of any alternative supply or automatically controlled switches between the trunk feeders of the meshed network. Therefore, this scenario analyses the 'inherent' reliability performance of the network, as if it was operating radially without any type of additional support, considering only the collected MTTR values from Table 2.7 (Page 36), and all previous assumptions on protection settings and contributions of permanent vs. temporary faults, so the customers' supply is only restored in network components' repair time, with no consideration to SQS requirements.

Three different cases (1.a, 1.b and 1.c) are proposed for analysis within Scenario 1. Therefore, as assessment proceeds from Scenario 1.a) to Scenario 1.c), different functionalities are added to the reliability analysis, such as the consideration of a varying demand profile over the day (Scenario 1.b), or the addition of the aggregate/equivalent LV network models to expand the bulk load points at LV level (Scenario 1.c). Scenario 1.a) is considered as the base case to compare any added functionality, and thus models only the maximum peak loading conditions at every load point. Any customer interruption would only count the rated/installed power at the point of supply. Obviously, after including the load profile in the analysis, it will be seen that the network reliability performance is more accurately assessed, so this condition will be kept for the rest of scenarios to analyse.

Regarding the inclusion of a time-varying load profile into MCS analysis, the residential load model from Figure 3.8 (Page 61) is selected to represent the demand at the network supply points, providing a demand decomposition into different load types during the 24 hours of the day, and therefore affecting the different values of both power factor and reactive power demand. Another concept taken into account with the MCS procedure is how the probability of outages in the network is affected by the overall system loading, hence the probability profiles of both SIs and LIs (i.e. time of the day when interruptions occurred) previously presented in Figure 5.17, Section 5.4, are also incorporated in the MCS algorithm.

The three analysed cases within *Scenario 1* can be summarised as follows:

1.a) No alternative supply (MTTR values, no SQS Reg.) + Constant peak load

1.b) No alternative supply (MTTR values, no SQS Reg.) + Time-varying load profile

1.c) No alternative supply (MTTR values, no SQS Reg.) + Equivalent LV network models + Time-varying load profile

***Scenario 2*: Impact of SQS and Regulator requirements for TTRS on network performance (manual back-up action)**

The three cases considered in *Scenario 2* aim to investigate the effect of different backup functionalities on the distribution network reliability. This will help to identify the benefits of operating a meshed network, as, for example, in case of a metropolitan underground system. Scenario, 2.a), only applies the SQS regulation depending on the power interrupted and classes of supply as specified in the network diagram of Figure 6.6 and Table 2.4. This case considers the 'manual' (i.e. not automatic) switching of alternative supply with the applicable time limits of 3 h, 15 min, etc, while faulted parts of the network supplying a demand less than 1 MW (according to SQS requirements) should be restored in network component's repair times (MTTR), provided in Table 2.7.

Scenario 2.b), evaluates the impact of the maximum duration of interruptions requirement (18 h) for domestic customers set by the regulator (Table 2.5), assuming the restoration of supply depends on the action of crew members sent by the DNO to the specific fault location, as there are no backup functionalities at LV level. Thus, faults that before were restored within component's MTTR, for PCs with MTTR > 18 h, now have a maximum restoration time of 18 hours, by allocating a random outage duration (LIs) uniformly distributed between 3 min (i.e. > SIs) and 18 h. This analysis adds up to the previous study in Section 6.2, which assessed the response of power supply systems to targets imposed by Regulator to protect customers from extremely long interruptions. The base backup functionalities of Scenario 2.a) remain the same for Scenario 2.b). Finally, Scenario 2.c), incorporates the equivalent LV networks to the analysis proposed in scenario 2.b). *Scenario 2* can be summarised as follows:

2.a) Alternative supply (Restoration < SQS Reg.) + MTTR values (No 18h Reg.) + Time-varying load profile

2.b) Alternative supply (Restoration < SQS Reg. + 18h Reg.) + Time-varying load profile

2.c) Alternative supply (Restoration < SQS Reg. + 18h Reg.) + Equivalent LV network models + Time-varying load profile

***Scenario 3*: Impact of automatic reclosing in combination with SQS/Regulator requirements for TTRS on network performance**

Scenario 3 considers the same cases as 2.b) and 2.c), i.e. meshed network with backup functionalities and complete application of SQS regulation, however in this case the switches between trunk feeders and the alternative supply are allocated an automatic switching functionality. This could be considered as a 'smart grid' case with a very high flexibility and low impact on customer's supply. In this way, interruptions that before were counted as long interruptions (LIs), now are restored in less than 3 minutes, so they are not contributing to the frequency of long interruptions (i.e. SAIFI index). However this will have a counter effect, as the switching

action is expected to cause a transient fault (< 3 min) that will increase the frequency of short interruptions (i.e. MAIFI index) and therefore lower the power quality performance of the network. The two analysed cases within *Scenario 3* can be summarised as follows:

3.a) Alternative supply (Automatic Switching < 3min + 18h Reg.) + Time-varying load profile

3.b) Alternative supply (Automatic Switching < 3min + 18h Reg.) + Equivalent LV network models + Time-varying load profile

6.3.3 Reliability Results: MCS vs. Analytical Contingency Analysis

The resulting mean values of the reliability indicators after applying the aforementioned scenarios and simulation techniques (i.e. MCS vs. analytical) are presented in Table 6.3 and Table 6.4 below. First, Table 6.3 shows the results from Monte Carlo simulation method, where the mean reliability indicators are at this point the first results to assess any change or benefit from each added network functionality (from Scenario 1.a to 3.b). The probability distribution functions corresponding to these average values will be presented in following sections.

MCS Results:

Table 6.3: Mean reliability indices (urban network) following Monte Carlo simulation.

Urban MV Network	**Scenario 1**			**Scenario 2**			**Scenario 3**	
	1.a	**1.b**	**1.c**	**2.a**	**2.b**	**2.c**	**3.a**	**3.b**
SAIFI (LIs/cust/yr)	0.283	0.201	0.071	0.204	0.204	0.07	0.017	0.061
MAIFI (SIs/cust/yr)	0.305	0.21	0.082	0.213	0.213	0.083	0.393	0.091
SAIDI (h/cust/yr)	35.02	24.35	2.202	1.6	0.643	0.661	0.358	0.647
CAIDI (h/cust int)	73.139	59.932	24.575	19.271	4.501	9.732	11.553	10.579
ENS (MWh/cust/yr)	15.042	6.79	0.598	0.396	0.143	0.1703	0.093	0.168
Avg. No. of LIs (per year)	13.606	9.648	64.752	9.799	9.794	63.714	0.803	55.768
Avg. No. of SIs (per year)	14.634	10.082	75.114	10.223	10.224	75.298	18.879	83.058
Avg. Duration of all LIs (h)	123.54	29.8	21.35	7.83	3.15	9.45	21.4	10.58

Scenario 1.a), with its frequency, duration and average number of interruptions per year can be considered as the base case to which the rest of scenarios will be compared. Considering its basic network assumptions, Scenario 1.a) does not offer a complete comprehension of the system, therefore, it can also be directly compared with results from the analytical/deterministic approach in which the system is simplified for analysis. In Scenario 1.a) no action is taken in the network (i.e. backup reconfiguration and control), so any component fault will result in a

number of customer interruptions depending on historical reliability data from Table 2.7, so duration-based indicators are relatively high (i.e. SAIDI and CAIDI). Regarding the past network recordings on fault statistics (SIs and LIs) presented in Section 5.2, it is still possible to see how the resulting SI/LI ratio is maintained in 54/46%, both for average number of interruptions and frequency-based indices (SAIFI and MAIFI). As for the ENS index, in Scenario 1.a) each network fault is assumed to interrupt maximum loading conditions in all cases, resulting in such a high value for energy not supplied.

One finding that can be derived from Table 6.3 is the impact of the use of a varying load profile (from Scenario 1.a to 1.b). There is a considerable reduction in the frequency of LIs (SAIFI) and SIs (MAIFI), which obviously is affecting the value of the rest of results. This effect is mainly due to the normal operation of the supplying 33/11 kV substation. If a component of one of the parallel branches trips (e.g. a transformer), the loading conditions in the other branch (transformer, circuit breakers, etc.) are checked, so if they exceed 100%, the branch is disconnected in order to protect the overloaded network components. Therefore, if the network loads are modelled considering a simple demand equal to their peak maximum value (including P and Q), the tripping situation in the supplying substation will occur more often than if the loads are modelled with a varying load profile over the simulation period. This situation was previously illustrated in the case presented in Figure 5.2, Section 5.2.2, where the inclusion of actual load profiles in MCS was discussed.

In Scenario 1.c), the equivalent LV networks are included in the analysis, so this results in a higher number of LIs and SIs per year (64.752 and 75.114 respectively), due to the fact that all power components within the LV networks are now contributing to the frequency of interruptions in the overall system. Accordingly, this gives an estimation of the number of outages that conventional reliability studies neglect when modelling the network load points as BSPs. With this new scenario, another factor to consider is that the rest of average results change according to the new number of served customers (48 x 19 = 912), to which all reliability indices are now normalised, but provide a more accurate estimation of the actual network reliability performance. This will be validated with the PDFs of reliability indices provided in next sections.

Regarding the results from cases in *Scenario 2* (2.a), 2.b) and 2.c)), the aim is to emphasise the action of different backup functionalities on network reliability performance. In these scenarios, the initial SI/LI ratio is maintained regarding the frequency of interruptions, as the incorporation of an alternative supply (in accordance with SQS and Regulator imposed requirements) only offer corrective measures affecting the duration, but not the frequency of interruptions occurring in the network. Therefore, there is a progressive reduction in duration-based indicators (SAIDI, CAIDI, and also ENS) due to the implementation of SQS time limits, from Scenario 2.a to Scenario 2.c, in which the equivalent LV networks are modelled for a more accurate reliability estimation.

Finally, *Scenario 3* (3.a) and 3.b)) confirms the improvement in the number of LIs taking place per year (0.803 (< than 1) and 55.768 respectively), as SAIFI index is almost brought down to zero due to the automatic switching action in less than 3 minutes. Therefore, LIs are now converted into SIs, which make MAIFI index to increase and therefore worsen the power quality performance of the network. It must be noted that the reduction in Scenario 3.b) is not as considerable as in Scenario 3.a. This is due to the fact that the switching functionalities are available in the MV part of the network, so they cannot prevent most of the events occurring at LV level, which are considered with the equivalent LV networks in case 3.b).

Analytical Results:

In order to validate the MCS-based results, Table 6.4 provides the mean reliability results by applying a deterministic analysis to the scenarios directly comparable with this approach.

Table 6.4: Mean reliability indices (urban network) following analytical contingency analysis.

Urban MV Network	Base Case (1.a)	with Aggregate LV Networks (1.c)
SAIFI (LIs/cust.)	0.266	0.075
MAIFI (SIs/cust.)	0.312	0.088
SAIDI (h/cust.)	115.464	6.088
ENS (MWh/cust.)	49.8	2.626
Avg. No. of LIs	12.759	68.07
Avg. No. of SIs	14.978	79.908

All the previously proposed scenarios consider the effect of network corrective actions on the duration of LIs, thus, only the 'base' scenarios (i.e. 1.a, base case, and 1.c, base case with aggregate LV networks) are calculated following an analytical approach, which are the ones directly comparable with their corresponding average values obtained using MCS. From Table 6.4, it can be seen that the frequency-based results (i.e. SAIFI, MAIFI and Avg. No. of LIs/SIs) are able to match the mean values resulting from MCS with a very low error. Although the analytical simulation only provides a 'snapshot' of the network reliability performance, on average, the frequency of events is maintained for both simulation approaches.

A different outcome is obtained when trying to match duration and energy-based results (i.e. SAIDI and ENS). MCS offers the possibility of testing different network components over a set number of samples/years of operation, resulting in different numbers and durations of customer interruptions in each case. Also, as PDFs are used to model the initial conditions for the calculation of TTR values, random restoration times (taken from the PDFs) are allocated to each component in case of failure, which enables the consideration of very long/short interruption events. This concept was illustrated and discussed in Section 5.2.3, with the assessment of different input probability distributions. However, the analytical approach, based on a single-run simulation, only considers the MTTR value of each and every component in the network (for all outage events), allocating always that value to the TTRS due to their failure, and thus offering a very stiff capability for modelling network components' repair time. This obviously

overestimates the resulting duration-based indices, providing unrealistic results, which are not capable of modelling the different network functionalities proposed in this section, such as the use of a time-varying load profile, probability of network faults, etc. Moreover, only a constant peak load is considered for the computation of ENS at the different BSPs in the network.

6.3.4 Monte Carlo Simulation Results: Network Stochastic Behaviour

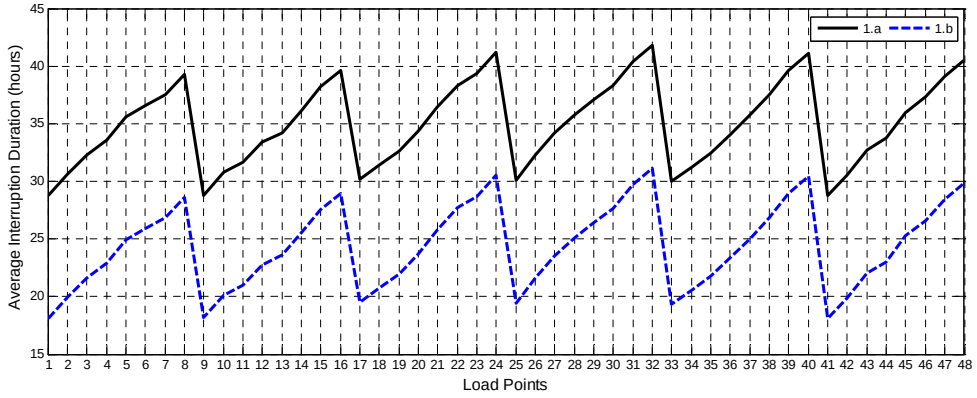

(a) Cases 1.a) and 1.b): No Backup (MTTR values)

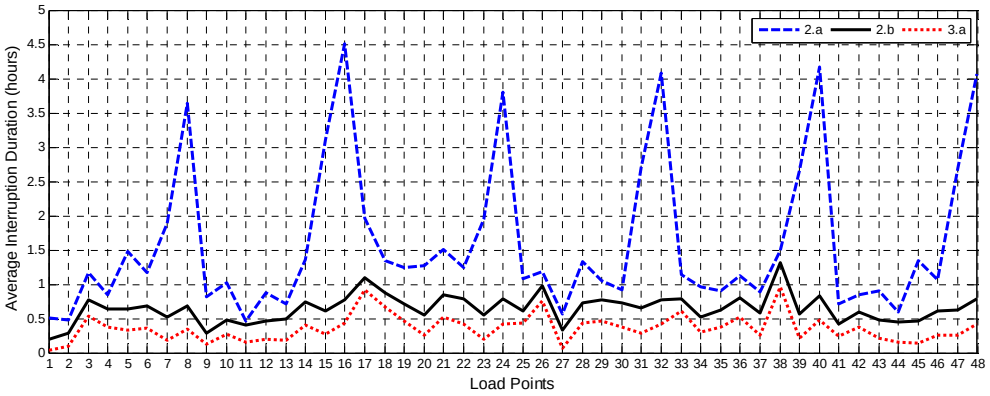

(b) Cases 2.a), 2.b) and 3.a): Inclusion of Backup Functionalities

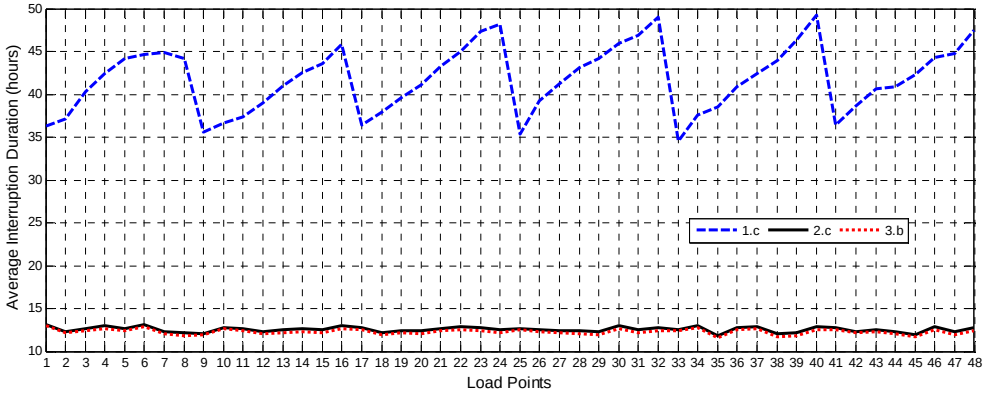

(c) Cases 1.c), 2.c) and 3.b): Inclusion of Equivalent LV Networks

Figure 6.7: Average duration of interruptions for 48 load points and all network scenarios.

The results presented for all considered scenarios (from 1.a to 3.b) in Figure 6.7 illustrate the assessed network reliability performance as a consequence of the inclusion of new functionalities in the system operation. They represent the network "stochastic behaviour", as those curves are the result of performing an integrated reliability assessment following the proposed MCS procedure. In Figure 6.7 above, the expected average duration of interruptions is provided for the different load points in the urban test network of Figure 6.6. Moreover, as there is a high dependency of the energy-related indices (i.e. ENS) on the duration of customer interruptions in each case, the results obtained for the expected ENS per load point of the network follow a similar pattern as the durations provided in Figure 6.7 above. Accordingly, the corresponding variations in ENS values will be provided in the form of PDFs in next sections.

Considering the design and structure of the urban network, Figure 6.7(a) illustrates the reliability performance of the system (expressed as average duration of interruptions) operated radially, i.e. with lack of alternative supply and when no system reconfiguration is applied. Therefore, it is possible to see how the expected duration of interruptions increases from load points closer to the supplying 33/11 kV substation, in comparison with those located further in the 11 kV trunk feeder. The first network functionality affecting the simulation results, which is quantifiable from Figure 6.7(a), is the impact of the time-varying load models, which considerably decrease the expected duration of interruptions (from Scenario 1.a to 1.b) for the 48 load points in the urban network. However, the resulting average values are still unrealistic, as mean values of 35.02 h and 24.35 h are obtained for Scenarios 1.a) and 1.b) respectively.

In the case of Figure 6.7(b), the expected durations are provided after SQS and Regulator-imposed requirements are included in the form of alternative supply in the network, which result in more realistic outage durations as compared with reported DNOs' values. These results again emphasise the importance of including the 18-hour time thresholds in order to protect customers from extremely long interruptions. In Scenario 2.a), load points located at the end of the 11 kV trunk feeder (corresponding to class A, < 1 MW interrupted) are not completely protected from LIs, and therefore their expected outage durations sharply increases in comparison with the rest of load points. As soon as all reconfiguration and automatic switching functionalities are modelled in the simulation (i.e. Scenarios 2.b and 3.a), a considerable reduction is obtained for all supplied load points. Accordingly, the impact of each action can be quantified with respect to the others, which can potentially be used by DNOs for decision-making and network planning processes.

Lastly, Figure 6.7(c) provides the average outage durations when the LV networks are included in the simulation by using the LV equivalent/aggregate models. For this case, all faults within LV levels are computed in the final values, so that is the reason for such an increase in the average duration times. In these scenarios, it must be noted that the final reliability indices are per-unitised by the total number of served customers, which is 912 (48 MV nodes $\times$ 19 LV nodes). However, although network reconfiguration and alternative supply are also considered

in Scenarios 2.c and 3.b, Figure 6.7(c) is split into the 48 MV load points, in order to highlight the impact of LV network equivalents on the assessment of network reliability, as system faults within LV networks are typically neglected in conventional MCS procedures.

Frequency of Interruptions: SAIFI and MAIFI Indices

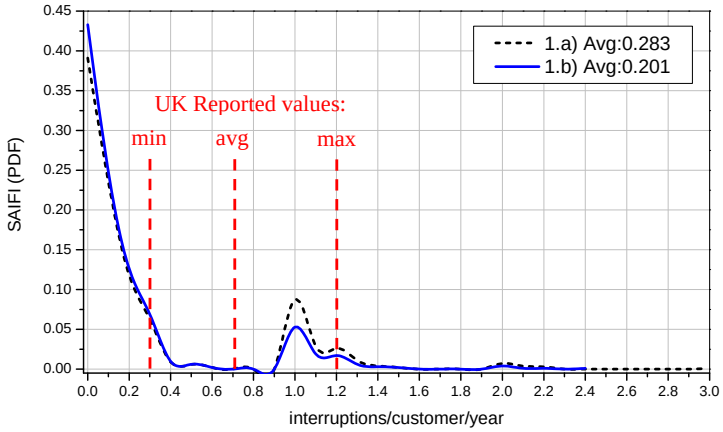

(a) Cases 1.a) and 1.b): No Backup (MTTR values)

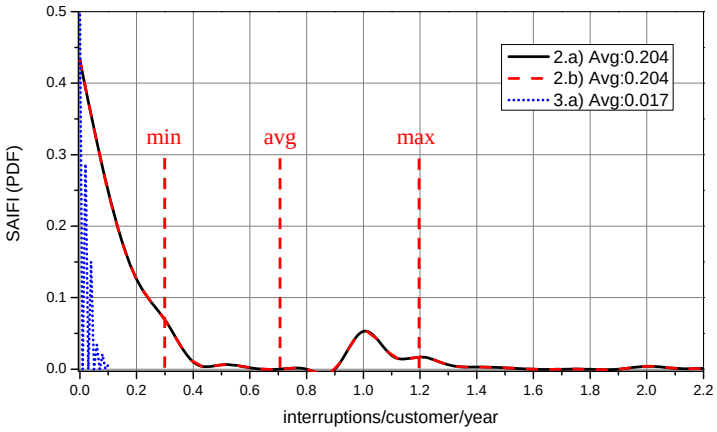

(b) Cases 2.a), 2.b) and 3.a): Inclusion of Backup Functionalities

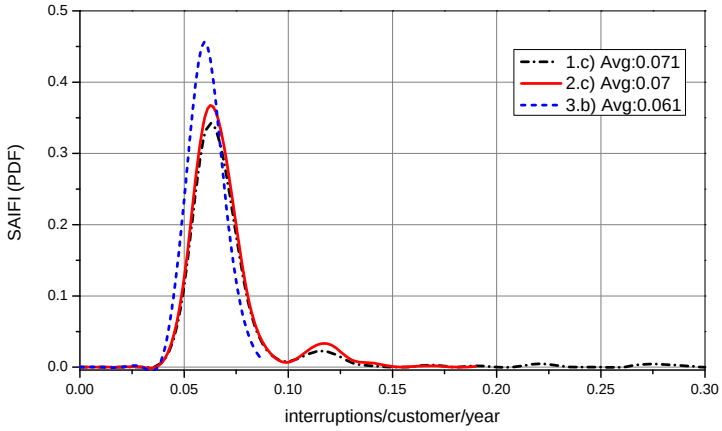

(c) Cases 1.c), 2.c) and 3.b): Inclusion of Equivalent LV Networks

Figure 6.8: Frequency of long interruptions analysis: SAIFI index for all network scenarios.

The probability density functions (PDFs) of the frequency-based reliability indices (SAIFI for LIs, MAIFI for SIs) are provided in this section together with the reliability values reported by DNOs in the UK, as previously presented in Table 2.3, Page 32. These annually reported values are used to validate the obtained results, and to assess to what extent they are capable of providing realistic results for the estimation of the urban network reliability performance. In addition, this validation can be used by DNOs in order to quantify the (%) probability that falls within the different reported thresholds, which can potentially help to assess parts of their networks in need of reinforcement.

First, the frequency probability of LIs is provided in Figure 6.8 for all the proposed scenarios, with the corresponding mean values previously provided in Table 6.3. In the first case comparison, Figure 6.8(a), an improvement is identified in the PDF of LIs from Scenario 1.a) to 1.b), after the time-varying load models are included in the analysis. This effect is also maintained in Scenarios 2.a) and 2.b), due to the impact of the load profile acknowledgment on the frequency of interruptions. However, no change is experienced in the number of system faults when SQS and Regulator-imposed requirements are included in the simulation (Scenarios 2.a and 2.b), as these scenarios mostly affect the duration of interruptions. For these cases, the PDFs show a sudden increase in the values around 1 interruption/customer/year, which corresponds to the network faults affecting the total number of supplied customers (load points) in the system, e.g. faults taking place in the supplying 33/11 kV substation or associated components. As reliability indices are per-unitised by the total number of customers, when all of them are interrupted, SAIFI (and MAIFI) index is computed as 1 interruption/customer/year, therefore it contributes to the probability of faults around that value. This probability can again be used by DNOs in order to assess and improve the reliability performance of the MV GSP.

Another network characteristic to highlight, is the one offered by Scenario 3.a), which shifts the resulting PDF to values in the vicinity of zero. Again, this effect is due to the automatic switching action (in < 3 min), avoiding the occurrence of the majority of LI events and transforming them into transient faults, which obviously will have a strong impact on network's PQ. This counter effect is shown in Figure 6.9(b), where the resulting PDF for MAIFI index (Scenario 3.a) presents a higher probability of SIs as compared with the previous cases.

Finally, a completely different scenario is obtained for SAIFI and MAIFI indicators in Figures 6.8(c) and 6.9(c). In this case, faults in the LV networks are acknowledged, therefore they have a big contribution to the overall network reliability performance. The resulting PDFs for both indices present a different curve shape, with a probability distribution concentrated around an average value, which provides a more realistic estimation of the actual number of interruptions actually taking place in the network (per served customer). Therefore, with this methodology, the dispersion of results (as seen in PDFs of previous scenarios) is drastically reduced. With the inclusion of equivalent LV networks in MCS, the number of faults considered in the simulation increases, and so does the number of served customers for the computation of

final reliability indices, which offers a more realistic approach to the actual network behaviour as compared with the reported values by DNOs.

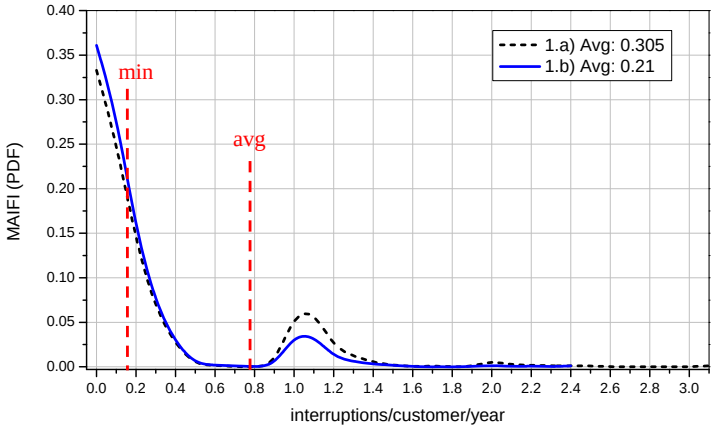

(a) Cases 1.a) and 1.b): No Backup (MTTR values)

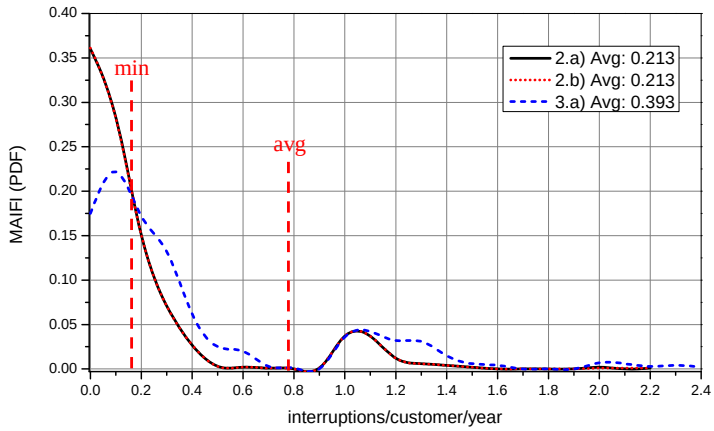

(b) Cases 2.a), 2.b) and 3.a): Inclusion of Backup Functionalities

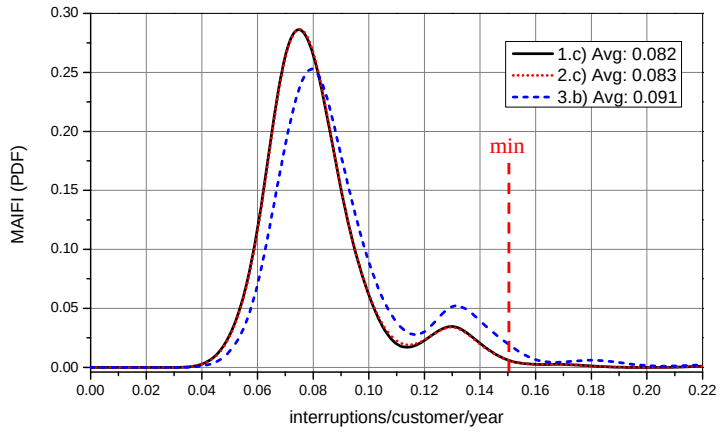

(c) Cases 1.c), 2.c) and 3.b): Inclusion of Equivalent LV Networks

Figure 6.9: Frequency of short interruptions analysis: MAIFI index for all network scenarios.

The validation of previous scenarios against reported values to Regulator can serve as a reference for network planning and operation strategy. However, these figures include the whole system operated by DNOs (i.e. from weak radial to strong meshed networks), so they may not

be directly comparable to the number of faults expected in the 'isolated' urban network for analysis in this section. Therefore, the frequency-based PDFs presented in Figures 6.8(c) and 6.9(c) are considered to provide a closest match to the 'real' reliability performance expected in this type of urban networks. Also, Figures 6.8(c) and 6.9(c) illustrate how the probability of SAIFI and MAIFI indices is reduced and increased respectively when Scenario 3.b ('smart grid' automatic switching) is assessed, affecting the final number of LIs and SIs.

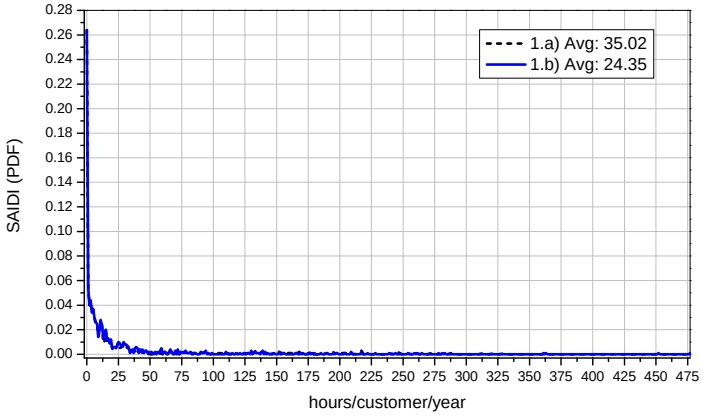

(a) Cases 1.a) and 1.b): No Backup (MTTR values)

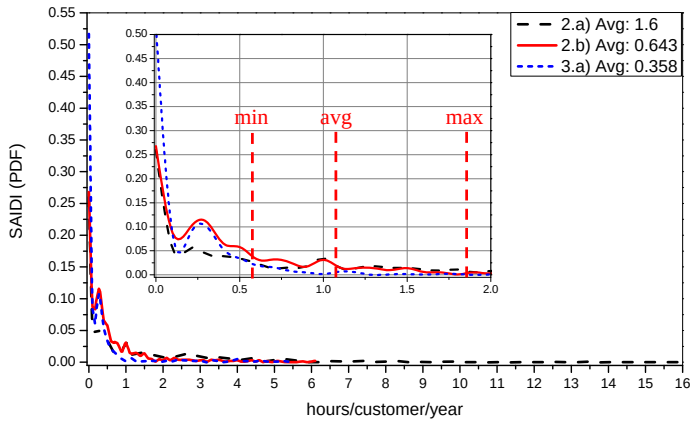

(b) Cases 2.a), 2.b) and 3.a): Inclusion of Backup Functionalities

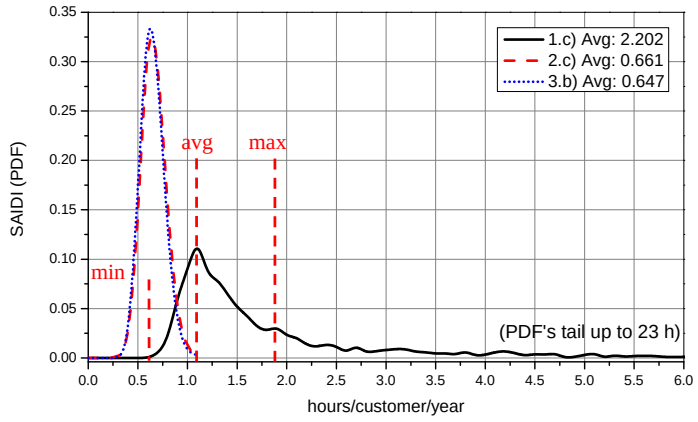

(c) Cases 1.c), 2.c) and 3.b): Inclusion of Equivalent LV Networks

Figure 6.10: Duration of long interruptions analysis: SAIDI index for all network scenarios.

Duration of Interruptions: SAIDI Index

In order to assess the effectiveness of all the proposed scenarios (1.a to 3.b), which are specifically designed to reduce the frequency and duration of interruptions by applying the use of alternative supply and reconfiguration functionalities, Figure 6.10 shows the duration-based PDFs obtained for SAIDI index. Opposite to the situation with the frequency of interruptions, in which the validation of SAIFI and MAIFI indices for an 'isolated' network was not directly compared with reported indices by DNOs for their distribution systems, in this case the duration of interruptions is a common factor for every type of network (i.e. varying from radial to meshed systems, according to the generalised SQS and Regulator-imposed requirements), and thus can be directly compared with DNOs' reported values for the quantification of each network functionality.

As seen in Figure 6.10 above, the first scenarios (1.a and 1.b) provide unrealistic values for the outage durations as no backup supply is considered in the simulation. Therefore, as soon as SQS time thresholds are included in the model (i.e. depending on group demand classes), the resulting PDF (Scenario 2.a) starts to provide SAIDI values closer to (or within) stipulated values. Again, as previously demonstrated in Figure 6.5 (Section 6.2), there is an improvement in the reported distribution for SAIDI index when Regulator-imposed requirements (i.e. time thresholds of 18 h, etc.) are also implemented in the network model. Moreover, Scenario 3.a (automatic switching) provides a considerable reduction in the durations probability, which is only applicable to benefits obtained at the MV level of the system, as load points are still modelled as BSPs and no faults are considered within LV networks.

Again, the PDFs for SAIDI index presented in Figure 6.10(c) provide more accurate results, as now all the faults within LV networks contribute with their corresponding durations, which are much longer than those outages at MV level, due to the fact that no backup actions can be taken to restore the supply (class A demand). This higher fault contribution makes the resulting PDFs to acknowledge more durations of interruptions at the time of computing SAIDI index, and therefore the distribution functions tend to concentrate over a clear mean value (i.e. there is less dispersion of results). This concept can be deduced from the resulting SAIDI PDFs in Figure 6.10(c), where a percentage of the durations probability is outside the DNOs' reported limits, but still provides a more realistic comparison with the reported figures.

Overall, Scenarios 2.c) and 3.b) would be the ones providing an optimal solution to the system reliability, as they consider all the possible network functionalities, and now the results offered by the automatic switching are not overestimated as it was the case with Scenario 3.a). It must be noted that, although Scenarios 2.b) and 2.c) provide similar mean values for SAIDI, the resulting PDF from Scenario 2.c) presents a much lower dispersion of probabilities, and therefore emphasise the benefits from the use of LV reliability equivalent models. All these effects will be validated in next section with the actual durations of interruptions obtained from MCS, which will avoid masking the results by normalising over the total number of customers.

Duration of Customer Interruptions

According to previous assumptions, all network restoring functionalities can be more easily quantified if the actual recordings of customer interruptions (as a result of MCS procedure) are directly analysed and compared. Therefore, the impact of the different scenarios on network outages is illustrated in Figure 6.11.

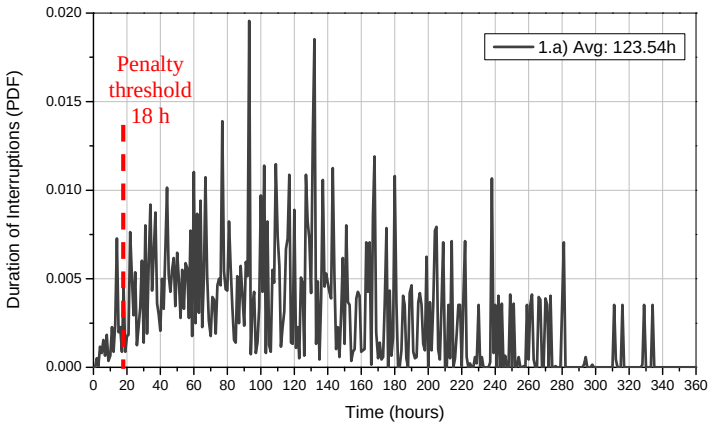

(a) Case 1.a): No Backup (MTTR values)

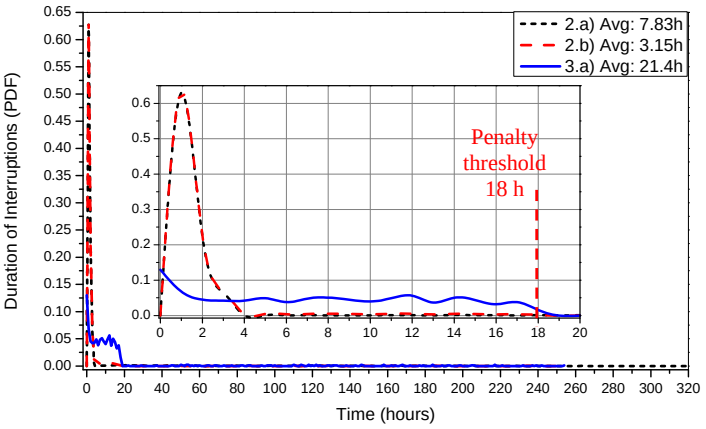

(b) Cases 2.a), 2.b) and 3.a): Inclusion of Backup Functionalities

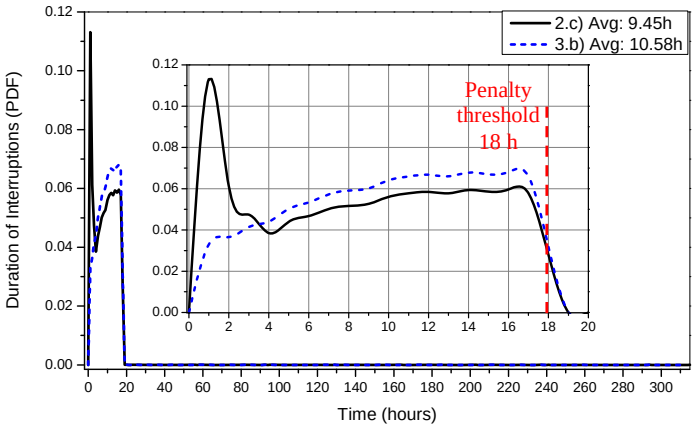

(c) Cases 2.c) and 3.b): Inclusion of Equivalent LV Networks

Figure 6.11: Impact of network functionalities on duration of customer interruptions.

As a 'base case' example, Figure 6.11(a) presents the raw probability for the duration of interruptions after applying a simplified MCS to the urban network. This illustrates the 'natural' behaviour of network components, reacting to actual MTTR values, and resulting in very long interruptions (compared against the 18 h penalty threshold) as no backup action is implemented in the model. Scenarios 1.b) and 1.c) provide similar results (network behaviour), however the average value is progressively reduced, as previously shown in Table 6.3.

The impact of SQS restoration (i.e. alternative supply and automatic reclosing functionalities) on the urban network performance is presented in Figures 6.11(b) and 6.11(c), for both scenarios, with and without the equivalent/aggregate LV networks. In the first case, Figure 6.11(b), where load points are only modelled as BSPs, the probability for the duration of interruptions is modified according to SQS requirements (i.e. classes of group demands) which mainly affect the reliability performance of the MV level of the network (the one directly connected to the backup supply and reconfiguration switches). Therefore, as previously specified in the urban network model of Figure 6.6, most network components at MV level belong to the SQS 'class demand' B (i.e. interrupt group demands between 1 MW and 12 MW), so the supply in those cases must be restored within 3 hours. This backup effect can be seen for the durations probabilities of Scenarios 2.a) and 2.b), presenting an accumulated probability within 3 hours, however the curve's tail of the first PDF (Scenario 2.a) is much longer (affecting the resulting average duration) as the penalty threshold of 18 hours (Scenario 2.b) is still not implemented in the network model. Moreover, the 'smart grid' automatic switching introduced by Scenario 3.a) drastically eliminates the peak probability of LIs (< 3 h) as now those interruptions are restored in less than 3 minutes, so they do not compute as LIs anymore. Thus, the resulting PDF of Scenario 3.a) only considers the probability of a reduced number of LIs in the network.

Finally, the results provided in Figure 6.11(c) emphasise the need of including the equivalent LV networks in the overall model, so all the interruptions taking place in the network (also at LV level) are considered for a more accurate reliability estimation of network performance. Basically, the results obtained for Scenarios 2.c) and 3.b) maintain the same assumptions as those obtained for previous Scenarios 2.b) and 3.a) (including the effects from SQS restoration and automatic reclosing), however the resulting durations PDFs in Figure 6.11(c) show the high percentage/contribution of faults occurring within LV networks (GD class A, < 1 MW interrupted) which are usually neglected by conventional MCS procedures.

These final results, considering the behaviour of outage durations in the overall system, can be validated by comparing the resulting probabilities and interruption durations of Figure 6.11(c) against the 'real' probability data for outages in the networks operated by SPEN (UK DNO). This data was previously processed and presented in Figure 2.11, Page 43, providing the PDF representing the duration of unplanned LIs for the reporting year 09/10. A high correlation between both sets of PDFs is identified, showing how the network reacts to the different SQS and switching/restoration actions.

Energy Not Supplied: ENS Index

In order to estimate how system outages affect energy not supplied to customers, Figure 6.12 shows the variation of ENS index according the functionalities applied to the urban network model. There exists a high dependency in the computation of ENS index with the durations of customer interruptions (i.e. SAIDI index), therefore all the assumptions previously discussed for the resulting probability of SAIDI are directly applicable for the PDFs representing ENS.

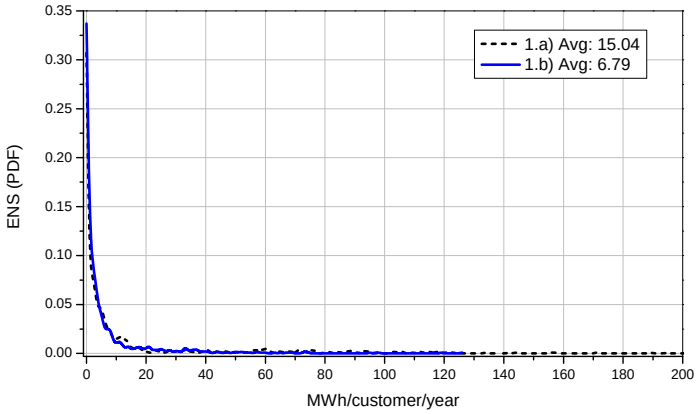

(a) Cases 1.a) and 1.b): No Backup (MTTR values)

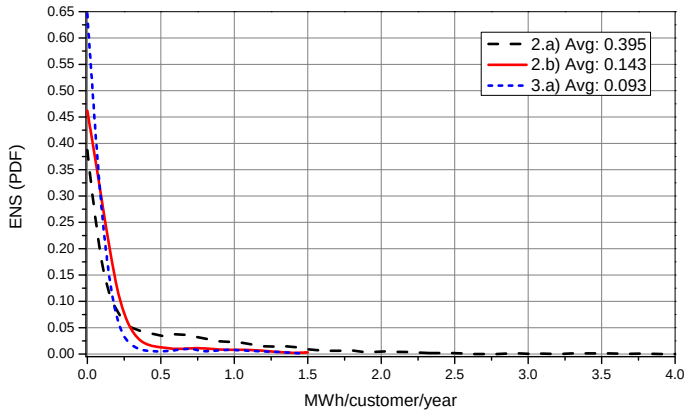

(b) Cases 2.a), 2.b) and 3.a): Inclusion of Backup Functionalities

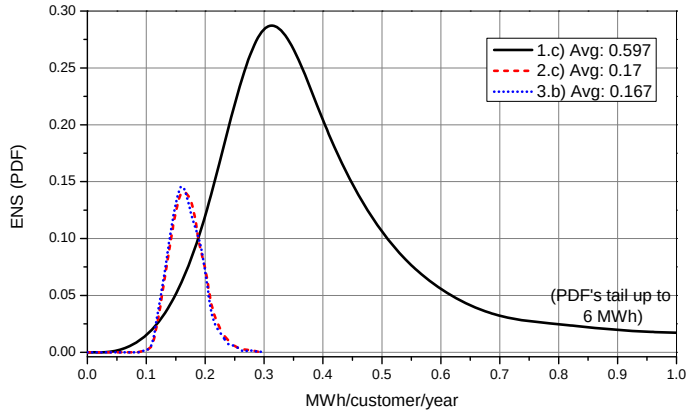

(c) Cases 1.c), 2.c) and 3.b): Inclusion of Equivalent LV Networks

Figure 6.12: Energy not supplied analysis: ENS index for all network scenarios.

6.4 "Smart Grid" Reliability Performance Assessment

This section analyses the influence of distributed energy resource functionalities on reliability performance of actively managed networks (so called "smart grids"). All the previously defined modelling assumptions (e.g. reliability and network equivalent models, theoretical interruption model for classification of LIs and SIs, etc.) in combination with the proposed MCS procedure, are used to assess the potential improvements that different demand-side management (DSM) and energy storage (ES) schemes will have on the frequency and duration of customer interruptions. Particular attention is given to energy-related reliability indices (e.g. ENS) which measure the energy and power not supplied to residential and commercial customers. For further reference on this topic, the reader is referred to additional work published by the author in [22, 23, 25, 34], which analyses the impacts of DSM, renewable-based micro-generation (MG) systems and ES schemes on actively managed distribution networks.

ES and DSM resources will provide not only residential LV customers, but also MV commercial and industrial customers with the capability for reducing their overall electricity consumption and energy bills, as well as contributing to the general improvement of network reliability performance. The previously published work concluded that energy-related reliability indices are the most appropriate to measure the potential benefits of 'smart grid' applications on the continuity of supply of LV residential customers, as they allow for a more accurate assessment of demand-manageable loads and energy storage functionalities. However, the probability of faults in the overall distribution network (including both LV and MV levels) is mainly influenced by larger commercial and industrial loads with a peak consumption taking place over the working hours of the day. Therefore, the proposed analysis considers an appropriate load profile at each voltage level, according to the demand decomposition (residential, commercial and industrial) presented in Section 5.2.2 of this thesis.

6.4.1 Application of Energy Storage and Demand-side Management Resources

A realistic assessment is undertaken by applying the load decomposition approach described in Section 3.4.2 to build an accurate equivalent representation of the aggregate demand for the network performance analysis. This is represented by different component-based load models of UK residential and commercial sector loads, based on available statistics on load mixes and device ownerships [128]. Figure 6.13 shows the results of the load decomposition for typical UK residential and commercial loads, based on demand profiles recorded by the DNO for the maximum winter day. For this analysis, no industrial demand is considered to participate in any DSM scheme.

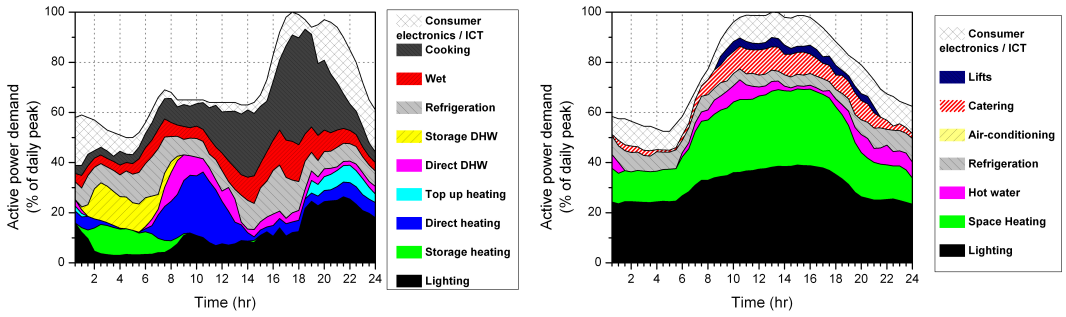

(a) Residential sector **(b)** Commercial sector

Figure 6.13: Decomposition of typical UK daily load curves for maximum demand (winter).

Demand-side Management

The load types presented in Figure 6.13 allow various DSM scenarios to be modelled by adjusting the corresponding load components in the aggregate demand. The portion of the load potentially available for DSM, and the times during the day at which they are available, can be easily identified. Therefore, the potential for each load type (e.g. residential "wet" load, commercial refrigeration, etc.) to provide network reliability improvements and their effects on the resulting reliability indices can be evaluated. The analysis considers two load types for DSM: a) residential "wet load" (including domestic washing machines, dishwashers and clothes dryers); b) commercial refrigeration load. This assumes each load type is fully controllable (e.g. 100% of each load type can be disconnected at a given time instant). The reconnection of deferred load is not considered, as this will depend on the method by which loads are controlled (e.g. by a price signal or frequency control to smart appliances). The two proposed DSM scenarios, including both residential and commercial demands, can be categorised as following:

1) DSM for peak load reduction:

50% of the residential loads in the test network participate in this scheme by reducing the consumption from "wet loads" present during the evening peak hours (16:00 - 22:00) to zero.

2) DSM for reliability improvement:

The reduction in demand is applied to both domestic and commercial loads when the probability of fault occurrence is higher (as in Figure 5.16, Section 5.4). Thus, the duration of interruptions and the energy not supplied during that period are expected to decrease. Accordingly, this scenario considers the participation of the other 50% of residential loads in the test network, disconnecting their "wet demand" during the hours between the morning and the evening ramp period (5:00 - 15:00). As for the commercial demand, the refrigeration loads are reduced over the hours with higher consumption (5:00 - 21:00).

Energy Storage

A relatively high penetration of ES and DSM, with backup capacity provided, can have a considerable impact on continuity of supply if appropriate control schemes are implemented. This work analyses the capability of MG to operate in islanded mode, through the coordinated control of energy storage, to potentially relieve the effects of faults in the upstream network. The analysis builds on previously defined 'smart grid' schemes in Section 4.5.2, where the daily MG power output is stored during the day to provide a backup capability of around 3.67 kWh per domestic customer. This is expected to reduce the ENS and the duration of customer interruptions in the event of a fault.

6.4.2 Reliability Performance Analysis with ES and DSM

The reliability performance of the previously analysed suburban test network, in Figure 5.5, Page 132, is used as a benchmark study to assess any reliability benefits from the proposed 'smart grid' scenarios. The suburban test system represents a radial MV overhead feeder supplying 10 secondary transformers, which serve a maximum average load of 1.82 MVA (760 residential customers, i.e. loads L1 to L10). In addition, a commercial load (L11) is included in the analysis, with an installed demand of 2.2 MVA. Both residential and commercial demands are represented with their corresponding load profiles and load mix as shown in Figure 6.13.

For this analysis, half of the residential demand (load points L1 to L5) participate in the "peak reduction" DSM scheme, while the other half (L6 to L10) and the commercial load (L11) contribute to the DSM scheme for reliability improvement. By grouping the load supply points into different DSM schemes, it is possible to assess and compare the potential reliability improvements that each scenario will offer to the DNO. As for the energy storage scheme, it is applied to the residential loads only (L1-L10), considering that each domestic customer (76 per load point) have a backup capacity of 3.67 kWh at their disposal to help supply part of their demand in the event of a fault in the upstream network. This builds up a total backup capability of around 2.8 MWh, which is considered as the maximum contribution residential customers could have through the use of this energy storage scheme to the improvement of network reliability.

Regarding the system modelling approach, the resulting indices are calculated using the network and reliability equivalent models presented in Chapter 4 for LV suburban networks (i.e. $Z_{eq,LV}$ = 8 + j2.164 p.u., λ_{eq} = 1.21 failures/year, d_{eq} = 18 hours/year). In this way, the electrical characteristics, failure rates and repair times of all network components within the lumped LV networks are included in the MCS analysis. Also, it must be noted that the aim of this analysis is to assess the potential benefits that ES/DSM schemes can provide at the different network's load points. Therefore, in order to simplify the analysis of results, the calculated indices will not be per-unitised by the total number of LV customers, but only to the 11 load supply points (residential + commercial) in the suburban network.

System Reliability Results with 'Smart Grid' Scenarios

The standard set of reliability indices (SAIFI, MAIFI, SAIDI and ENS) are analysed for the proposed ES and DSM scenarios by adjusting the various components in the load mix. Figure 6.14 presents the PDFs and average values of the obtained reliability indices measuring the frequency of LIs and SIs in the test network. For this particular analysis, the introduction of ES and DSM functionalities in the distribution network has an almost negligible effect on the expected frequency of supply interruptions. This is mainly due to the radial configuration of the network (low interconnectivity level), as well as to the low loading conditions, which prevent the 'smart grid' scenarios from gaining relevance with respect to the overloading conditions of the non-faulted components.

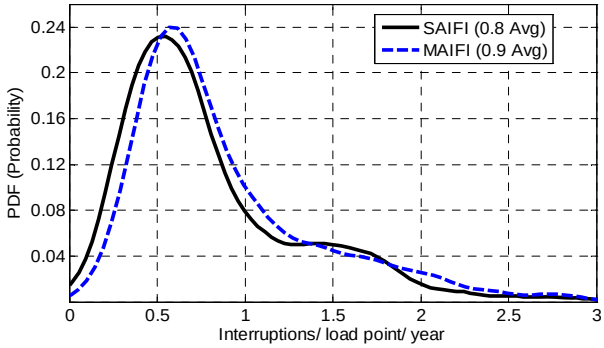

Figure 6.14: Frequency of interruptions probability (SAIFI and MAIFI Indices).

1) Effect of Energy Storage on the Duration of LIs:

A completely different result is obtained when analysing the effect of the considered ES scenario on the duration of LIs at the load points supplying the residential demand (loads L1-L10). In case of a network fault, each domestic customer has its own capacity to supply the local demand for a specific time; consequently, the energy consumed during that period is no longer counted as ENS and the total duration of each interruption is significantly reduced. This effect is shown in Figure 6.15(a), where the PDF of SAIDI index is notably shifted to the left (from 13.1 h to 11.3 h average values), providing a higher probability for the occurrence of shorter interruptions. The proposed energy storage scenario, considering 100% of domestic customers participating in the scheme, can provide up to a 13.6% reduction in SAIDI index. In addition, Figure 6.15(b) presents the different probabilities for the actual duration of faults taking place in the overall distribution network.

The energy storage scheme increases the probability of having shorter interruptions, as well as reducing the maximum value of the expected range of interruptions (i.e. the end of the long tail of the PDFs). Figure 6.15(b) also illustrates the protection behaviour of the network, as it is possible to see two different peaks in the probability of faults. The first one (i.e. faults < 3h) is due to the switching action of the alternative supply point at the end of the MV radial feeder.

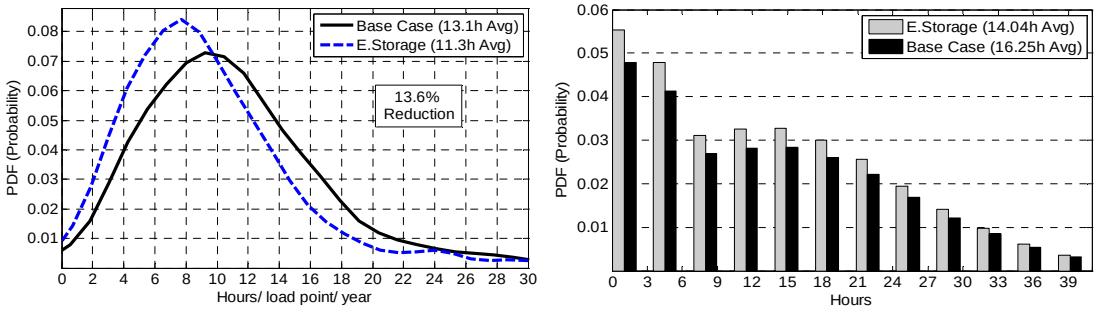

(a) SAIDI Index (b) Duration of LIs probability

Figure 6.15: Effect of energy storage on the duration of LIs (Base case vs. E. Storage).

This is due to SQS requirements [89] for the interrupted demand (between 1 MW and 12 MW) in this type of distribution networks. The second peak, which strongly affects the average value of interruptions, is due to longer faults happening within the LV networks, which are affected by the manual restoration in component's repair time (MTTR) for each fault.

2) Impact of 'Smart Grid' Scenarios on ENS:

As shown in Figure 6.16, the reliability indicator mostly affected by the introduction of 'smart grid' schemes in the suburban network is the ENS index. These results, which consider both residential (L1-L10) and commercial (L11) demand, include the PDFs and average values for each applied scenario. Considering the base case as reference, the combination of both DSM and ES can provide the largest benefits to the reliability performance of the system, being the latter the one with higher impact. This is due to the large amount of residential loads in comparison to the commercial demand, as well as to the fact that the proposed ES scheme represents a post-fault corrective action, while the DSM scenarios are only defined as a preventive measure to reduce the ENS during the peak and reliability-related periods. Figure 6.16(b) presents the average ENS at each load point and their potential reduction from ES and DSM scenarios, while Table 6.5 quantifies these benefits providing percentages for each considered 'smart grid' scenario.

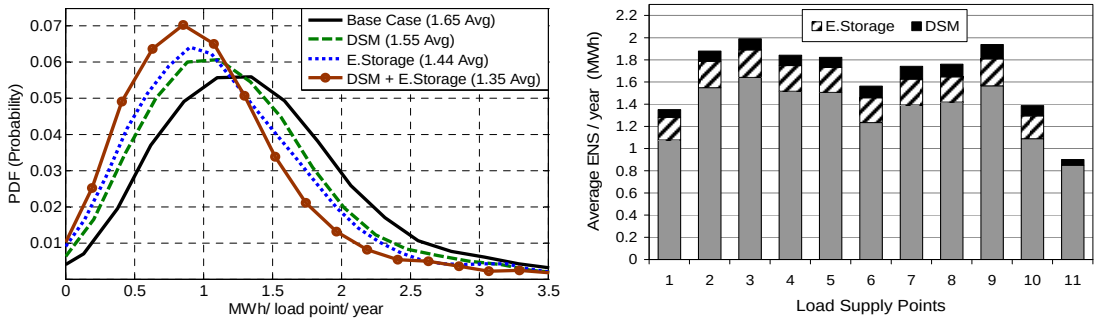

(a) ENS Index ('smart' scenarios) (b) Average ENS per load point (L1 to L11)

Figure 6.16: Impact of 'smart grid' scenarios on energy not supplied (ENS).

Table 6.5: Average reduction of energy not supplied (ENS) for different 'smart grid' scenarios.

ENS Average Reduction ('smart' scenarios)	Residential Demand		Commercial Demand	Total
	Load Points (1-5) (peak reduction)	Load Points (6-10) (reliability improv.)	Load Point 11	Overall Network
DSM	5.03%	6.66%	5.75%	5.82%
E. Storage	13.18%		0%	12.52%
DSM + E. Storage	18.04%	20.22%	5.75%	18.26%

The obtained results suggest that properly devised 'smart grid' control actions (i.e. introducing ES, DSM, MG, etc.) might be an efficient tool for DNOs to reduce network congestion and improve reliability and quality of supply in their networks. Moreover, this method could potentially help DNOs to decide the optimal location, time and portion of the load available for implementation of reliability-based scenarios. The additional results for energy-related indices further emphasise the positive impact of the considered "smart grid" schemes on both residential and commercial customers' reliability.

6.5 Conclusions

The main aim of this chapter was to demonstrate the applicability of the developed Monte Carlo simulation methodology, in combination with different network functionalities and equivalent models, for an integrated (i.e. all-condition inclusive) reliability analysis of actively managed distribution networks. In the previous chapter, a new theoretical interruption model was introduced for assessing more accurately the moment in time when customer interruptions take place in the network. Therefore, in order to further assess its effectiveness to model the initial conditions of the MCS procedure, the methodology is applied to the reliability performance assessment of a 'realistic' power distribution system, represented with typical/generic UK LV/MV network models.

Regarding the estimation of ENS index, significant differences have only been achieved for individual or group(s) of customers, with the theoretical model having less, but not negligible, effect on the global ENS index (evaluated for the whole system). Additional reliability indices, SAIFI, SAIDI and MAIFI have been quantified in order to validate the proposed interruption model against reported figures and decide which of the probability distributions shall be assumed in similar studies for modelling the initial conditions of the MCS procedure. The results suggested that the theoretical interruption model, combined with the exponential distribution, provides the most realistic estimations, always considering that its impact on reliability estimations (i.e. ENS) depends on how reliable the analysed system is (e.g. meshed or radial network configurations, etc.).

Moreover, by considering the UK Energy Regulator requirements (methodology also applicable to similar regulatory environments in other countries), a new analytical reliability algorithm has been developed in this chapter in order to acknowledge the protection of electricity

customers from excessively long durations of interruptions. The proposed methodology allows estimating the risk of interruption times above the Regulator-imposed limits when the reliability performance of the analysed system is tested to respond to those targets.

An additional study is presented in this chapter to assess and evaluate, by using different approaches and equivalent models, the impact of several network functionalities on the accuracy of reliability performance results provided by the MCS methodology. A comparison is also provided after analysing the same network conditions and scenarios using time-sequential MCS, and analytical approaches, in an attempt to fully match the mean values of the resulting reliability indices. Accordingly, the stochastic behaviour of the generic urban distribution network is assessed by applying different reconfiguration, switching, and security of supply schemes available to DNOs.

Finally, this chapter analyses the influence of distributed energy resources on reliability performance of active networks (so called "smart grids"). The proposed time-sequential MCS methodology, including all developed modelling assumptions, is used to assess the potential improvements that different demand-side management and energy storage schemes will have on the frequency and duration of customer interruptions. Particular attention is given to energy-related reliability indices (e.g. ENS), measuring the energy not supplied to residential and commercial customers.

Chapter 7

Summary and Conclusions

7.1 Synopsis

This thesis presents a number of methodologies intended for the modelling and aggregation of typical power distribution networks in combination with different load models and distributed energy resource functionalities, as well as the assessment of the aggregate impact of these equivalent models and technologies on distribution system quality of supply.

Chapter 2 introduces the main background and literature review related to network reliability and power quality, i.e. overall quality of supply assessment of power distribution systems, focusing particularly on the expected challenges posed by the most widely used reliability metrics and concepts. A review of security and regulator-imposed requirements applied in the UK for supply restoration times is also presented, in combination with a comprehensive database with failure rates and mean repair times for the wide range of network components. In addition, this chapter provides several reliability case studies with the analysis of actual component failure statistics and reliability performance of different European distribution/transmission network operators.

Chapter 3 describes an integrated modelling procedure in order to develop different generic models, which are capable of accurately representing typical sub-transmission and power distribution systems. Accordingly, their equivalent representations are provided at different network locations, load subsectors and voltage levels. First, the work focuses on the development of a comprehensive component database for network modelling, which provides a wide range of specifications and parameters of actual power equipment. Moreover, this chapter reviews the main principles of load modelling for power system analysis, identifies typical load structures at different residential subsectors, and proposes an aggregate residential load model for an accurate network design and operation.

Chapter 4 deals with the modelling, aggregation and analysis of distribution network equivalents, with a particular focus on the different network models (per load subsector) previously described in Chapter 3. A more accurate approach is also proposed for the calculation of public supply network impedances at different voltage levels. A methodology for aggregating LV and MV distribution networks, which allows for the correct assessment of network reliability at

bulk supply points including microgeneration models and distributed generation/storage functionalities, is presented and validated. Accordingly, accurate electrical and reliability equivalent models are formulated for different distribution networks and load subsectors.

Chapter 5 describes the main reliability criteria and techniques used in this thesis for the calculation of system and end-users' reliability indices. The conventional Monte Carlo Simulation method is modified with the inclusion of actual load profiles, the use of different input probability distributions, as well as the impact analysis of time-varying failure rates of network components. The uncertainty and convergence of the resulting reliability indices is also discussed, in combination with a study of multiple-fault occurrence. Finally, a new theoretical outage model is introduced for assessing more accurately the moment in time when interruptions of electricity customers are likely to occur.

Chapter 6 applies all the reliability assessment procedures and equivalent models of distribution networks and 'smart grid' technologies/functionalities (i.e. renewable-based microgeneration, energy storage and demand-responsive loads) developed in previous chapters for an integrated reliability analysis of actively-managed distribution systems. The applicability of the proposed Monte Carlo simulation algorithm, previously introduced in Chapter 5, is fully assessed by quantifying the impact of different network functionalities on the overall system reliability performance. In addition, a reliability deterministic approach is undertaken in order to acknowledge the protection of electricity customers from extremely long outages. The integrated time-sequential methodology is used to assess the potential improvements that different demand-side management and energy storage schemes could have on the frequency and duration of customer interruptions.

7.2 Implications of Results

The presented PhD work aims to extend the standard three-phase calculation engine by providing multiple numerical software models offering new capabilities and distinctive properties for the correct assessment of quality of supply in future electricity networks.

7.2.1 Modelling of Generic Networks and Load Identification

The work presented in Chapter 3 was designed to identify and develop missing power component models, update the existing ones, and apply them after identifying typical UK and European network models. Therefore, a detailed database with configurations and parameters of electricity distribution systems was built in order to provide a set of generic models that can easily represent actual sub-transmission and distribution networks supplying a mix of residential, commercial and industrial demand, while allowing the efficient modelling and simulation of current and future power system functionalities (e.g. DG, ES and DSM).

For different load sectors, from metropolitan to rural areas, detailed demand decomposition and generic network models were identified, which are considered essential for steady state network analysis, such as active/reactive power flows, system losses, voltage profiles, etc., as well as for any network planning stage, where issues such as security and reliability of supply are of primary importance.

In addition, a realistic assessment is undertaken by applying the load decomposition approach described in Chapter 3 to build an accurate, equivalent representation of the aggregate demand within the networks of analysis. This is represented by different component-based load models of UK residential and commercial sector loads, based on available statistics on load mix and device ownership [41]. This information is then used to build a load/network aggregation methodology in Chapter 4. One major advantage of this approach is that the resulting load-/network models are flexible, as the aggregate demands can easily be built to incorporate future or expected changes in the load composition. By adjusting the contributions from each load type and load sector, the load/network models are particularly well suited to the modelling of DSM, as well as to the inclusion of MG/ES models.

7.2.2 Electrical and Reliability Network Equivalents

Based on the generic models presented in Chapter 3, the modelling, aggregation and network analysis of distribution system equivalents have been discussed in Chapter 4. In order to avoid the underestimation of network's performance at bulk supply points, a general methodology is developed for reducing system complexity by calculating the electrical and reliability equivalent models of LV and MV distribution networks. These equivalent models, based on the aggregation of individual component models, help to reduce calculation times while preserving the accuracy of the assessment of power system reliability performance.

According to the research outcome, these aggregate models and distribution network equivalents were validated in order to prove that fundamental steady-state and reliability network characteristics are preserved when the aggregation methodology is applied. These aggregate network models were used to develop improved MV aggregate load models, considering different contribution from residential and commercial demand. In addition, the aggregation methodology also served to analyse the impacts of different MG, ES and DSM scenarios on network quality of supply performance. The analysis also includes relevant security of supply requirements, in order to correctly analyse modern meshed distribution networks with alternative supply points, for which supply restoration times are empirically determined.

7.2.3 Impact of the Smart Grid Functionalities on QoS Performance

Regarding the expected 'smart grid' functionalities to be applied in future power distribution systems, the network equivalent models developed in Chapter 4 for different load subsectors also incorporate capabilities for the integrated assessment of MG models, DSM and ES functionalities on network quality of supply performance.

Different 'smart grid' scenarios were specifically tailored for reliability purposes in order to assess the potential improvements that different DSM and ES schemes could have on the frequency and duration of customer interruptions. Particular attention was given to energy-related reliability indices (e.g. ENS), which were found to be the most appropriate for estimating the optimal continuity of supply to residential and commercial customers.

According to the work presented in Chapter 5, the probability of faults in the overall distribution network (including both LV and MV levels) is mainly influenced by larger commercial and industrial loads with a peak consumption taking place over the working hours of the day. Therefore, the proposed analysis considers an appropriate load profile at each voltage level, according to the demand decomposition (residential, commercial and industrial) presented in Section 5.2.2 of this thesis.

7.2.4 Integrated Reliability Analysis of Active Distribution Networks

First, analytical (i.e. deterministic) approaches, and then simulation techniques (i.e. Monte Carlo Simulation method) are both employed to improve service quality by reducing the frequency and duration of customer interruptions for different scenarios and test distribution networks. Recordings and contingency statistics related to the analysed network models are used as inputs for the simulation method, in which output reliability indices (e.g. SAIFI, SAIDI, MAIFI, CAIDI, ENS, etc. [33]) are expressed as probability distributions, rather than simple average values and standard deviations. Accordingly, the effectiveness of several probability distributions (i.e. exponential, Weibull, Rayleigh, Gamma, etc.) to model the initial conditions of the MCS procedure is assessed and validated in Chapters 5 and 6. Therefore, an integrated methodology is proposed for quantifying in a most realistic manner the standard set of indices reported annually to energy regulators.

Conventional reliability assessment procedures are extended to include accurate reliability equivalent models (developed in Chapter 4), actual load profiles (i.e. residential, commercial and industrial demands), and empirical (i.e. recorded non-uniform) fault probability distributions, allowing to make a clear distinction between short and long supply interruptions. Besides these modifications, the conventional MCS approach is modified to include UK security of supply legislation, imposing required times to restore supply for interrupted customers. The accuracy and applicability of the proposed methodology is validated through different network scenarios.

7.3 Research Limitations

Validation of generic distribution systems and aggregate network/load models

One of the most challenging aspects of this work is the validation of the developed aggregate network/load models, as a result of the proposed generic models representing typical distribution systems for different load subsectors. This would require a large number of measurements performed on specifics areas of the power system where the networks and load configurations are relatively well known. As these measurements are not currently available, this final level of validation was not possible within the time-frame of this research. However, it was possible to validate other stages of the process, which provides confidence in the final result.

For this purpose, a disaggregated sample (i.e. a 'real' system comprising 10 to 100 buses) of an actual DNO's MV/LV distribution network, which would ideally supply a high percentage of residential customers, would be required for validation of results at the four different load/network subsectors. This information is considered essential for validation as it would provide full network specifications (i.e. circuit ratings, transformer loads, etc.) and layout for systems with different characteristics, such as meshed networks with backup/reconfiguration capabilities and radial networks with mainly overhead configurations. Additional data would also be required to provide number of customers supplied per bus/load point, considering their aggregate load profiles and rated power considered for individual households.

Integration of network/load models

The development of new modelling tools can only be considered successful if they are compatible with widely used softwares. In this case, the proposed models are developed by using PSSE simulator and Matlab (Simulink) Power Systems Toolbox, as these are amongst the most common and flexible power-flow solvers in the market, and the rest of algorithms are coded and solved in Python and Matlab programming tools. Accordingly, the modelling approach presented in this thesis could still be further validated by integrating the developed models in additional software/simulators such as Powerworld, DIgSILENT, or OpenDSS. However, the flexibility contained within the network/load modelling approach goes a long way to resolving these issues.

Considering the practical implementation of the aggregate network/load models, the majority of results were represented by the exponential and polynomial/ZIP load models, which are still the most widely used load model forms. However, if further information of the aggregate load must be retained in the network aggregation process (i.e. dynamic modelling approach), the use of the detailed network/load models must be extended to develop highly accurate models for power-quality related analyses. This approach was applied in the work published by the author in [21, 28, 31].

Modelling of GSP loads and DSM

As a new feature of MCS method, the identification of load sectors which compose the BSP's aggregate demand is introduced in Chapter 5, which is based on comparing the aggregate demand at each node with the "typical" residential, commercial and industrial load profile. However, the success of this approach depends on how accurately the "typical" load profiles represent each load sector (generally well performed for residential and commercial sectors), as for example, in the case of industrial loads, the daily load profiles can vary considerably depending on the exact type of industry. This issue could potentially be overcome by adding more load sectors and categories. However, since that is not of primary importance to the work in this thesis, this line of research was not pursued further.

The decomposition of aggregate load demands into load types and categories is carried out using measurements at 33 kV supply points throughout the SPTL system. Ideally, the load identification and decomposition should be validated using detailed measurements of the load at the secondary (11 kV) substations, or even at each LV feeder, to ensure that the load sectors and categories identified in the analysis are correct.

Finally, the assumptions around the proposed 'smart grid' schemes (by applying MG, ES and DSM functionalities) can serve as a good reference for assessing possible reliability benefits in power systems; however, some of the scenarios described (specially those for reliability improvement) might present a new challenge to the actual regulatory and operational framework for electricity distribution. It is generally envisaged that DSM or storage technologies will mainly be applied for energy arbitrage, i.e. to take advantage of high electricity prices by selling/reducing demand at times of high prices. However, the current context for electricity distribution still does not consider a situation in which the users will apply DSM or storage purely for reliability purposes, i.e. to store/reduce energy consumption for reducing their frequency and duration of supply interruptions.

Reliability uncertainty modelling

The accuracy in the calculation of reliability indices after applying the proposed MCS procedure strongly depends on the available information on past system performance, consisting of historical data and records of failure and repair rates of network components. In this thesis, access to measurements was used to remove as much of the uncertainty as possible. However, this type of data is not always readily available, thus a large number of data sources, ranging from technical literature to DNOs' datasheets, were used to address uncertainty gaps.

The range of reliability indices reported by 14 UK DNOs (Table 2.3) is used in this thesis for the validation of different reliability results. However, the presented analysis is applied to generic networks designed for operation in specific network locations (i.e. from highly-urban to rural areas), thus a direct comparison with the overall UK reported indices is not always possible. Therefore, additional information is essential for further work in order to validate the

reliability assessment procedures proposed in this thesis. For this purpose, the *real* reliability performance (i.e. information on CI, CML, SIs) and fault record data from part of an actual DNO's distribution network, could be reproduced and validated by the reliability models of this work. Another identified option would be to use a well-known reliability test system (e.g. provided by IEEE [187, 188] for reliability analysis), which would allow for direct comparison with other methods in the literature and for others to easily reproduce results.

As proved in this thesis, the methods currently used for network reliability analysis must be adapted for a correct assessment of the expected 'smart grid' functionalities (e.g. DG, ES and DSM). However, time-sequential MCS represents a highly-demanding computational method, from which the accuracy of results depends on the number of samples in the simulation and variance of the estimate. Accordingly, a considerable modelling effort was made to find an optimal precision of the obtained reliability indices, by applying parallel calculation methods and the combination of MCS with analytical equivalent models. Acceleration methods and techniques for variance reduction are thus proposed to be addressed in further research.

7.4 Recommendations for Further Work

The following outlines the most important areas in which the proposed methodologies could be improved and further applied in analysis of quality of supply in future electricity networks.

Analytical LV/MV transformation

The equivalent network impedance has been shown in Chapter 4 to allow for the quick, but accurate, transformation of aggregate LV load characteristics to the MV level. However, this requires the representation of the equivalent network components, i.e. the equivalent feeder and secondary distribution transformer, in power system simulation software and must also include a voltage sweep to allow for fitting of the exponential or polynomial/ZIP load model coefficients. A mathematical derivation of the equivalent network impedance load flow will allow for the quick transformation of LV load model parameters to the MV, without the need for any software, or simulation of multiple voltage conditions. The value of this would be significantly increased if large penetrations of MG were present, as this method could be combined with probabilistic techniques which are typically used when simulating this particular scenario.

Reliability modelling with stochastic behaviour of intermittent renewable resources

The 'smart grid' scenarios analysed in this thesis could be improved by fully considering the interdependencies between different renewable-based technologies, and the time constraints and variability associated with them. For example, some of the backup capabilities, as a result of the energy stored from solar/wind microgeneration systems, might not always be applicable for a fast-response (e.g. a cloudy/non-windy day with no solar/wind MG output to store).

Therefore, in those cases, no storage capacity would be available. Other situations include cases when the energy could not be stored for a long enough period, or when some users might have decided to sell into the grid instead.

Methods for building simplified, aggregate models of the most relevant DG/DSM/Storage technologies, such as [189, 190, 191] could be used to build a stochastic representation of the 'smart grid' technologies, and their potential to provide reliability/backup services. This would allow to include the time constraints and interdependencies between these technologies in the model and provide a more accurate assessment of the impacts of the 'smart grid' on network's reliability.

In addition, there is currently great interest in many parts of the world in microgrid applications and technologies for a local improvement of the supply quality. Accordingly, all the aforementioned capabilities could be combined and implemented in order to assess the effects these new applications/technologies will have on bulk system reliability, as it will require changes in the way the bulk power system is planned and operated.

High-accuracy and full time-domain simulations for reliability analysis

This next stage of the work would concentrate on the analysis of transient operating conditions of future electricity networks. Due to an increased number of distributed active elements, located much closer to the end-user's loads, there will be a substantially higher level of system-load interactions affecting network's reliability. The correct solution for the dynamic performance will, therefore, require the implementation of a full time-domain analysis, capable of providing output results with a high resolution. For example, the analysis engine should be capable of modeling system wide propagation of harmonics and unbalances, as well as the inclusion of relevant inter-compatible models of all control, coordination and protection equipment.

In this case, the developed models of DSM-load will be able to respond to relevant voltage, frequency or price signals, and accordingly change their mode of operation. Models of DG units, on the other hand, will include a set of autonomous and/or coordinated controls, which will allow them to participate in voltage and frequency regulation, based on system-wide intermittent/renewable resources, or to provide some additional system/user support functionalities.

Regarding the process of stochastic convergence in time-sequential Monte Carlo Simulation, different acceleration methods (i.e. decrease number of samples) and techniques can be applied, by improving the accuracy and precision of results, in order to reduce the simulation's variance/uncertainty. Five main techniques are used in power system analysis to accelerate the MCS procedure [48, 181], which imply the substitution of "natural" sampling with a more sophisticated sampling.

Incorporation of a cost-benefit reliability assessment

The reliability work presented in this thesis could be complemented by defining a set of 'cost-benefit' indicators, capable of quantifying, in economical terms, any improvement or deterioration of the quality of supply performance due to, for example, a change in system configuration, installation of new components, or the application of new automation/control functionalities. This would allow for a direct correlation of the achieved economical benefits with the known or estimated costs of each applied action.

In that way, a more accurate cost-benefit analysis and economic assessment tools will be applied in order to allocate the correct value to different planned or unplanned changes in the system and end-user's assets, functions and services. This cost-benefit approach will, perhaps, increase the motivation for network operators to further explore the potential of 'smart grid' applications for network support and improvement of system performance.

References

[1] "Carbon emissions reduction target (CERT)," Department of Energy and Climate Change (DECC), UK, Tech. Rep., April 2008 - March 2011.

[2] (2010) Driving the low carbon economy. Paper 1: Renewing our ambitions. Scottish Renewables. [Online]. Available: www.scotland.gov.uk/News/Releases/2010/09/23134359

[3] SuperGen Flexnet Consortium, "Making networks fit for renewables," in *Proceedings of IET SuperGen Flexnet Consortium, London, UK*, London, UK, October 2008.

[4] NERC, "Potential reliability impacts of emerging flexible resources," North American Electric Reliability Corporation, Tech. Rep., 2010.

[5] E. Lannoye, D. Flynn, and M. O'Malley, "Evaluation of power system flexibility," *Power Systems, IEEE Transactions on*, vol. 2, pp. 922–931, 2012.

[6] S. Djokic and J. Milanovic, "Power quality and compatibility levels: A general approach," *Power Delivery, IEEE Transactions on*, vol. 22, no. 3, pp. 1857–1862, 2007.

[7] S. Djokic, J. Milanovic, and M. Kayikci, "The influence of distributed generation and power conditioning equipment on distribution network performance," in *13th Int. Symposium on Power Electronics - Ee 2005*, 2005.

[8] S. Djokic, "Assessment of the quality of supply in networks with distributed generators based on measurements and computer simulations," in *15th Int. Electrical Equipment Conf. on the Electric Network of the Future and Distributed Generation, IEEC 2005*, 2005.

[9] "The costs and impacts of intermittency," UK Energy Research Centre and Carbon Trust (UKERC), Tech. Rep., 2006.

[10] S. Z. Djokic, I.-S. Ilie, and I. Hernando-Gil, "Integrated assessment of quality of supply in future electricity networks," March 2010-September 2013, (UK) EPRSC Grant EP/G052530/1.

[11] R. Billinton and R. Allan, "Power-system reliability in perspective," *Electronics and Power*, vol. 30, no. 3, pp. 231–236, 1984.

[12] R. Allan and R. Billinton, "Power system reliability and its assessment. I. Background and generating capacity," *Power Engineering Journal*, vol. 6, no. 4, pp. 191–196, 1992.

[13] ——, "Power system reliability and its assessment. II. Composite generation and transmission systems," *Power Engineering Journal*, vol. 6, no. 6, pp. 291–297, 1992.

[14] ——, "Power system reliability and its assessment. III. Distribution systems and economic considerations," *Power Engineering Journal*, vol. 7, no. 4, pp. 185–192, 1993.

[15] R. Billinton and R. N. Allan, *Reliability Evaluation of Power Systems*, 2nd ed. Plenum Press, New York, 1996.

[16] T. McDermott and R. Dugan, "Distributed generation impact on reliability and power quality indices," in *Rural Electric Power Conference, IEEE*, 2002, pp. D3–D3–7.

[17] "Review of planning and operational contingency criteria," GB SQSS Steering Group, Working Group 4 Report, April 2010.

[18] Q. Chen, "The probability, identification, and prevention of rare events in power systems," Ph.D. dissertation, Iowa State University, 2004.

[19] A. Collin, I. Hernando-Gil, J. Acosta, and S. Djokic, "An 11 kV steady state residential aggregate load model. Part 1: Aggregation methodology," in *PowerTech, 2011 IEEE Trondheim*, 2011, pp. 1–8.

[20] I. Hernando-Gil, S. Ilie, A. Collin, J. Acosta, B. Hayes, and S. Djokic, "Coordinated control of micro-generation and demand-side management in smart grids," in *IEEE PES MixGenera Conference, Madrid.* IEEE, 2011.

[21] A. Collin, I. Hernando-Gil, J. Acosta, I.-S. Ilie, and S. Djokic, "Realising the potential of smart grids in LV networks. Part 1: Demand-side management," in *Innovative Smart Grid Technologies (ISGT Europe), 2011 2nd IEEE PES International Conference and Exhibition on*, 2011, pp. 1–7.

[22] I.-S. Ilie, I. Hernando-Gil, A. Collin, J. Acosta, and S. Djokic, "Reliability performance assessment in smart grids with demand-side management," in *Innovative Smart Grid Technologies (ISGT Europe), 2011 2nd IEEE PES International Conference and Exhibition on*, 2011, pp. 1–7.

[23] I. Hernando-Gil, I.-S. Ilie, A. Collin, J. Acosta, and S. Djokic, "Impact of DG and energy storage on distribution network reliability: A comparative analysis," in *Energy Conference and Exhibition (ENERGYCON), 2012 IEEE International*, 2012, pp. 605–611.

[24] I.-S. Ilie, I. Hernando-Gil, and S. Djokic, "Reliability equivalents of LV and MV distribution networks," in *Energy Conference and Exhibition (ENERGYCON), 2012 IEEE International*, 2012, pp. 343–348.

[25] I. Hernando-Gil, I. Ilie, and S. Djokic, "Reliability performance of smart grids with demand-side management and distributed generation/storage technologies," in *Innovative Smart Grid Technologies (ISGT Europe), 2012 3rd IEEE PES International Conference and Exhibition on*, 2012, pp. 1–8.

[26] I. Hernando-Gil, B. Hayes, A. Collin, and S. Djokic, "Distribution network equivalents for reliability analysis. Part 1: Aggregation methodology," in *Innovative Smart Grid Technologies Europe (ISGT EUROPE), 2013 4th IEEE/PES*, 2013, pp. 1–5.

[27] "Electricity distribution quality of service report," OFGEM, UK, Annual Report, December 2009.

[28] J. Acosta, K. Combe, S. Djokic, and I. Hernando-Gil, "Performance assessment of micro and small-scale wind turbines in urban areas," *Systems Journal, IEEE*, vol. 6, no. 1, pp. 152–163, 2012.

[29] B. Hayes, I. Hernando-Gil, A. Collin, G. Harrison, and S. Djokic, "Optimal power flow for maximizing network benefits from demand-side management," *Power Systems, IEEE Transactions on*, no. 99, pp. 1–9, 2014.

[30] A. Collin, J. Acosta, I. Hernando-Gil, and S. Djokic, "An 11 kV steady state residential aggregate load model. Part 2: Microgeneration and demand-side management," in *PowerTech, 2011 IEEE Trondheim*, 2011, pp. 1–8.

[31] A. Collin, I. Hernando-Gil, J. Acosta, I.-S. Ilie, and S. Djokic, "Realising the potential of smart grids in LV networks. Part 2: Microgeneration," in *Innovative Smart Grid Technologies (ISGT Europe), 2011 2nd IEEE PES International Conference and Exhibition on*, 2011, pp. 1–8.

[32] B. Hayes, A. Collin, I. Hernando-Gil, J. Acosta, S. Hawkins, G. Harrison, and S. Djokić, "All-scale modelling of wind generation and responsive demand in power system studies," in *Proceedings of the IEEE PES General Meeting, San Diego, CA*, 2012.

[33] "IEEE guide for electric power distribution reliability indices," *IEEE Std 1366-2012 (Revision of IEEE Std 1366-2003)*, pp. 1–43, 2012.

[34] I. Hernando-Gil, B. Hayes, A. Collin, and S. Djokic, "Distribution network equivalents for reliability analysis. Part 2: Storage and demand-side resources," in *Innovative Smart Grid Technologies Europe (ISGT EUROPE), 2013 4th IEEE/PES*, 2013, pp. 1–5.

[35] I.-S. Ilie, I. Hernando-Gil, and S. Z. Djokic, "Risk assessment of interruption times affecting domestic and non-domestic electricity customers," *International Journal of Electrical Power & Energy Systems*, vol. 55, pp. 59–65, 2014.

[36] ——, "Theoretical interruption model for reliability assessment of power supply systems," *IET Generation, Transmission & Distribution*, vol. 8, no. 4, pp. 670–681, 2013.

[37] J. Taylor, "Bulk system reliability assessment and the smart grid," Electric Power Research Institute (EPRI), White Paper, August 2012.

[38] R. Ball, "The probability of faults and trips on the grid system," National Grid, UK, Internal Report (ENI Policy: SC&M), July 2012.

[39] J. Acosta, "Micro and small-scale generation in urban distribution networks," Ph.D. dissertation, The University of Edinburgh, 2012.

[40] B. P. Hayes, "Distributed generation and demand side management: Applications to transmission system operation," Ph.D. dissertation, The University of Edinburgh, 2013.

[41] A. Collin, "Advanced load modelling for power system studies," Ph.D. dissertation, The University of Edinburgh, 2013.

[42] "Guidance and proposals on best practice - electricity distribution," OFGEM, UK, Guaranteed Standards, April 2006.

[43] "The 4^{th} benchmarking report on quality of electricity supply," Council of European Energy Regulators, Tech. Rep., 2008.

[44] *Voltage Characteristics of Electricity Supplied by Public Electricity Networks*, Std. EN50 160, 2010.

[45] "Quality of service regulatory instructions and guidance," RIGS, UK, Tech. Rep., 2005.

[46] A. B. Baggini *et al.*, *Handbook of power quality*. Wiley Online Library, 2008.

[47] R. E. Brown, *Electric power distribution reliability*. CRC Press, 2002.

[48] R. Billinton and W. Li, *Reliability assessment of electrical power systems using Monte Carlo methods*. Springer, 1994.

[49] N. Hadjsaïd and J. C. Sabonnadière, *Electrical distribution networks*, Technology & Engineering ed. John Wiley & Sons, January 2013.

[50] *UK National Electricity Transmission System Security and Quality of Supply Standard*, Std., Rev. Version 2.1, March 7 2011.

[51] A. Chowdhury and D. O. Koval, "Two views of utility performance indices," *Industry Applications Magazine, IEEE*, vol. 15, no. 5, pp. 14–20, 2009.

[52] *Recommended Practice for Monitoring Electric Power Quality*, IEEE Std. 1159, June 2009.

[53] E. Hirst and B. Kirby, "Bulk-power basics: Reliability and commerce," *Consulting in Electric-Industry Restructuring, Oak Ridge, Tennessee*, vol. 37830, 2000.

[54] North American Electric Reliability Council (NERC), Glossary and Terms, August 1996.

[55] D. J. Smith, *Reliability, maintainability and risk: Practical safety-related systems engineering methods.* Access Online via Elsevier, 2011.

[56] P. Wikstrom, L. A. Terens, and H. Kobi, "Reliability, availability, and maintainability of high-power variable-speed drive systems," *Industry Applications, IEEE Transactions on*, vol. 36, no. 1, pp. 231–241, 2000.

[57] S. Djokic, "Generalised methodology for the assessment of voltage sag performance indices and equipment sensitivity," Ph.D. dissertation, University of Manchester, February 2004.

[58] *Dependability and Quality of Service*, Part 191-19-01 IEC 60 050, 1990.

[59] *Quality Vocabulary. Part 2: Quality Concepts and Related Definitions*, British Standard BS 4778-2, 1991.

[60] *Recommended Practice for Powering and Grounding Electronic Equipment*, IEEE Std. 1100, December 2005.

[61] *Part 1: "Overview of implementation of standard and procedures", Part 2: "Minimum Standards"*, Electricity Supply - Quality of Supply Std. NRS 048-1,2,3,4, 1996.

[62] *Electromagnetic compatibility - Part 4-30: Testing and measurement techniques - Power quality measurement methods*, British Standards Std. IEC 61 000-4-30, January 2009.

[63] *Electromagnetic Compatibility Series*, IEC Std. 61 000.

[64] *International electrotechnical vocabulary*, Series IEC 60 050.

[65] R. Dugan, M. F. McGranaghan, and H. W. Beaty, *Electric power systems quality*. McGraw-Hill, 2002.

[66] D. Chapman, "Introduction to power quality," *Leonardo Energy Application Guide*, 2001.

[67] G. T. Heydt and J. Spindler, "Effects of electronic equipment on plant power quality," *Plant Engineering;(United States)*, vol. 46, no. 15, 1992.

[68] E. Fuchs and M. A. Masoum, *Power quality in power systems and electrical machines*. Academic press, 2011.

[69] C. Sankaran, *Power quality*. CRC press, 2001.

[70] N. Balijepalli, S. S. Venkata, and R. D. Christie, "Modeling and analysis of distribution reliability indices," *Power Delivery, IEEE Transactions on*, vol. 19, no. 4, pp. 1950–1955, 2004.

[71] R. Allan and R. Billinton, "Probabilistic assessment of power systems," *Proceedings of the IEEE*, vol. 88, no. 2, pp. 140–162, 2000.

[72] R. Billinton and E. Wojczynski, "Distributional variation of distribution system reliability indices," *Power Apparatus and Systems, IEEE Transactions on*, no. 11, pp. 3151–3160, 1985.

[73] "E-ON Central Networks plc, Long term development statement," Central Networks West, Tech. Rep., 2009.

[74] National Grid. (2011) National electricity transmission system (NETS) seven year statement. [Online]. Available: http://www.nationalgrid.com/uk/Electricity/SYS/current/

[75] R. Billinton, M. Fotuhi-Firuzabad, and S. Faried, "Power system reliability enhancement using a thyristor controlled series capacitor," *Power Systems, IEEE Transactions on*, vol. 14, no. 1, pp. 369–374, 1999.

[76] L. Goel and R. Billinton, "A comparison of three fundamentally different methods for generating capacity reliability evaluation," *Electric power systems research*, vol. 29, no. 1, pp. 1–8, 1994.

[77] F. Bouffard and F. D. Galiana, "An electricity market with a probabilistic spinning reserve criterion," *Power Systems, IEEE Transactions on*, vol. 19, no. 1, pp. 300–307, 2004.

[78] W. Wangdee and R. Billinton, "Utilization of time varying event-based customer interruption cost load shedding schemes," *International Journal of Electrical Power & Energy Systems*, vol. 27, no. 9, pp. 674–681, 2005.

[79] J. Sinclair and I. Gray, "Assessing the potential for arc suppression coil technology to reduce customer interruptions and customer minutes lost," in *Electricity Distribution - Part 1, 2009. CIRED 2009. 20th International Conference and Exhibition on*, June 2009, pp. 1–4.

[80] E. Weber, B. Adler, R. Allan, S. Agarwal, M. Bhavaraju, R. Billinton, M. Blanchard, R. D'Aquanni, R. Ellis, J. Endrenyi *et al.*, "Reporting bulk power system delivery point reliability," *Power Systems, IEEE Transactions on*, vol. 11, no. 3, pp. 1262–1268, 1996.

[81] J. Horak, "Power quality: Measurements of sags and interruptions," in *Transmission and Distribution Conference and Exhibition, 2005/2006 IEEE PES*. IEEE, 2006, pp. 733–739.

[82] T. Ortmeyer, "A unified index for power distribution reliability/power quality indices," in *Harmonics and Quality of Power (ICHQP), 2010 14th International Conference on*. IEEE, 2010, pp. 1–6.

[83] T. H. Ortmeyer, J. A. Reeves, D. Hou, and P. McGrath, "Evaluation of sustained and momentary interruption impacts in reliability-based distribution system design," *Power Delivery, IEEE Transactions on*, vol. 25, no. 4, pp. 3133–3138, 2010.

[84] B. W. Kennedy, *Power quality primer*. McGraw Hill Professional, 2000.

[85] D. L. Brooks, R. C. Dugan, M. Waclawiak, and A. Sundaram, "Indices for assessing utility distribution system rms variation performance," *Power Delivery, IEEE Transactions on*, vol. 13, no. 1, pp. 254–259, 1998.

[86] Quality of Service Guaranteed Standards. OFGEM. [Online]. Available: https://www.ofgem.gov.uk/licences-codes-and-standards/standards/quality-service-guaranteed-standards

[87] *The electricity standard of performance regulations*, OFGEM Statuory Instruments 698, 2010. [Online]. Available: http://www.legislation.gov.uk/

[88] Interruption Incentive Scheme (Quality of Service Incentives). OFGEM. [Online]. Available: https://www.ofgem.gov.uk/electricity/distribution-networks/network-price-controls/quality-service/quality-service-incentives

[89] *Security of Supply*, Energy Networks Association (ENA) Engineering Reccommendations P2/6, March 2005.

[90] "Long term development statement for Scottish hydro electric power distribution plc's electricity distribution system," Scottish and Southern Energy Power Distribution, Tech. Rep., November 2009.

[91] "Distribution long term development statement for the year 2011/12 to 2015/16," SP Distribution and SP Manweb, Tech. Rep., November 2011.

[92] R. Billinton and J. Billinton, "Distribution system reliability indices," *Power Delivery, IEEE Transactions on*, vol. 4, no. 1, pp. 561–568, 1989.

[93] "National system and equipment performance," National Fault and Interruption Reporting Scheme, ENA Report, December 2010.

[94] R. Allan, M. De Oliveira, A. Kozlowski, and G. Williams, "Evaluating the reliability of electrical auxiliary systems in multi-unit generating stations," in *Generation, Transmission and Distribution, IEE Proceedings C*, vol. 127, no. 2. IET, 1980, pp. 65–71.

[95] E. Stanek and S. Venkata, "Mine power system reliability," *Industry Applications, IEEE Transactions on*, vol. 24, no. 5, pp. 827–838, 1988.

[96] A. Farag, C. Wang, T. Cheng, G. Zheng, Y. Du, L. Hu, B. Palk, and M. Moon, "Failure analysis of composite dielectric of power capacitors in distribution systems," *Dielectrics and Electrical Insulation, IEEE Transactions on*, vol. 5, no. 4, pp. 583–588, 1998.

[97] "The performance of networks using alternative network splitting configurations," Final Report on Technical Steering Group Workstream 3, August 2004.

[98] F. Roos and S. Lindah, "Distribution system component failure rates and repair times–an overview," in *Conf. Rec. the Nordic Distribution and Asset Management Conference*. Citeseer, 2004.

[99] G. J. Anders, H. Maciejewski, B. Jesus, and F. Remtulla, "A comprehensive study of outage rates of air blast breakers," *Power Systems, IEEE Transactions on*, vol. 21, no. 1, pp. 202–210, 2006.

[100] "Review of electricity transmission output measures," PB Power, OFGEM Final Report, October 2008.

[101] Y. He, "Study and analysis of distribution equipment reliability data," Sweden, Elforsk Report, March 2010.

[102] B. Retterath, S. Venkata, and A. A. Chowdhury, "Impact of time-varying failure rates on distribution reliability," *International Journal of Electrical Power & Energy Systems*, vol. 27, no. 9, pp. 682–688, 2005.

[103] "Drifthändelsestatistik (DARWin)," Svensk Energi, in Swedish, 2010. [Online]. Available: http://www.svenskenergi.se

[104] D. Torstensson, M. Bollen, and R. Kolessar, "The Swedish benchmarking report on continuity of supply," in *Electricity Distribution (CIRED 2011), 21st International Conference and Exhibition on*, no. 0233. IET, June 2011, pp. 1–4.

[105] "Leveranssäkerhet i elnäten - Statistik och analys av elavbrotten i de Svenska elnäten 1998-2008," Energy Markets Inspectorate, in Swedish EIR 2010:05, April 2010. [Online]. Available: http://www.ei.se

[106] "Long Term Development Statement," Electricity North West plc, Tech. Rep., 2010.

[107] "Long Term Development Statement for the Electricity Distribution System of South Wales & South West," Western Power Distribution plc, Tech. Rep., April 2010.

[108] "Long Term Development Statement," EDF Energy Networks, Tech. Rep., 2009.

[109] "Long Term Development Statement," CE Electric UK, Tech. Rep., 2009.

[110] "The distribution code of licensed distribution operators of Great Britain," DCode, Tech. Rep., September 2013. [Online]. Available: http://www.dcode.org.uk/

[111] C. Foote, P. Djapic, G. Ault, J. Mutale, and G. Strbac, "United Kingdom Generic Distribution System (UKGDS), Typical UK Distribution Networks," DTI Centre for Distributed Generation and Sustainable Electrical Energy, Tech. Rep., July 2005.

[112] ——, "United Kingdom Generic Distribution System (UKGDS), Review of Long Term Development Statements," DTI Centre for Distributed Generation and Sustainable Electrical Energy, Tech. Rep., June 2005.

[113] "DRAKA Product Range, Cable Specifications," DRAKA UK Limited, Tech. Rep., 2010. [Online]. Available: www.drakauk.com

[114] "Cable Specifications," NKT Cables, NKT Cables Product Catalogue. [Online]. Available: www.nktcables.cz

[115] UK GDS, United Kingdom Generic Distribution System. [Online]. Available: http://www.sedg.ac.uk/

[116] "Central Networks Grid Transformer Specification (Including 66/11.5/11.5 kV three winwind transformers)," E-ON Central Networks plc, Tech. Rep., May 2008.

[117] L. Freris and A. Sasson, "Investigation of the load-flow problem," in *Proceedings of the Institution of Electrical Engineers*, vol. 115, no. 10. IET, 1968, pp. 1459–1470.

[118] U. of Washington Department of Electrical Engineering. (2010) Power systems test case archive. [Online]. Available: http://www.ee.washington.edu/research/pstca/

[119] IEEExplore Database. [Online]. Available: http://ieeexplore.ieee.org

[120] H. Saadat, Ed., *Power System Analysis*, 3rd ed. McGraw-Hill, 2010.

[121] J. J. Grainger and W. D. Stevenson, *Power system analysis*. McGraw-Hill New York, 2003, vol. 621.

[122] D. Kothari and I. Nagrath, *Modern power system analysis*. Tata McGraw-Hill Education, 2008.

[123] Siemens Energy, "Power System Simulator for Engineering," http://www.ptius.com/pti/software/psse/index.cfm, 2012.

[124] C. Cresswell, "Steady state load models for power system analysis," Ph.D. dissertation, The University of Edinburgh, 2009.

[125] P. Kundur, *Power System Stability and Control.* McGraw-Hill, 1994.

[126] Department of Energy and Climate Change. (2011) Sub-national electricity consumption data, regional and local authority electricity consumption statistics: 2005-2010. [Online]. Available: https://www.gov.uk/government/collections/sub-national-electricity-consumption-data

[127] ——. (2012) Digest of UK energy statistics (DUKES). [Online]. Available: http://www.decc.gov.uk/en/content/cms/statistics/publications/dukes/

[128] C. Pout, F. MacKenzie, and E. Olluqui, "The impact of changing energy patterns in buildings on peak electricity demand in the UK," Department of Energy and Climate Change, Tech. Rep., 2008.

[129] M. MacDonald, "Renewables Network Impact Study Annex 3: Distribution Network Topography Analysis," The Carbon Trust & DTI, Tech. Rep., November 2003.

[130] S. Drenos, "Power system operation: Demand side management (DSM) and load aggregation," Master's thesis, The University of Edinburgh, 2010.

[131] S. Ingram, S. Probert, and K. Jackson, "The impact of small scale embedded generation on the operating parameters of distribution networks," *PB Power, Department of Trade and Industry (DTI)*, 2003.

[132] P. Trichakis, P. Taylor, P. Lyons, and R. Hair, "Predicting the technical impacts of high levels of small-scale embedded generators on low-voltage networks," *IET Renewable Power Generation*, vol. 2, no. 4, pp. 249–262, 2008.

[133] J. Ribeiro and F. Lange, "A new aggregation method for determining composite load characteristics," *Power Apparatus and Systems, IEEE Transactions on*, no. 8, pp. 2869–2875, 1982.

[134] UKERC. (1997) Electricity user load profiles by profile class. Electricity Association (supplied by Elexon Ltd). [Online]. Available: http://data.ukedc.rl.ac.uk/browse/edc/Electricity/LoadProfile/doc/MetaDataLoadProfileClass.html

[135] D. McQueen, M. Mcqueen, P. Hyland, and S. Watson, "Simulation of power quality in residential electricity networks," in *Power Quality*.

[136] Department of Energy and Climate Change, "Sub-national electricity consumption statistics for 2009," DECC, Special feature, December 2010.

[137] I. Hernando-Gil, "Energy Efficiency Management and Monitoring Services for the Domestic Sector," Master's thesis, Heriot Watt University, September 2009.

[138] "Primary Network Design Manual," E-ON Central Networks plc, Tech. Rep., October 2007.

[139] H. Joshi, *Residential, Commercial and Industrial Electrical Systems: Network and installation.* Tata McGraw-Hill Education, 2008, vol. 2.

[140] E. Lakervi and E. J. Holmes, *Electricity distribution network design*, 2nd ed., ser. 21, P. P. Ltd., Ed. IEE Power Engineering, 2003.

[141] S. Papathanassiou, N. Hatziargyriou, K. Strunz *et al.*, "A benchmark low voltage microgrid network," in *Proceedings of the CIGRE Symposium: Power Systems with Dispersed Generation*, 2005, pp. 1–8.

[142] "Specification for overhead line work used during the installation of new connections," Scottish & Southern Energy Power Distribution, Tech. Rep., October 2001.

[143] "Specification for electricity service and distribution cables for use during the installation of new connections," Scottish & Southern Energy Power Distribution, Tech. Rep., July 2010.

[144] "SP Distribution plc. Technical specification for power cables up to and including 33kV and associated auxiliary cables," SP Transmission and Manweb Networks, Tech. Rep. Issue 6, February 2005.

[145] S. Y. TOLEDANO, *Técnicas y procesos en las instalaciones eléctricas en media y baja tensión.* Editorial Paraninfo, 2007 (in Spanish).

[146] "Information to assist third parties in the design and installation of secondary substations for adoption or use by SSE Power Distribution," SSE Power Distribution, Tech. Rep., November 2007.

[147] F. Garnacho Vecino, "Transformadores. Curso sobre material eléctrico de media tensión," Fundación para el fomento de la innovación industrial, Ministerio de Ciencia y Tecnología, Spain, Tech. Rep., 1999 (in Spanish).

[148] "Long term development statement," Gas Natural Fenosa Distribution plc, Spain, Tech. Rep., 2001.

[149] Mathworks. (2012) Matlab SimPowerSystems. [Online]. Available: http://www.mathworks.co.uk/products/simpower/

[150] W. H. Kersting, *Distribution system modeling and analysis.* CRC press, 2012.

[151] C. Barbier, A. Maloyd, and G. Putrus, "Embedded controller for LV networks with distributed generation," DTI, UK, Tech. Rep., May 2007.

[152] "Consideration of reference impedances and public supply network impedances for use in determining disturbance characteristics of electrical equipment having a rated current $\leq$75 A per phase," BSI, IEC Technical Report IEC/TR 60725, 2005.

[153] G. Jasmon and L. Lee, "Distribution network reduction for voltage stability analysis and loadflow calculations," *International Journal of Electrical Power & Energy Systems*, vol. 13, no. 1, pp. 9–13, 1991.

[154] A. Collin, G. Tsagarakis, A. Kiprakis, and S. McLaughlin, "Multi-scale electrical load modelling for demand-side management," in *Innovative Smart Grid Technologies (ISGT Europe), 2012 3rd IEEE PES International Conference and Exhibition on*, Oct 2012, pp. 1–8.

[155] L. Korunovic, D. Stojanovic, and J. Milanovic, "Identification of static load characteristics based on measurements in medium-voltage distribution network," *Generation, Transmission Distribution, IET*, vol. 2, no. 2, pp. 227–234, March 2008.

[156] BWEA, "Small wind systems," British Wind Energy Association, UK, Market Report, 2010.

[157] "Technology roadmap: Solar photovoltaic technology," International Energy Agency, OECD/IEA, 2010.

[158] M. Thomson and D. Infield, "Impact of widespread photovoltaics generation on distribution systems," *Renewable Power Generation, IET*, vol. 1, no. 1, pp. 33 –40, March 2007.

[159] SMA Technology, "Windy boy 2500/3000 inverter for wind energy power plants," Niestetal, Germany, 2010.

[160] *Engineering Recommendation G83/1: Recommendations for the Connection of Small-Scale Embedded Generators (Up to 16A per phase) in Parallel with Public Low-Voltage Distribution Networks*, Energy Networks Association, London, UK, September 2003.

[161] *Electricity Safety, Quality and Continuity Regulations 2002*, UK Statutory Instruments Std. 2665, January 2003.

[162] R. Billinton and P. Wang, "Reliability-network-equivalent approach to distribution-system-reliability evaluation," *Generation, Transmission and Distribution, IEE Proceedings-*, vol. 145, no. 2, pp. 149–153, Mar 1998.

[163] R. Y. Rubinstein and D. P. Kroese, *Simulation and the Monte Carlo method*. John Wiley & Sons, 2011, vol. 707.

[164] J. Ubeda and R. Allan, "Sequential simulation applied to composite system reliability evaluation," *Generation, Transmission and Distribution, IEE Proceedings C*, vol. 139, no. 2, pp. 81–86, Mar 1992.

[165] R. Billinton and P. Wang, "Teaching distribution system reliability evaluation using Monte Carlo simulation," *Power Systems, IEEE Transactions on*, vol. 14, no. 2, pp. 397–403, May 1999.

[166] M. Rios, K. Bell, D. Kirschen, and R. Allan, "Computation of the value of security," *Manchester Centre for Electrical Energy, UMIST, EPSRC/ERCOS reference nGR/K*, vol. 80310, 1999.

[167] A. Sankarakrishnan and R. Billinton, "Sequential Monte Carlo simulation for composite power system reliability analysis with time varying loads," *Power Systems, IEEE Transactions on*, vol. 10, no. 3, pp. 1540–1545, Aug 1995.

[168] M. R. Bhuiyan and R. Allan, "Modelling multistate problems in sequential simulation of power system reliability studies," *Generation, Transmission and Distribution, IEE Proceedings-*, vol. 142, no. 4, pp. 343–349, Jul 1995.

[169] Z. Bie, P. Zhang, G. Li, B. Hua, M. Meehan, and X. Wang, "Reliability evaluation of active distribution systems including microgrids," *Power Systems, IEEE Transactions on*, vol. 27, no. 4, pp. 2342–2350, Nov 2012.

[170] K. Alvehag and L. Soder, "Risk-based method for distribution system reliability investment decisions under performance-based regulation," *Generation, Transmission Distribution, IET*, vol. 5, no. 10, pp. 1062–1072, October 2011.

[171] L. Arya, S. Choube, R. Arya, and A. Tiwary, "Evaluation of reliability indices accounting omission of random repair time for distribution systems using Monte Carlo simulation," *International Journal of Electrical Power & Energy Systems*, vol. 42, no. 1, pp. 533–541, 2012.

[172] H. Zhang and P. Li, "Probabilistic analysis for optimal power flow under uncertainty," *Generation, Transmission Distribution, IET*, vol. 4, no. 5, pp. 553–561, May 2010.

[173] R. Allan and M. da Silva, "Evaluation of reliability indices and outage costs in distribution systems," *Power Systems, IEEE Transactions on*, vol. 10, no. 1, pp. 413–419, Feb 1995.

[174] E. Carpaneto and G. Chicco, "Evaluation of the probability density functions of distribution system reliability indices with a characteristic functions-based approach," *Power Systems, IEEE Transactions on*, vol. 19, no. 2, pp. 724–734, May 2004.

[175] J. Haakana, J. Lassila, T. Kaipia, and J. Partanen, "Comparison of reliability indices from the perspective of network automation devices," *Power Delivery, IEEE Transactions on*, vol. 25, no. 3, pp. 1547–1555, July 2010.

[176] L. Arya, S. Choube, and R. Arya, "Probabilistic reliability indices evaluation of electrical distribution system accounting outage due to overloading and repair time omission," *International Journal of Electrical Power & Energy Systems*, vol. 33, no. 2, pp. 296–302, 2011.

[177] R. Ashok Bakkiyaraj and N. Kumarappan, "Optimal reliability planning for a composite electric power system based on Monte Carlo simulation using particle swarm optimization," *International Journal of Electrical Power & Energy Systems*, vol. 47, pp. 109–116, 2013.

[178] L. Arya, A. Koshti, and S. Choube, "Frequency-duration analysis of composite distribution system using a non-sequential Monte Carlo simulation," *International Journal of Electrical Power & Energy Systems*, vol. 46, pp. 17–25, 2013.

[179] O. Dzobo, C. Gaunt, and R. Herman, "Investigating the use of probability distribution functions in reliability-worth analysis of electric power systems," *International Journal of Electrical Power & Energy Systems*, vol. 37, no. 1, pp. 110–116, 2012.

[180] M. Simab and M. R. Haghifam, "Quality performance based regulation through designing reward and penalty scheme for electric distribution companies," *International Journal of Electrical Power & Energy Systems*, vol. 43, no. 1, pp. 539–545, 2012.

[181] R. Billinton and R. N. Allan, *Reliability evaluation of engineering systems*. Springer, 1992.

[182] D. C. Montgomery and G. C. Runger, *Applied statistics and probability for engineers*. John Wiley & Sons, 2010.

[183] P. Wang and R. Billinton, "Reliability cost/worth assessment of distribution systems incorporating time-varying weather conditions and restoration resources," *Power Delivery, IEEE Transactions on*, vol. 17, no. 1, pp. 260–265, Jan 2002.

[184] J.-F. Moon, J.-C. Kim, H.-T. Lee, S.-S. Lee, Y.-T. Yoon, and K.-B. Song, "Time-varying failure rate extraction in electric power distribution equipment," in *Probabilistic Methods Applied to Power Systems, 2006. PMAPS 2006. International Conference on*, June 2006, pp. 1–6.

[185] A. B. Ocnasu, Y. Bésanger, J. P. Rognon, and P. Carer, "Distribution system availability assessment Monte Carlo and antithetic variates method," in *proc. 19th International Conference on Electricity Distribution, CIRED*, 2007.

[186] G. E. Noether, "Elements of nonparametric statistics," 1967.

[187] R. Allan, R. Billinton, I. Sjarief, L. Goel, and K. S. So, "A reliability test system for educational purposes-basic distribution system data and results," *Power Systems, IEEE Transactions on*, vol. 6, no. 2, pp. 813–820, May 1991.

[188] C. Grigg, P. Wong, P. Albrecht, R. Allan, M. Bhavaraju, R. Billinton, Q. Chen, C. Fong, S. Haddad, S. Kuruganty, W. Li, R. Mukerji, D. Patton, N. Rau, D. Reppen, A. Schneider, M. Shahidehpour, and C. Singh, "The IEEE reliability test system-1996. a report prepared by the reliability test system task force of the application of probability methods subcommittee," *Power Systems, IEEE Transactions on*, vol. 14, no. 3, pp. 1010–1020, Aug 1999.

[189] K. Heussen, S. Koch, A. Ulbig, and G. Andersson, "Unified system-level modeling of intermittent renewable energy sources and energy storage for power system operation," *Systems Journal, IEEE*, vol. 6, no. 1, pp. 140–151, March 2012.

[190] G. Koeppel and G. Andersson, "Reliability modeling of multi-carrier energy systems," *Energy*, vol. 34, no. 3, pp. 235–244, 2009.

[191] Z. Qin, W. Li, and X. Xiong, "Generation system reliability evaluation incorporating correlations of wind speeds with different distributions," *Power Systems, IEEE Transactions on*, vol. 28, no. 1, pp. 551–558, Feb 2013.

[192] "ABC, Copper, AAAC and ACSR Conductor Specifications," Clydesdale Ltd., Clydesdale Technical Specification.

[193] *Conductors for overhead lines - Round wire concentric lay stranded conductors*, British Standards Std. BS EN 50 182, 2001.

[194] *Current rating guide for high voltage overhead lines operating in the UK distribution system*, Electricity Association (EA) Engineering Recommendation P27, 1986.

[195] "Medium voltage 19000/33000V cable characteristics," Prysmian Cables and Systems, Utilities Cables.

[196] *LV and MV polymeric insulated cables for use by distribution and generation utilities*, British Standards Std. BS 7870.

[197] "Short-circuit ccurrent in three-phase a.c. systems - Part 2: Data of electrical equipment for short-circuit current calculations," BSI, IEC Technical Report IEC/TR 60909-2 Ed. 2.0, 2008-2011.

[198] M. Heathcote, *J & P Transformer Book*. Newnes, 2011.

[199] ORMAZABAL, "Electrical Distribution Transformers: Dielectric Liquid Immersed Transformers," Technical Specifications (Insulation level 24 & 36 kV).

Appendix A

Reliability Case Studies: DNOs/TSOs Performance Analysis

A.1 Analysis of Swedish Reliability Performance

The following tables (Table A.1, A.2, A.3 and A.4) provide a direct comparison between the actual Swedish reliability data in year 2010 (covering statistics for 114 DNOs), and the customer interruption recordings provided by 64 Swedish local DNOs. Whilst the national interruption statistics represent 93% of Sweden's 5.2 million electricity consumers, the real recordings from 64 local DNOs only cover interruption data for 920,438 customers. In addition, the voltage levels at which the data refer in each case is not exactly the same. The Swedish regulator data only cover customers at 24, 12, 10 and 0.4 kV, however actual DNOs recordings cover a wider range of voltages, from which 99.8% correspond to LV (0.4 kV) customers. The data is also divided into unplanned, planned and total long customer interruptions, with an additional table for short interruptions.

A.1.1 Aggregate Customer Impact in Year 2010

Table A.1: Unplanned long customer interruptions.

YEAR 2010	**From Files/Recordings (64 DNOs)** 920,438 Customers All Voltage Levels (99.84% at 0.4kV)					**Svensk Energi Data (114 DNOs)** [103] ˜4,836,000 Customers Only at 24kV, 12kV, 10kV and 0.4kV			
	Customer Interruptions		**SAIFI**	**SAIDI**	**CAIDI**	**Customer Interrupt.**	**SAIFI**	**SAIDI**	**CAIDI**
	No.	Duration (min)	(Int./ cust.)	(mins /cust.)	(mins /int.)	No.	(Int./ cust.)	(mins /cust.)	(mins /int.)
< 12 h	1,043,068	49,979,445	1.13	54.3	47.92	-	-	-	-
> 12 h	1,497	2,052,890	0.002	2.23	1371.34	-	-	-	-
Inside Network	786,390	37,073,076	0.85	40.28	47.14	5,303,936	1.10	76.78	69.55
Outside Network	258,175	14,959,259	0.28	16.25	57.94	-	-	-	-
TOTAL	**1,044,565**	**52,032,335**	**1.13**	**56.53**	**49.81**	**6,798,848**	**1.42**	**86.81**	**61.35**

Table A.2: Planned long customer interruptions.

YEAR 2010	From Files/Recordings (64 DNOs) 920,438 Customers All Voltage Levels (99.84% at 0.4kV)					Svensk Energi Data (114 DNOs) [103] ˜4,836,000 Customers Only at 24kV, 12kV, 10kV and 0.4kV			
	Customer Interruptions		SAIFI	SAIDI	CAIDI	Customer Interrupt.	SAIFI	SAIDI	CAIDI
	No.	Duration (min)	(Int./ cust.)	(mins /cust.)	(mins /int.)	No.	(Int./ cust.)	(mins /cust.)	(mins /int.)
Inside Network	88,635	9,981,854	0.096	10.84	112.62	677,565	0.14	16.26	115.30
Outside Network	2,280	76,955	0.002	0.08	33.75	-	-	-	-
TOTAL	**90,915**	**10,058,809**	**0.098**	**10.92**	**110.64**	**750,671**	**0.16**	**17.15**	**109.76**

Table A.3: Total (planned + unplanned) long customer interruptions.

YEAR 2010	From Files/Recordings (64 DNOs) 920,438 Customers All Voltage Levels (99.84% at 0.4kV)					Svensk Energi Data (114 DNOs) [103] ˜4,836,000 Customers Only at 24kV, 12kV, 10kV and 0.4kV			
	Customer Interruptions		SAIFI	SAIDI	CAIDI	Customer Interrupt.	SAIFI	SAIDI	CAIDI
	No.	Duration (min)	(Int./ cust.)	(mins /cust.)	(mins /int.)	No.	(Int./ cust.)	(mins /cust.)	(mins /int.)
Inside Network	875,025	47,054,930	0.95	51.12	53.78	5,981,501	1.24	93.04	74.73
Outside Network	260,455	15,036,214	0.28	16.34	57.73	-	-	-	-
TOTAL	**1,135,480**	**62,091,144**	**1.23**	**67.46**	**54.68**	**7,549,519**	**1.57**	**103.96**	**66.16**

Table A.4: Short customer interruptions.

From Files/Recordings (64 DNOs) 920,438 Customers All Voltage Levels (99.84% at 0.4kV)		
YEAR 2010	Customer Interruptions	MAIFI
	No.	(Interrupt./customer)
Inside Network	417,712	0.45
Outside Network	88,740	0.10
TOTAL	**506,452**	**0.55**

A.1.2 Classification of SAIFI and CAIDI Indices by Type of Customer Interruptions (Year 2010)

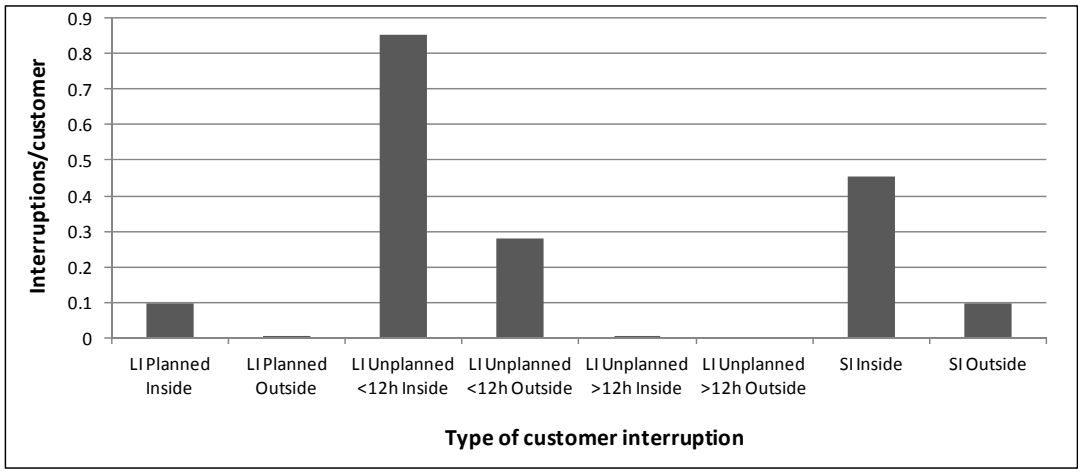

(a) Frequency of customer interruptions (SAIFI) – Year 2010

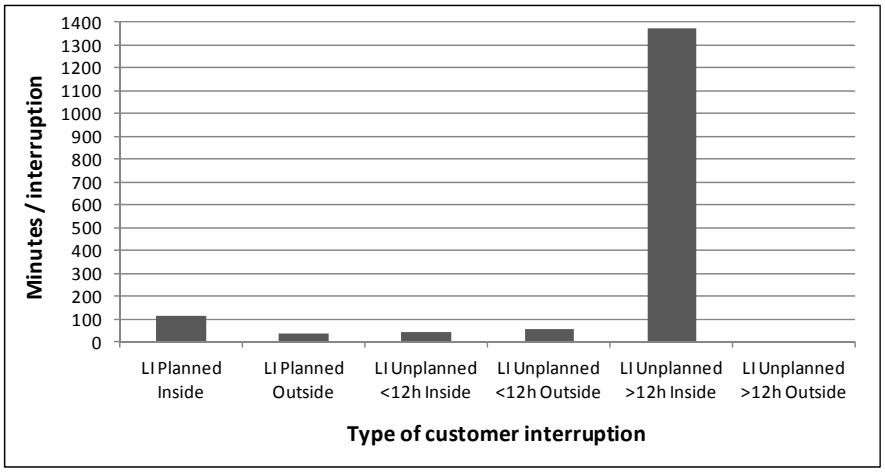

(b) Average duration of customer interruptions (CAIDI) – Year 2010

Figure A.1: Frequency and average outage duration by type of customer interruptions.

A.1.3 Classification of Customer Interruptions by Voltage Level (Year 2010)

Shown overleaf.

Table A.5: Type of customer interruptions by voltage level.

YEAR 2010			CUSTOMER LONG INTERRUPTIONS												CUSTOMER SHORT INTERRUPTIONS	
V (kV)	Customers		Planned				Unplanned < 12 h				Unplanned > 12 h					
	No.	% of Total	Inside		Outside		Inside		Outside		Inside		Outside		Inside	Outside
			No.	Dur.	No.	Dur.	No.	Dur.	No.	Dur.	No.	Dur.	No.	Dur.	No.	No.
138	1	0.000	0	0	0	0	0	0	1	70	0	0	0	0	0	0
130	5	0.001	0	0	0	0	0	0	1	70	0	0	0	0	0	0
72	2	0.000	0	0	0	0	0	0	4	220	0	0	0	0	0	0
50	1	0.000	0	0	0	0	0	0	0	0	0	0	0	0	0	0
40	2	0.000	0	0	0	0	0	0	0	0	0	0	0	0	0	0
24	102	0.011	6	536	0	0	62	1402	6	249	0	0	0	0	114	15
23	1	0.000	0	0	0	0	2	45	1	6	0	0	0	0	0	0
22	33	0.004	0	0	0	0	4	384	0	0	0	0	0	0	0	0
20	96	0.010	5	1067	0	0	27	1367	37	677	0	0	0	0	2	0
12	169	0.018	10	2108	0	0	103	2639	29	700	0	0	0	0	171	10
11	298	0.032	77	7380	0	0	514	27537	346	37996	21	20770	0	0	1	12
10	742	0.081	19	2466	0	0	181	8380	121	2998	3	4360	0	0	70	34
7	7	0.001	0	0	0	0	0	0	0	0	0	0	0	0	0	0
6	36	0.004	0	0	0	0	12	264	1	70	0	0	0	0	1	0
0.4	918943	**99.84**	88518	9968297	2280	76955	783988	34978168	257630	14916343	1473	2027760	0	0	417353	88669
TOTAL	**920438**		**88635**	**9981854**	**2280**	**76955**	**784893**	**35020186**	**258175**	**14959259**	**1497**	**2052890**	**0**	**0**	**417712**	**88740**

*Note: 99.84% of customers are supplied at LV (0.4 kV)

Further clarification is needed in order to identify the relationship between customer interruptions taking place inside and outside the own network. In addition, since most of customer interruptions occur at LV, they should be a consequence of a fault occurring at a higher voltage level. For example, in Table A.5, all the planned customer interruptions with an origin outside the own network affect customers at 0.4 kV and no further information is provided. These could be a result of an interruption event happening at MV level outside the network or even due to DSM actions resulting in the disconnection of a high number of LV customers.

Table A.6: Reliability indicators per voltage level.

V (kV)	Customers	SAIFI	SAIDI (min)	CAIDI (min)	MAIFI
	No.	Planned + Unplanned (In & Out)			
138	1	1.086E-06	7.605E-05	70	0
130	5	0	0	0	0
72	2	4.346E-06	0.00024	55	0
50	1	0	0	0	0
40	2	0	0	0	0
24	102	8.04E-05	0.00238	29.55	0.00014015
23	1	3.259E-06	5.541E-05	17	0
22	33	4.346E-06	0.00042	96	0
20	96	7.496E-05	0.00338	45.09	2.1729E-06
12	169	0.0002	0.00592	38.36	0.00020
11	298	0.0010	0.10178	97.79	1.4124E-05
10	742	0.0004	0.01978	56.19	0.00011
7	7	0	0	0	0
6	36	1.304E-05	0.00029	22	1.0864E-06
0.4	918943	1.232	67.324	54.65	0.5498
TOTAL	**920438**	**1.234**	**67.46**	**54.68**	**0.55**

*Note: LV (0.4 kV) indicators strongly affect total values

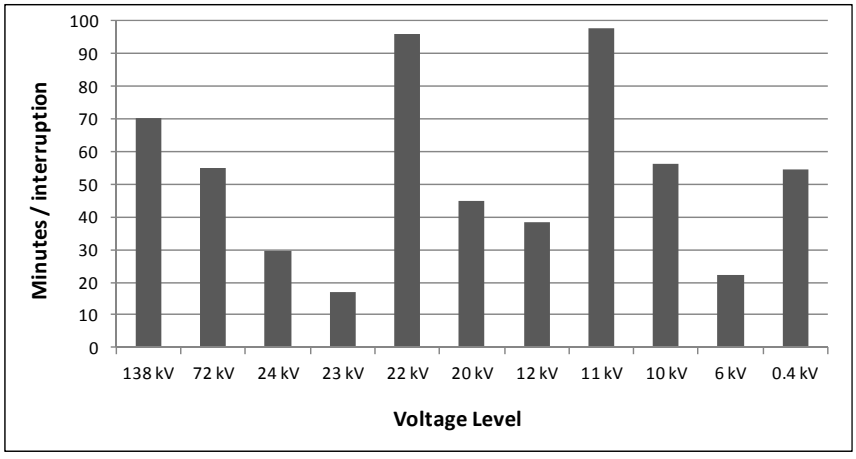

Figure A.2: Average duration of customer interruptions (CAIDI) per voltage.

A.1.4 Comparison of 64 Swedish DNOs' Data (Years 2008 vs. 2010)

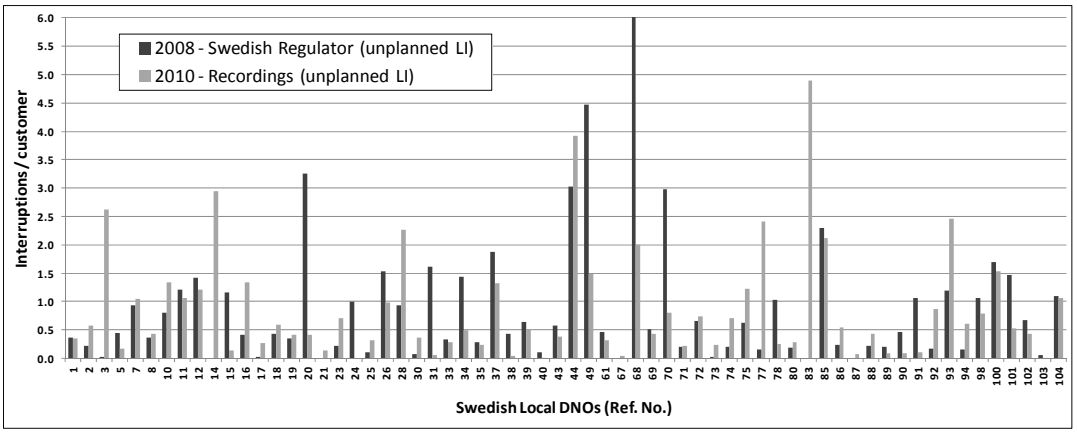

(a) Frequency of customer interruptions (SAIFI) per DNO (Years 2008–2010)

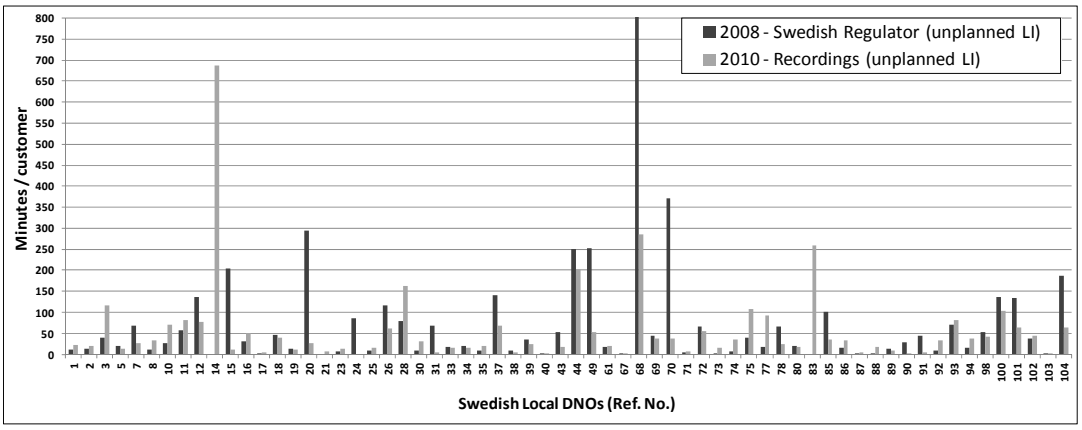

(b) Duration of interruption per customer (SAIDI) for each DNO (Years 2008–2010)

Figure A.3: SAIFI and SAIDI indices - Unplanned long customer interruptions inside own network [105].

A.2 SPEN - Distribution Reliability Performance 2009/10

A.2.1 Analysis of Pre-arranged Network Interruptions

This section provides additional information and results, considering the probabilistic assessment of the frequency and duration of customer interruptions, on the planned (i.e. pre-arranged) LIs in the Scottish (SPEN) distribution networks:

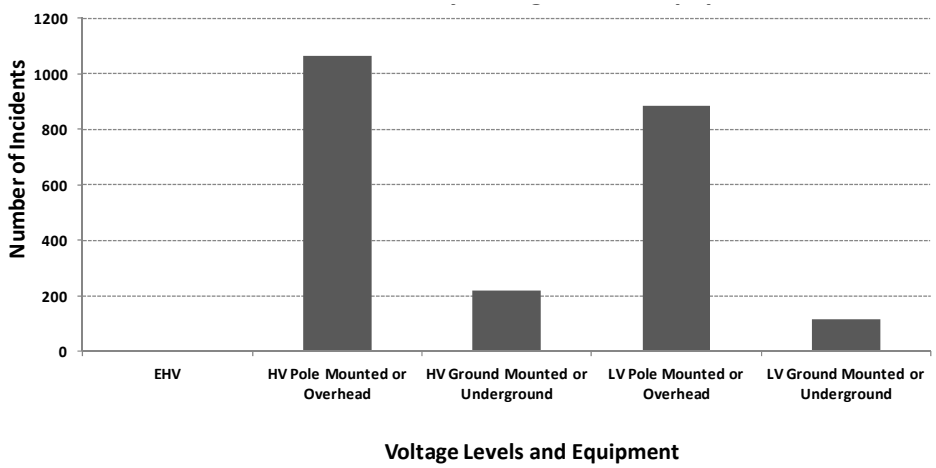

Figure A.4: SPEN - Number of planned LIs by voltage level and equipment (09/10).

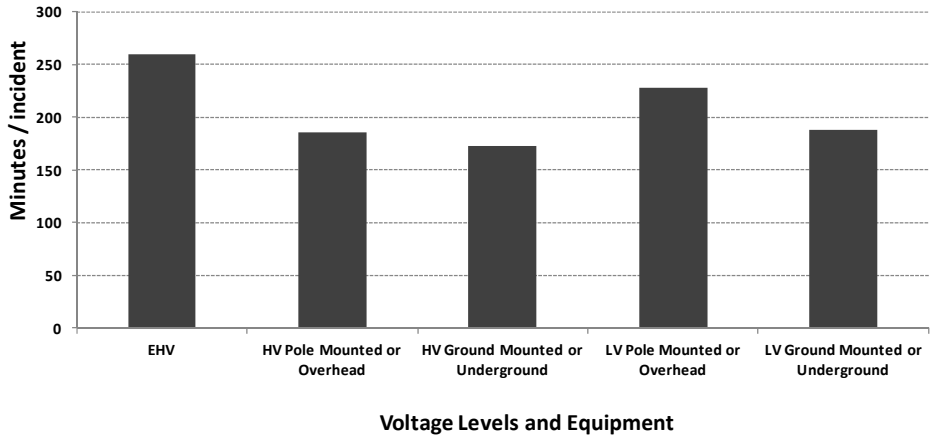

Figure A.5: SPEN - Average duration of planned LIs (09/10).

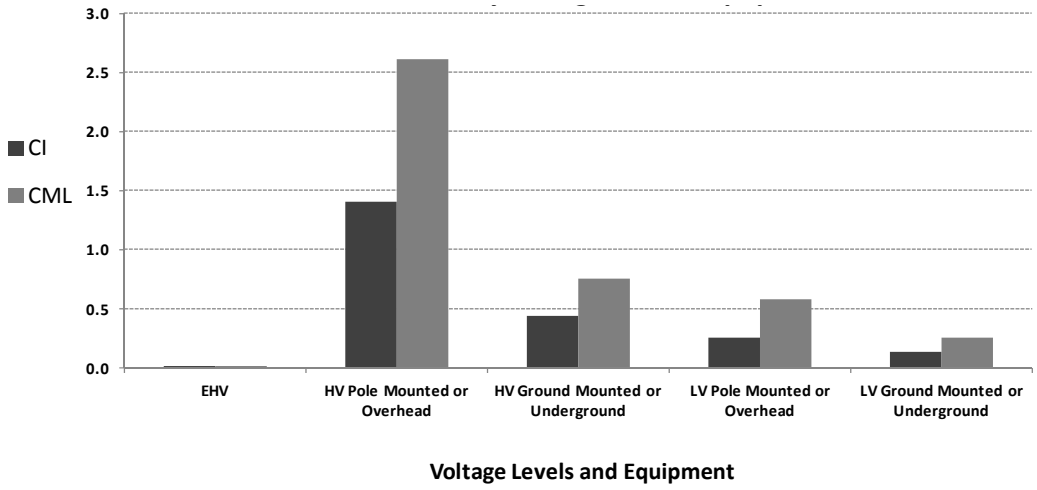

Figure A.6: SPEN - Planned CI and CML by voltage level and equipment (09/10).

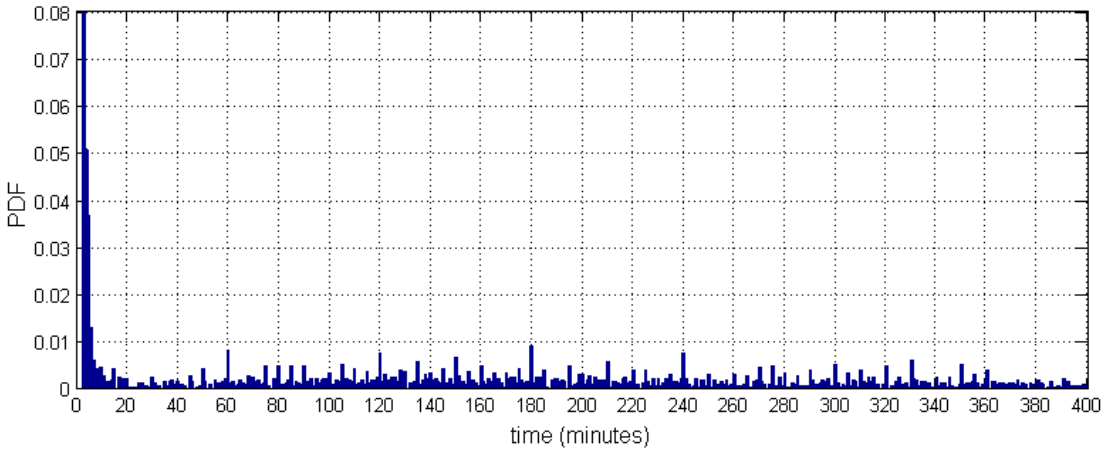

Figure A.7: SPEN - Probability of duration of planned LIs (09/10).

A.3 NG - Fault Probability Analysis (6-10 years data)

Considering past statistics of the UK transmission network (National Grid data), this section provides additional information and results on the probabilistic analysis of the transient, sustained, and planned circuit outages over a 10-year period between 2002 and 2011.

A.3.1 NG - Transient/Sustained Transformer Trips

Figure A.8 provides a general classification of different transmission transformers according to the number of outages experienced during the time of the sampled data (6 years in this case, 2006-2011) and the corresponding outage duration range in which each category falls. Therefore, these results provide a correlation between sub-categories (i.e. voltage levels and number/duration of outages) in order to assess the operation availability for each type of transformer.

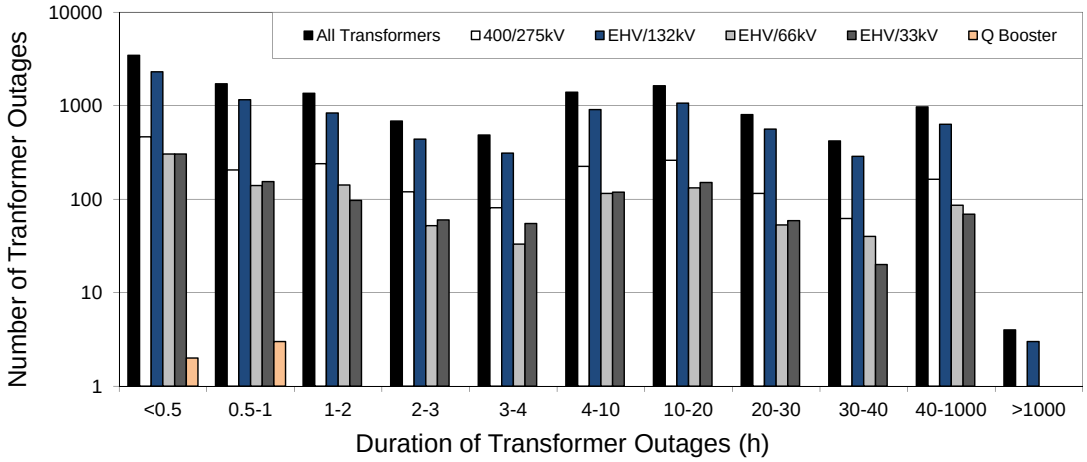

Figure A.8: NG - Number and duration of outages for different transformer types.

A.3.2 NG - Planned Circuit Outages

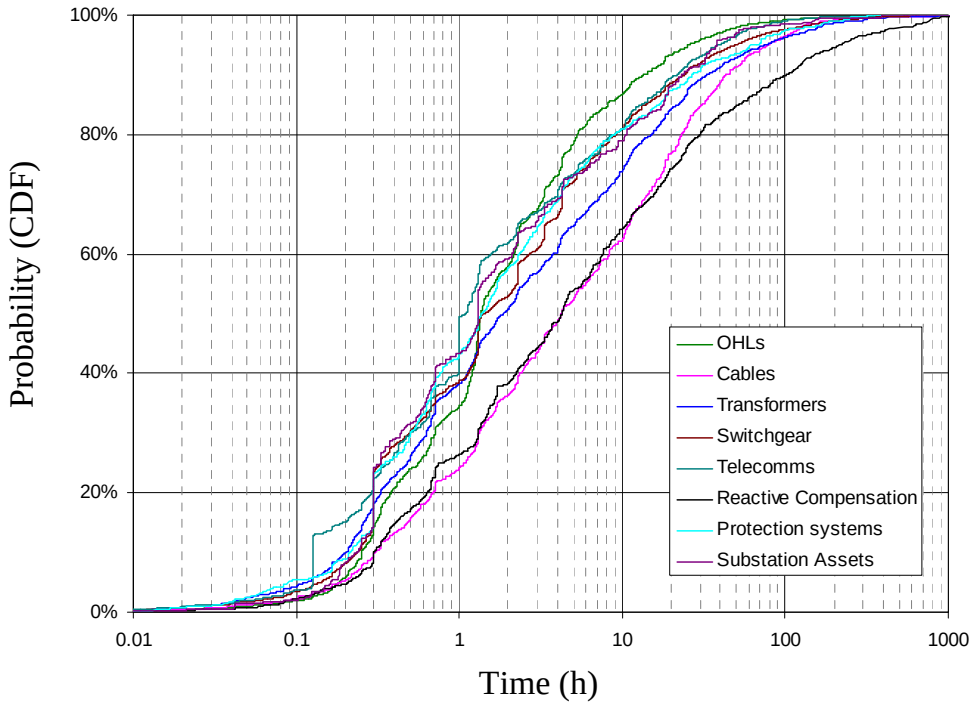

Figure A.9: NG - Cumulative distribution of the duration of planned outages.

A.3.3 NG - Overall Component Fault Statistics

Shown overleaf.

Table A.7: NG - Overall component fault statistics (6-10 years) [38].

	OHL	Cable	Transf.	Switchg.	Protect.	Reactive Comp.	Substation Assets	Telecoms	OHL in lightning storm	Double Circuits	Double Circuits in lightning storm
Number of Assets	13,767 km	589 km	721	1,585	972 ends	187	N/A	N/A	13,767 km	6,276 km	6,276 km
- TRANSIENT:											
No. of transient trips (in 6 years)	128	10	21	22	64	6	N/A	N/A	122	2	4
Occurrences per asset per year	0.002/km	0.003/km	0.005	0.002	0.011	0.005	N/A	N/A	0.0015/km	0.00005/km	0.00011/km
- SUSTAINED:											
No. of sustained trips (in 6 years)	43	19	80	122	132	378	N/A	N/A	23	2	0
Occurrences per asset per year	0.001/km	0.005/km	0.018	0.013	0.023	0.337	N/A	N/A	0.0003/km	0.00005/km	0.000/km
Mean duration (days)	0.41	15.35	9.33	3.31	7.62	28.81	N/A	N/A	1.00	0.13	0.00
- PLANNED:											
Number of planned outages (10 years)	1095	904	1941	4704	629	889	312	100	N/A	N/A	N/A
Occurrences per asset per year	0.008/km	0.153/km	0.269	0.297	0.065	0.475	-	-	N/A	N/A	N/A
Mean duration (days)	9.40	20.84	17.77	12.03	12.39	43.63	9.95	8.52	N/A	N/A	N/A

Appendix B

Power Component Database Sample

B.1 Sample Database: Circuits

This section of the database provides an extended set of data regarding the typical cables and overhead lines (OHLs) commonly used at different voltage levels in UK distribution networks. This information has been extracted after reviewing manufacturer's data, British standards, Engineering Recommendations and DNOs documentation. However, the application and length of cables or OHLs will depend on the type of network configuration (meshed, radial or mixed), as issues such as load density and voltage regulation must be carefully considered.

B.1.1 Overhead Lines

Technical specifications and sections of aerial conductors are provided, including typical OHLs for distribution network upgrading [73, 107], bare, insulated and covered overhead conductors from manufacturers [113, 192], and typical OHLs specified by Standards [193, 194]. The different types of aerial conductors included in the database are:

- Aluminium / Aluminium Alloy Conductor (AAC / AAAC)
- Aluminium / Aluminium Alloy Conductor Steel Reinforced (ACSR / AACSR)
- Aerial Bundled Conductor (ABC)
- Hard Drawn Copper / Aluminium (HDC / HDA)

In addition, Table B.1 shows a part of the extended database created from information provided by UK DNOs [73, 74, 90, 91, 106, 107, 108, 109], providing detailed data (at different voltage levels) of typical circuit lengths, electrical specifications, power ratings, etc.

Table B.1: MV Overhead lines data (11, 33 & 132 kV).

Operating Voltage (kV)	Circuit Length (km)	Ratings(Amps)			Positive seq. Z/km		Zero-phase seq. Z/km		B/km
		Winter	Spring/ Autumn	Summer	R/km	X/km	R/km	X/km	
					(p.u. on 100 MVA base)				
11	1.9	290	281	265	0.22469	0.25247	0.54166	1.24999	2.10044E-05
	2.9	395	383	335	0.14412	0.18579	0.56173	0.91317	6.93165E-05
33	5.4	466	419	350	0.01676	0.03279	0.03037	0.15557	3.58475E-05
	4.7	457	419	350	0.01662	0.03240	0.03062	0.15305	5.69475E-05
132	8.8	660	585	585	0.00038	0.00183	0.00150	0.00448	0.006700997
	9.2	817	700	659	0.00067	0.00324	0.00191	0.00834	0.002720833

B.1.2 Cables

Typical configurations, sections, lengths, electrical and constructional data of MV Cables have been collected to create this part of the component database. In this case, the specifications of 11 kV, 33 kV and 132 kV cables for electricity distribution and network upgrading have been extracted from different cable manufacturers [114, 195], DNOs documentation [143, 144] and British Standards [196, 197].

As a rough summary, the most typical cables used for power distribution in the UK (always depending on the cross-section/rating, voltage and installation) are Single Core, XLPE-Cu, XLPE-Al, Triplexed EPR-Al, and PICAS. Extended information, such as the standard and preferred sizes for each voltage level, can be accessed through the database created during this research project. Also, a summary is provided in Table B.2, giving useful information for modelling this type of MV distribution cables.

Table B.2: MV Distribution cable data (11, 33 & 132 kV).

Operating Voltage (kV)	Circuit Length (km)	Ratings(Amps)			Positive seq. Z/km		Zero-phase seq. Z/km		B/km
		Winter	Spring/ Autumn	Summer	R/km	X/km	R/km	X/km	
					(p.u. on 100 MVA base)				
11	0.83	355	344	337	0.14403	0.06662	1.00824	0.23318	0.00017803
	1	415	403	394	0.12271	0.06575	0.85896	0.23011	0.00023954
33	3.5	474	474	420	0.00810	0.01042	0.09299	0.00606	0.00128542
	2.8	457	457	405	0.00836	0.01048	0.08647	0.00599	0.00128452
132	6.31	328	328	328	0.00057	0.00062	0.00389	0.00132	0.01608511
	5.56	315	289	263	0.00050	0.00060	0.00392	0.00127	0.01719888

B.2 Sample Database: Reactive Compensation & FACTS Devices

These devices increase the reliability of ac grids, reduce power delivery costs, and improve the quality and efficiency of the power transmission by supplying inductive or reactive power to the grid. In this case, information is provided about:

- Typical static VAr compensators (SVC) parameters and ratings (40 < MVAr < 800) used at transmission level [74];
- Power capacitors (variable/fixed banks) characteristics for distribution networks, provided by manufacturers (e.g. Nokian Capacitors, ABB, Schneider Electric MV, etc.);
- Shunt reactors technical features provided by manufacturers (e.g. ABB). Typically, unit ratings vary up to 250 MVAr (three-phase) and 130 MVAr (single-phase).

Table B.3 provides a summary of typical reactive compensation equipment operated in the UK by transmission and distribution network operators.

Table B.3: Sample of typical reactive compensation equipment [74].

DNOs & TSO	MVAr Generation	MVAr Absorption	Compensation Type	Connection Voltage (kV)
SHETL	-	42	Shunt Reactor	132
	-	60	Shunt Reactor	
	-	30	Shunt Reactor	
	225	75	SVC	275
	45	-	Mechanically Switched Capacitor	132
SPT	-	150	Reactor	400
	-	60	Reactor	33
NGET	-	60	Reactor	
	60	-	Mechanically Switched Capacitor	66
	60	-	Mechanically Switched Capacitor	132
	55	-	Mechanically Switched Capacitor	
	45	-	Mechanically Switched Capacitor	
	20	-	Mechanically Switched Capacitor	
	-	60	Reactor	
	-	15	Reactor	

B.3 Sample Database: Protections

The information collected in this section covers specifications of switchgear and protections typically used to protect components of the UK power distribution networks. The database includes:

- Typical switchgear for distribution network upgrading [73, 107] (circuit breakers, ring main units, pole mounted auto-reclosers, air break switch disconnectors, sectionalisers, auto sectionalising links and expulsion fuses);
- Fault levels at 11, 25, 33 and 132 kV [74];
- Indicative ratings of circuit breakers at 33, 66 and 132 kV, provided by National Grid Electricity Transmission (NGET) [74];
- Protection system characteristics of transformers and feeders (OHLs and underground cables) at 11, 33, 66 and 132 kV.

Table B.4: UK network fault clearance times.

Index	Voltage level (kV)	Fault clearance time (ms)
1	400	80
2	275	100
3	$\leq$132	120

Table B.5: Back-up protection fault clearance times.

Main protection provided	Clear fault side	Voltage level (kV)	Back-up protection provider	Back-up fault clearance time (ms)	Operation conditions	Fault location
one	HV	400	Gen. units	300	normal	HV
		275				
		$\leq$132				
two	HV	400	Gen. units and NGET	800 ms (for England, Wales and offshore)	normal	HV
		275		300 ms (for Scotland)		
one or two	HV	$\leq$132	Gen. units and NGET	800 ms (for England, Wales and offshore)	normal	HV
				300 ms (for Scotland)		

B.4 MV Distribution Transformers: Specifications Summary

Nominal Voltage (kV)	66/11.5/11.5	132/33	132/33	132/33	132/11	132/11	132/11/11	132/11/11	132/66	132/66
Nominal Rating (MVA)	30/60	22.5/45	45/90	30/60	15/30	15/30	30/60	30/60	30/60	45/90
Vector Group	Yyn0yn0	YNd1/ YNd11	YNd1/ YNd11	YNd1/ YNd11	YNd1/ YNd11	YNyn0	YNd1d1/ YNd11d11	YNyn0yn0	YNd1/ YNd11	YNd1/ YNd11
Short Circuit (MVA) Primary Secondary	3500 350	5000 1500	5000 1500	5000 1500	5000 350	5000 350	5000 350	5000 350	5000 2500	5000 2500
BIL kV Primary Secondary	325 95	550 170	550 170	550 170	550 95	550 95	550 95	550 95	550 325	550 325
Nominal Impedance on CMR Base	33% HV/LV1+LV2 on 60 MVA 20% HV/LV on 30 MVA HV 13% on 30 MVA LV each 7% on 30 MVA [Alternative 24% on 30MVA 40% on 60MVA]	10% on 45MVA	20% HV/LV on 90 MVA [Alternative 13.5%]	14% on 60MVA	28% HV/LV on 30 MVA	28% HV/LV on 30MVA	40% HV/LV1+LV2 on 60 MVA 24% HV/LV on 30 MVA HV 16% on 30 MVA LV each 8% on 30 MVA	40% HV/LV1+LV2 on 60 MVA 24% HV/LV on 30 MVA HV 16% on 30 MVA LV each 8% on 30 MVA	12% HV/LV on 60 MVA	18% HV/LV on 90MVA
Primary Terminals	Bushings	Bushings	Bushings	Bushings	Bushings	Bushings	Bushings	Bushings	Bushings	Bushings
Primary Neutral	Not Brought Out	Bushing for Solid Earth	Bushing for Solid Earth	Bushing for Solid Earth	Bushing for Solid Earth	Bushing for Solid Earth	Bushing for Solid Earth	Bushing for Solid Earth	Bushing for Solid Earth	Bushing for Solid Earth
Secondary Terminals	Cable box with 6 sockets for each secy winding	Cable box or boxes	Cable box or boxes	Cable box or boxes	Cable box with 6 sockets	Cable box with 6 sockets	Cable box or boxes with 6 sockets for each secy winding	Cable box or boxes with 6 sockets for each secy winding	Bushing	Bushing
Secondary Neutral	Connector Socket for cable to NER	Provided by Earthing Tx	Provided by Earthing Tx	Provided by Earthing Tx	Provided by Earthing Tx	Connector Socket for cable to NER	Provided by Earthing Transformer	Connector Socket for cable to NER	Provided by Earthing Tx	Provided by Earthing Tx
Transformer main protection	800/1 Class PxB	400/1 Class PxB	500/1 Class PxB	400/1 Class PxB	200/1 Class PxB	200/1 Class PxB	400/1 Class PxB	400/1 Class PxB	400/1 Class PxB	500/1 Class PxB
Transformer backup protection	800/1 Class 5P20	400/1 Class 5P20	500/1 Class 5P20	400/1 Class 5P20	200/1 Class 5P20	200/1 Class 5P20	400/1 Class 5P20	400/1 Class 5P20	400/1 Class 5P20	500/1 Class 5P20
Feeder Back Up Protection	1200/600/1 5P20	1200/600/1 5P20	1200/600/1 5P20	1200/600/1 5P20	1200/600/1 5P20	1200/600/1 5P20	1200/600/1 5P20	1200/600/1 5P20	1200/600/1 5P20	1200/600/1 5P20
Feeder/Busbar Main Protection	1200/600/1 Class PxA	1200/600/1 Class PxA	1200/600/1 Class PxA	1200/600/1 Class PxA	1200/600/1 Class PxA	1200/600/1 Class PxA	1200/600/1 Class PxA	1200/600/1 Class PxA	1200/600/1 Class PxA	1200/600/1 Class PxA
HV Winding Temperature "L2" phase only	656/5 Class 3	246/5 Class 3	492/5 Class 3	328/5 Class 3	164/5 Class 3	164/5 Class 3	328/5 Class 3	328/5 Class 3	328/5 Class 3	492/5 Class 3
HV Neutral CTs REF	Not Brought Out	400/1 Class PxB	500/1 Class PxB	400/1 Class PxB	200/1 Class PxB	200/1 Class PxB	400/1 Class PxB	400/1 Class PxB	400/1 Class PxB	500/1 Class PxB
LV Winding Temperature "L2" phase only	1506/5 Class3	787/5 Class3	1575/5 Class3	1050/5 Class3	1575/5 Class3	1575/5 Class3	1575/5 Class3	1575/5 Class3	525/5 Class3	787/5 Class3
LV Neutral CTs REF	2000/1 Class PxB	2000/1 Class PxB	2000/1 Class PxB	2000/1 Class PxB	2000/1 Class PxB	2000/1 Class PxB	2000/1 Class PxB	2000/1 Class PxB	800/1 Class PxB	800/1 Class PxB
STBY E/F	2000/1 Class 5P10	2000/1 Class 5P10	2000/1 Class 5P10	2000/1 Class 5P10	2000/1 Class 5P10	2000/1 Class 5P10	2000/1 Class 5P10	2000/1 Class 5P10	800/1 Class 5P10	800/1 Class 5P10
Max Noise dB(A)	65	65	65	65	65	65	65	65	65	65
Max Iron Loss KW Max Cu loss KW at CMR	20 400	15 250	30 300	20 280	10 200	10 200	20 380	20 380	20 220	30 250

Figure B.1: Specifications summary of MV power distribution transformers [116].

Appendix C

Report on Typical UK Transformer Ratings

The report presented overleaf provides a comprehensive study and analysis of the most typical characteristics and parameters of power distribution transformers operated by Scottish and Southern Energy (SSE) [90] in the south of England (by Southern Electric Power) and in the north of Scotland (by Scottish Hydro Electric Power Distribution) in year 2010.

The aim of the report is to identify the typical transformer ratings for all the UK networks, and for each power rating, the different parameters, voltage ratio, vector group, impedance, etc. This information is considered essential for the modelling effort of the typical/generic UK power distribution networks presented and analysed in this thesis.

TYPICAL TRANSFORMER RATINGS

POWER DISTRIBUTION NETWORK

South-Central England

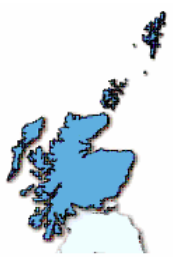

North Scotland

SCOTTISH & SOUTHERN ENERGY - 2010

(Southern Electric Power & Scottish Hydro Electric Power Distribution)

Report by:

Ignacio Hernando Gil

CONTENTS

1. S&S Energy TRANSFORMER CHARACTERISTICS (General).....2
1.1 SHE North Scotland Transformer Characteristics.....2
1.2 SE South-Central England Transformer Characteristics.....3
2. Typical Transformer Ratings.....4
3. Detailed Transformer Characteristics (S&S Energy Network).....5
132/33 kV Transformers
132/22 kV Transformers
132/11 kV Transformers.....5

66/33 kV Transformers
66/25 kV Transformers
66/22 kV Transformers
66/11 kV Transformers.....6

33/33 kV Transformers (Voltage Regulators).....7

33/11 kV Transformers (SHE North-Scotland).....8
33/11 kV Transformers (SE South-Central England).....9

Most Typical Coincident 33/11 kV Transformers
Most Typical Characteristics of Coincident 33/11 kV Transformers.....10

33/7 kV Transformers
33/6.6 kV Transformers
33/3 kV Transformers
22/11 kV Transformers.....11

22/6.6 kV Transformers
11/11 kV Transformers (Voltage Regulators).....12

1. S&S Energy TRANSFORMER CHARACTERISTICS (General)

1.1 SHE North Scotland Transformer Characteristics

- **33kV System:**

- **Voltage Regulators**

Vector Group	Auto transformer
Voltage Ratio	33/33 kV
Rating	Between 5 MVA and 32 MVA
Tapping Range	-18% to + 4%

- **Primary Transformers**

° **Voltage Ratio**	**33/11 kV**
Vector Group	YY0
Rating	1 MVA, 2.5 MVA, 4/8 MVA, 6 MVA, 7.5/15MVA, 10 MVA, 12/24 MVA, 15/30 MVA, 20/40 MVA
Tapping Range	-18% to +4% (on load)
Rating	0.1 MVA, 0.15 MVA, 0.2 MVA, 0.3 MVA, 0.5 MVA
Tapping Range	-5% to +5% (off-load)

° **Voltage Ratio**	**33 kV/LV (433V, 480V or 250V)**
Rating	300 kVA and less
Tapping Range	-5% to +5% (off load)

- **11kV System:**

- **Voltage Regulators**

Vector Group	Auto transformer
Voltage Ratio	11/11 kV
Rating	Between 1 MVA and 8 MVA
Tapping Range	-18% to + 4%

- **Transformers**

Vector Group	DY11
Voltage Ratio	11 kV/LV (433 V, 500 V or 250 V)
Rating	1000, 500, 315, 200 kVA and less
Tapping Range	-5% to 5% (off load)

1.2 SE South-Central England Transformer Characteristics

- **132 and 66 kV System:**

- **Bulk Supply Point Transformers**

° **Voltage Ratio**	**132/33 kV**
Vector Group	YD1, YD11
Rating	90, 60, 45, 30 MVA
Tapping Range	-10% to +20% and -10% to +10% (on load)
° **Voltage Ratio**	**132/22 kV**
Vector Group	YD1
Rating	60, 45 MVA
Tapping Range	-10% to +20% and -10% to +10% (on load)
° **Voltage Ratio**	**132/11 kV**
Vector Group	YD1, YD11
Rating	45, 30, 20, 15 MVA
Tapping Range	-10% to +20% and -10% to +10% (on load)
° **Voltage Ratio**	**66/22 and 66/11 kV**
Vector Group	DY1, YY6
Rating	60, 40, 30, 20 MVA
Tapping Range	-10% to +20% and -5% to +15% (on load)

- **33 and 22 kV System:**

- **Primary Transformers**

° **Voltage Ratio**	**33/11 and 33/6.6 kV**
Vector Group	DY1, YY0, DY11
Rating	3, 5, 7.5, 7.5/15, 10, 15, 12/24,15/30, 20/40 MVA
Tapping Range	-5% to +15%, -10% to +10% (on load)
° **Voltage Ratio**	**22/11 and 22/6.6 kV**
Vector Group	DY1
Rating	5, 10, 12.5, 14 MVA
Tapping Range	-5% to +15%, -10% to +10% (on load)
° **Voltage Ratio**	**33 kV/LV (433V)**
Rating	300 kVA and less
Tapping Range	-5% to +5% (off load)

- **HV System:**

- **Distribution Transformers**

Vector Group	DY11
Voltage Ratio	11 or 6.6 kV/LV (433 V, 500 V or 250 V)
Rating	1000, 500, 315, 200 kVA and less
Tapping Range	-5% to +5% (off load)

2. Typical Transformer Ratings

Power Distribution Transformers used by SHE in Scotland	
Voltage Ratio (kV)	**Volume (%)**
132/33	0.34
33/33	1.87
33/11	96.39
11/11	1.02
33/7	0.17
33/3	0.17

$\sum (\%) = 100\%$

Power Distribution Transformers used by SE in South-England	
Voltage Ratio (kV)	**Volume (%)**
132/33	21.43
132/22	0.86
132/11	4.26
66/33	0.12
66/25	0.12
66/22	0.25
66/11	2.72
33/11	65.47
33/6.6	1.11
22/11	1.48
22/6.6	2.16

$\sum (\%) = 100\%$

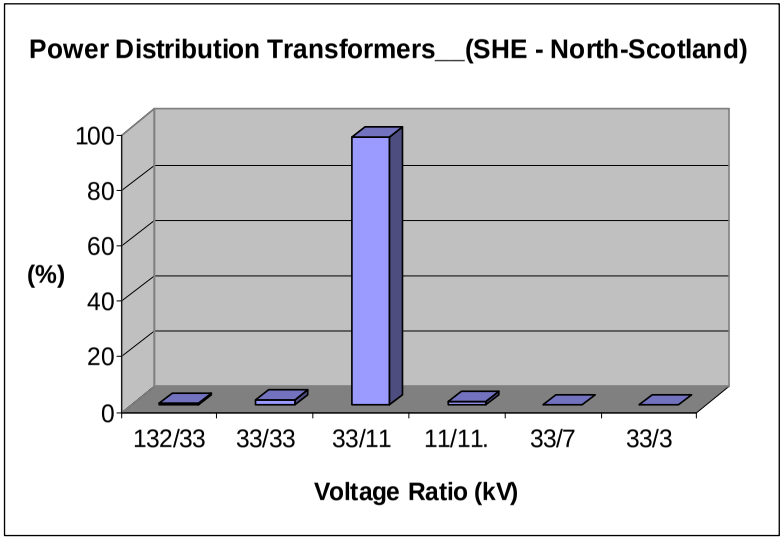

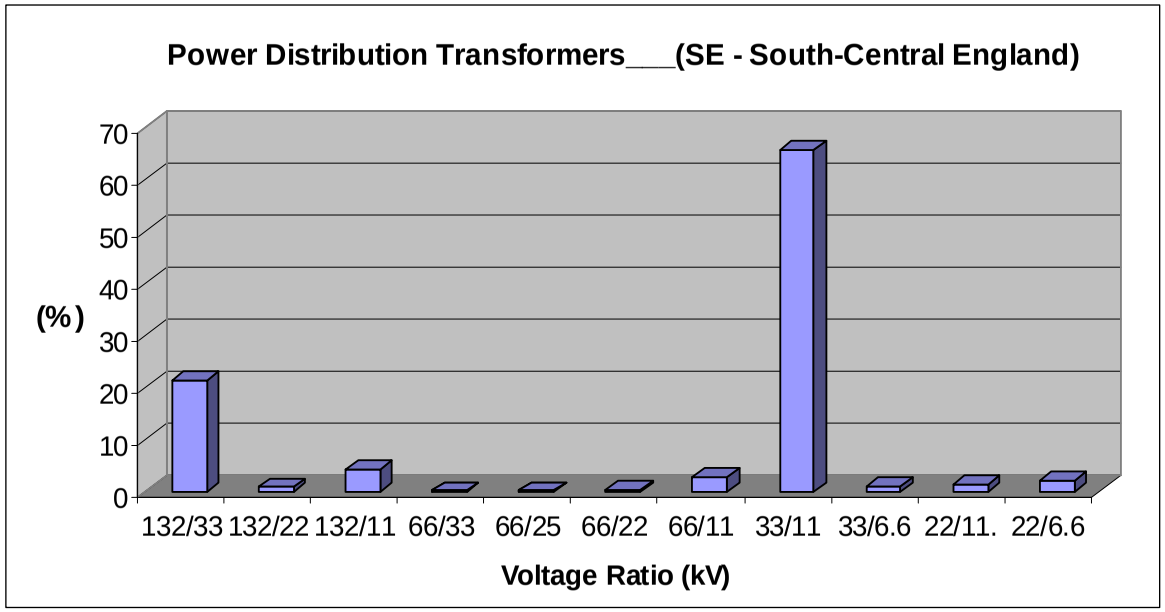

3. Detailed Transformer Characteristics (S&S Energy Network)

Note: * p.u. on 100 MVA.

132/33 kV Transformers

SHE - North-Scotland								
Nameplate Rating *S* (MVA)	Volume (%)	Vector Group	Resistance *R* (p.u.)*	Reactance *X* (p.u.)*	R/X (p.u.)*	Tap Range		Method of Earthing
						Min	Max	
30	100	Yy0	0.0233	0.299	0.0779	0.8	1.1	Resistance

SE - South-Central England									
Nameplate Rating *S* (MVA)	Volume (%)	Vector Group	Resistance *R* (p.u.)*	Reactance *X* (p.u.)*	R/X (p.u.)*	Zero Seq. X (p.u.)*	Tap Range		Method of Earthing
							Min	Max	
30	0.86	YD1	0.016	0.333	0.047	0.333	0.8	1.1	Resistance
45	26.22		0.014	0.267	0.052	0.269			
60	14.70		0.010	0.208	0.047	0.208			
75	1.15		0.007	0.193	0.037	0.193			
90	56.48		0.008	0.253	0.031	0.260			
120	0.58		0.007	0.244	0.029	0.246			

132/22 kV Transformers

SE - South-Central England									
Nameplate Rating *S* (MVA)	Volume (%)	Vector Group	Resistance *R* (p.u.)*	Reactance *X* (p.u.)*	R/X (p.u.)*	Zero Seq. X (p.u.)*	Tap Range		Method of Earthing
							Min	Max	
45	42.86	YD1	0.0157	0.4688667	0.033	0.468833	0.8	1.1	Resistance
60	57.14		0.015	0.33	0.045	0.21			

132/11 kV Transformers

SE - South-Central England									
Nameplate Rating *S* (MVA)	Volume (%)	Vector Group	Resistance *R* (p.u.)*	Reactance *X* (p.u.)*	R/X (p.u.)*	Zero Seq. X (p.u.)*	Tap Range		Method of Earthing
							Min	Max	
15	5.80	YD1	0.0504	0.6913	0.073	0.6913	0.8	1.1	Resistance
17	1.45		0.044	0.65	0.068	0.65			
18.5	8.70		0.0266	0.665	0.04	0.665			
20	17.39		0.0405	1.014	0.04	1.014			
			0.0294	0.623	0.047	0.623			
24	2.90		0.0333	0.675	0.049	0.675	0.8	1.05	
30	37.68		0.0188	0.337	0.056	0.337	0.8	1.1	
			0.0314	0.674	0.047	0.674			
40	5.80		0.03	0.647	0.046	0.259			
45	4.35	YY6	0.0741	0.7787	0.095	0.7787	0.8	1.11	
50	15.94	YD1	0.0143	0.334	0.043	0.334	0.8	1.1	

66/33 kV Transformers

SE - South-Central England									
Nameplate Rating *S* (MVA)	Volume (%)	Vector Group	Resistance *R* (p.u.)*	Reactance *X* (p.u.)*	R/X (p.u.)*	Zero Seq. X (p.u.)*	Tap Range		Method of Earthing
							Min	Max	
72	100	DY1	0.0052	0.1375	0.038	0.0833	1	1.05	Resistance

66/25 kV Transformers

SE - South-Central England									
Nameplate Rating *S* (MVA)	Volume (%)	Vector Group	Resistance *R* (p.u.)*	Reactance *X* (p.u.)*	R/X (p.u.)*	Zero Seq. X (p.u.)*	Tap Range		Method of Earthing
							Min	Max	
10	100	YY6	0.00	0.08	0	0.0001	0.9	1.1	Resistance

66/22 kV Transformers

SE - South-Central England									
Nameplate Rating *S* (MVA)	Volume (%)	Vector Group	Resistance *R* (p.u.)*	Reactance *X* (p.u.)*	R/X (p.u.)*	Zero Seq. X (p.u.)*	Tap Range		Method of Earthing
							Min	Max	
40	50	YY6	0.0179	0.4813	0.037	0.4813	1	1.1	Resistance
			0.013	0.295	0.044	0.2953	1	1.13	
45	50		0.025	0.797	0.031	0.797	0.9	1.1	

66/11 kV Transformers

SE - South-Central England									
Nameplate Rating *S* (MVA)	Volume (%)	Vector Group	Resistance *R* (p.u.)*	Reactance *X* (p.u.)*	R/X (p.u.)*	Zero Seq. X (p.u.)*	Tap Range		Method of Earthing
							Min	Max	
20	11.36	YY6	0.0275	0.977	0.028	3.9	0.8	1.1	Resistance
			0.03	0.75	0.04	3			
28	6.82		0.039	0.976	0.04	3.9			
30	22.73		0.0308	0.8753	0.035	3.6	0.9	1.05	
			0.03	1.12	0.027	4.48	0.8	1.1	
			0.037	0.9333	0.04	3.73	0.9		
37.5	4.55		0.0264	0.7417	0.036	3	0.8		
40	45.45		0.0228	0.768	0.03	0.768			
			0.0277	0.6782	0.041	2.76			
			0.03	0.745	0.04	3			
			0.0544	1	0.054	4			
			0.0249	0.825	0.03	5.05	0.9		
60	9.09		0.035	0.733	0.048	4	0.9	1.06	
			0.035	0.733	0.048	0.033	0.9	1.1	

33/33 kV Transformers
(Voltage Regulators)

SHE – North-Scotland								
Nameplate Rating *S* (MVA)	Volume (%)	Vector Group	Resistance *R* (p.u.)*	Reactance *X* (p.u.)*	R/X (p.u.)*	Tap Range		Method of Earthing
						Min	Max	
5	9	Yy0	0.013	0.0466	0.279	0.857	1.086	Solid
7			0.01	0.05	0.2	0.8141	1.0429	
10								
15	45.4							
20	9							
21			0.21	0.833	0.252			
30			0.01	0.0413	0.2421			

33/11 kV Transformers

SHE – North-Scotland

Nameplate Rating *S* (MVA)	Volume (%)	Vector Group	Resistance *R* (p.u.)*	Reactance *X* (p.u.)*	R/X (p.u.)*	Tap Range		Method of Earthing
						Min	Max	
0.05	0.7		18.4648	140	0.1319			
0.1	1.8		7.8939	60	0.1316			
0.15	1.1		5.9058	45	0.1312			
0.2	0.7		3.9275	30	0.1309			
0.3	0.7		2.6119	20	0.1306			
0.5	1.8		1.5596	12	0.13			
0.6	0.2		1.063	8.2	0.1296			Solid
0.75	0.2		1.0346	8	0.1293			
0.8	0.4		0.8076	6.26	0.129	0.8141	1.0429	
1	5.7		0.7722	6	0.1287			
1.2	0.2		0.6451	5	0.129			
1.5	0.2		0.5157	4	0.1289			
1.8	0.2		0.5154	4	0.1289			
2	1.1		0.3861	3	0.1287			
2.1	1.4		0.0402	1	0.0402			Resistance
2.5	12.6		0.3609	2.8	0.1289			Solid
3.5	1.2		0.2528	2	0.1264			
4	1.1	Yyo	0.2247	1.75	0.1284	0.8641	1.0929	Solid/Resistance
5	11		0.1313	1.4	0.0938			Resistance/Solid
6	1.9		0.1066	1.2	0.0888	0.8141	1.0429	Solid/Resistance
6.25	2.1		0.1107	1.2	0.0923			
7	0.3		0.1379	1.52	0.0907	0.8715	1.0715	Resistance
7.5	1.1		0.0927	1.067	0.0869			Solid/Resistance
8	8.4		0.0704	1	0.0704			Resistance/Solid
10	8.2		0.0681	1	0.0681	0.8141	1.0429	
12	0.2		0.0365	1	0.0365			Resistance
12.5	4.2		0.0668	1	0.0668			Resistance/Solid
14	0.7		0.0649	1	0.0649	0.85	1.05	Resistance
15	15.5		0.0596	1	0.0596			Resistance/Solid
18	0.1		0.0425	1.0117	0.042			Resistance
20	0.2		0.0444	1	0.0444			Solid
23	4.4		0.0385	1	0.0385	0.8141	1.0429	Resistance/Solid
24	9.6		0.0365	1	0.0365			
30	0.4		0.034	1	0.034			Resistance
40	0.4		0.032	0.75	0.0427			

∑ (%) = 100%

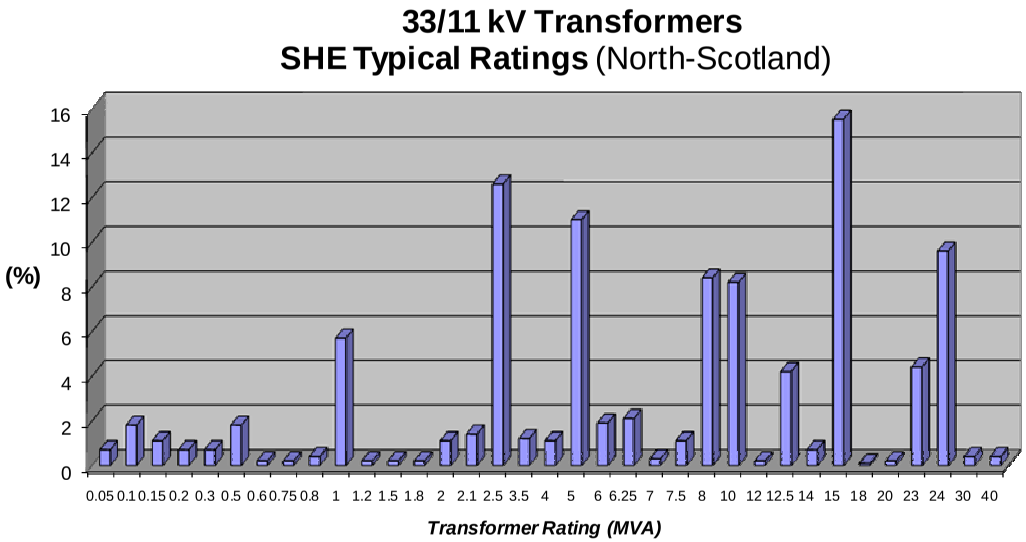

Notes: Most typical Transformers (Volume > 8%);
Coincident Transformers (MVA Rating) with SE, South-Central England.

33/11 kV Transformers

SE - South-Central England

Nameplate Rating *S* (MVA)	Volume (%)	Vector Group	Resistance *R* (p.u.)*	Reactance *X* (p.u.)*	R/X (p.u.)*	Zero Seq. X (p.u.)*	Tap Range Min	Tap Range Max	Method of Earthing
2	1.04	YY0	0.5325	3.55	0.15	10.65	0.9	1.05	Resistance
			0.55	3.665	0.1501	1.5			Solid
			→ 0.35	3.555	0.0985	1.7775			
			0.459	3.63	0.1264	11.28			
3	2.26		0.3127	2.383	0.1312	1.21			
4	0.19		0.315	2.865	0.1099	2.865	0.9	1	Resistance
		DY11	→ 0.1792	1.6	0.112	1.69	0.9	1.05	Solid
5	5.19	YY0	0.155	1.588	0.0976	0.8	0.9		Solid/Resistance
7.5	6.51		0.0988	1.097	0.0901	0.52			Resistance
8	0.09		0.4	1.6063	0.249	0.82			Solid
9	0.28	DY11	0.086	0.9586	0.0897	0.9586	0.9	1.06	
9.4	0.28		0.066	0.9467	0.0697	0.95			
10	12.26		0.0698	0.992	0.0704	0.5	0.9	1.05	Resistance
10.5	0.28	YY0	0.101	1.12	0.0902	0.56	0.9	1.06	
11.2	0.47		0.083	1.0373	0.08	5	0.9	1.05	
11.5	1.42		0.0964	1.067	0.0903	0.8			
			0.072	1.03	0.0699	5	0.8	1.06	Solid
11.9	0.38		0.072	1.024	0.0703	5	0.8	1.04	
12	0.38		0.07	1.358	0.0515	0.7	0.9	1.05	
			0.1027	1	0.1027	0.0047			
			→ 0.03	1.05	0.0286	0.79			
13	1.32		0.069	0.985	0.0701	0.5			
14	0.85		0.0668	1	0.0668	0.5			
15	14.43		→ 0.0586	1.047	0.056	5	0.8	1.06	
			0.0833	1.088	0.0766	0.54	0.9	1.05	
			0.0416	0.667	0.0624	0.333	0.9		
			0.192	1.094	0.1755	0.0001	0.9		
16.2	0.09		0.07	0.867	0.0807	0.33	0.9		Resistance
17	0.19		0.098	1.067	0.0918	0.53			
18.6	0.19		0.041	0.667	0.0615	0.333			
18.7	0.57	DY11	0.05	0.9067	0.0551	0.9067	0.9	1.06	
18.8	0.09	YY0	0.04	0.727	0.055	4	0.8	1.04	
19.5	0.57	DY11	0.0883	0.6663	0.1325	0.663	0.9	1.06	
			0.055	0.882	0.0624	0.882			
20	5.94	YY0	0.0303	0.74	0.0409	0.325	0.9	1.05	
21	2.45		0.048	0.86	0.0558	0.5			
21.2	0.19	DY11	0.043	0.8676	0.0496	0.8675	0.9	1.06	
21.5	0.28	YY0	0.039	0.633	0.0616	0.333	0.9	1.05	
22.5	0.94		0.035	0.9213	0.038	4			
23	4.43		0.03	0.963	0.0312	4	0.8	1.06	
24	7.83		→ 0.03	0.93	0.0323	0.45	0.9	1.1	
			0.1265	1.0538	0.12	0.5	0.8	1.06	
			0.0737	1	0.0737	0.335	0.9	1.05	
			0.0933	0.8013	0.1164	0.516			
		DY11	0.0883	0.6663	0.1325	0.663		1.06	
24.5	0.09		0.03	0.76	0.0395	0.76	0.8		

Nameplate Rating *S* (MVA)	Volume (%)	Vector Group	Resistance *R* (p.u.)*	Reactance *X* (p.u.)*	R/X (p.u.)*	Zero Seq. X (p.u.)*	Tap Range Min	Tap Range Max	Method of Earthing
26	0.19	YY0	0.0303	0.74	0.0409	0.56	0.9	1.05	
27	0.19		0.025	0.649	0.0385	0.324	0.9		
28	0.57		0.0355	0.745	0.0477	0.37	0.9		
		DY1	0.0381	0.9755	0.0391	0.97	0.9	1.06	
30	24.43	YY0	→ 0.03	0.78	0.0385	4	0.8	1.04	Resistance
			0.035	0.78	0.0449	0.5			
			0.0917	1.0453	0.0877	1	0.9		
32	0.09		0.07	0.964	0.0726	0.5	0.9	1.05	
40	2.83	DY11	0.0568	0.8045	0.0706	0.8045	0.8		
		YY0	0.06	0.7975	0.0752	0.0001	0.9		
			→ 0.035	0.7075	0.0495	0.317	0.9		
50	0.19		0.012	0.2522	0.0476	0.25	0.9	1.1	Resistance/Solid

$\sum (\%) = 100\%$

33/11 kV Transformers
SE Typical Ratings (South-Central England)

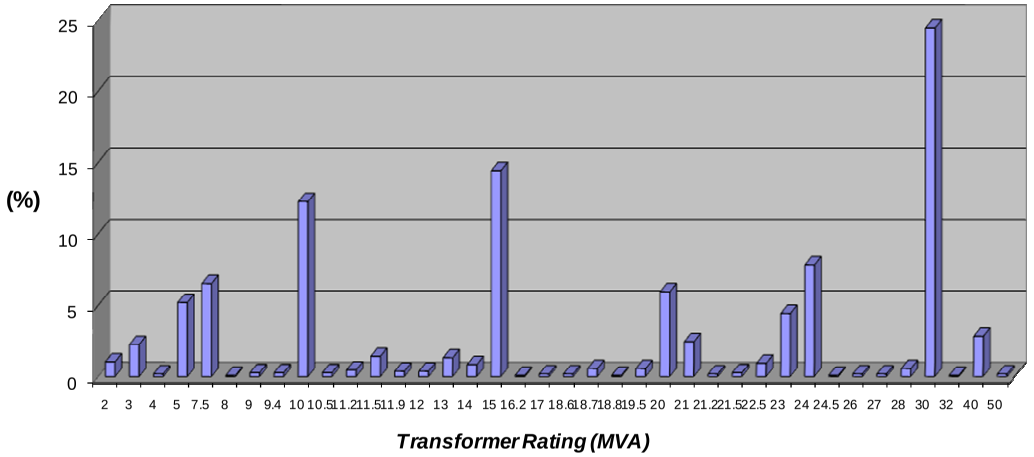

Notes: Most typical Transformers (Volume > 10%);
Coincident Transformers (MVA Rating) with SHE, Scotland;
Similar values to coincident transformers of SE South-England.

33/11 kV Transformers

→ Most Typical Coincident 33/11 kV Transformers (SHE Scotland + SE England)

	Power Rating	Site Volume (%)	Area
1)	**15 MVA**	15% in each area	Scotland + England
2)	**30 MVA**	25%	England
3)	**10 MVA**	~10% in each area	Scotland + England

4) The rest of 'predominant' Transformers are located in Scotland:

2.5 MVA (12.6%)

5 MVA (11%)

24 MVA (9.6%)

8 MVA (8.4%)

→ Most Typical Characteristics of Coincident 33/11 kV Transformers

Nameplate Rating *S* (MVA)	Vector Group	Resistance *R* (p.u.)*	Reactance *X* (p.u.)*	R/X (p.u.)*	Zero Seq. X (p.u.)*	Tap Range		Method of Earthing
						Min	Max	
2	YY0	0.37	3.3	0.1121	1.77	0.85	1.045	Solid
4	YY0/DY11	0.2	1.7	0.1176	1.69	0.9	1.07	
5	YY0	0.14	1.5	0.0933	0.8	0.85	1.045	Solid/Resistance
7.5		0.095	1.08	0.088	0.52			Resistance
10		0.069	1	0.069	0.5			
12		0.035	1.02	0.0343	0.79			
14		0.065	1	0.065	0.5	0.9	1.05	
15		0.06	1	0.06	5	0.8	1.05	
23		0.035	1	0.035	4	0.8	1.05	
24		0.035	1	0.035	0.45	0.85	1.05	
30		0.03	0.78	0.0385	4	0.8	1.04	
40		0.035	0.71	0.0493	0.317	0.9	1.05	

Notes: sorted by increasing power rating;

: Most typical Coincident 33/11 kV Transformers (Total Volume > 20%).

33/7 kV Transformers

SHE – North-Scotland								
Nameplate Rating *S* (MVA)	Volume (%)	Vector Group	Resistance *R* (p.u.)*	Reactance *X* (p.u.)*	R/X (p.u.)*	Tap Range		Method of Earthing
						Min	Max	
6.5	100	Yy0	0.1053	1.15	0.0915	0.8141	1.0429	Solid

33/6.6 kV Transformers

SE - South-Central England									
Nameplate Rating *S* (MVA)	Volume (%)	Vector Group	Resistance *R* (p.u.)*	Reactance *X* (p.u.)*	R/X (p.u.)*	Zero Seq. X (p.u.)*	Tap Range		Method of Earthing
							Min	Max	
10	44.44	YY0	0.0925	1.069	0.087	0.5	0.9	1.05	Resistance
			0.067	1.04	0.064	0.5			
			0.072	1.06	0.068	0.8			
11.3	11.11		0.08	1.013	0.079	5			
14.4	16.67	DY11	0.0676	1.0958	0.062	0.964	0.9	1.06	
22.5	11.11	YY0	0.036	0.9333	0.039	0.5	0.9	1.05	
24	16.67		0.0553	1.15	0.048	5	1	1.15	

33/3 kV Transformers

SHE – North-Scotland								
Nameplate Rating *S* (MVA)	Volume (%)	Vector Group	Resistance *R* (p.u.)*	Reactance *X* (p.u.)*	R/X (p.u.)*	Tap Range		Method of Earthing
						Min	Max	
3	100	Yy0	0.2945	2.3	0.12804	0.8141	1.0429	Solid

22/11 kV Transformers

SE - South-Central England									
Nameplate Rating *S* (MVA)	Volume (%)	Vector Group	Resistance *R* (p.u.)*	Reactance *X* (p.u.)*	R/X (p.u.)*	Zero Seq. X (p.u.)*	Tap Range		Method of Earthing
							Min	Max	
10	50	DY11	0.07	1	0.07	1	0.9	1.06	Resistance
		DY1	0.0655	0.99	0.066	0.5			
			0.0674	1.012	0.067	1.012	0.8	1.2	Solid
11.5	8.33	DY11	0.0787	0.992	0.079	0.99	0.9	1.06	Resistance
12.5	33.33		0.069	0.987	0.07	0.98			
			0.0732	0.977	0.075	0.97	0.9	1.1	
		DY1	0.063	0.99	0.064	0.99	0.5	1.5	Solid
24	8.33		0.075	1.0758	0.07	1.07	0.9	1.06	Resistance

22/6.6 kV Transformers

SE - South-Central England									
Nameplate Rating *S* (MVA)	Volume (%)	Vector Group	Resistance *R* (p.u.)*	Reactance *X* (p.u.)*	R/X (p.u.)*	Zero Seq. X (p.u.)*	Tap Range		Method of Earthing
							Min	Max	
5	5.71	DY1	0.136	1.392	0.098	1.39	0.9	1.06	Resistance
10	37.14		0.0686	1.05	0.065	1.05	0.8	1.04	
			0.072	1	0.072	1	0.9	1.06	
		DY11	0.0749	0.975	0.077	0.957			
11.5	11.43		0.067	0.958	0.07	0.96			
12.5	37.14		0.07	1	0.07	1			
14	8.57	DY1	0.08	1.075	0.074	1.41			

11/11 kV Transformers
(Voltage Regulators)

SHE – North-Scotland								
Nameplate Rating *S* (MVA)	Volume (%)	Vector Group	Resistance *R* (p.u.)*	Reactance *X* (p.u.)*	R/X (p.u.)*	Tap Range		Method of Earthing
						Min	Max	
1.6	16.6	Yy0	0.5154	4	0.12885	0.8141	1.0429	Solid
2			0.3861	3	0.1287	0.9	1.1	
2.5	33.3		0.3609	2.8	0.1289	0.8141	1.0429	
8			0.0704	1.7475	0.0402			

Appendix D

Full-Specification Modelling of Secondary Distribution Transformers

This appendix provides the full specifications and parameters required to model the different types of secondary distribution transformers presented in Section 3.6. This includes all the phase constants and parameters of the transformer model, allowing for a full transient and dynamic network simulation such as the study presented in [21] and [31], where these models were particularly useful for the network implementation with Matlab Simulink software (i.e. SimPowerSystems Toolbox [149]). For each particular load subsector presented in Section 3.4.3 (i.e. HU, U, SU and Ru), the most representative 2^{ary} transformer at each subsector is selected to model the generic distribution networks proposed for analysis in Section 3.6. The full specifications for the implementation of these transformer models are provided in Tables D.1, D.2, D.3 and D.4 in Section D.2 at the end of this appendix.

D.1 Development of Full Transformer Models

Manufacturers of power transformers usually provide limited specifications, i.e. not enough, for an accurate modelling of these components. As an example, the most typical parameters provided [73, 107, 146, 147] include transformer rating, (load and no-load) losses, winding connection, tapping range and the overall winding impedance (as a % of transformer's rating). These limited specifications are those presented in the first 9 columns of Tables D.1, D.2, D.3 and D.4 at the end of this appendix.

Let us consider the 500 kVA (urban subsector) transformer as an example. Apart from the manufacturer's voltage ratio of 11,000/433 V, the only parameter provided regarding the winding impedance is $Z = 4.75\%$ on transformer's rating, which is the same as considering an overall impedance of $|Z| = 0.0475 p.u.$ on 500 kVA base. Thus, the first step would be to decompose this value into their corresponding *active* (R_{TOTAL}) and *reactive* (X_{TOTAL}) parameters, in order to build the simple equivalent circuit presented in Figure D.1.

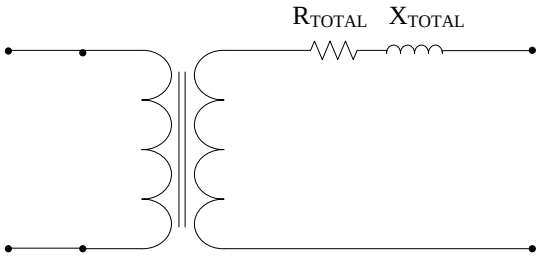

Figure D.1: Simplified transformer equivalent circuit.

First, the transformer base impedance (referred to the LV side) must be calculated:

$$Z_{BASE} = \frac{U^2}{S_{BASE}} = \frac{(433V)^2}{500 \cdot 10^3 VA} = 0.374978\Omega \tag{D.1}$$

Considering the transformer's load losses (W_{cu}) of 5,100 W in Table D.2, which are mainly due to losses in the copper (Cu) winding, they contribute with 1.02% of the transformer's base power S_{BASE}:

$$P_{Lcu} = \frac{W_{cu}}{S_{BASE}} = 0.0102 = 1.02\% S_{BASE} \tag{D.2}$$

Thus, as the copper losses are due to the resistive component of the winding, R_{TOTAL} can be easily calculated:

$$R_{TOTAL} = \frac{U^2}{W_{cu}} = \frac{U^2}{0.0102 \cdot S_{BASE}} = 0.00382\Omega \tag{D.3}$$

From this value and Z_{BASE}, it is possible to calculate both active and reactive components of the transformer's impedance in p.u., which are the values provided in Table 3.11 of Section 3.6 in the main body of the thesis:

$$R_{TOTAL}(p.u.) = \frac{R_{TOTAL}(\Omega)}{Z_{BASE}} = 0.0102 p.u. \tag{D.4}$$

$$|X_{TOTAL}| = \sqrt{|Z|^2 - |R_{TOTAL}|^2} = \sqrt{0.0475^2 - 0.0102^2} = 0.0464 p.u. = 0.0174\Omega \text{(converted to ohms)} \tag{D.5}$$

As a result:

$$Z = R_{TOTAL} + jX_{TOTAL} = 0.00382 + j0.0174\Omega = 0.0102 + j0.0464 \text{(p.u. on 500 kVA base)} \tag{D.6}$$

Once we are able to build the basic transformer model of Figure D.1, it is possible to further develop this model to obtain a more accurate representation. For this purpose, there exist two option models, as shown in Figures D.2 and D.3.

1. with each component of R_{TOTAL} and X_{TOTAL} referred to its own winding:

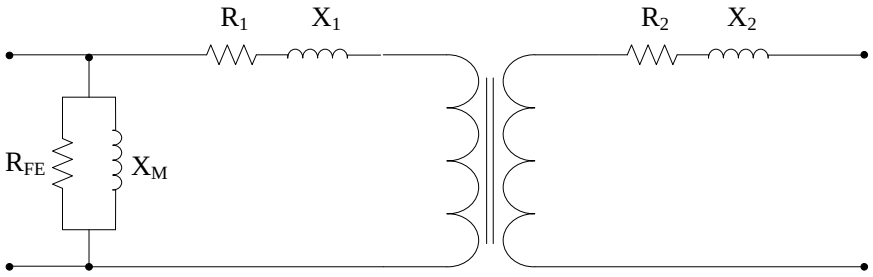

Figure D.2: Transformer equivalent circuit: Z_{TOT} components referred to their own winding.

2. with both components of R_{TOTAL} and X_{TOTAL} referred to the secondary winding:

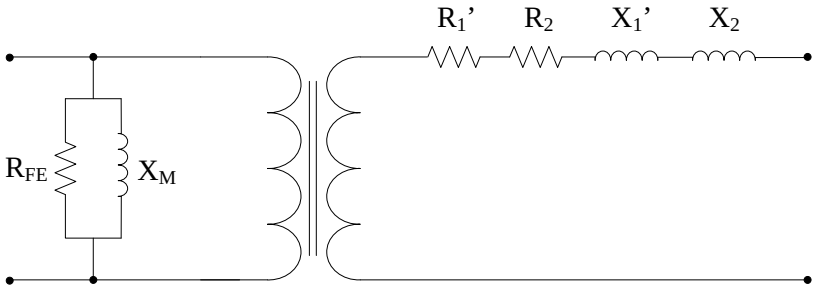

Figure D.3: Transformer equivalent circuit: Z_{TOT} components referred to the secondary winding.

After the corresponding calculations explained below, all the transformer phase parameters represented in these models are provided in Tables D.1, D.2, D.3 and D.4 in Section D.2 at the end of this appendix.

D.1.1 Transformer's Series Impedance Calculation

First of all, let us focus on the series impedance of the transformer (referred to the secondary winding, option 2), for the parameters R_1', R_2, X_1' and X_2.

$$X_{TOTAL} = 0.0174\Omega = X_1' + X_2 \tag{D.7}$$

Assuming the reactive voltage drop to be equal in the primary and secondary winding [198] gives:

$$X_1' = X_2 = \frac{X_{TOT}}{2} = 0.0087\Omega \tag{D.8}$$

Following the same assumption, and taking into account several examples of tests undertaken for this type of transformers [198], the active voltage drop in the secondary winding is normally about 43.1% of the total. Thus, if R_{TOTAL} is:

$$R_{TOTAL} = 0.00382\Omega = R'_1 + R_2 \tag{D.9}$$

Its decomposed value can be calculated as following:

$$R_2 = R_{TOTAL} \cdot 0.431 = 0.00165\Omega \tag{D.10}$$

$$R'_1 = R_{TOTAL} - R_2 = 0.00217\Omega \tag{D.11}$$

If any of these values must be calculated referred to the primary winding, then the transformer's phase voltage ratio must be considered. As the transformer's connection is delta/star:

$$n_T = \frac{11000 \cdot \sqrt{3}}{433} = 44 \tag{D.12}$$

and therefore: $n_T^2 = 44^2 = 1936$

So, for example, in order to calculate R_1 and X_1 values referred to the primary winding:

$$R_1 = R'_1 \cdot n_T^2 = 0.002 \cdot 1936 = 4.2081\Omega \tag{D.13}$$

$$X_1 = X'_1 \cdot n_T^2 = 0.008 \cdot 1936 = 16.84\Omega \tag{D.14}$$

D.1.2 Transformer's Parallel Impedance Calculation

Considering that the parallel impedance of the transformer is formed by R_{FE} and X_m parameters, first of all, in order to calculate R_{FE} we need to consider losses in the iron (i.e. 'No-load Losses' in Table D.2, equal to 680 W).

Thus, the core loss per phase, $P_{IRON} = 680/3 = 226.6W$

The current flowing through R_{FE}, (I_C), can be calculated:

$$I_C(perphase) = \frac{226.6}{11000} = 0.0206A \tag{D.15}$$

Thus,

$$R_{FE} = \frac{P_{IRON}}{I_C^2} = \frac{226.6}{0.0206^2} = 533.82k\Omega \tag{D.16}$$

For the calculation of X_m we need to know the current flowing through the parallel branch of the transformer when it is no loaded (i.e. no-load current 'I_0'), from which we will be able to calculate the current ('I_m') flowing through the magnetising reactance X_m.

$$\overline{I_m} = \overline{I_0} - \overline{I_C} \tag{D.17}$$

However, the 'no-load current' 'I_0' is not always readily available, so it will be necessary to check manufacturer's data [199]. Accordingly, Figure D.4 provides an example table with specifications for different transformers:

ELECTRICAL CHARACTERISTICS										
Rated Power kVA			**250**	**400**	**630**	**800**	**1000**	**1250**	**1600**	**2000**	**2500**
Rated	Primary	Maximum Voltage 24 kV								
Voltage	Secondary no load*	420 V between phases - no load								
Tapping Range*		± 2,5 ± 5% 6 +2,5 + 5 + 7,5 + 10% (other regulation voltages on demand)								
Vector Group*		Dyn 11								
No Load Losses (W)*			650	930	1300	1550	1700	2130	2600	3100	3800
Load Losses (W)*			3250	4600	6500	8100	10500	13500	17000	20200	26500
Short Circuit Impedance % at 75° C *			4	4	4	6	6	6	6	6	6
No Load current at 100% of Vn*			2	1,8	1,6	1,4	1,3	1,2	1,1	1	0,9
Max. Sound Power Level (dB)*			62	65	67	68	68	70	71	73	76
Voltage drop		cos φ = 1	1,4	1,2	1,1	1,2	1,2	1,3	1,2	1,2	1,2
at full load %		cos φ = 0,8	3,3	3,2	3,1	4,4	4,4	4,4	4,4	4,4	4,4
Efficiency (%)	Load 100%	cos φ = 1	98,5	98,6	98,8	98,8	98,8	98,8	98,8	98,9	98,8
		cos φ = 0,8	98,1	98,3	98,5	98,5	98,5	98,5	98,5	98,6	98,5
	Load 75%	cos φ = 1	98,7	98,8	99,0	99,0	99,0	99,0	99,0	99,1	99,0
		cos φ = 0,8	98,4	98,6	98,7	98,7	98,8	98,7	98,8	98,8	98,8

* Other characteristics on demand

Figure D.4: Electrical characteristics of MV distribution transformers (Ormazabal) [199].

This table provides values of 'I_0' (in % of nominal current) for different transformer ratings in the row with title: 'No Load current at 100% of V_n'. There is not a specific value for a 500 kVA transformer, but it is possible to deduct from other values (1.8% for 400 kVA and 1.6% for 630 kVA) that the value needed for I_0 will be 1.7% of the transformer's nominal current, which for the 500 kVA transformer can be calculated as:

$$I_{NOM} = \frac{S_{NOM}}{\sqrt{3} \cdot U} = \frac{500 \cdot 10^3}{\sqrt{3} \cdot 11000} = 26.24A \tag{D.18}$$

$$I_0 = 1.7\% I_{NOM} = 0.017 \times I_{NOM} = 0.44608A \tag{D.19}$$

Therefore, we can calculate the current I_m:

$$\overline{I_m} = \overline{I_0} - \overline{I_C} = \sqrt{0.44608^2 - 0.0206^2} = 0.4456A \tag{D.20}$$

So the value of X_m is:

$$X_m = \frac{U}{I_m} = \frac{11000}{0.4456} = 24.68k\Omega \tag{D.21}$$

D.2 Transformer Full-Specification Models per Load Subsector

As a result of all the calculations for the correct modelling of secondary distribution transformers (per load subsector, i.e. HU, U, SU and Ru), the full set of parameters and phase constants are provided in the tables shown overleaf.

Table D.1: Full specification of phase constants for secondary transformers in highly-urban areas.

HIGHLY URBAN Subsector																	
Voltage (kV)	**Type**	**Rating (kVA)**	**Connect.**	**Tapping Range**	**Impulse Level (kV)**	**Losses at 75∘C (W)**	**No-Load Losses (W)**	**Z (%)**	**Transformer Model Parameters**								
									$R_{TOT}(\Omega)$	$X_{TOT}(\Omega)$	$R_1(\Omega)$	$R'_1(\Omega)$	$X_1(\Omega)$	$X'_1(\Omega)$	$R_2(\Omega)$	$X_2(\Omega)$	$R_{FE}(k\Omega)$	$X_M(k\Omega)$
11/0.4	Ground / Pad Mounted	1000	Dyn11	± 5% in 2.5% taps	75	11,000	1,350	4.75	0.00206	0.00866	2.2693	0.00117	8.38	0.00433	0.00089	0.00433	268.90	16.15

Table D.2: Full specification of phase constants for secondary transformers in urban areas.

URBAN Subsector																	
Voltage (kV)	**Type**	**Rating (kVA)**	**Connect.**	**Tapping Range**	**Impulse Level (kV)**	**Losses at 75∘C (W)**	**No-Load Losses (W)**	**Z (%)**	**Transformer Model Parameters**								
									$R_{TOT}(\Omega)$	$X_{TOT}(\Omega)$	$R_1(\Omega)$	$R'_1(\Omega)$	$X_1(\Omega)$	$X'_1(\Omega)$	$R_2(\Omega)$	$X_2(\Omega)$	$R_{FE}(k\Omega)$	$X_M(k\Omega)$
11/0.4	Ground / Pad Mounted	500	Dyn11	± 5% in 2.5% taps	75	5,100	680	4.75	0.00382	0.01740	4.2081	0.00217	16.84	0.00870	0.00165	0.00870	533.82	24.68

Table D.3: Full specification of phase constants for secondary transformers in suburban areas.

SUBURBAN Subsector																	
Voltage (kV)	**Type**	**Rating (kVA)**	**Connect.**	**Tapping Range**	**Impulse Level (kV)**	**Losses at 75∘C (W)**	**No-Load Losses (W)**	**Z (%)**	**Transformer Model Parameters**								
									$R_{TOT}(\Omega)$	$X_{TOT}(\Omega)$	$R_1(\Omega)$	$R'_1(\Omega)$	$X_1(\Omega)$	$X'_1(\Omega)$	$R_2(\Omega)$	$X_2(\Omega)$	$R_{FE}(k\Omega)$	$X_M(k\Omega)$
11/0.4	Ground / Pad Mounted	200	Dyn11	± 5% in 2.5% taps	75	2,900	540	4.75	0.01406	0.04218	15.4880	0.00800	40.83	0.02109	0.00606	0.02109	672.22	52.56

Table D.4: Full specification of phase constants for secondary transformers in rural areas.

RURAL Subsector																	
Voltage (kV)	**Type**	**Rating (kVA)**	**Connect.**	**Tapping Range**	**Impulse Level (kV)**	**Losses at 75∘C (W)**	**No-Load Losses (W)**	**Z (%)**	**Transformer Model Parameters**								
									$R_{TOT}(\Omega)$	$X_{TOT}(\Omega)$	$R_1(\Omega)$	$R'_1(\Omega)$	$X_1(\Omega)$	$X'_1(\Omega)$	$R_2(\Omega)$	$X_2(\Omega)$	$R_{FE}(k\Omega)$	$X_M(k\Omega)$
11/0.4	Ground / Pad Mounted	50	Dyn11	± 5% in 2.5% taps	75	1,100	190	4.75	0.08197	0.14736	90.2968	0.04664	142.60	0.07368	0.03533	0.07368	1910.52	191.50

Appendix E

MV Load Subsector Classification in the SPTL System

The results of the load subsector classification carried out for the interconnecting MV and LV networks at all 89 GSPs in the Scottish Power Transmission Limited (SPTL) network are given in Table E.1 overleaf. Each node is classified as either HU (Highly-Urban), U (Urban), SU (Suburban), or Ru (Rural), according to Section 4.3.1 of this thesis.

Table E.1: Results from load subsector classification at the 89 GSPs in the SPTL network [91].

GSP code	Subsector	Peak Demand (MW)	GSP code	Subsector	Peak Demand (MW)
AYR	U	33	GOVA	U	25.9
BAGA	SU	23.7	GRMO A	SU	20.2
BAIN	U	20.6	GRMO C	SU	15.7
BERW	SU	16.1	HAGR	U	33
BONN	U	26.8	HAWI	U	13.2
BRAP	U	25.1	HELE	U	12.8
BROX	U	31.1	HUNF	Ru	4.9
CAFA	Ru	0	INKE	SU	29.7
CATY	SU	30.6	JOHN	U	25.9
CHAP	U	26.8	KAIM	SU	42.9
CHAS	HU	55.3	KEOO	Ru	0.2
CLYM	SU	43.8	KIER	SU	41.6
COAT A	U	17.8	KILB 11	SU	6.2
COAT C	U	22.2	KILB 33	SU	13.3
COCK	U	23.6	KILS	SU	19.2
COYL	U	19	KILT	SU	62.9
CROO A	U	29.3	KILW	SU	7.8
CROO B	SU	10.9	LEVE	U	23.3
CUMB	U	27.7	LING	SU	48.1
CUPA	U	31.5	LINM	SU	7.7
CURR	SU	7.3	MAYB	SU	9
DEVM	SU	19.6	NEAR	SU	50.2
DEVO	Ru	35.7	NETS	Ru	5.3
DEWP	HU	44.6	PAIS	U	25.4
DRCR	SU	14	PART	SU	23.7
DRUM	SU	46	POOB	SU	51.3
DUMF1	SU	9.8	PORD	SU	47.6
DUMF3	SU	17.9	RAVE	SU	20.8
DUMFT3	SU	9	REDH	U	23
DUNB	SU	11.7	SACO A	SU	21.4
DUNF	Ru	22.4	SACO B	U	16.9
EAST	Ru	0	SANX	U	16.7
ECCL	SU	8.8	SHRU	U	43.2
EERH	SU	62	SIGH	U	59.4
EKIL	U	37.9	SPAV	SU	24.7
EKIS	SU	15.1	STHA	U	30.4
ELDE	U	18.4	STIR	SU	38.9
ERSK	U	16.2	STLE	U	29.7
GALA	U	15.4	TELR	SU	26.2
GIFF	SU	16.7	TONG	SU	-9.3
GLNI	Ru	0	WFIE	SU	12.1
GLLE	SU	11	WGEO	HU	47.6
GLLU	U	14.8	WHHO	U	36.4
GLRO	U	24.1	WISH	SU	42.2
GORG	U	24.6			

Appendix F

Matlab Model for Monte Carlo Simulation

This appendix provides an example of the Matlab code which is used to implement the integrated Monte Carlo simulation described in Section 5.2. The code is divided in different sections, including the probabilistic processing of input failure rates and repair times, acknowledgment of time-varying fault probabilities and load profiles, backup supply actions for classification of outages into LIs and SIs, as well as details on the adjustment of simulation accuracy (e.g. 1000 years in 30 min time-steps) for a time-sequential MCS analysis. Several variants of this base code have been developed during this PhD work in order to obtain the different simulation results presented in this thesis.

Input Data and Main MCS Code Development

```
% Input data preparation (Lambdas and Mus)

%number of Power Components (e.g. for Test Radial Network, with 134 PCs)
buses33=4;
buses11=43;
busesLV=20;
lines11=10;
CBs33=3;
CBs11=32;
fuses=10;
trafos3311=2;
trafos1104=10;

% Length of lines/cables: (km)
length_lines=0.5; %(km)  % define length for each particular line/cable
% In this case, all 11kV lines (10 O/H lines) have the same length

%Definition of lambdas and Mus-------------------------------------------
lambda_bus_33=0.08;
lambda_bus_11=0.005;
lambda_bus_LV=0.005;
```

```
lambda_line_11=0.091;  % This is per km (not per unit), to multiply by length.

lambda_CB_33=0.0041;
lambda_CB_11=0.0033;

lambda_fuse=0.0004;

lambda_trafo_3311=0.01;
lambda_trafo_1104=0.002;

% For Weibull (and RAYLEIGH) Distribution, MTTR values are assigned to mus:
mu_bus_33=140;
mu_bus_11=120;
mu_bus_LV=24;

mu_line_11=9.5;

mu_CB_33=140;
mu_CB_11=120.9;

mu_fuse=35.3;

mu_trafo_3311=205.5;
mu_trafo_1104=75;

%Structure of input arrays for Lambda----------------------------------------
l_bus_33=lambda_bus_33*ones(1,buses33);
l_bus_11=lambda_bus_11*ones(1,buses11);
l_bus_LV=lambda_bus_LV*ones(1,busesLV);
l_bus=[l_bus_33 l_bus_11 l_bus_LV];

l_line=lambda_line_11*length_lines*ones(1,lines11);

l_CB_33=lambda_CB_33*ones(1,CBs33);
l_CB_11=lambda_CB_11*ones(1,CBs11);
l_CB=[l_CB_33 l_CB_11];

l_fuse=lambda_fuse*ones(1,fuses);

l_trafo_3311=lambda_trafo_3311*ones(1,trafos3311);
l_trafo_1104=lambda_trafo_1104*ones(1,trafos1104);
l_trafo=[l_trafo_3311 l_trafo_1104];

%Structure of input arrays for Mu----------------------------------------
m_bus_33=mu_bus_33*ones(1,buses33);
m_bus_11=mu_bus_11*ones(1,buses11);
m_bus_LV=mu_bus_LV*ones(1,busesLV);
m_bus=[m_bus_33 m_bus_11 m_bus_LV];
```

```
m_line=mu_line_11*ones(1,lines11);

m_CB_33=mu_CB_33*ones(1,CBs33);
m_CB_11=mu_CB_11*ones(1,CBs11);
m_CB=[m_CB_33 m_CB_11];

m_fuse=mu_fuse*ones(1,fuses);

m_trafo_3311=mu_trafo_3311*ones(1,trafos3311);
m_trafo_1104=mu_trafo_1104*ones(1,trafos1104);
m_trafo=[m_trafo_3311 m_trafo_1104];

%--------------------------------------------------------------------------
% Variables to define: (Simulation Time)

years=1000;
multiplier=365; % down to days scale
days=years*multiplier;

lambda1=[l_bus l_line l_CB l_fuse l_trafo];
mu=[m_bus m_line m_CB m_fuse m_trafo];
lambda=lambda1/multiplier;   %failure/day

%--------------------------------------------------------------------------
% Variation of Fault Rates (lambdas) with time (40 years: Bathtube)

bathtube = 40*multiplier;  % 40 years in days
step=bathtube+1;
% Different steps of the Bathtub over 14600 days (40 years)
x=1/step : 1/step : 1-1/step;
y=zeros(bathtube,length(lambda));

% Each value of vector 'lambda' is expanded (following Beta PDF) over 14600 days
%(40years):
for n=1:length(lambda)
    y(:,n)=(lambda(n))./(pi*sqrt(x.*(1-x))); % Beta PDF with mean value = lambda(n)
end

dim=size(y);
a=1;
b=dim(1);
% The Beta PDFs over 40 years (matrix 'y' for all the PCs) is repeated to complete
% simulation time (e.g. 1000 years)

for m=1:25  % (40years * 25 times = 1000 years of simulation)
    LAMBDA(a:b,:)=y;
    a=a+dim(1);
```

```
    b=b+dim(1);
end

%-------------------------------------------------------------------------
% Weibull parameters Short Interruptions (SIs):
G1=14.25;
b1=1.95;                                          % (Fitted apart in Excel)
% Weibull parameters Long Interruptions (LIs):
G2=14.35;
b2=2.35;
%-------------------------------------------------------------------------
%-------------------------------------------------------------------------
%MAIN CODE (MCS):

U1=rand(days,length(lambda));
U2=rand(days,length(mu));

TTF=zeros(days,length(lambda));
TTR=zeros(days,length(lambda));

% Application of desired Distribution Functions for Modelling TTF/TTR
b3=2;   % e.g. RAYLEIGH Distribution: b=2  (different PDFs applicable here)
G3=mu/(gamma(1+(1/b3)));

for k=1:days
    for i=1:length(lambda)
        % Inverse Exponential CDF for Fault Rates
        TTF(k,i)=-1/LAMBDA(k,i)*log(U1(k,i));
        % This LAMBDA considers time variation over 40 years steps

        % Inverse Weibull CDF for TTR times
        TTR(k,i)=G3(i)*(-log(U2(k,i)))^(1/b3); %given in hours
    end
end

f=find(TTF<1);
% Accounting Statistics on LIs/SIs classification:
SI_LI=randsrc(length(f),1,[0 2;0.54 0.46]); % 0='SIs' 54%prob , 2='LIs' 46%prob
LI=find(SI_LI);
SI=find(SI_LI<2);

f1=TTR(f);  % duration of interr. in hours
f1(SI)=0;   % vector divided in SIs and LIs (in hours)
f0=f1*2;   % (in 30min divisions) (i.e. adjustable accuracy)
f0(f0<2 & f0>0)=2;
% In this case, the minimum duration (max.accuracy) for LIs is 1h (2x30min)
% This is because the time-step is 30min (1 time-step = SI)
f2=round(f0);
```

```
%-----------------------------------
% Weibull (Random Variables) for SI and LI Distributions (over the day)
% This defines the exact time (in hours) at which SI-LI happen in day

U3=rand(length(SI),1);
T_SI=zeros(length(SI),1);
for j=1:length(SI)
    T_SI(j)=G1*(-log(U3(j)))^(1/b1);  % Times SIs
    while T_SI(j)>24
       U4=rand;
       T_SI(j)=G1*(-log(U4))^(1/b1);
    end
end

U5=rand(length(LI),1);
T_LI=zeros(length(LI),1);
for l=1:length(LI)
    T_LI(l)=G2*(-log(U5(l)))^(1/b2);  % Times LIs
    while T_LI(l)>24
       U6=rand;
       T_LI(l)=G2*(-log(U6))^(1/b2);
    end
end

max_t_SI=max(T_SI);
min_t_SI=min(T_SI);

max_t_LI=max(T_LI);
min_t_LI=min(T_LI);

% Time (in 30min divisions) at which SI-LI happen in day
T_SI_2=T_SI*2;
T_LI_2=T_LI*2;
T_SI_30min=round(T_SI_2); %rounded values (30min) of occurrence (SIs)
T_LI_30min=round(T_LI_2); % " (LIs)

T_SI_30min(T_SI_30min<1)=1; % This is to make sure that the round value
T_LI_30min(T_LI_30min<1)=1; % doesn't give a failure in time '0'
%-------------------------------------------------------------------------
% Output Matrix 'B' for PSS/E (iterations=days):

B=ones(days,length(lambda));
B(f)=f1;  % 0='SIs' , 1=Normal Operation , 'duration of 'LIs' (value in hours)
%-----------------------------------------------
% 'C', same Matrix 'B', but with time of occurrence of faults
B_SIs=find(B==0);
B_LIs=find(B~=0 & B~=1);
```

```
C=zeros(days,length(lambda));
% it must be a 'zeros' matrix to avoid confusion with other values (ones)
% C(B_SIs)=T_SI;  %(in h over the day)
% C(B_LIs)=T_LI;
C(B_SIs)=T_SI_30min;  %(in rounded 30min over the day)
C(B_LIs)=T_LI_30min;
%----------------------------------------
save MCS_BetaFR_RaleTTR B C f2 % (output variables for postprocessing)
```

Accuracy Adjustment of MCS

```
% This code adjust/expands the accuracy of the simulation to 30 min time-steps
% for implementing a time-sequential analysis with load profile acknowledgment

load C
dim=size(C);
exp_n=48;    % Value to change (number of copies desired for each element)
             % 48 = 24h * 2 (30min)
for k=1:dim(1,2)

    p = 1;
    for n = 5000:5000:365000   % Iteration step = 5000, up to 1000years
        m = n - 4999;            % this speeds up simulation

        a=C(m:n,k);

        for i=1:length(a)

            a0=sprintf('a%d', i);
            if a(i)==0
                S.(a0) = ones(exp_n,1);
            else
                b=ones(exp_n,1);
                b(a(i))=0;        % a(i) must be an integer
                S.(a0) = b;
            end
        end

        P=zeros(exp_n*i,1);
        startpoint1 = 1;
        endpoint1 = 1;

        for j = 1:i
            endpoint1 = startpoint1+(exp_n-1);
            P(startpoint1:endpoint1,1) = eval(['S.a' num2str(j)]);
            startpoint1 = endpoint1+1;
        end
```

```
        x0=sprintf('P%d', p);
        SP.(x0) = P;
        p = p + 1;
    end

    p = p - 1;
    A=zeros(length(P)*p,1);

    startpoint2 = 1;
    endpoint2 = 1;

    for q = 1:p

        endpoint2 = startpoint2+(length(P)-1);
        A(startpoint2:endpoint2,1) = eval(['SP.P' num2str(q)]);
        startpoint2 = endpoint2+1;
    end

    x=sprintf('A%d', k);
    S1.(x) = A;
end

D=zeros(length(A),k);

for l=1:dim(1,2)
    D(:,l) = eval(['S1.A' num2str(l)]);
end
% D is the output Matrix (mostly ones)
% with the exact time (zeros) at which LIs/SIs happen (in 30min time steps)
```

Classification of LIs and SIs

```
f0=find(D==0); % find interruptions in Matrix D (simulation time)
D(f0)=f2;      % allocate interruption durations (from vector f2)

% Extend those durations (for LIs only) to the corresponding time steps:
f1=find(D>1);

for m=1:length(f1)
    for p=0:(D(f1(m))-1)
        D(f1(m)+p)=0;
    end
end
% The new matrix D is the OUTPUT MATRIX to export for analysis in PSS/E
% i.e. Risk & Power Flow Analysis in 30min time steps
save Dnew D
```

Example Application of Backup Action

```
% First, from Dnew, which is the input matrix for PSS/E, a new sub-matrix must
% be created (Dnew_backup_2) with only those PCs that are affected by the backup
% action in the network (i.e. SoS legislation: 3h, 15 min, etc., depending on
% power interrupted)

% According to the test network, this code applies backup action:
% (max 3h = 6x30min time steps), and generates a matrix B
% (to be renamed 'Dnew_backup_3') with the required backup action for each
% PC (in each column)

load Dnew_backup_2
B = zeros(size(Dnew_backup_2));
dim = size(Dnew_backup_2);

for j = 1:dim(1,2)

    A = Dnew_backup_2(:,j);

    n = diff ([2; A; 2]==0);
    f1 = find(n==1);
    dur = (find(n==-1) - find(n==1));

    for m = 1:length(f1)

        if dur(m)>6
        % For each LI, this is the limit value to track (max backup time =3h)
        %(6x30min steps)

            q = randsrc(1,1,[2 3 4 5 6]);
            % If the interruption is >6 (3h), then q is the random (uniform)
            % time limit for backup:
            % either 2(1h), 3(1.5h), 4(2h), 5(2.5h) or 6(3h) time steps

            for p=q:(dur(m)-1)
                B(f1(m)+p,j)=1;
            end
        end
    end
end       % Matrix B is the output (to be renamed: 'Dnew_backup_3')

Dnew_backup_3 = B;

%--------------------------------------------------------------------------
% Aggregation of all backup values into a common vector for modelling
% the switching actions in PSS/E:
% This code sums the columns of Dnew_backup_3 matrix in order to
% unify into a one vector for backup action (those values different to '0',
```

```
% when there is backup action, are reset to '1'

Backup_vector = sum(Dnew_backup_3,2);

Backup_vector(Backup_vector~=0)=1;

save Backup_vector Backup_vector

% Backup_vector is the input for the backup switch in PSS/E
```

Appendix G

DNO's Interruption Probability Analysis

According to the work presented in this thesis on network predictive fault performance (Section 5.4), the reliability assessment of power distribution networks can be more accurate if the actual probability distribution of customer interruptions (i.e. LIs > 3 min and SIs < 3 min) is incorporated in the empirical interruption model. Therefore, this appendix provides further probabilistic analysis of the outage data provided by Scottish Power Energy Networks (SPEN) for the reporting years 2009 and 2010, covering sustained/long and momentary/short interruptions in their electricity distribution networks. The fault recordings are used to determine the daily probability distributions of both customer long and short interruptions.

G.1 Probability Distributions of Long Interruptions

For LI assessment, the following figures provide the corresponding analysis of one-year data recordings on unplanned, planned and LIs due to incidents on other systems (e.g. NG transmission system) for the year 2009 on SPEN networks. The processed statistics cover the wide range of different voltage levels (33 kV, 11 kV and LV) and main equipment involved (OHLs, underground cables, switchgear, fusegear, LV services, etc.).

For example, Figure G.1 contains the overall processed probabilities for both unplanned and planned LIs within SPEN networks. As previously shown in Figure 5.16 (Page 144), it is also possible to identify a close correlation between (only) the unplanned LI probabilities in SPEN networks and the typical aggregate load profile at the GSP level. In addition, Figure G.2 demonstrates the typical time range when DNOs undertake maintenance services on the network, and Figure G.3 provides the supply interruption probabilities corresponding to faults taking place at system's transmission level.

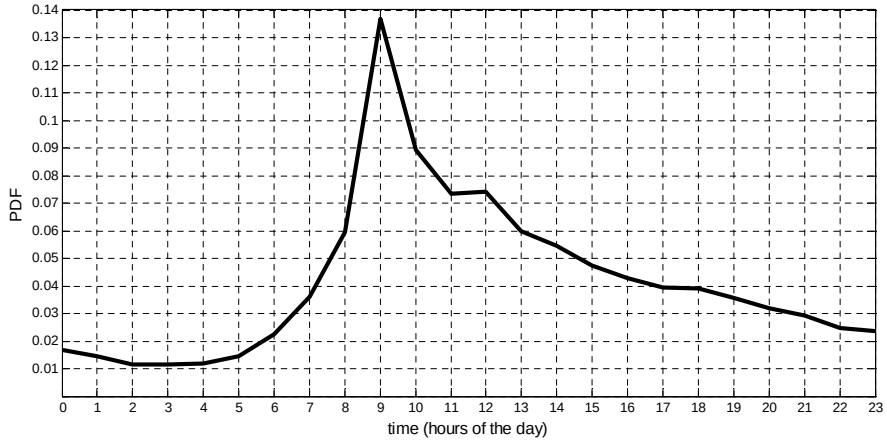

Figure G.1: SPEN - Daily probability of all long interruptions in year 2009.

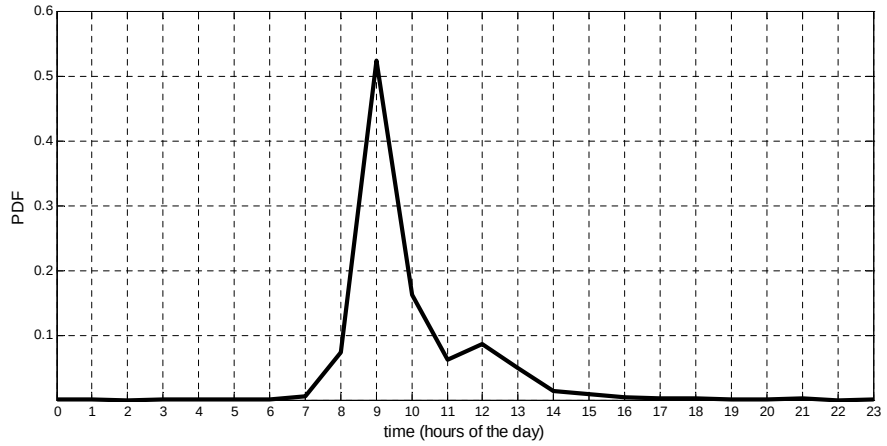

Figure G.2: SPEN - Daily probability of planned long interruptions in year 2009.

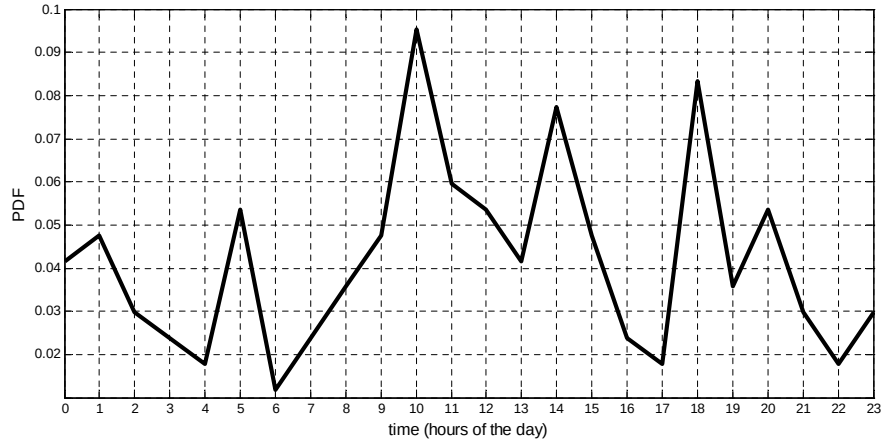

Figure G.3: SPEN - Daily probability of LIs due to incidents on other systems in year 2009.

G.2 Probability Distributions of Short Interruptions

Regarding the SI assessment (i.e. PQ-related analysis), the following figures divide the probabilistic analysis into different time ranges (e.g. yearly seasons, week-days, weekend-days, etc.) over the analysed period, covering years 2009 and 2010. These probability density functions (PDFs) will enable to understand how the SIs are typically distributed over the year, incurring on more or less risk of occurrence. In this case, the processed statistics also cover different SPEN voltage levels (i.e. 33 kV, 11 kV and LV) and main equipment involved (OHLs, underground cables, switchgear, fusegear, LV services, etc.).

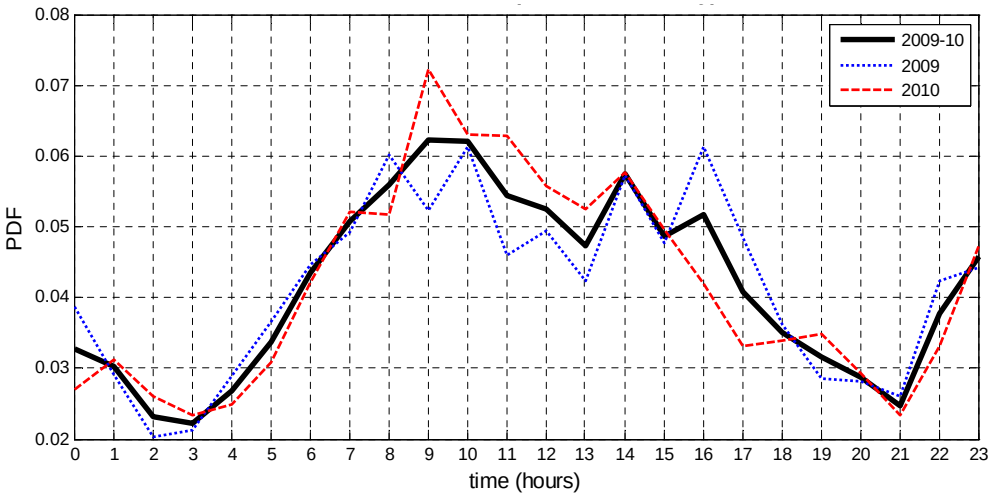

Figure G.4: SPEN - Daily probability of all short interruptions in years 2009/10.

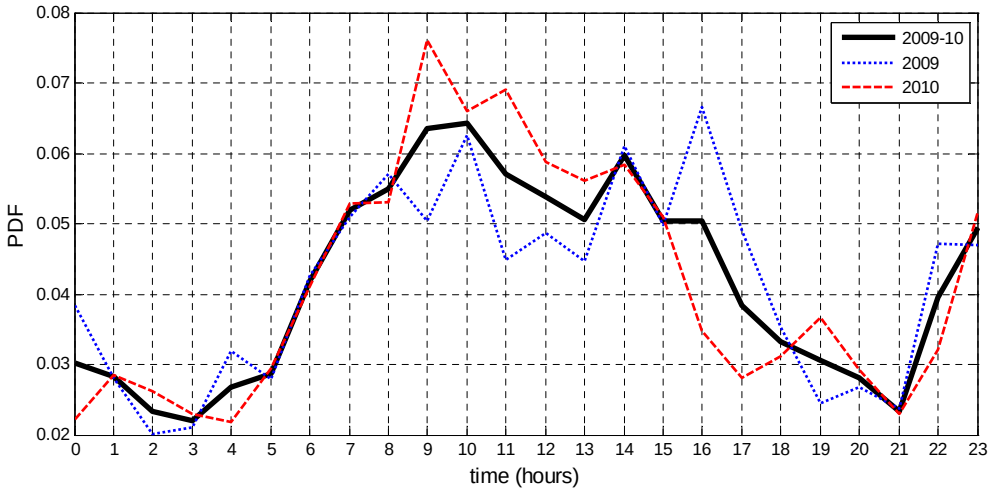

Figure G.5: SPEN - Daily probability of week-day short interruptions in years 2009/10.

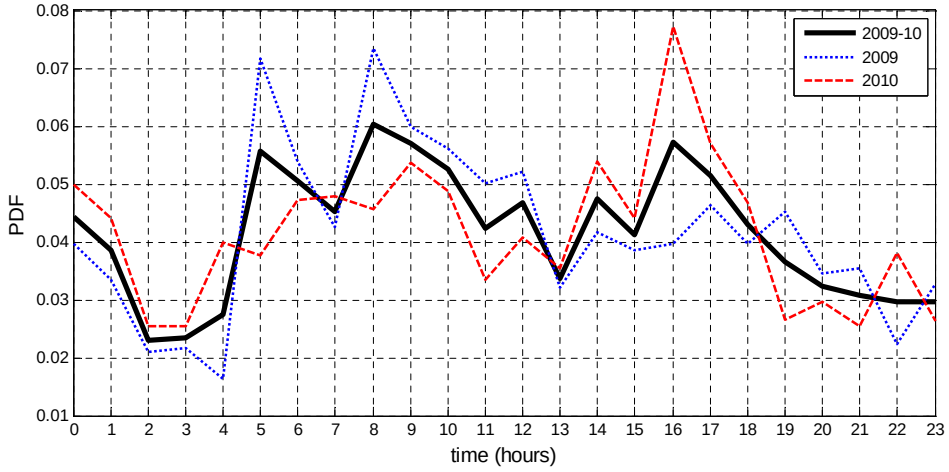

Figure G.6: SPEN - Daily probability of weekend-day short interruptions in years 2009/10.

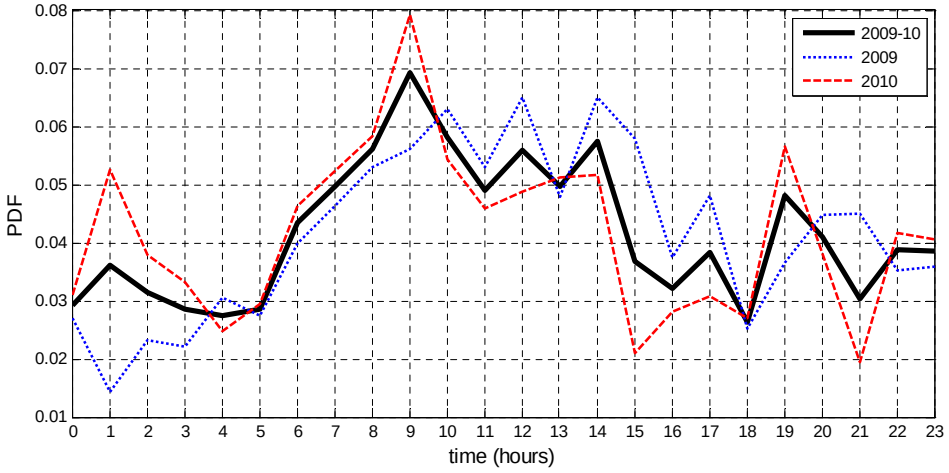

Figure G.7: SPEN - Daily probability of spring-time short interruptions in years 2009/10.

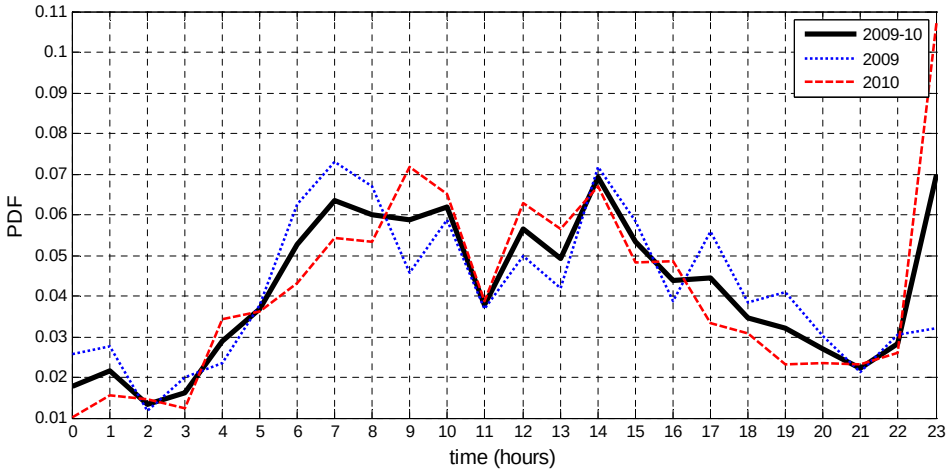

Figure G.8: SPEN - Daily probability of summer-time short interruptions in years 2009/10.

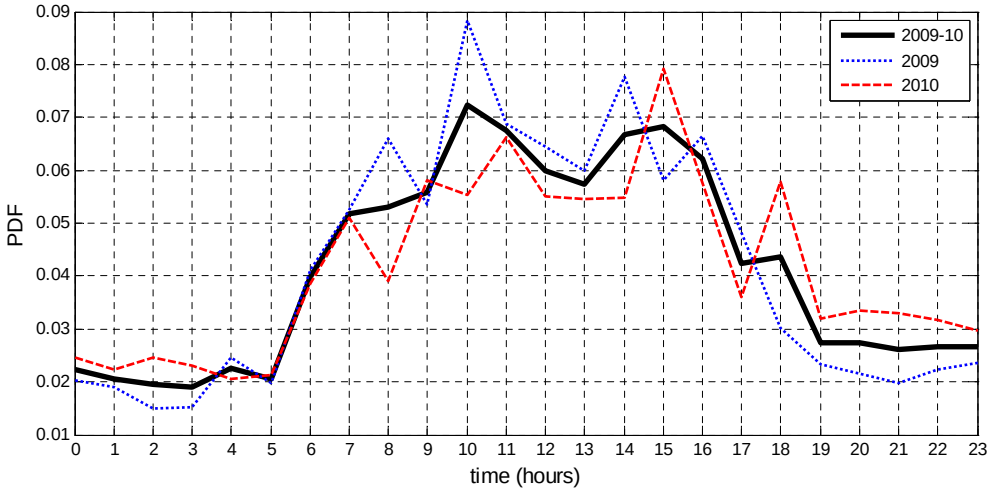

Figure G.9: SPEN - Daily probability of autumn-time short interruptions in years 2009/10.

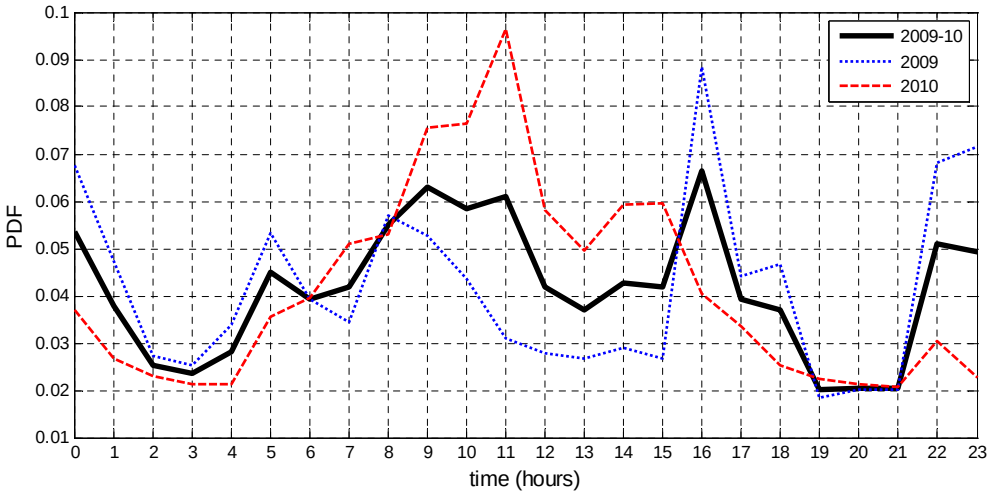

Figure G.10: SPEN - Daily probability of winter-time short interruptions in years 2009/10.

As a general/common trend, the most probable time of having a PQ-related short interruption is in all cases between 9:00 h and 10:00 h in the morning. Annual and week-days probability are basically equal, so weekends do not seem to have a big effect on annual SI probability. Also, the weekend probability is within the range of 2% and 6%, with no visible upwards or downwards trend, therefore, it can be considered as a constant average value of around 4% probability.

Regarding the yearly seasonal analysis, there is not a big difference from season to season to the annual disturbance probability. Spring and autumn SI probability are more equal to the aggregate annual, and on the other hand, summer and winter disturbance probabilities are surprisingly distributed in quite a similar way.